

**THE PERFORMANCE CHARACTERISTICS OF
POLYMER NANOCOMPOSITE MODIFIED
BINDERS AND ASPHALT MIXTURES**

**A THESIS SUBMITTED TO THE INSTITUTE OF
GRADUATE STUDIES
OF
NEAR EAST UNIVERSITY**

**By
MUSTAFA ALAS**

**In Partial Fulfilment of the Requirements for the Degree
of Doctor of Philosophy in Civil Engineering**

NICOSIA, 2021

MUSTAFA ALAS

**THE PERFORMANCE CHARACTERISTICS OF POLYMER
NANOCOMPOSITE MODIFIED BINDERS AND ASPHALT MIXTURES**

**NEU
2021**

**THE PERFORMANCE CHARACTERISTICS OF
POLYMER NANOCOMPOSITE MODIFIED
BINDERS AND ASPHALT MIXTURES**

**A THESIS SUBMITTED TO THE INSTITUTE OF
GRADUATE STUDIES
OF
NEAR EAST UNIVERSITY**

**By
MUSTAFA ALAS**

**In Partial Fulfilment of the Requirements for the Degree
of Doctor of Philosophy in Civil Engineering**

NICOSIA, 2021

**Mustafa ALAS: THE PERFORMANCE CHARACTERISTICS OF POLYMER
NANOCOMPOSITE MODIFIED BINDERS AND ASPHALT MIXTURES**

Approval of Director of Institute of Graduate Studies

Prof. Dr. K. Hüsnü Can BAŞER

**We certify this thesis is satisfactory for the award of the degree of Doctor of
Philosophy in Civil Engineering**

Thesis defence was held online. The jury members declared their acceptance verbally which is recorded.

Examining committee in charge:

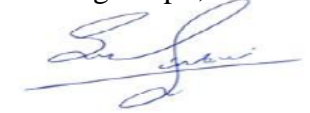
Prof. Dr. Hüseyin Gökçekuş

Committee chairman, Supervisor, Civil
Eng. Dept., NEU/ TRNC



Dr. Shaban Albrka

Co-supervisor, Civil Eng. Dept., NEU/
TRNC



Prof. Dr. Özgür Eren

Civil Eng. Dept., EMU/ TRNC



Prof. Dr. Khaled Hamed Marar

Civil Eng. Dept., EMU/ TRNC



Assoc. Prof. Dr. Beste Çubukçuoğlu

Civil Eng. Dept., NEU/ TRNC



Assoc. Prof. Dr. Walid El-kamash

Civil Eng. Dept., Suez Canal
University/ Egypt



Assoc. Prof. Dr. Hasan Tapkın

Civil Eng. Dept., Çankaya University/
Turkey



I hereby declare that all information in this document has been obtained and presented in accordance with academic rules and ethical conduct. I also declare that, as required by these rules and conduct, I have fully cited and referenced all material and results that are not original to this work.

Name, Last name: Mustafa Alas

Signature:

Date: 19/02/2021

ACKNOWLEDGEMENT

This thesis would not have been possible without the help, support and patience of my principal and co-supervisor. I would like to express my deep and sincere gratitude to Prof. Dr. Hüseyin Gökçekus and Dr. Shaban Albrka for their constant encouragement and assistance during my studies. I am extending my heartfelt thanks to my co-supervisor for his friendship, empathy and for providing me the opportunity to travel to Malaysia for conducting the thesis experiments.

Eventually, after visiting three different institutions namely, the Universiti Sains Malaysia, Universiti Teknologi Malaysia and Universiti Tun Hussein Onn Malaysia for completing my research, there is a long list of academic staff, technicians and fellow researchers that I would like to thank. I cannot mention them all but I would like to express my sincerest gratitude to all of those with whom I have had the pleasure to work with while conducting my research.

Above all, I am extremely grateful to my parents for their love, prayers, caring and sacrifices for educating and preparing me for my future. I am very much thankful to my fiancée Dilan Kalaycı for her love, understanding and continuing support to complete this research work. Without their unconditional love and support throughout my academic career, none of this would have been possible.

To my parents...

ABSTRACT

The current research focuses on the influence of polymer nanocomposite (PNC) modifiers regarding to performance characterisation of neat and modified asphalt cement (AC) and the design and moisture susceptibility of PNC modified asphaltic concrete mixtures. Seven original blends including neat AC, Acrylate-Styrene-Acrylonitrile (ASA)/ Nanosilica (Si) and ASA/ Nanoironoxide (Fe) were the subject of experimental investigations. ASA was used at 5% for all modified blends while the nanomaterials were blended in 3, 5 and 7% concentrations by the weight of AC. Physical and rheological testing procedures were conducted as well as morphology analysis. Temperature susceptibility, storage stability and aging resistance of AC were analysed by the physical test results while, the viscoelastic properties of AC were evaluated by the isochronal plots, master curves and the creep compliance curves. Morphology analysis aided to observe the newly formed chemical and structures changes in the chemical composition of AC to understand and validate the findings from the conventional and DSR test outcomes. Additionally, heuristic modelling techniques were utilised to predict experimental outcomes over a wider range of testing parameters. Furthermore, by using the optimum performing compositions for each type of PNC modified AC, the mix design procedures were employed to evaluate the performance of additives at the mixture level. Volumetric characteristics and the effect of modifiers on the moisture sensitivity of Hot Mix Asphalt (HMA) were evaluated. Rheological characterisation revealed that, viscoelastic properties of PNC modified AC were improved significantly compared to the base AC. ASA/Fe composites yielded lower rutting depths and a lower fatigue resistance parameter, while ASA/Si composites demonstrated ability to resist rutting and possessed elastic properties concurrently. The coefficient of determination (R^2) values showed that, ANN's were able to predict experimental outcomes with higher accuracy than the ANFIS. The optimum performing ASA/Si and ASA/Fe composites which were the 5% and 3% compositions respectively were designed at the mixture level and evaluated for moisture susceptibility. ASA/Fe modified AC-HMA demonstrated the most enhanced moisture susceptibility.

Keywords: Rheological characterisation; morphology; moisture susceptibility; heuristic modelling; polymer/nanocomposite

ÖZET

Araştırmada polimer nanokompozit (PNK) katkı maddesi ile modifiye edilmiş asfalt bağlayıcıların karakteristik performans özellikleri incelenmiş, bağlayıcıların karışım seviyesinde tasarımı ve nem duyarlılığı üzerindeki etkisi üzerinde durulmuştur. Katkısız bağlayıcı ile birlikte, bitüm ağırlığının %5 oranında Akrilet-Stiren-Akrilonitril ve 3%, 5% ve 7% oranlarında nano silika (SiO₂) ve nano demiroksit (Fe₃O₄) katkı maddelerinin karışımı sonucunda yedi farklı asfalt bağlayıcı elde edilmiş ve bu bağlayıcılar fiziksel, morfolojik ve reolojik değerlendirmeye tabi tutulmuştur. Araştırmada konvansiyonel ve Dinamik Kayma Reometresi (DKR) test prosedürlerinin uygulanmasına ilaveten morfoloji analizi yapılmıştır. Bağlayıcıların sıcaklık duyarlılığı, depolama kararlılığı ve yaşlanma direnci fiziksel test sonuçlarıyla analiz edilirken; viskoelastik özellikleri, izokronal grafikler, ana eğriler ve devingen sürünme eğrileri ile değerlendirilmiştir. Morfoloji analizi, konvansiyonel ve DKR test sonuçlarından elde edilen bulguları tahkik etmek ve bağlayıcıların kimyasal yapısında oluşan değişikliklerin gözlemlenmesi için kullanılmıştır. Yapay sinir ağları (YSA) ve uyarlanabilir nöro bulanık çıkarım sistemleri (UNBÇS), daha geniş test parametreleri yelpazesinde deneysel sonuçları tahmin edebilmek amacı ile modellenmiştir. Ayrıca, “Superpave” tasarım prensipleri benimsenerek, katkısız bağlayıcı ve en iyi performans gösteren PNK katkılı bağlayıcılar için sıcak karışım asfalt (SKA) tasarımları hazırlanmıştır. Tasarlanan karışımların hacimsel özellikleri ve katkı maddelerinin SKA üzerindeki nem duyarlılığına etkisi incelenmiştir. Reolojik karakterizasyon sonucunda, PNK katkı maddeli bağlayıcıların viskoelastik özelliklerinin katkısız bağlayıcıya kıyasla önemli ölçüde geliştiği gözlemlenmiştir. ASA/Fe kompozitleri, en yüksek tekerlek izi ve en düşük yorulma direnci parametrelerini verirken; ASA/Si kompozitleri, tekerlek izine direnme ve aynı zamanda elastik özelliklere sahip olma kabiliyetini sergilemiştir. Belirleme katsayısı (R²) değerleri deneysel sonuçları YSA'nın UNBÇS'den daha yüksek doğrulukla tahmin edebildiğini göstermiştir. En iyi performansı gösteren bağlayıcılar (ASA/Fe 3% ve ASA/Si 5%) karışım düzeyinde tasarlanmış ve SKA'ların nem duyarlılığı incelenmiştir. En az nem duyarlılığı bulunan karışımın ASA/Fe 3% PNK bağlayıcı ile tasarlanan karışım olduğu saptanmıştır.

Anahtar kelimeler: Reolojik karakterizasyon; morfoloji; nem duyarlılığı; buluşsal modelleme; Polimer/nanokompozit

TABLE OF CONTENTS

ACKNOWLEDGEMENTS	i
ABSTRACT	iii
ÖZET	iv
TABLE OF CONTENTS	v
LIST OF FIGURES	ix
LIST OF TABLES	xii
LIST OF ABBREVIATIONS	xiv
LIST OF SYMBOLS	xvii

CHAPTER 1: INTRODUCTION

1.1 Background.....	1
1.2 Problem Statement	2
1.3 Research Objectives	3
1.4 Scope and Research Methods	4
1.5 Research Limitations.....	6
1.6 Thesis Organisation.....	7

CHAPTER 2: LITERATURE REVIEW

2.1 Asphalt Cement Characteristics	9
2.1.1 Asphalt composition and structure	10
2.1.2 Physical characterisation.....	12
2.1.3 Rheological characterisation	18

2.1.4 Chemical characterisation	27
2.1.5 Durability of asphalt cement	32
2.2 Asphalt Cement Modification.....	35
2.2.1 Polymer modified asphalt cement	36
2.2.2 Nano materials in AC	40
2.2.3 Polymer/nanocomposite AC	43
2.3 Modelling the Performance Characteristics of Asphalt Cement	48
2.3.1 Experimental modelling of AC	48
2.3.2 Soft computing modelling of performance parameters	54
2.4 Hot Mix Asphalt Design.....	64
2.4.1 Requirements of HMA.....	65
2.4.2 Superpave mix design methods	68
2.4.3 HMA characteristics and behaviour	72
2.4.4 HMA Moisture susceptibility.....	81

CHAPTER 3: EXPERIMENTAL PROCEDURES AND DATA ANALYSIS

3.1 Materials and Sample Preparation	83
3.2 Testing Procedures.....	84
3.2.1 Penetration test	86
3.2.2 Ring and ball softening point	86
3.2.3 Rotational viscosity	87
3.2.4 Ductility	88
3.2.5 Storage stability test.....	89
3.2.6 Morphology analysis.....	89
3.2.7 Sample conditioning	92

3.2.8 Dynamic shear rheometer	93
3.3 Heuristic Modelling for Viscoelastic Characteristics of Asphalt Cement	96
3.3.1 Multilayer perceptron neural networks.....	96
3.3.2 Adaptive neuro fuzzy inference system (ANFIS)	99
3.4 Hot Mix Asphalt Design.....	102
3.4.1 Mixing and compaction temperatures.....	103
3.4.2 Volumetric properties and the optimum binder content	104
3.4.3 Moisture susceptibility	111

CHAPTER 4: RESULTS AND DISCUSSION

4.1 Conventional Properties	113
4.1.1 Penetration and softening point test results	114
4.1.2 Rotational viscosity test results.....	117
4.1.3 Ductility test results.....	119
4.1.4 Temperature sensitivity analysis.....	120
4.1.5 Storage stability analysis	121
4.1.6 Aging index for AC.....	122
4.2 Chemical Structure and Morphology Analysis.....	124
4.2.1 X-ray diffraction	125
4.2.2 Fourier infrared spectroscopy	127
4.3 Performance Characteristics	131
4.3.1 Frequency sweep test.....	132
4.3.2 MSCR test.....	140
4.4 Heuristic Modelling Of Performance Characteristics	143
4.4.1 Artificial neural network	144

4.4.2 Adaptive neuro fuzzy inference system	148
4.5 Hot Mix Asphalt Design.....	151
4.5.1 Mix design parameters and volumetric properties	151
4.5.2 Moisture susceptibility	154
 CHAPTER 5: CONCLUSION	
5.1 Summary of the Findings	157
5.2 Future Research Recommendations.....	158
 REFERENCES	
	160
 APPENDICES	
Appendix 1: XRD analysis results for ASA/Si and ASA/Fe composites	182
Appendix 2: FTIR analysis results for ASA/Si composites	183
Appendix 3: FTIR analysis results for ASA/Fe composites	184
Appendix 4: Complex modulus for ASA/Si and ASA/Fe composites	185
Appendix 5: MSCR test results for ASA/Si composites at 100 and 3200 Pa	186
Appendix 6: MSCR test results for ASA/Fe composites at 100 and 3200 Pa	187
Appendix 7: ANN model results	188
Appendix 8: ANFIS model results.....	189
 CURRICULUM VITAE	
	190

LIST OF FIGURES

Figure 1.1: Research outline.....	5
Figure 2.1: S.A.R.A fractions	11
Figure 2.2: Time lag between shear stress and shear strain	20
Figure 2.3: Viscous and elastic components of AC.....	20
Figure 2.4: DSR testing configuration	22
Figure 2.5: Viscoelastic region.....	22
Figure 2.6: Time-temperature superposition	24
Figure 2.7: Schematic representation of MSCR test results.....	25
Figure 2.8: Asphalt cement response to creep loading-unloading cycle.....	26
Figure 2.9: XRD characteristics peaks.....	29
Figure 2.10: Typical groups present in FTIR spectra	31
Figure 2.11: Asphalt dimensions from macro to quantum levels.....	41
Figure 2.12: Asphalt/polymer nanocomposite matrix internal structure	44
Figure 2.13: Penetration grading of three different pen 60/70 grade AC samples	50
Figure 2.14: Superpave grade selection	53
Figure 2.15: Superpave PG testing protocols	54
Figure 2.16: A three-layered feed-forward neural network with BP	58
Figure 2.17: General structure of ANFIS.....	62
Figure 2.18: Federal Highway Administration 045 power chart.....	70
Figure 2.19: Superpave gyratory compaction	71
Figure 2.20: Compacted asphalt concrete cross section and volumetric phase diagram.....	73
Figure 2.21: Relationship between air voids and asphalt content in the HMA.....	81

Figure 3.1: Penetration test apparatus assembly	86
Figure 3.2: Ring and ball softening point test	87
Figure 3.3: Rotational viscosity test	88
Figure 3.4: Ductility test	89
Figure 3.5: X-ray crystallography.....	90
Figure 3.6: FTIR working principle.....	91
Figure 3.7: Rolling thin film oven test.....	92
Figure 3.8: Dynamic shear rheometer.....	95
Figure 3.9: Schematic of FFNNM with backpropagation network.....	98
Figure 3.10: The general structure of ANFIS.....	101
Figure 3.11: Rice method procedure.....	108
Figure 3.12: Determination of Bulk specific gravity of the mixture	109
Figure 4.1: Penetration test results.....	114
Figure 4.2: Softening points for the base and PNC modified AC	116
Figure 4.3a: Rotational viscosity test results for ASA/Si composites.....	117
Figure 4.3b: Rotational viscosity test results for ASA/Fe composites	117
Figure 4.4: Ductility test results	118
Figure 4.5: Storage stability results	121
Figure 4.6: Viscosity aging index at elevated temperatures.....	123
Figure 4.7a: XRD plot for ASA/Si composites.....	125
Figure 4.7b: XRD plot for ASA/Fe composites.....	126
Figure 4.8: D-spacing for PNC modified AC.....	126
Figure 4.9a: Spectrum pattern for the ASA/Si composite binders	128
Figure 4.9b: Spectrum pattern for the ASA/Fe composite binders	128
Figure 4.10a: Aliphatic index.....	130

Figure 4.10b: Aromatics index	130
Figure 4.10c: Sulfoxide index	131
Figure 4.10d: Carbonyl index.....	131
Figure 4.11: Isochronal plots for ASA/Si composites	134
Figure 4.12: Isochronal plots for ASA/Fe composites	134
Figure 4.13a: G* for unaged base and ASA/Si modified AC	136
Figure 4.13b: G* for RTFO aged base and ASA/Si modified AC.....	137
Figure 4.14a: G* for unaged base and ASA/Fe modified AC	137
Figure 4.14b: G* for RTFO aged base and ASA/Fe modified AC	138
Figure 4.15: Rutting resistance parameter	139
Figure 4.16: Fatigue resistance parameter	140
Figure 4.17: Creep compliance for ASA/Si composites	141
Figure 4.18: Creep compliance for ASA/Fe composites	142
Figure 4.19: Elastic recovery for base, ASA/Si and ASA/Fe composites	143
Figure 4.20: Non-recoverable creep compliance for base, ASA/Si and ASA/Fe composites.....	143
Figure 4.21: Total number of epochs for Scenario 1 and Scenario 2	145
Figure 4.22: Measure of goodness of fit for Scenario 1 and Scenario 2.....	147
Figure 4.23: ANFIS model regression performance.....	149
Figure 4.24: Discrepancy between actual and predicted data	150
Figure 4.25: Mixing and compaction temperatures	152
Figure 4.26: Tensile strength of control and modified HMA.....	155
Figure 4.27: Tensile strength ratio	156

LIST OF TABLES

Table 1.1: Research limitations	6
Table 2.1: Asphalt composition	11
Table 2.2: Viscosity measurement testing methods.....	16
Table 2.3: Jnr classification for specific volume of traffic.....	26
Table 2.4: Minimum requirement for delayed elastic response	26
Table 2.5: Characteristics IR bands	30
Table 2.6: Classification and characterisation of common polymers used to modify AC.....	38
Table 2.7: Review of common nanomaterials used to modify neat asphalt.....	42
Table 2.8: Superpave PG specification	51
Table 2.9: Superpave grade bumping.....	53
Table 2.10: Superpave design compaction gyrations.....	72
Table 2.11: Superpave compaction density requirements.....	72
Table 2.12: Apparent, bulk and effective specific gravities of aggregates	74
Table 2.13: Superpave hot mix asphalt VMA requirements	78
Table 2.14: Superpave hot mix asphalt VFA requirements	79
Table 3.1: Physical properties of the base binder and the modifiers	84
Table 3.2: Testing procedures for asphalt binders	85
Table 3.3: Testing procedures for hot mix asphalt concrete	85
Table 3.4: AC-14 Gradation	103
Table 4.1: PI index and PVN.....	120
Table 4.2: Softening point aging index	124
Table 4.3: Model Scenarios and descriptive statistics for the input and output parameters	144

Table 4.4: Statistical indicator metrics.....	149
Table 4.5: Mixing and compaction temperatures	152
Table 4.6: Volumetric characteristics of HMA	154

LIST OF ABBREVIATIONS

AASHTO:	American Association of State Highway and Transportation Officials
AC:	Asphalt Cement
AFM:	Atomic Force Microscopy
ALF:	Accelerated Loading Facility
ANFIS:	Adaptive Neuro Fuzzy Inference System
ANN:	Artificial Neural Network
APE:	Average Percentage Error
ASA:	Acrylate Styrene Acrylonitrile
ASTM:	American Society for Testing and Materials
ATR:	Attenuated Total Reflectance
BBR:	Bending Beam Rheometer
BSN:	Branch SBS-Nanocomposite
CKE:	Centrifuge Kerosene Equivalent
CNT:	Carbon Nano Tubes
CR:	Crumb Rubber
D/A:	Dust to Asphalt Ratio
DSR:	Dynamic Shear Rheometer
DTT:	Direct Tension Tester
ESAL:	Equivalent Single Axle Load
EVA:	Ethylene Vinyl Acetate
FE-SEM:	Field Emission Scanning Electron Microscope
FFMLPNN:	Feed Forward Multi-Layer Perceptron Neural Network
FHWA:	Federal Highway Administration

FIS:	Fuzzy Inference System
FRT:	French Rutting Tester
FTIR:	Fourier Infrared Spectroscopy
GA:	Genetic Algorithm
GD:	Gradient Descent
HMA:	Hot Mix Asphalt
HWTD:	Hamburg Wheel Tracking Device
ITS:	Indirect tensile strength
LSN:	Linear SBS-Nanocomposite
LM:	Levenberg-Marquardt
MAE:	Average Mean Error
MLP:	Multi-Layer Perceptron
MLR:	Multiple Linear Regression
M-RTFO:	Modified Rolling Thin Film Oven
MSCR:	Multiple Stress Creep Recovery
MSE:	Mean Squared Error
OBC:	Optimum binder content
PAV:	Pressure Aging Vessel
PE:	Polyethylene
PG:	Performance grade
PI:	Penetration Index
PMB:	Polymer Modified Bitumen
PNC:	Polymer Nanocomposite
PNCMAC:	Polymer Nanocomposite Modified Asphalt Cement
PP:	Polypropylene

PVN:	Penetration Viscosity Number
R:	Correlation Coefficient
R²:	Coefficient of Determination
RBF:	Radial Basis Function
RMSE:	Root Mean Squared Error
RTFO:	Rolling Thin Film Oven
RV:	Rotational Viscosity
SB:	Styrene Butadiene
SBR:	Styrene Butadiene Rubber
SBS:	Styrene Butadiene Styrene
SCG:	Scaled Conjugate Gradient
SGC:	Superpave Gyrotory Compactor
SHRP:	Strategic Highway Research Program
SMA:	Stone Matrix Asphalt
SSD:	Saturated Surface Dry
SVM:	Support Vector Machine
TSR:	Tensile Strength Ratio
UTM:	Universal Testing Machine
UV:	Ultra Violet
VAI:	Viscosity Aging Index
VFA:	Voids Filled with Asphalt
VMA:	Voids in Mineral Aggregates
XRD:	X-Ray Diffraction

LIST OF SYMBOLS

%R:	Percentage recovery
\hat{Y}_i :	Data predicted in AI model
W_c :	Dissipated work in frequency sweep
γ_i :	Data observed from the experiments
ϵ_1 :	Strain at the end of creep portion of each cycle in MSCRT
ϵ_{10} :	Strain at the end of recovery portion of each cycle in MSCRT
ϵ_c :	Final strain in the creep stage of MSCRT
ϵ_{nr} :	Total non-recovered shear strain
ϵ_o :	Initial strain in the creep stage of MSCRT
ϵ_r :	Final strain in the recovery stage of MSCRT
ϵ_t :	Total strain
Δt :	Time lag of phase angle
D/A:	Dust to asphalt ratio
Fe₃O₄:	Iron oxide
G*.sin δ:	Fatigue resistance parameter
G*/sin δ:	Rutting resistance parameter
G*:	Complex shear modulus
G':	Storage modulus
G'':	Loss modulus
G_b:	Specific gravity of the asphalt binder
G_{mb}:	Bulk specific gravity of the mixture
G_{mm}:	Theoretical maximum specific gravity of the mixture
G_{sa}:	Apparent specific gravity of the aggregates

G_{sb}:	Bulk specific gravity of the aggregates
G_{se}:	Effective specific gravity of the aggregates
$J_{nr(diff)}$:	Difference between non-recoverable creep compliance at 0.1 and 3.2 kPa.
J_{nr}:	Non-recoverable creep compliance
P_{ba}:	Percentage asphalt binder absorbed by the mineral aggregates
P_{be}:	Percentage asphalt binder content
P_s:	Percentage of aggregates in the mixture
R^2:	Coefficient of determination
SiO_2:	Silicon dioxide
S_{mix}:	Creep modulus
S_t:	Tensile strength
V_a:	Total air voids in the mixture
γ:	Shear rate
δ:	Phase angle
η:	Rotational viscosity
τ:	Torque
σ:	Applied stress
ϵ:	Axial strain

CHAPTER 1

INTRODUCTION

1.1 Background

Asphalt (bitumen), an adhesive hydrocarbon which is naturally occurring in asphalt lakes in very small quantities or obtained from the distillation of crude oil in refineries has been the most suitable material which is used in combination with the mineral aggregates and optionally with filler materials to construct flexible pavement roads (Sotiriadis, 2016). Asphalt that is used for paving applications is referred to as asphalt cement (AC). AC has thermoplastic features because it softens as it is heated and hardens as it is cooled. This unique combination of characteristics along with other useful properties such as being a water proof and a durable material are the fundamental reasons why asphalt is a suitable paving material (Handbook, 2007). The performance characteristics and the durability of asphalt pavements are under the influence of climatic conditions and dynamic vehicular loading. Higher stiffness at high temperatures and low frequencies to prevent permanent deformation and higher elasticity at low temperatures and high frequencies to prevent fatigue failure for the pavement roads are favourable properties of AC (Lee et al., 2007). Historically, AC has been graded based on its consistency which was determined by empirical testing methods such as the penetration and viscosity measurements. However, with the increase in traffic volumes and erratic climate conditions, the concern to improving the standards of AC and the experimental techniques to measure those standards accurately have arisen. On this basis, the Strategic Highway Research Program (SHRP) was developed in 1993 (Read et al., 2003). Along with the new testing technologies, SHRP enabled the introduction to asphalt modification with polymeric materials which was then followed by introducing new additives such as nano materials and polymer nanocomposites to modify neat asphalt with the pursue to achieving superior performing pavements (Moghaddam et al., 2011). Findings of numerous researchers regarding to polymer and nanomaterial modified AC have already been implemented in the paving industry. Polymer nanocomposite modified AC has been the most recent innovation to improve the performance and durability of pavement roads. However, before field application further

research to understanding the behaviour and influence of PNC's on the AC is required which is the objective of the present study to present findings that are useful to the pavement engineering community.

1.2 Problem Statement

The viscoelastic nature of asphaltic mixtures makes it a suitable option for flexible pavement design as it possesses valuable engineering properties to resist dynamic vehicular loading and extreme climatic conditions which the pavement roads encounter during the service life. However, from the previous reports of field observations and the research conducted in the literature, it has been acknowledged that, the neat asphalt binder used for paving applications may not always ensure sufficient stability, durability and desired performance characteristics. In the search for enhancing the performance of asphalt cement and mixtures, numerous investigations have been concentrated on asphalt modification with polymers, nanomaterials and polymer nanocomposites due to their versatile properties needed to design superior performing asphalt pavements. Despite a remarkable enhancement of asphalt properties is achieved this way, the success of the modification process has been mostly suffered from certain limitations such as the phase separation between the polymer and the asphalt and/or agglomeration of the nanoparticles. Other issues associated with the modification process regards to the workability and high storage stability of asphalt during production and construction stages due to increased viscosities. Also, it should be noted that, there exist no superior modifier to improve durability (aging resistance and moisture susceptibility) and all performance characteristics (high temperature and low temperature characteristics) of asphalt. Often, targeting to enhance a specific characteristic of asphalt is at the expense of losing another one. Additionally, from the economic standpoint, the cost of modification should not undermine the performance enhancement achieved with the modification process. ASA, nanosilica and nanoironoxide have been previously utilized as sole additives to modify base AC and they are known to be capable of enhancing the high and low temperature performance characteristics as well as improving the durability of neat asphalt. Along with the positive effect of these materials on the performance of AC, it has been reported in numerous studies that, they have been limited to address multiple concerns at the same time when used as sole additives. Based on the literature, polymer

nanocomposite modified AC can mitigate the certain drawbacks of additives and offers a promising potential to address major distresses such as the rutting and thermal fatigue that the pavements experience during the service time. Since the anticipated field conditions (climate and traffic loading) are erratic and there exists no superior asphalt, the perspective of the pavement engineers is to attain a fine balanced asphalt design that is durable and can remediate major forms of distresses. Although, polymer nanocomposites are an effective way to achieve this, they are relatively new and there exists a gap in the literature on this matter. The lack of understanding regarding to the behaviour of polymer nanocomposites in modified asphalt cement drew the incentives for the current study.

1.3 Research Objectives

The focus of this research was to investigate the influence of ASA/SiO₂ and ASA/Fe₃O₄ polymer nanocomposites on the durability and performance characteristics of AC by using physical, morphological and rheological analysis. The influence of additives at different concentrations (3, 5 and 7% by wt.) were the subject of investigations. To finding the optimum performing composition for the PNC modified AC, the conventional and dynamic shear rheometer testing procedures were focused on evaluating the critical parameters of AC which included, the temperature susceptibility, workability, storage stability, aging resistance and the performance parameters such as the creep compliance, rutting and fatigue resistance parameters. Morphology analysis was further conducted in order to observe the formations of new chemical and structural changes in the asphalt matrix due to the modification process and to understand the performance variation of the PNC modified AC. Heuristic modelling techniques such as ANN and ANFIS were implemented to predict the experimental outcomes from physical and rheological properties of AC to estimating the performance behaviour over a wider range of testing and aging conditions which the pavement may experience during its service time. Furthermore, the performance of the PNC modified AC was investigated at the mixture level by conducting volumetric analysis for the designed HMA which was then followed by the moisture susceptibility analysis to evaluating the stripping potential of the base and PNC modified AC in HMA design.

1.4 Scope and Research Methods

The scope of the study covers the performance evaluation for two different polymer nanocomposites at the binder and mixture levels. The effects of nanomaterials namely, the nano silica and nano ironoxide at three different concentrations blended with 5% ASA by the weight and a base AC of 80/100 penetration grade as the control sample comprised the research concern. The research objectives were executed in three primary stages. According to a number of researchers, the performance of flexible asphalt pavements is vigorously influenced by the asphalt cement characteristics. Therefore, the first stage of the research was focused on characterising the asphalt cement by its physical, morphological and rheological properties. Empirical testing methods conducted for the conventional properties of AC included; Penetration, softening point, viscosity and ductility testing procedures. By using the outcomes from the physical tests, the temperature susceptibility, storage stability and the aging index for the AC were evaluated. The performance characteristics of AC were investigated by the DSR test outcomes. Two DSR testing procedures namely, the frequency sweep test and the multiple stress creep recovery (MSCR) test were performed to characterise the AC by its rheological properties. Creep compliance, rutting and fatigue resistance parameters were analysed from the outcomes of the DSR investigations to evaluating the viscoelastic properties of AC. The chemical composition of the PNC modified AC was analysed by using X-Ray diffraction (XRD) and Fourier infrared spectroscopy (FTIR) in order to understand the chemical and structural changes that occurred due to the modification process which might have influenced the results observed from the performance evaluation. In the second stage of the research, ANN and ANFIS were employed as artificial intelligence modelling techniques to predict the experimental outcomes. The heuristic approach enabled the experimental observations be analysed over a wider range of testing conditions which may also be the conditions that the constructed pavement experience during its service life. A considerable number of researchers stated in the literature that, a sole investigation of the asphalt cement characteristics may not always provide adequate analysis to determining the actual field performance of a constructed pavement. Since factors such as aggregate properties and gradation also have influence on volumetric properties of the mix design and the overall performance of the asphalt mixture, the third stage of the study was concentrated on the performance evaluation for the PNC

modified AC mix design. Using the weight volume relationships and specific gravities of the mixtures, the volumetric properties of the mix design were established. From the volumetric properties of the mix design, optimum binder content (OBC) was determined for each sample and moisture susceptibility evaluation was performed. Moisture susceptibility test was performed by the indirect tension test after conditioning the samples by using the modified Lottman method. Thoroughly, the testing protocols which were followed in order to achieve the objectives stated for the present study is illustrated in Figure 1.1.

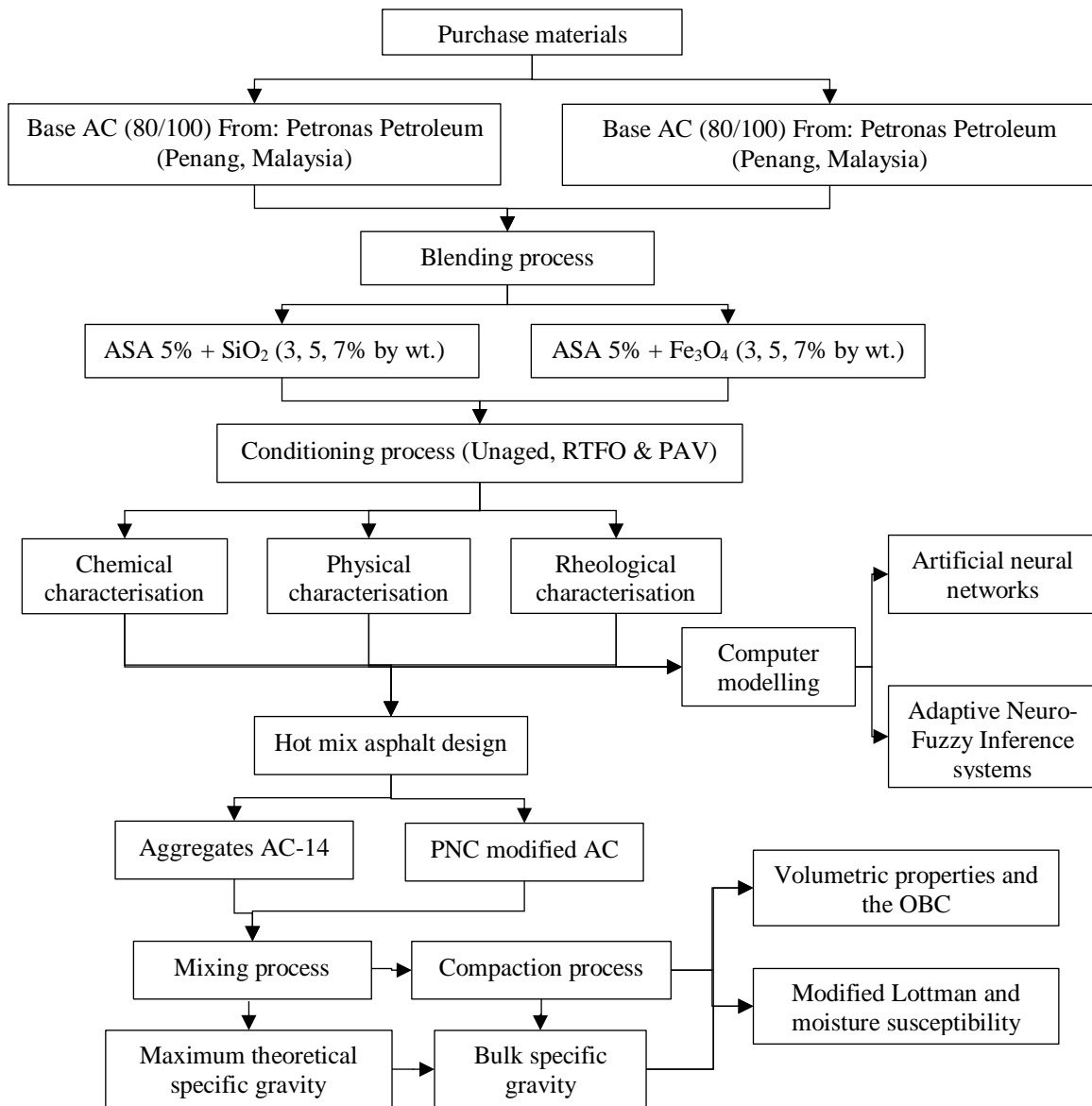


Figure 1.1: Research outline

1.5 Research Limitations

The present study demonstrated the experimental findings that were based on the most recent available experimental investigation techniques however, as it has been encountered in all previous research regarding to the investigation of modified asphalt binders and mixtures inevitably, the present study also suffered from certain limitations which were related to the efficiency of the experimental techniques and availability and capability of the testing equipment and the local sources. Additionally, the lack of previous research regarding to the materials of concern for the present study was a constraint towards being able to analyse the test results more comprehensively. A list of limitations and the researchers approach to address these limitations are demonstrated in Table 1.1.

Table 1.1: Research limitations

Related to;	Associated with;	Limitation	Proposed solution
Experimental techniques	Frequency sweep test	According to a number of researchers the frequency sweep test is performed at low strain levels which is valid for neat asphalt binders but does not accurately represent the actual deformations that take place in modified asphalt cement since the polymer phase is not activated.	Additionally, conduct experimental investigations by using the MSCR test.
	MSCR test	MSCR test is a relatively new technique used to measure permanent deformation of asphalt which requires further research to improve the technique. Most agencies still accept the frequency sweep test results rather than the MSCRT results.	Use the results from the frequency sweep test to validate the test results.
	HMA Mixing and compaction temperatures	Laboratory mixing and compaction temperatures for neat asphalt are determined based on the viscosity temperature relationship. For modified AC, this procedure may result in unreasonably high mixing and compaction temperatures.	None. Since no any other technique to determine the mixing and compaction temperatures is yet to be available in the literature and since the mixing and compaction temperatures did not reach beyond 200°C as suggested in the literature, the researcher did not find necessity to take any measure on this matter.

Table 1 continued

Related to;	Associated with;	Limitation	Proposed solution
Experimental techniques	Compaction process	Although Marshall compaction method is widely utilized owing to the economic reasons (low cost of equipment and low maintenance costs) many researchers reported that, the Marshall compaction process cannot truly represent the actual compaction effort in the field.	Superpave gyratory compaction method can better simulate the actual field compaction. However, the researcher was obliged to visit another institution to perform the sample mixing and compaction procedures.
Availability of the testing equipment and resources	Sample preparation, conditioning process and performance testing	Lack or malfunctioning of the testing equipment.	The testing protocols required advanced laboratory with well-maintained experimental equipment. The researcher visited three different institutions in different parts of Malaysia. Yet, testing procedures such as low temperature HMA characteristics were not able to be investigated due to lack of experimental equipment.
Literature and fieldwork implementation	Aggregates selection Availability of data from previous research and data from field observations	The aggregate selection was limited to the locally available sources. Polymer nanocomposites modified asphalt is a recently emerging topic. There exists a gap in the literature particularly on the materials of concern presented in the present study regarding to combined utilization to forming a polymer nanocomposite that can remediate certain drawbacks of the each individual additive. Additionally, due to the originality of the designed product, laboratory test results were not able to be compared with the data from the field observations.	None. The results from the previous work of other researchers which utilized similar additives as sole modifiers to asphalt cement were reviewed. No action could have been taken to investigate the correlation between the laboratory tested and field observed data since such data were not available.

1.6 Thesis Organisation

The study is organised in five main chapters which are the introduction, literature review, research methodology, results and discussion and conclusion. A brief conjuncture of the problem and the objectives of the study along with an overview of the methods which were followed to achieve the objectives were outlined in the introduction section. In chapter two,

an extensive background regarding to the experimental and computer modelling methods for the asphalt binder and mixture performance characteristics were presented. Previously conducted research with various types of modifiers and their effect on the physical, chemical and performance characteristics of AC and HMA design were acknowledged in this section. Chapter three presented the sample preparation techniques and the experimental procedures which were followed to evaluate the influence of the additives. Heuristic modelling methods were employed to develop artificial intelligence models that are able to predict the experimental outcomes. The findings from the experimental investigations were presented in chapter four. A detailed analysis of the test results and the corresponding discussions were presented. Finally, the findings of the research were emphasized in the conclusion section and future work recommendation were presented.

CHAPTER 2

LITERATURE REVIEW

2.1 Asphalt Cement Characteristics

Asphalt is a by-product that is derived from distillation of crude oil. The production of crude oil dates back to 1859 and the use of asphalt from the crude oil sources was started in early 1900's for application of asphaltic concrete (Bitumen, 1995). Numerous researchers attempted to characterize the structure of asphalt to obtain generalised knowledge about its physical and rheological properties however, asphalt being an organic material that has complex structure, many of these attempts have failed to acquire knowledge that relates the asphalt chemical structure to its physical and rheological properties (Redelius & Soenen, 2015). The chemical structure of asphalt majorly consists of hydrocarbons and other minor heteroatoms which are as explained in Chapter 2.1.1 in more detail. The proportion of constituents and the quality of asphalt depends on the source from which it is obtained as well as the production and processing procedures of crude oil (Zhang et al., 2015). Heavier crude oil was found to produce better asphalt yields and better physical and rheological properties (Ghaffari et al., 2017). It is worthy to mention that, chemical characterisation of asphalt alone was found to provide limited information regarding to its performance characteristics and therefore, advanced testing procedures are required for the physical and rheological characteristics assessment of asphalt cement (Redelius & Soenen, 2015). On the other hand, having knowledge about the chemical characteristics of AC is essential particularly in the case of modified asphalt to understanding the changes in physical and characteristic properties of the materials such as poor dispersion of particles in the asphalt matrix, agglomeration and phase separation concerns that results in instability of modified asphalt cement (Porto et al., 2019).

Commercially, asphalt cement is a thermoplastic and viscoelastic material that is used in flexible pavement construction due to its initial low cost of construction and suitable properties compared to other paving options such as concrete material which is principally used in rigid pavement construction applications (Jain et al., 2013). From functional perspective, asphalt is desired to have optimum fluidity and workability to be pumped and

processed during the manufacturing and construction processes. Also, higher stiffness at high temperatures and low frequencies and higher elasticity at low temperatures and high frequencies are favourable properties of asphalt cement in order to improve its performance characteristics which are under the influence of the climatic conditions and dynamic vehicular loading (Al-Mansob et al., 2016). In addition, in terms of manufacturing long-lasting durable asphalt pavements, the chemical composition of asphalt is found to have a considerable role in the aging properties of neat and modified asphalt cement. (Fernández-Gómez et al., 2013). It is reported in almost all studies that, neat asphalt that is used in the construction of pavements may be insufficient to address growing concerns regarding to increased traffic loading and extreme climatic conditions due to nature of the asphalt material. In this respect, numerous research have been dedicated to modify neat asphalt with polymers, nanomaterials and polymer nanocomposites in order to produce better performing and longer lasting pavement roads (Fang et al., 2013; Zhu et al., 2014). Herein, the fundamental basis of the current study is focused on exploring new polymer nanocomposite modifiers that are suitable to enhance the performance characteristics and durability of asphalt pavements.

2.1.1 Asphalt composition and structure

Chemically, asphalt has a complex structure since it is made up of a mixture of organic molecules. Numerous researchers have investigated the relationship between asphalt chemical composition and its ties to rheological properties of asphalt cement. However, most of these studies have not been proven to provide a solid knowledge about this relationship yet (Behnood & Gharehveran, 2019; Petersen, 2000). Composition variations in constituents of asphalt due to its origin and the type of distillation process of crude oil is a major factor that limits the generalisation ability to clarify the chemical structure of asphalt and its relation to engineering properties of asphalt cement (Petersen, 2000). It is also difficult to breakdown composition of asphalt precisely. However, studies that were conducted during the strategic highway research program that has been developed in 1993 using various sources of crude oil showed that, the elementary composition of asphalt is majorly formed of carbon and hydrogen atoms. In addition to that, other heteroatoms such as sulphur, nitrogen and oxygen are generally present. Traces of metals are also found where the most

numerous ones being the vanadium and nickel. The concentration of the constituents of asphalt are given in Table 2.1 (Branthaver, 1993).

Table 2.1: Asphalt composition

Elemental analysis	Concentration
Carbon	82-88%
Hydrogen	8-11%
Sulphur	0-6%
Oxygen	0-1.5%
Nitrogen	0-1%
Vanadium, Nickel, Iron, Aluminium, Silicon	Traces

In order to fully understand the fundamental engineering properties of asphalt at the molecular level, asphalt composition can be described by four main components which are the asphaltenes, resins, aromatics and saturates, also known as the S.A.R.A fractions (García-Morales et al., 2007). It has to be noted that the percent of each S.A.R.A fractions depends on the crude oil origin, manufacturing process and grade of the analysed asphalt. Moreover, many researchers reported the occurrences of alterations in S.A.R.A composition under different experimental conditions and after aging procedures (Galooyak et al., 2010). The relative quantity of S.A.R.A fractions are given in Figure 2.1.

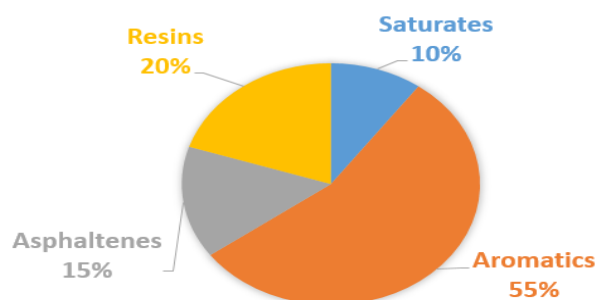


Figure 2.1: S.A.R.A fractions

Asphaltenes are defined as the soluble part of asphalt. They are in the form of black powder and are responsible for the brown to black asphalt colour. Asphaltenes comprises 5% to 25%

of the weight of asphalt. The concentration of asphaltenes has considerable effect on the rheological characteristics of asphalt. More asphaltenes level indicate better performance at high temperatures due to increased stiffness. However, an adverse impact of higher asphaltenes level is observed under the effect of long-term aging because of excessive hardening due to photo-oxygenation and results in lower aging resistance of asphalt cement (Rahman, 2004).

Resins are another constituent of the asphalt which gives asphalt its adhesion properties due to its highly polar nature. However, their primary role is to act as dispersing agents for asphaltenes. Approximately, they constitute from 15% to 25% of asphalt and increase in resins content results in solution structure whereas, reduction of resin content results in gelatinous structure of asphalt. Resins play crucial role in the stability of asphalt since they act as a stabilizer for the asphaltenes (Porto et al., 2019).

Saturates constituents typically forms 0%-15% by the weight of the overall fractions of asphalt. Saturates are known to give fluid properties to asphalt. Increase in the saturate concentration results in lower complex shear modulus and higher phase angle where, the opposite leads to versa. This indicates that, asphalt with higher saturates fractions are more preferred to be used in pavement construction under cold climate conditions in order to prevent fatigue and thermal cracking failures (Galooyak et al., 2010).

Aromatics are the most abundant constituent of asphalt which constitutes 40%-65% of the asphalt fractions. Aliphaticity and aromaticity are the two structural groups commonly used as aging indices for asphalt cement. Aliphatic structures are the light components which volatilizes during the aging process. Aliphatic structures are also absorbed by the aromatic structures during this process. Therefore, observing the changes in aromatic fractions under aging conditions, the rate of volatilization can be evaluated (H. Wang et al., 2020).

2.1.2 Physical characterisation

Historically, asphalt cement (AC) was used to be described by its physical properties such as the penetration value and the rotational viscosity. Additional testing procedures that were adopted for physical characterisation of asphalt cement included ductility test and the softening point tests (Hardin, 1995). However, due to viscoelastic nature of asphalt material

and its complex organic structure, its physical failure properties and the damage resistance properties are influenced by the temperature and the loading rate. Therefore, conventional testing procedures being a single point measurement was found not to be effective and reliable test methods in the modelling of the performance characteristics of AC (Kim, 2008). In addition to that, it is a common application to modify neat asphalt with polymeric materials, agents and nanomaterials in order to improve its performance and durability which further increases the complexity of its structure and makes it difficult to model the performance of AC by utilizing the above mentioned physical properties (Al-Mansob et al., 2017). With this concern, many agencies abandoned conventional physical testing procedures and adopted new testing technologies and modelling techniques such as chemical characterisation by Fourier Infrared Spectroscopy (FTIR) and rheological properties and failure parameters assessment by using Dynamic Shear Rheometer (DSR) (Yao et al., 2013). Although, more advanced testing methods are currently available and adopted as standard requirements by many authorisation agencies, conventional testing procedures are still required by agencies and they are also conducted for research purposes in the classification of AC. Moreover, numerous studies showed that, physical properties of AC could be used in analytical and computational modelling for fundamental engineering characteristics of AC which can be useful in terms of reducing the time, effort and resource consumption and the requirement for advanced technical testing equipment for further testing protocols (Kok et al., 2010). Penetration, softening point, viscosity and ductility tests were utilized in the current study to be used in classification of AC and also they were used for the computational prediction modelling of the performance parameters for neat and modified AC.

2.1.2.1 Penetration

Asphalt is predominantly used as binders in hot mix design for road construction and it is available in number of grades. The grading of asphalt is done based on its consistency. The consistency is determined by measuring the penetration of asphalt by using a standard penetrometer. The penetration of asphalt is the distance travelled by a standard needle of specific size, weight (100 grams) and shape under specified conditions of time (5 seconds) and temperature (25°C) in one tenths of a millimetre (Al-Omari et al., 2018). ASTM D5 and AASHTO T-49 are the common test protocols utilized for penetration testing for asphalt

cement. Favourable penetration values of asphalt are lower in warmer regions in order to avoid rutting failure due to softening of asphalt due to exposure to high temperatures and the use of asphalt which has higher penetration value is favourable in colder climate in order to prevent high stiffness related excessive brittleness that results in thermal and fatigue cracking failures (Handbook, 2007). Test results have been widely accepted as an indicator for rheological behaviour of neat asphalt however, penetration being a single point measurement, limits its suitability to be considered as a complete evaluation for such a complex viscoelastic material (Kim, 2008). Therefore, more recently the test results are used by numerous researchers solely as a physical property that aids in the assessment of temperature susceptibility parameter of asphalt cement (Ehinola et al., 2012). Along with the penetration test, softening point and rotational viscosity test results are also required in the assessment for temperature sensitivity of asphalt by using two indices called the penetration index (PI) and penetration-viscosity index (PVN) which are explained in Chapter 2.1.2.2 and Chapter 2.1.2.3 respectively. Another significance of the test is that, for modified asphalt cement, the performance characteristics are highly dependent on the penetration grade of the base asphalt. It is therefore noteworthy to mention that, for different penetration grade asphalt used as a base in the modified asphalt cement, up to 10^3 differences in complex modulus (G^*) value that is related to the stiffness of asphalt cement had been observed in a number of researches (Junaid et al., 2018; Pasandín & Pérez, 2014).

2.1.2.2 Softening Point

The ring and ball softening point test is another empirical test method that is used to measure the consistency of AC. The asphalt softening point is referred to as the temperature at which AC can change from the solid to the liquid phase under specific conditions. The test is used to determine the temperature up to which asphalt cement should be heated for different applications for road use. (Dahunsi et al., 2013). ASTM: D-36 and AASHTO: T-53 are the common testing protocols adopted in testing of asphalt for softening point although other testing procedures such as BS: 2000 Part: 58 and EN 1457: 2015 are used depending on the standards defined by authorisation agencies in particular regions in the world (Nicholls et al., 2006). The range of allowable softening point values for asphalt cement is specified for various road use applications in combination with the penetration grade of the asphalt by

various standards that are in use by different authorisation agencies. Softening point and penetration of asphalt cement are inversely proportional. In general, increase in softening point results in reduction of penetration value of asphalt cement (stiffening) and the opposite is versa (softening) (Ezzat et al., 2016). However, this rule may be disobeyed for asphalt cement that is modified with certain additives. For example, a research conducted by (Zaumanis, 2011) reported that, up to 3% addition of sasobit by the mass of base asphalt yielded decrease in softening point 20°C - 35°C and also the penetration of asphalt cement was reduced by 15-20 in one tenths of a millimetre.

Penetration value and softening point test results can further be used in conjunction for the assessment of temperature susceptibility of asphalt cement by a parameter called the Penetration index (PI). The formula for computing the PI number for asphalt cement is as given in eq. 2.1 (Al-Mansob et al., 2017).

$$PI = \frac{1952 - 500 \log(\text{Pen}25) - 20S.P}{50 \log(\text{Pen}25) - S.P - 120} \quad (2.1)$$

Where; Pen(25) is the penetration test result at 25°C in one tenths of a millimetre and S. P is the ring and ball softening point test result in °C.

The PI value for base asphalt cement ranges from -3 to +7, where lower values indicate a more temperature susceptible AC and higher values represent lower temperature susceptibility (Al-Mansob et al., 2017).

2.1.2.3 Rotational Viscosity

Viscosity denoted as (η) of a material is defined as its ability to resist flow and it is used as a measure of consistency for asphalt cement in pavement engineering. Rotational viscosity (RV) test is used to measure the viscosity of AC in a range of temperatures at which the asphalt is anticipated to undergo for manufacturing and construction processes. The test is commonly conducted at 135°C and 165°C since these temperatures are typically the mixing and compaction temperatures for neat asphalt (Al-Khateeb & Al-Akhras, 2011). However, the test may be conducted at various temperatures commonly with 10°C and 15°C increments

from 100°C to 200°C for modified AC for observing the variations in viscosity and to be able to plot a smooth viscosity temperature curve that is used in the determination of hot mix asphalt design temperatures (You et al., 2011). The aim of the test is to ensure that, AC has sufficient pumpability, mixability and workability. Pumpability is the ability to pump asphalt between storage facilities or to pump it into an asphalt manufacturing plant for hot mixes. Mixability is the ability of asphalt to be properly mixed in the processing plant with the aggregates or other asphalt elements of the hot mix. Workability is the ability to place and compact hot mix asphalt with reasonable effort in field application. (Jadidirendi, 2017).

Previously, various testing methods such as ford cup, falling ball experiment and capillary viscometers have been adopted in the literature each one having its appropriate uses but also significant weaknesses. Description of these techniques and their weaknesses are as given in Table 2.2 along with more recent and advanced viscosity measurement technique with a rotational viscometer (Viswanath et al., 2007). Currently, AASHTO T-316 and ASTM D-4402 specifications are used to measure rotational viscosity with a Brookfield viscometer.

Table 2.2: Viscosity measurement testing methods

Test Method	Test description	Weaknesses of the test procedures
Ford cup	Measure the time it takes for a given sample volume to pass through a nozzle.	No temperature control, does not work for non-Newtonian fluids.
Falling ball	Tests the time in a tube of 10° inclination that the ball has to fall over a gap of 100 mm.	Application restricted to Newtonian thin, transparent fluids.
Capillary viscometer	Measure the time for a sample to flow under a controlled head or vacuum through a narrow tube.	It takes a long time to run and modified asphalt binders may get stuck in the tube.
Rotational viscometer	Measures torque needed to sustain a cylindrical spindle's constant rotational speed when submerged in an asphalt binder at a constant temperature.	Inaccuracy of measurement is at least $\pm 10\%$.

It is desirable that asphalt cement has low viscosity in order to minimise the energy consumption that is needed in the manufacturing and construction processes (Hamid et al.,

2019). However, it is noteworthy to mention that, AC with low viscosity, merely lubricates the aggregate particles instead of providing a thin film for binding action and similarly AC with high viscosity does not allow complete compaction and the resulting mix presents heterogeneous character and hence, low stability. The degree of fluidity at the application temperature greatly influences the ability of asphalt to spread, penetrate into voids and also coat the aggregate and hence effect the strength and characteristics of resulting paving mixes (Nikhil, 2013). On this basis, allowable viscosity values are standardised by agencies and it is also dependent on the penetration and softening point of asphalt cement. In addition to that, rotational viscosity test results are also used in the determination of temperature susceptibility of asphalt cement by using an index called the Penetration-viscosity number (PVN). Similar to PI index, increase in PVN is an indication of improved temperature susceptibility for asphalt cement. PVN is calculated by using eq. 2.2 - 2.4 based on the penetration and rotational viscosity test results at reference temperatures of 25°C and 135°C, respectively (Al-Mansob et al., 2017).

$$PVN = \frac{\text{LogL} - \text{LogX}}{\text{LogL} - \text{LogM}} \times 1.5 \quad (2.2)$$

Where L is the rotational viscosity value at 135°C for a PVN of 0.00,

$$\text{LogL} = 4.25800 - 0.79670\text{LogPen} \quad (2.3)$$

M is the rotational viscosity value at 135°C for a PVN of -1.50,

$$M = 3.46289 - 0.61094\text{LogPen} \quad (2.4)$$

X is the rotational viscosity value at 25°C and LogPen is the logarithmic penetration value for bitumen at 25°C.

2.1.2.4 Ductility

Ductility of a material is the property by virtue of which it can be pulled without breaking apart. The asphalt cement used in road construction should be ductile such that, it can take up the deflections that occur in them (Al-Omari et al., 2018). The ductility test can be performed by following the AASHTO T-51 and ASTM D113. ASTM standards specify that, for neat asphalt the minimum ductility requirement is 100cm. Similar to other conventional tests, due to the empirical nature of testing procedures and ductility being measured only at one standard temperature at 25°C, the test has limitations (Kim, 2008). In addition to that, with the development of the multiple stress creep recovery (MSCR) test which is explained in Chapter 2.1.3.2, the researchers have been gravitated towards utilizing the more advanced MSCR test since it provides more fundamental knowledge regarding to materials elastic recovery, tenacity and ductile properties all at once (Anderson, 2014). However, due to rules and regulations by many authorisation agencies, the test results are still required for performance assessment since the MSCR test requires advanced testing equipment that is not available widely. Also the test is conducted for research purposes with the pursuit to acknowledge ductile properties of asphalt cement which particularly has significant role on asphalt cements' low and intermediate temperature performance characteristics (Al-Omari et al., 2018).

2.1.3 Rheological characterisation

Asphalt exhibits viscoelastic behaviour meaning that, its rheological properties are dependent on its viscous and elastic components. Therefore, it is more reliable to characterise the viscous and elastic components of asphalt cement rather than evaluating its chemical structure and physical properties to understanding its rheological characteristics which influence the overall performance characteristics of flexible pavement roads (Crucho et al., 2019). A dynamic shear rheometer (DSR) is used in the characterisation of asphalt cement. DSR apparatus is capable of performing two major tests that are, the frequency sweep test or the temperature sweep test and the MSCR test. Both tests are able to measure the rutting resistance parameter of asphalt cement at intermediate and high temperatures by measuring different parameters under fresh and RTFO states, while frequency sweep test can also be

used to measure the asphalt cement low temperature properties and fatigue cracking resistance parameter in long-term aged state (Gama et al., 2016). The principle of the frequency sweep tests is to measure the viscous and elastic properties of asphalt cement, while MSCR test is used to determine the recoverable and non-recoverable compliance of the asphalt cement (Gama et al., 2016). Detailed information regarding to the frequency sweep test and MSCR test are given in chapters 2.1.3.1 and 2.1.3.2 respectively.

2.1.3.1 Frequency sweep tests

Frequency sweep tests have long been utilized in the rheological characterisation of asphalt cement. It is a rule rather than a fact that, asphalt roads experience extreme weather conditions and dynamic vehicular loading during its service life. Escalation of these conditions have strong impact on the performance and durability of asphalt pavement that needs to be addressed (Ali et al., 2015). Although, asphalt is a suitable material for paving flexible pavement roads, it has limitations due to its viscoelastic nature. Under the conditions of high temperatures and low frequencies, asphalt tends to soften and it becomes brittle when exposed to low temperatures and high frequencies. However, the required engineering properties of asphalt in order to resist failure in terms of rutting and fatigue are the opposite (Al-Mansob et al., 2016). One way to evaluate the viscoelastic properties of asphalt cement is the frequency sweep test that is performed by using a DSR. DSR is able to measure viscous and elastic behaviour of asphalt cement over a range of temperatures and frequencies. DSR oscillation tests can be performed by the temperature sweep or the frequency sweep methods which fundamentally yields the same parameters. These parameters are called the complex shear modulus (G^*) and the phase angle (δ). G^* is the materials stiffness and it is related to the materials resistance to permanent deformation (rutting) when repeated shear loading is applied. δ is the gap between the applied shear stress and the corresponding shear strain. The viscoelastic range of δ for asphalt cement lies between 0° and 90° where, higher δ indicates more viscous material and lower δ represents more elasticity. The definition of phase angle and its relation with the complex shear modulus are given in Figures 2.2 and 2.3 respectively (Abedali, 2015).

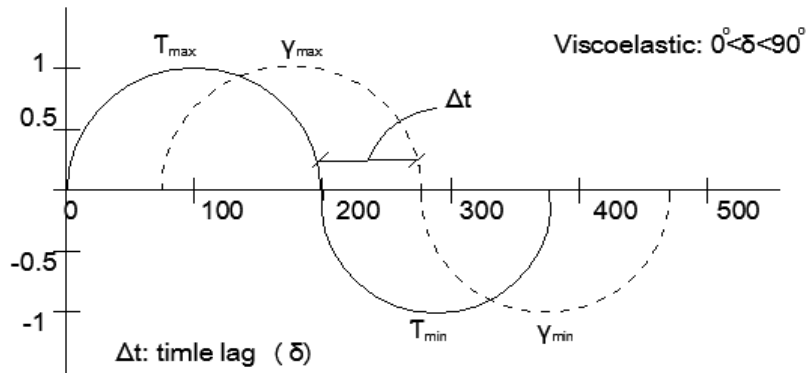


Figure 2.2: Time lag between shear stress and shear strain

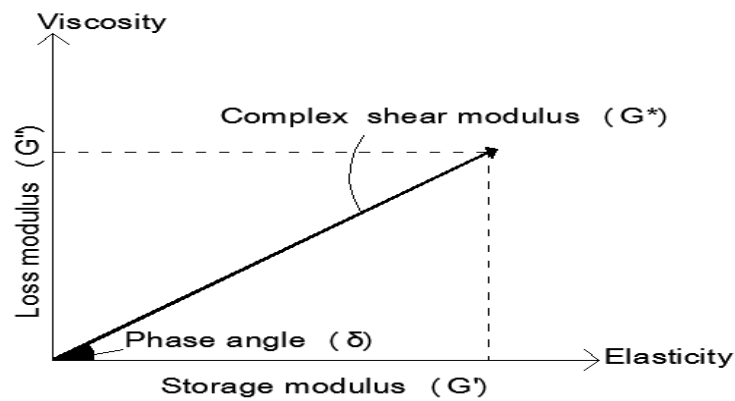


Figure 2.3: Viscous and elastic components of AC

According to Superpave specifications, G^* and δ are the two parameters that can be used in the modelling of asphalt concretes rutting and fatigue cracking behaviour. In order to prevent rutting, asphalt should demonstrate stiff behaviour meaning that, it should not deform excessively and at the same time, it should be sufficiently elastic to recover after the load is removed (Al-Khateeb & Ramadan, 2015). The formula G^*/δ is used to explain the rutting resistance of asphalt at high temperatures. Rutting failure is of concern during the early and mid-life of the asphalt concrete pavement. According to Superpave standards, at a loading rate of 1.592 Hz, a minimum of 1 kPa for fresh and 2.2 kPa for short-term aged asphalt cement is the allowable limits in order to prevent rutting failure. Rutting is a cyclic conjuncture where the work is been dissipated with each traffic cycle. After each cycle, asphalt is partially returned to its original shape and some of the work is dissipated in the

form of permanent deformation of asphalt pavement. Under constant stress conditions, the work dissipated can be calculated by using eq. 2.5 (Al-Khateeb & Ramadan, 2015). Eq. 2.5 clearly defines that, in order to prevent rutting failure of asphalt pavement, either the work dissipation should be minimized or the rutting resistance parameter should be maximised. Since, the former is inevitable, the aim is to maximizing the latter.

$$W_c = \pi\sigma_0^2 \left[\frac{1}{G^* \sin\delta} \right] \quad (2.5)$$

Where; W_c is the dissipated work, σ is the applied stress, G^* is the complex shear modulus and δ is the phase angle.

Another mode of failure for asphalt concrete pavement is the fatigue cracking. Asphalt cement should be less stiff and more elastic to be able to recover by rebounding rather than converting the energy dissipated into a form of cracking. Fatigue cracking is a major concern during the late life of asphalt pavement particularly due to stiffening of the material after long term oxidative aging. The viscous portion of G^* (see Figure 2.3) should therefore be minimised in order to prevent fatigue cracking (Ali et al., 2015). The mechanical test conditions that the frequency sweep tests are conducted are different for fatigue resistance investigation than that of conditions set for rutting evaluation since the primary concern for fatigue cracking is the low temperature and long-term aged conditions. The fatigue cracking resistance is described by $G^* \times \sin\delta$. Similar to rutting, fatigue cracking is a stress or strain controlled condition. With repeated loading of traffic cycles, a load is being exerted on the pavement surface and some of these forces are recovered by rebounding and the rest results in irreversible cracking deformation. It can be observed in eq. 2.6 which is used for calculating the work dissipated that, the fatigue cracking resistance parameter should be minimised in order to reduce the work dissipated for reducing the propagation of cracking (Al-Khateeb & Ramadan, 2015). Therefore Superpave standards have specified a maximum value of 5000 kPa for the fatigue cracking resistance parameter.

$$W_c = \pi\sigma_0^2 [(G^*)(\sin\delta)] \quad (2.6)$$

Where; W_c is the dissipated work, σ is the applied stress, G^* is the complex shear modulus and δ is the phase angle.

Testing procedures that are followed for the frequency sweep test is the AASHTO: T-315. The schematic of the working principle of a DSR is as shown in Figure 2.4. The frequency sweep test can be performed under stress or strain controlled conditions. Strain controlled testing allows the test to be conducted within the linear viscoelastic region. Beyond this point the asphalt is permanently deformed and the test results are considered to be unreliable. In order to ensure, that the test is conducted within the linear viscoelastic region, prior to starting the testing procedures, strain sweeps are performed on neat asphalt for determining the maximum strain that is required to deform it irreversibly. Linear viscoelastic region is denoted as the point at which the G^* of the material is decreased by 95% of zero strain condition which is as expressed in Figure 2.5 (Al-Mansob et al., 2016).

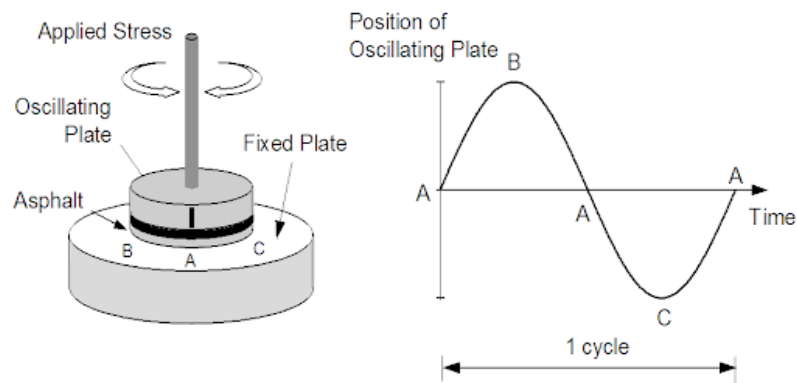


Figure 2.4: DSR testing configuration

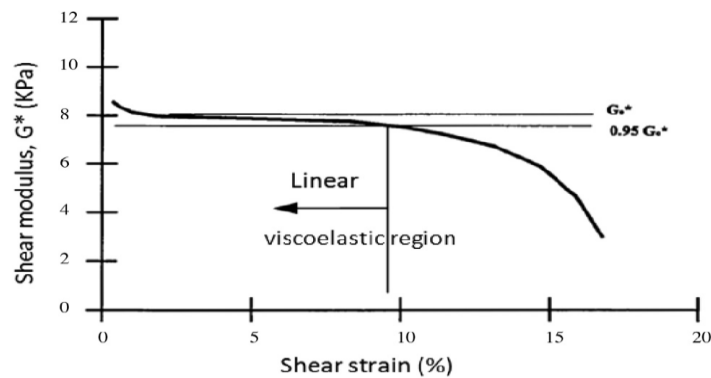


Figure 2.5: Viscoelastic region

G^* and the δ are the two outcomes from the frequency sweep test. To evaluating the above mentioned parameters under fresh and aged states (short-term and long-term ageing conditions) and at different test temperatures, specific plate geometries of DSR are used. Above 46°C at which the samples are tested under fresh and short-term aged conditions, sample size of 25mm diameter and 1mm thickness and for test conditions under long-term aging and test temperatures between 4°C - 46°C, an 8mm sample diameter and 2mm thickness is used. The use of latter mentioned plate geometry is due to excessive stiffening of asphalt material at low temperatures that is resulting in very low phase angle values that cannot be determined by the DSR software (Ali et al., 2015). Typical values for neat asphalt cement in terms of G^* is between 500 Pa - 6000 Pa and for the δ , the range is usually between 50°C - 90°C where, 90°C indicates a completely viscous material and 0°C represents completely elastic material. Generally, modified binders demonstrate higher stiffness and lower elastic properties (Joshi et al., 2013).

The representation and analysis of the outcomes of the oscillatory DSR tests are performed by constructing, isochronal plots, isothermal plots, black diagrams and master curves. Furthermore, rutting resistance and fatigue cracking resistance parameter plots are used in the evaluation of performance characteristics of asphalt cement (Mantilla-Forero & Castañeda-Pinzón, 2019). Isochronal plots are used to plot the variations in G^* or δ over a range of temperatures at constant frequency whereas, isothermal plots are used to plot these parameters over a range of frequencies at a constant temperature (Airey, 2002). Black diagram is essentially the plot of G^* and δ on the same graph that enables the representation of variations in both parameters over a range of temperatures and frequencies at the same time (Gallego et al., 2016). The most fundamental and useful representation that is adopted without exception in high class investigations is the master curves. Master curves enable the G^* and/or δ values to be displayed in one graph under various temperature and frequency conditions (Mantilla-Forero & Castañeda-Pinzón, 2019). In order to construct a single curve known as the master curve, time-temperature superposition theorem is used. Time-temperature superposition theorem is applied by specifying a reference temperature and moving rheological data at other temperatures relative to the axis of frequency by using an appropriate function which is as illustrated in Figure 2.6 (Airey et al., 2016). Although there are numerous functions are available in the literature that essentially performs the same task

for obtaining the best fitting master curve, the shifting is commonly performed by the log-linear approach due to its practical use (Ali et al., 2015).

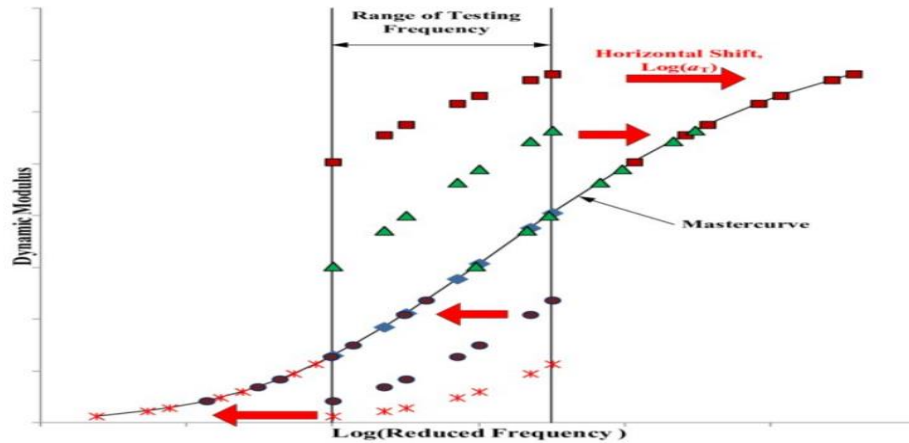


Figure 2.6: Time-temperature superposition

2.1.3.2 Multiple stress creep recovery tests (MSCR)

MSCR test, also mentioned as the repeated creep and creep recovery test in the literature has been utilized in the investigation of the amount of rutting that occurs in the asphalt cement. MSCR test can be conducted on fresh and short-term aged samples where, the rutting resistance parameter is of major concern during the early life of asphalt concrete pavement. The test is not suitable to be performed on long-term aged conditions since, it is particularly designed to measure the rutting potential of asphalt cement (Canestrari & Partl, 2015). Additionally, MSCR test also provides information about other asphalt properties such as the elastic recovery, toughness and tenacity and it can be used as a single test which can be used to replace testing procedures for these parameters that are particularly designed for modified asphalt cement (Anderson, 2014). The MSCR test is commonly performed by the standard protocols specified in ASTM: D7405- 15 and/or AASHTO: TP-70. The testing temperature is determined by the performance grade (see Chapter 2.3.1.3) of asphalt cement and the test stress levels are 100 Pa and 3200 Pa to represent high speed and low speed traffic scenarios. The test configuration is as illustrated in Figure 2.7.

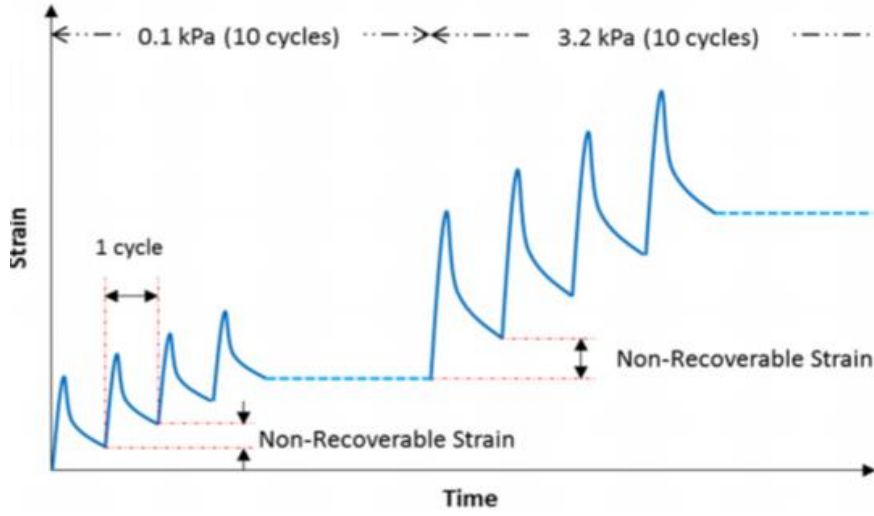


Figure 2.7: Schematic representation of MSCR test results.

The primary purpose of the MSCR test is to determine the non-recoverable compliance (J_{nr}), elastic recovery (%R) and the asphalt sensitivity to variations of stress levels ($J_{nr, diff}$). J_{nr} is the ratio of non-recoverable creep compliance to the applied testing stress. %R is calculated as the ratio of recoverable shear strain to instantaneous shear strain. $J_{nr, diff}$ is the percentage difference between the J_{nr} at two different loading states (100 Pa and 3200 Pa). Calculations of these parameters are performed according to eq. 2.7 - 2.9 which are represented in Figure 2.8 (Bastos et al., 2017). J_{nr} evaluated at 3200 Pa is used as a parameter to classify the asphalt cement based on a specific traffic volume that is as expressed in table 2.3 (Bukowski, 2011). Currently, available specifications have not released a standard criteria for percentage recovery values for asphalt cement. However, it is suggested in AASHTO TP-70 that, recommended %R values corresponding to specific J_{nr} values are as represented in Table 2.4 (Arshad et al., 2017). Also, in order to minimize the concerns that is related to sensitivity of asphalt to changes in stress levels, $J_{nr, diff}$ ratio is recommended to be lower than 75% according to AASHTO: MP-19 (Bastos et al., 2017).

$$\%R = \frac{\epsilon_r}{\epsilon_t} \times 100\% \quad (2.7)$$

$$J_{nr} = \frac{\epsilon_{nr}}{\sigma} \quad (2.8)$$

$$J_{nr,diff} = \frac{j_{nr,3200} - J_{nr,100}}{J_{nr,100}} \times 100\% \quad (2.9)$$

Where; %R is the percentage recovery, J_{nr} is the non-recoverable creep compliance, $J_{nr,diff}$ is the difference between the non-recoverable compliance at 3200 Pa and 100 Pa, ϵ_r is the recovered strain, ϵ_t is the total strain and ϵ_{nr} is the non-recovered shear strain.

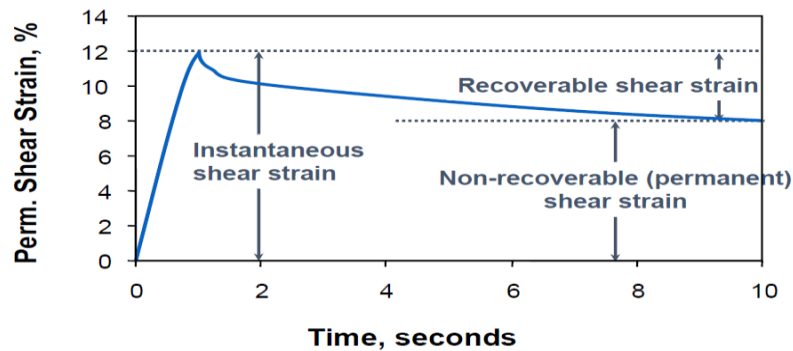


Figure 2.8: Asphalt cement response to creep loading-unloading cycle

Table 2.3: J_{nr} classification for specific volume of traffic

Limits $J_{nr,3200}$	MSCR class	Equivalent single axle loading (ESAL)
≤ 4.5 kPa-1	S-Standard	<10 million and more than traffic speed (>70 km/h)
≤ 2.0 kPa-1	H-Heavy	>10-30 million or slow moving traffic (20-70 km/h)
≤ 1.0 kPa-1	V-Very heavy	>30 million or standing traffic (<20 km/h)
≤ 0.5 kPa-1	E-Extreme	>30 million and standing traffic (<20 km/h)

Table 2.4: Minimum requirement for delayed elastic response

J_{nr} , 3200 Pa	Minimum %R
2.0-1.01	30%
1-0.51	35%
0.50-0.251	45%
0.25-0.125	50%

The relationship of the J_{nr} parameter that has been evaluated using the MSCR test to the rutting evaluation of asphalt concrete performed by accelerated loading facilities (ALF) and the actual rutting phenomena that is anticipated in the field have previously been investigated

extensively in the literature. Notable investigations include the works of the Federal Highway Administration (FHWA). Full scale analysis of rutting has been performed on numerous neat and modified asphalt cement samples. The outcomes of their analysis showed that, J_{nr} and %R in MSCR test has higher correlation with actual rutting performance of asphalt cement compared to the rutting parameter ($G^*/\sin \delta$) that is obtained by the oscillatory frequency sweep tests. This finding has also been validated by the Asphalt Institute (Bukowski, 2011). A major upside of the MSCR test from the frequency sweep test is considered to be the low stress levels that are used in frequency sweep tests. In MSCR test, the form of distresses that actually occur during the life time of the asphalt pavement is more realistically simulated due to high levels of stress and strains where the polymer/nano modified phase is activated and also the delayed elastic response is captured. On the other hand, frequency sweep tests have to be conducted at low stress and strain levels within the linear viscoelastic region. According to some researchers, this prevents the activation of modifier phase and also underestimates the performance of asphalt cement (Mahali & Sahoo, 2019). It is noteworthy to mention that, currently, the frequency sweep testing method to determine the rutting resistance parameter is still the most widely accepted method by many highway agencies, although some researchers reported that MSCR test method outperforms the frequency sweep tests. Furthermore, the requirement for the frequency sweep test is also due to measuring the crack resistance and durability of asphalt cement since MSCR test is not able to evaluate these parameters (Bastos et al., 2017).

2.1.4 Chemical characterisation

From chemical characteristics perspective, asphalt that is used in pavement construction is a complex material and behaves differently depending on its origin and the manufacturing process in terms of its performance characteristics under various stress and climate conditions. The complexity of asphalt cement is further escalated in the cases which neat asphalt is modified with additives which is a common practice to explore better performing and longer lasting asphalt cement (Fernández-Gómez et al., 2013). Therefore, it is of paramount importance to chemically characterize asphalt cement in order to understand the nature of its behaviour. Numerous techniques are available today for chemical characterisation of asphalt cement. The most widely accepted methods include; Atomic

Force Microscopy (AFM), Field Emission Scanning Electron Microscopy (FE-SEM), X-Ray diffraction (XRD) and Fourier Transform Infrared Spectroscopy (FT-IR) (Sembiring et al., 2019). Chemical reactivity of base asphalt and the modifier materials, the dispersibility of the particles within the asphalt matrix and the formation of new functional and structural groups, particularly in the cases of hybrid systems which the polymers and/or nanomaterials are used as modifiers to base asphalt are among the most essential parameters that are investigated in the chemical characterisation of asphalt cement (Yao et al., 2013). XRD and the FTIR as discussed in Chapters 2.1.4.1 and 2.1.4.2 are the most popular techniques in the literature that are used to investigate the above mentioned characteristics of base and modified AC (Abhilash et al., 2016; Dony et al., 2016).

2.1.4.1 X-Ray Diffraction

XRD is a non-destructive procedure which is utilized in characterising and optimizing the interactions that take place between the base asphalt and modifiers such as polymers, nanomaterials and polymer/nanocomposites that are used to modify neat asphalt cement. XRD has been conventionally used to gather information about the chemical structure of asphalt cement as well as investigating the crystallite size, lattice strain and the interlayer spacing between the particles (Abhilash et al., 2016). A major advantage of conducting XRD is to gain knowledge about the materials chemical structure. Asphalt cement can be in three different chemical structures which are; Amorphous, semi crystalline and highly crystalline. In amorphous structure, the XRD plot follows a straight plateau with a smooth curve that is also called the mountain valley. The presence of small peaks in the XRD plot, indicates that, the material has a semi crystalline structure whereas, for materials having highly crystalline structure, a number of strong and high peaks are observed (Zhu et al., 2014). Figure 2.9 illustrates the chemical structures for the materials that are used in the current study except for nonaluminum which is deducted from an investigation conducted by (Murali et al., 2017) since, none of the materials of concern in the current study possessed highly crystalline structure. Crystallinity of composite materials is related to their reactivity. Amorphous structure indicates low reactivity whereas, materials having crystallite structures are considered as reactive in the modified composition of asphalt cement (Ali et al., 2015).

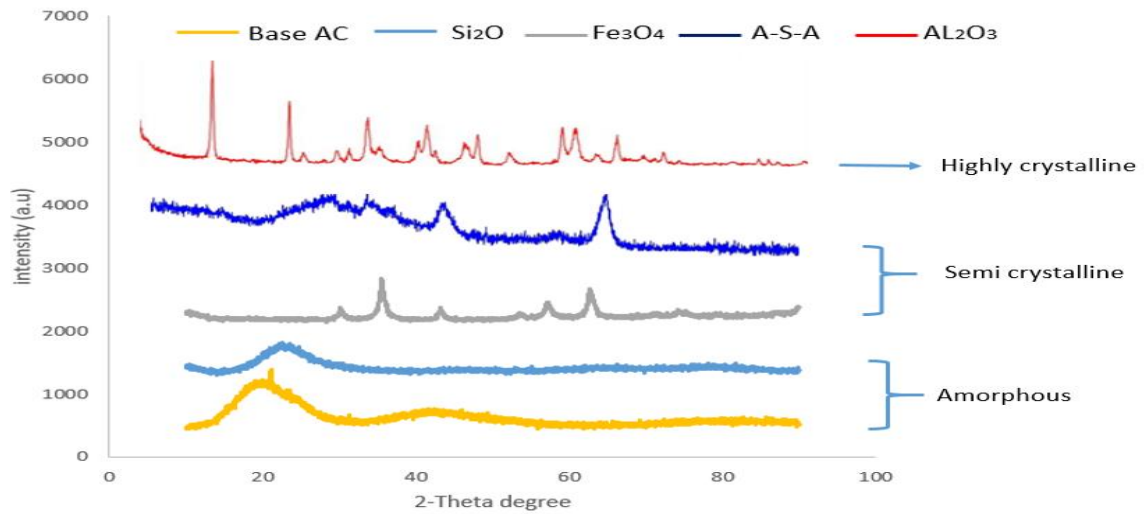


Figure 2.9: XRD characteristics peaks

XRD works by shooting X-rays of fixed length in λ and measuring the diffraction pattern of materials in the 2-theta angle range. This way, the working principle for XRD is by analysing the arrangement of particles in the asphalt cement. Experimentally, the investigations may be conducted by the Laue method or the powder diffraction method where, in the former, the θ is kept constant and λ is varied and in the latter is versa (Abhilash et al., 2016). The measured intensity of the diffracted x-ray beams is used to compute the interlayer spacing (d-spacing) between the particles using the Bragg's law as given in eq. 3.1 (Golestani et al., 2012). Nanomaterials in particular have a layered structure. D-spacing is the distance between these layers. Increase in d-spacing indicates insertion of polymers in-between the layered structure. As can be seen in Figure 2.12, polymer nanocomposite modified asphalt cement may have three different structure which are; phase separated, intercalated and exfoliated structures (Samiey et al., 2014). Phase separation is an undesired phenomenon that is due to the incompatibility between the polymer and base asphalt which results in instability of the modified asphalt cement. A higher d-spacing value indicates penetration of polymer particles inside the layered structure of nanomaterials and therefore it is a desirable characteristic in order to prevent phase separation (Golestani et al., 2012). Numerous nanomaterials and coupling agents as detailed in Chapter 2.2 have been researched and commonly used to prevent the occurrence of phase separation. Although there is a gap in the literature regarding to the correlation between phase separation and agglomeration, many

researchers reported that, in phase separated structure modified asphalt cement, the tendency for agglomeration is more likely to occur (Zhu et al., 2014). It is also noteworthy to mention that, the chemical structure of asphalt cement has significant role in determining the aging rate due to volatilization and oxidative reactions, since exfoliated structure would trap the light weight components of asphalt as well as inhibiting the entering of oxygen molecules (Fang et al., 2013).

2.1.4.2 Fourier Transform Infrared Spectroscopy (FTIR)

FTIR is a powerful method to determine the changes in chemical bonding that occur in asphalt cement during the modification process and/or under different experimental test conditions. FTIR can be conducted in two different modes which are the transmission mode or the attenuated total reflectance mode (ATR). In both methods, the significant parameters that are observed in FTIR spectra are the absorption and the wavelength numbers (Yusoff et al., 2019). FTIR makes use of the infrared radiation absorbance of specific molecules as well as vibrational molecular structure of functional groups. FTIR spectra range is between 600 cm^{-1} and 4000 cm^{-1} however, most of the changes that occur in asphalt cement appear below 2000 cm^{-1} which is also called as the fingerprint region. The intensity of the absorbed wavelength and the position are significant in determining the structural characteristics of asphalt cement as well as, identifying the formation of new functional groups (Zhang et al., 2019). Typical characteristic of infrared radiation band positions for significant groups are given in Table 2.5 and Figure 2.10 (Zhang et al., 2019).

Table 2.5: Characteristics IR bands

Characteristic band (cm^{-1})	Functional group	Peak description
1034	S=O	Sulphur and oxygen double bonding
1376	C-H of CH_3	Symmetric carbon and hydrogen bending vibrations
1460	C-H of $(\text{CH}_2)_n$	Asymmetric carbon and hydrogen bending vibrations
1600	C=C	Carbon double bonds stretching vibrations in aromatics
1700	C=O	Carbon and oxygen double bonding
2850-2920	CH_2 , CH_3	Carbon and hydrogen stretching vibrations in aliphatic chains
>3500	O-H	Presence of hydroxyl groups

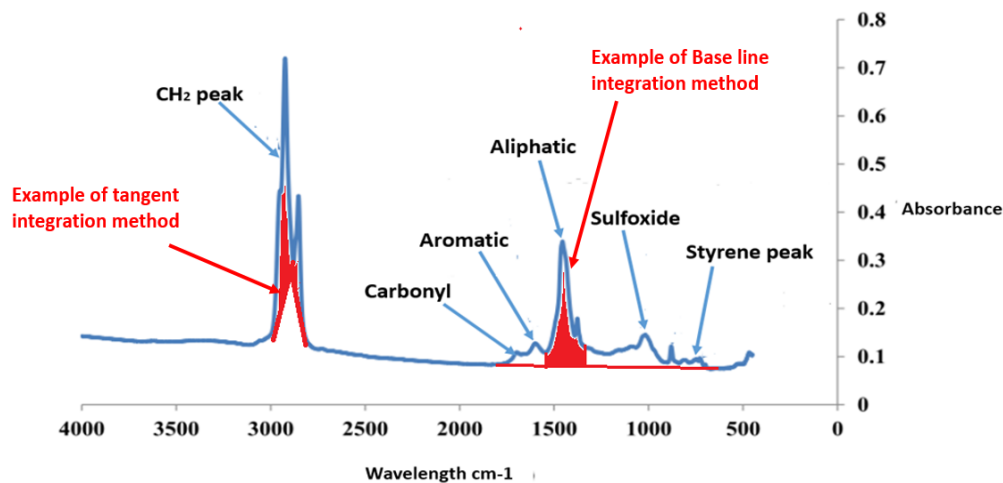


Figure 2.10: Typical groups present in FTIR spectra

FTIR is also capable of identifying the structural and functional changes that occur in asphalt cement due to aging. Volatilization and oxygenation are the irreversible aspects that change the chemical composition and hence, the performance characteristics and durability of asphalt cement (H. Wang et al., 2020). As mentioned in chapter 2.1.1, the composition of asphalt cement consists of S.A.R.A fractions. The aging of asphalt results in chemical and structural changes in these components resulting in altered behaviour of asphalt cement. Therefore it is important to monitor these changes by using a FTIR before and after the application of aging procedures to better understanding the behavioural changes related to performance and durability of asphalt cement (Khordehbinan & Kaymanesh, 2020). Formation of carbonyl and sulfoxide functional groups are related to aging index of asphalt cement. Sulfoxides appear at wavelengths around 1034 cm^{-1} whereas, carbonyl functional groups appear at around 1700 cm^{-1} in the FTIR spectra. Sulfoxides are more reactive than the carbonyl functional groups therefore, according to some researchers sulfoxides should be considered as the primary source of information in the quantitative aging analysis of asphalt cement. It is desirable that, minimum increase in both indexes are formed in order to achieve maximum aging resistance (Abed & Oudah, 2018). The peaks at 1376 cm^{-1} and 1456 cm^{-1} represents the aliphatic chains and the peaks at 1600 cm^{-1} is due to the presence aromatics. Aliphatic structures are the light weight components of asphalt. Therefore some of these fractions are volatilized and some are structurally converted to aromatic rings during the aging process. Also some of the aliphatic structures are absorbed by the additive

materials in the case of modified asphalt cement. However, the reduction in aliphatic compounds is not significantly obvious since they have low reactivity (H. Wang et al., 2020). The aromatic index of asphalt firstly, increases which corresponds to the reduction in the aliphatic compounds to form aromatic rings. However, in the modified asphalt cement case, aromatic compounds are also absorbed by the additive materials and also in the long term, the reduction trend is continued due to continued interaction between the modifier and the asphalt (Zhang et al., 2019). There are two methods available to compute the parameter indexes which are; the base line integration method and tangent integration method as illustrated Figure 2.10. The formula for computing these indices are given in eq. 2.10 (Hofko et al., 2017).

$$\text{Group index} = \frac{\text{Area under the associated infrared band width}}{\Sigma \text{Total area under the FTIR spectra}} \quad (2.10)$$

2.1.5 Durability of asphalt cement

Durability of asphalt cement is characterized as the ability of asphalt to resist the detrimental effects on the pavement. caused by adverse environmental factors over a period of time (Petersen, 2009). Among various factors, moisture susceptibility of asphalt and the effects of aging with time are the most widely accepted causes of asphalt pavement deterioration for a properly designed and constructed asphalt concrete as by following the standard specifications and regulations (Scholz, 1995). The age hardening of asphalt cement is discussed in this chapter and the reader's referred to Chapter 2.4.4 for the moisture susceptibility of HMA.

Aging of asphalt cement is an irreversible process which reduces its durability, causing early deterioration of asphalt pavement and hence, increasing the maintenance cost to restore and to maintain its service life (F. Wang et al., 2020). Recent advancements in self-healing modifiers, enables to partially recover the damage that occurs in asphalt cement to a certain degree by using micro capsules, rejuvenators and nanomaterials as additives (Tabaković & Schlangen, 2015). However, in the case of polymer modified asphalt cement, the polymer degradation due to aging is irreversible and the destruction of polymer network, permanently

deteriorates its engineering properties (Tauste et al., 2018). The incompatibility between the polymer and the asphalt matrix is also a determinant factor that influences the stability and aging resistance for a PMB (Bhargava et al., 2016).

Hardening of asphalt with time is referred to as 'age hardening'. The main mechanisms that cause age hardening in asphalt are the presence of oxygen, ultraviolet radiation and changes in weather conditions (Fernández-Gómez et al., 2013). Age hardening of asphalt to a certain extent is considered to be beneficial since, it increases the load spreading capacity as well as improving the permanent deformation resistance characteristics which is referred to as 'curing' (Wu, 2009). On the other hand, extreme age hardening leads to excessive brittleness of asphalt which in particular negatively influences its low temperature performance characteristics such as fatigue and thermal cracking properties. Formed cracks in the pavement surface rapidly propagates and discontinuities in the surface layer results in more vulnerable pavement structure against resisting the infiltration of oxygen and water to a further extent (Sirin et al., 2018). Since, asphalt becomes more exposed to environmental impact, it also loses its adhesion properties with mineral aggregates. As a result, damage mechanisms such as stripping, ravelling and potholes becomes inevitable (Hamedi & Tahami, 2018).

Asphalt cement aging is associated with two conditions that are; short-term and long-term aging. Short-term aging occurs during the production and construction stages. The primary factors that cause aging in the short-term are; asphalt exposure to oxygen (thermal oxygenation) and high temperatures that are required in storing and manufacturing of asphalt cement in the production plant. These conditions also prevail during the transportation and laying applications in the field (Cháves-Pabón et al., 2019). Another factor that causes aging in the short-term is the volatilization. Light constituents of asphalt material evaporates due to high temperatures during the manufacturing process. Because of the loss of these fractions, asphalt flow properties are reduced thus, the viscosity of asphalt is increased which indicates the hardening of asphalt cement. Previous researches showed that, the difference in viscosity of asphalt cement for up to 400% can be observed between the fresh and short-term aged asphalt samples (Fernández-Gómez et al., 2013).

In the long term aging, photo-oxygenation is the main cause for aging of asphalt cement. Atmospheric oxygen and ultraviolet (UV) rays from the sunlight reacts with the asphalt

pavement surface during its service lifetime (Cháves-Pabón et al., 2019). Given that, asphalt pavement cracks due to vehicular loading and aging with time, air percolates from these cracks into the asphalt layers and engages in oxygenation reactions. These reactions change the composition of S.A.R.A fractions of asphalt cement as well as forming new functional groups such as carbonyls (breaking of double carbon bonds and forming carbon-oxygen double bonds) and sulfoxides (sulphur double bonding with oxygen) (H. Wang et al., 2020). Also, an extensive research conducted by (Corbett & Merz, 1975) found that, three of the S.A.R.A fractions of asphalt exhibited significant variations in composition except for the saturates. The most noticeable change was the increase in asphaltene levels which results a reduction in penetration and an increase in viscosity for AC. In addition to that, due to the changes in chemical structure of asphalt particularly, the increase in carbonyl and sulfoxide indexes, asphalt pavement hardens and becomes more brittle which eventually results in excessive pavement cracking (H. Wang et al., 2020).

Other factors that essentially constitutes in the age hardening of asphalt cement are; polymerization, separation and steric hardening/thixotropy. Polymerization is defined as the clustering of asphalt molecules to forming larger molecules. Separation is the disassembling of the oily constituents, resins or asphaltenes from the asphalt binder through selective absorption of porous aggregates. Steric hardening is a progressive process which the molecules are reorganised and certain chemical components of asphalt crystalizes. Increase in asphalt viscosity and contraction in volume of asphalt mixture are the effects of steric hardening. As distinct from other aging mechanisms, steric hardening is a reversible process up to a certain degree by reheating the asphalt (Cháves-Pabón et al., 2019).

Laboratory simulations of aging conditions are crucial to understanding the as-laid properties of AC since there could be significant differences in the properties of aged and unaged asphalt cement. A rolling thin film oven (RTFO) is used to simulating the short-term aging whereas, pressure aging vessel (PAV) is used for the simulation of the long-term aging of asphalt cement. It should be noted that, until now, there have been no test invented yet to directly measure the aging of asphalt cement. However, the aging effects can be evaluated by conducting the physical, morphological and rheological tests in unaged, short-term aged and long-term aged conditions in order to observe the changes in properties of asphalt cement (F. Wang et al., 2020).

RTFO method involves placing a certain amount of asphalt into a glass tube and placing it into a rotating carousel. This creates a thin film of asphalt around the internal face of the tube. Hot air at 163°C is then blown onto the surface of asphalt as the carousel rotates for a period of time depending on the standards followed. Aging is then measured by the amount of change occurring in the abovementioned characteristics of asphalt cement. RTFO test was developed and replaced the thin film oven (TFO) test which lacked the efficiency of simulating the actual condition that occurs in the field. Currently, modified rolling thin film oven (M-RTFO) test has been developed and research conducted by numerous researchers reported that, M-RTFO outperforms the traditional RTFO test. However, their findings have not been validated and widely accepted yet and RTFO test is still the traditional method used and accepted by many agencies (Southern, 2015).

In order to simulate the long-term aging that may occur in the field, PAV method was developed. Having completed the RTFO process, the residual bitumen is placed on specified thin layers on trays and placed inside a PAV oven which applies elevated pressure and elevated temperature on the asphalt samples. The pressure is elevated to 2.1 MPa and the temperature depends on the testing protocol that is followed. The testing procedure is difficult to be correlated with the in-situ conditions since, it cannot effectively account for significant variables such as the ambient temperature, the amount of UV exposure and the structure of the asphalt pavement surface layers. Therefore, the PAV protocol is a method solely to benchmark on asphalt against another in standard conditions (Tauste et al., 2018).

2.2 Asphalt Cement Modification

The performance of AC used in the hot mix asphalt design depends on the quality of the crude oil it is extracted from. Virgin asphalt obtained from the distillation of crude oil may not always ensure desired performance across the entire service life of the asphalt mix concrete pavement (Redelius & Soenen, 2015). By choosing the correct starting crude, or tailoring the refinery processes used to produce asphalt, some improvements in asphalt properties have been achieved. Unfortunately, only a few crudes can produce very good asphalts, and only a small number of measures can be taken to regulate the process of refining to make better asphalts. Thus, modification of AC inevitably became an essential

research area to enhance the performance characteristics and durability of asphalt pavement roads (Becker et al., 2001). On this basis, polymers, nanomaterials, and polymer/nano-composite materials have previously been utilized to modify AC. The main rationales for asphalt cement modification include (Pyshyev et al., 2016);

- To improve high temperature performance by stiffening the asphalt cement to withstand rutting and permanent deformation.
- To improve low temperature performance by softening the asphalt cement to withstand thermal cracking.
- To improve fatigue resistance under the influence of repeated dynamic vehicular loading.
- To improve aging resistance for better durability.
- To improve workability, stability and strength of the mixtures.

The selection of a suitable modifier depends on the anticipated climatic conditions as well as the volume of traffic that the pavement is expected to carry. In the case of modified asphalt cement often, attaining enhancement in a certain performance characteristic is at the expense of losing another. Therefore, the designer should carefully assess the in-situ pavement conditions and then reach to a decision to select an appropriate modifier (Honarmand et al., 2019).

2.2.1 Polymer modified asphalt cement

A blend of polymer with the asphalt cement (also referred as bitumen) is denoted as polymer modified bitumen (PMB). Polymers are large molecules that are composed into a chain by incorporating several small molecules called monomers. It is possible to combine two different kinds of monomers into a single polymer that is then called a copolymer. This is a commonly used technique to gain the advantages of different types of monomers that would incorporate maximum benefits in the polymer modified asphalt cement (Behnood & Gharehveran, 2019). Polymer modifiers have proven to be effective in enhancing the physical and rheological properties as well as improving the durability of AC, thus reducing

the life cycle costs. Polymer modified bitumen is considered to be cost-effective in extending the service life of the pavements by up to 2-3 years, given that the cost of modification does not surpass the cost of base asphalt by more than 100%. (Ponniah & Kennepohl, 1996). Polymer addition in the asphalt cement increases the complexity of the molecular structure of asphalt. With polymer modification, asphalt cement can be in two distinct phases which are the continuous bitumen phase or the polymer phase. The phase which the asphalt would be continuous in matrix is influenced by the amount of modifier added in the asphalt (Sun & Lu, 2006). Polymer modification at low concentrations, typically below 4% polymer by the total weight of asphalt, the asphalt phase is the continuous phase while the polymer phase is dispersed through it. In this phase, a higher asphaltene proportion is dominant due to lowered oil content and as a result the elasticity and cohesion properties of asphalt are enhanced. Additionally, because of the dispersed polymer phase in the asphalt matrix, the stiffness modulus of the polymer phase is activated at extreme temperatures which reinforces the enhancement of mechanical properties of the asphalt and extends the temperatures at which it would be used (Pyshyev et al., 2016). Polymer modified asphalt cement around 5% by the weight of bitumen is considered as a moderate modifier content. This system possesses a microstructure that consists of both continuous asphalt and polymer phases. These systems are difficult to manage and typically display issues with low stability. (Porto et al., 2019). If the asphalt cement modification concentration is high, typically above 7%, the polymer phase is the major continuous phase in the asphalt matrix. The properties of such a system are controlled by the polymer phase and it acts as a thermoplastic adhesive. This type of modified asphalt is commonly applied as a sealing material for roofing rather than being used for paving applications (Pyshyev et al., 2016).

It should also be noted that, in addition to the amount of modifier used in the blend, different types of polymers cause different chemical reactions with asphalt and, as a result, each modified polymer of asphalt varies in its properties due to different molecular size, copolymer ratio and molecular structure. These parameters influence the mechanical properties of the polymer thus, the properties it brings to the PMB (Porto et al., 2019). Based on their characteristics, polymers are categorized into different groups. Elastomers and plastomers are the most widely utilized modifiers. A popular type of polymer used to modify asphalt is a copolymer of polystyrene and polybutadiene. It is usually called Styrene-

Butadiene (SB) or Styrene-Butadiene-Styrene (SBS). Since it adds viscosity and elasticity to the asphalt, this copolymer family is called an elastomer. SB and SBS constitutes to a percentage of more than 75% of the polymers used in asphalt modification. (Zhu et al., 2014). Another type of polymer type that is used in the asphalt modification is the plastomeric polymers which are commonly formed from copolymers of polyethylenes and polyesters. Since it adds stiffness and plasticity to the asphalt, this family of copolymers is called plastomers. Approximately, 15% of the polymers used in the modification of asphalt cement are acknowledged to be plastomers and the rest of the 10% is the asphalt modified with other polymeric materials such as natural rubber and epoxy resins being the most popular additives (Airey, 2003). The most widely used polymers in the modification of asphalt are as summarised in Table 2.6.

Table 2.6: Classification and characterisation of common polymers used to modify AC
(Behnood & Gharehveran, 2019; Pyshyev et al., 2016; Zhu et al., 2014)

Category	Polymer	Advantages	Disadvantages
Plastomers	Polyethylene (PE)	<ul style="list-style-type: none"> • Higher rutting resistance • Improved aging resistance • Relatively low cost 	<ul style="list-style-type: none"> • Stability problems • The desirable performance enhancement is achieved at high PE contents • Unremarkable enhancement in elastic
	Polypropylene (PP)	<ul style="list-style-type: none"> • Better temperature susceptibility • Improved plasticity range • Relatively low cost 	<ul style="list-style-type: none"> • Occurrence of phase separation due to insolubility in asphalt • Poor thermal fatigue cracking resistance
	Ethylene–vinyl acetate (EVA)	<ul style="list-style-type: none"> • Better temperature susceptibility • Good storage stability • Better resistance to rutting 	<ul style="list-style-type: none"> • No enhancement of elastic recovery • Minimum enhancement in low temperature properties
Thermoplastic Elastomers	Styrene–Butadiene–Styrene (SBS)	<ul style="list-style-type: none"> • Improved physical properties • Significant enhancement in both high and low temperature viscoelastic properties • Improved temperature susceptibility 	<ul style="list-style-type: none"> • Relatively high cost • Compatibility issues • Lower resistance to oxidation compared to plastomers • Increased optimum binder content and viscosity problems during paving applications

Table 2.6 Continued			
Category	Polymer	Advantages	Disadvantages
	Styrene-Butadiene-Rubber (SBR)	<ul style="list-style-type: none"> • Better cohesion and low temperature performance • Better viscous properties than SBS 	<ul style="list-style-type: none"> • Relatively high cost • Compatibility problems • Poor storage stability
Thermoplastic Elastomers	Acrylate-styrene-acrylonitrile (ASA)	<ul style="list-style-type: none"> • Higher resistance to rutting and permanent deformation • Better creep resistance • Improved aging resistance 	<ul style="list-style-type: none"> • Compatibility problems • Poor storage stability • Occurrence of phase separation

Polyolefin plastomers, such as Polyethylene (PE), polypropylene (PP) and ethylene vinyl acetate (EVA), have been acknowledged in the literature as they improve the high temperature performance of AC in the prevention of rutting failure (Porto et al., 2019). (Ameri et al., 2012; Brovelli et al., 2013) studied EVA modified binders by using different penetration grade base asphalt modified at various concentrations. Their findings showed an increase in the rutting parameter ($G^*/\sin\delta$) induced by the enhancement in the stiffness of modified binders. Furthermore, studies investigating the effect of recycled EVA modified binders have demonstrated promising results, which was evidential that, reclaimed plastomers also have the potential to improve the performance of modified binders at high service temperatures (Garcia-Morales et al., 2006; García-Morales et al., 2004). Research regarding PE and PP modified binders has demonstrated similar findings, such as that increased complex modulus and reduced phase angle generate better resistance to rutting failure. However, it is also reported in the literature that the addition of plastomeric modifiers commonly leads to more brittle behaviour of AC, thus exhibiting poor performance at low temperature. (Bala, Napiyah, et al., 2017; Yuanita et al., 2017). Consequently, coupling agents have been used with plastomers to eliminating the drawbacks regarding to the chemical and physical properties of plastomeric polymers (Brasileiro et al., 2019). A research conducted by (Yuanita et al., 2017) found that adding lignin to PP leads to better compatibility between the polymer and the base asphalt. Findings of (Bala, Napiyah, et al., 2017) also demonstrated that PE/nanosilica modified binders possess better morphological properties as well as improved low temperature performance.

In contrast to the plastomeric polymers, elastomeric polymers can resist permanent deformation and also demonstrate the ability to recover elastically after being loaded and

when exposed to low temperatures (Yilmaz et al., 2010). Elastomers that contain styrenic blocks such as SBS, SBR and ASA were found to be the most suitable modifiers since they extend to improve both the high temperature and low temperature performance characteristics of AC (Ali et al., 2015; Pyshyev et al., 2016; Zorn et al., 2011). According to Airey and Kok et al., (Airey, 2003; Kok et al., 2010), styrene block copolymers ensure higher strength and better rutting resistance due to the presence of polystyrene end-blocks, while the formation of polybutadiene mid-blocks is responsible for the better elastic properties. SBS and SBR copolymers have been investigated extensively by a number of researchers and their findings corroborated their positive influence such as increased aging resistance, prevention of high temperature rutting and low temperature fatigue failures of pavement roads (Fernandes et al., 2008; Rossi et al., 2015; Zorn et al., 2011). Ali et al. (Ali et al., 2015) investigated the morphology and rheological properties of ASA modified binders and their findings validated the advancements in the rheological properties. Although polymer-modified bitumen offers promising results, many researchers have noted a major shortcoming of the modification process, which is the compatibility issue between the polymer and bitumen (Galooyak et al., 2010; Polacco et al., 2015). (Al-Mansob et al., 2017) stated that, the incompatibility is correlated with the occurrence of phase separation due to the variations in density, molecular weight and solubility between the polymer and asphalt. Also according to (Lu et al., 1999), the phase separation is governed by the chemistry of asphalt and the characteristics of the polymer. Due to the shortcomings of the polymer modified bitumen, researchers have gravitated towards the investigation of the potential of nano-materials and nanocomposite materials as modifiers to asphalt cement.

2.2.2 Nano materials in AC

According to the definition of (Commission, 2011), nanomaterials are naturally occurring, incidentally occurred or engineering manufactured materials that have at least one dimension that is less than 100 nanometres. Previously, numerous types of rubbers, epoxy, resins, chemical agents and polymers have been utilised to modify asphalt and have been investigated in macro and micro levels (Iskender, 2016). More recently, the application of asphalt modification with materials in nano scale have been incorporated in pavement engineering. A number of special properties of nanomaterials such as increased surface area

to volume ratio and the quantum effects resulting from the spatial confinement added certain beneficial features to the modified asphalt cement such that; enabling better dispersion and stability in the mix, improving the aging resistance in the short and long term and enhancing the viscoelastic properties of the asphalt cement at extremely high and low temperatures (Bhargava et al., 2016). While asphalt is primarily used for road construction on a large scale and in large quantities, the mechanical properties of asphalt depend on the structure of the nanomaterials that are used to modify asphalt cement. Figure 2.11 shows the evolution of the longitudinal scales of an asphalt concrete material, from macro to meso, micro, nano and quantum scales. The microstructure has significant influence of macro properties of asphalt, hence, nano-modified asphalt offers a major improvement over the fundamental material properties, which is considered to be the most efficient method compared to other methods of asphalt modification (Fang et al., 2013).

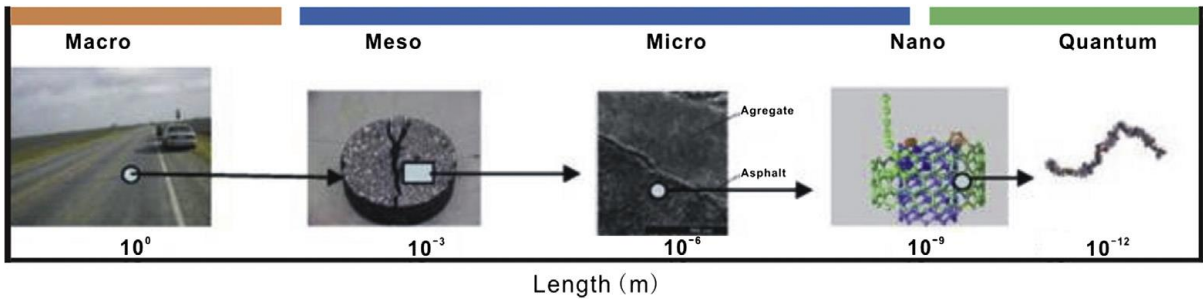


Figure 2.11: Asphalt dimensions from macro to quantum levels

Different nanomaterials add different benefits to the performance characteristics of asphalt. Although there exists certain nanomaterials in the literature to improve multiple features of asphalt cement concurrently, similar to those of polymer modified asphalt cements, usually improvement in one particular feature is at the expense of losing another. For nanomaterial modified asphalt, the enhancement or deterioration of asphalt properties such as aging resistance, workability, stability and rheological properties depend on the molecular structure and density of the nanomaterials. Also, particle size, specific surface area and purity of the nanomaterials are the influential factors that determine the new structural formations and changes in the performance characteristics of asphalt cement. Carbon nanotubes, nano silica, nano clay and nano iron are among the common nanomaterials that

were previously used in the modification of asphalt cement. Readers are referred to references included in Table 2.7 for further acknowledgment of the specific features and outcomes of the nanomaterial modification to asphalt cement.

Table 2.7: Review of common nanomaterials used to modify neat asphalt

Type	Designation	Particle size (nm)	Specific surface area (m ² /g)	Bulk density (g/cm ³)	Purity (%)	Reference
Nano silica	SiO ₂	<10	600	0.10	>99.0	(Hasaninia & Haddadi, 2017, 2018)
Nano silica	SiO ₂	15±3	160±12	0.14	>99.9	(Ghasemi et al., 2012)
Nano silica	SiO ₂	30	200±35	0.03-0.06	99.8	(Cai et al., 2018)
Nano silica	SiO ₂	70	64	-	-	(Crucho et al., 2018)
Nano clay	Cloisite-15A (Organophilic)	-	-	0.230	-	(Jahromi & Khodaii, 2009)
Nano clay	Polysiloxane (Organophilic)	-	-	0.251	-	(Goh et al., 2011)
Nano clay	Sodium Bentonite (Hydrophilic)	-	-	-	-	(Zare-Shahabadi et al., 2010)
Nano iron	Fe	50	25	-	>80	(Crucho et al., 2018)
Nano iron	Fe ₂ O ₃	38	-	-	-	(Kordi & Shafabakhsh, 2017)
Nano iron	Fe ₂ O ₃	20-40	40-60	-	>98	(Pirmohammad et al., 2019)

In addition to the nanomaterials mentioned in Table 2.7, positive effects of carbon nano tubes (CNT) have shown promising potential as modifier to asphalt cement which was reported in a number of studies. (Arabani & Faramarzi, 2015; Ziari et al., 2018) conducted research on CNT-modified asphalt binders and mixtures and concluded that the CNT modifiers enhanced the mechanical properties and also improved the aging resistance and self-healing mechanism of binders and hot mix asphalt (HMA).

According to (Crucho et al., 2019; You et al., 2011) nanoclay modified binders enhance the stiffness and elasticity of AC; however, due to the limited enhancement in the elastic behavior of AC, nanoclay is more frequently used as a second modifier to polymer modified AC. (Yang & Tighe, 2013) stated that the addition of a small amount of nanoclay into SBS

modified binders can enhance the thermal properties of AC at both high and at low temperatures while also improving the compatibility between the polymer and bitumen.

Numerous studies have reported that, based on its cost effectiveness and notable enhancements in physical and rheological properties, nanosilica is considered as one of the most substantial advancement in asphalt modification (Bhargava et al., 2016; Yang & Tighe, 2013). Studies conducted by (Yao et al., 2013; You et al., 2011) discovered that 2% to 4% use of nanosilica by the weight of bitumen can reduce the rut depth up to 50%. Additionally, Arabani et al. (Arabani et al., 2012) achieved remarkable enhancement in fatigue resistance of up to 37% than the neat asphalt. Nanosilica has also been utilized in numerous studies in order to build new polymer nanocomposites that can perform better over a longer life span. Similar studies also showed that, the drawbacks of well-known polymers such as SBS, PP and PE were found to be satisfactorily recovered with the addition of nanosilica (Bala, Kamaruddin, et al., 2017; Bala et al., 2018; Rezaei et al., 2016).

The use of nano iron to modify asphalt is designated as Fe or in the form of iron oxides such as FeO, Fe₂O₃ or Fe₃O₄. A study conducted by (Kordi & Shafabakhsh, 2017) with stone mastic asphalt modified by Fe₂O₃ nanoparticles demonstrated that, a small amount (0.9% by the weight of bitumen) of Fe₂O₃ modification to asphalt cement increased the fatigue life of samples by 15%-35% compared to the neat asphalt. Additionally, their research reported that, the amount of rut depth of asphalt samples containing 0.9% Nano Fe₂O₃ was about 25–40% lower than the neat asphalt samples. Further, (Pirmohammad et al., 2019) investigated the fracture properties of asphalt mixtures modified with Nano Fe₂O₃ and CNT's. The outcomes of their study showed that, 0.8% and 1.2% of modifier concentrations for Nano Fe₂O₃ and CNT's respectively resulted in remarkable improvement of fracture properties under two different types of mix loading modes. According to the findings of their study, enhancement in fracture properties for CNT's was 46% while it was 27% for the Nano Fe₂O₃ modified asphalt concrete.

2.2.3 Polymer/nanocomposite AC

Polymer/nanocomposite modified AC (PNC) is considered to be the latest advancement in the field of pavement engineering that facilitates the design of roads with superior

performance and increased durability (Porto et al., 2019). By blending polymers and nano layered silicates, PNC's are formed. The high silicate layer surface area gives rise to complex interactions, resulting in a new class of nanostructured materials known as polymer nanocomposites with a specific set of physical properties. (Gulzar & Underwood, 2019). A peculiar feature of polymer nanocomposites is the cost effectiveness compared to polymer modified and nanomaterial modified asphalt cements due to lowered modifier contents added in the blend (Bala et al., 2019). It is acknowledged in the literature that, certain polymeric additives have proven to improve the physical and mechanical properties of neat asphalt thereby resulting in longer lasting and better performing pavement roads. However, a drawback of such systems was the incompatibility of polymers with the asphalt, particularly in the case of elastomeric polymers such as SBS and SBR (Ponniiah & Kennepohl, 1996). The consequences of incompatibility between the asphalt and the polymer are the phase separation and clustering of the particles known as agglomeration which results in lower stability of the blends and further reduction in the performance characteristics of AC. The addition of nanomaterials in the PMB is known to mitigate the incompatibility issue between the asphalt and the polymer (Lu et al., 1999). (Mahali & Sahoo, 2019) stated that, the role of nanomaterials in the polymer modified asphalt cement is to act as a driving force to decreasing the differences in density between the polymer and the base binder thus, improving the compatibility. Based on their structures and depending on the strength of the interfacial interactions between the polymer matrix and the layered silicate structures of the nanomaterials, polymer nanocomposite modified asphalt cements can be in 3 different forms which are the phase separation intercalation and exfoliation as illustrated in Figure 2.12 (Porto et al., 2019).

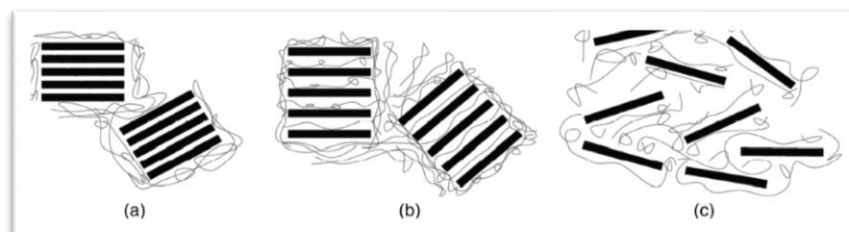


Figure 2.12: Asphalt/polymer nanocomposite matrix internal structure (a) Phase-separated (b) Intercalated and (c) Exfoliated

The formation of above-mentioned conditions is called in-situ polymerisation. In-situ means the reactions are getting developed while the blending process is going on by adding two independent elements where, in the case of polymer nanocomposites these are the polymer and the nanomaterial. The in-situ polymerisation is the dispersion of the layered structure of the nanomaterial in the polymer-asphalt matrix (Lee et al., 2011). The reversible inclusion or incorporation of a molecule or ion into materials with layered structures is called intercalation. The van der Waals distance between the silicate layers, which requires energy, is widened by intercalation. This energy is typically given by the transfer of charges between the polymer and the nanomaterial (Lee et al., 2011). The extreme case of intercalation is exfoliation, where the layers of the nanomaterial are completely nested while, in the case of phase separated structures, the reactions between the polymer and the nanomaterial are insufficient and they act like independent materials dispersed in the asphalt matrix (Golestani et al., 2012). It should be noted that un-separation of the silicate layers of the nanomaterials lead to phase separated structures which often results in agglomeration of the nano particles in the blend that is not desirable in terms of stability and performance of the asphalt cement (Zhu et al., 2014). (Fang et al., 2013) further stated that, the aging resistance of a polymer nanocomposite is affected by its phase structure since it is dependent on the stability and compatibility features which are the premise parameters for the anti-aging properties of the asphalt cement. According to the remarks of their study, a polymer nanocomposite modified asphalt cement that possesses an intercalated or exfoliated structure can produce an effective barrier to oxygen, water and organic solvents, while preventing the evaporation of the light components of the asphalt thus improving the aging resistance of the asphalt binder. X-ray diffraction analysis is commonly utilised as a measurement technique to observe the formation of phase structures. X-ray diffraction enables the measurement of the interlayer d-spacing between silicate layers of the nanomaterial. Higher interlayer d-spacing indicate to a formation of intercalated or exfoliated structures while the lower values indicate the versa. In a study conducted by (Golestani et al., 2012) with linear and nonlinear polymer nanocomposite modified asphalt cement by SBS and nano clay it was reported that, Linear SBS-nanocomposite modified asphalt (LSN) possessed an interlayer spacing of nanoclay more than 8.82 nm which was considered as exfoliation while Branch SBS-nanocomposite modified asphalt (BSN) possessed an interlayer spacing of nano clay around 4.69 nm and it was considered to have an intercalated structure. Rheological investigations of their study

also showed that, polymer nanocomposite modified asphalt with exfoliated structures showed improved aging resistance and better enhancement in the performance characteristics of the modified asphalt cement.

Although polymer nanocomposites are relatively new, not readily available and have received limited attention in the literature, a considerable amount of research have been published using numerous polymers and nanomaterials together to form polymer nanocomposites in the asphalt cement modification. Among the significant studies include the experimental investigations on the secondary modification to polymer modified asphalt cement with nano clay, nano silica, nano alumina, nano copper and nano calcium.

The use of nanoclay in the modification of polymer modified asphalt usually results in intercalated or exfoliated microstructures providing better performing and more durable asphalts. The above statement is validated by the references listed and the experimental outcomes of a study conducted by (Zhu et al., 2014). However, in the same study the authors highlighted certain downsides of nano clays such as, difficulties in obtaining the ideal exfoliated structure for the polymer nanocomposite and also poor enhancement in low temperature properties. Additionally, excessive clay concentration in the asphalt matrix was reported to negatively influence the elastic properties of the asphalt cement. A comparative analysis of nano clay modified (NMN) asphalt binders and polymer modified nano clay (PMN) asphalt binders was conducted (Gulzar & Underwood, 2019) and found that PMN asphalt binders performed much better than modified nano clay binders. When comparing their rheological properties, due to the addition of only nano clay, they find that viscosity increases while the addition of PMN enhances the properties of high temperature and complex shear modulus. It has also been found that the rutting and fatigue efficiency of the PMN asphalt blend was higher than that of the nano clay asphalt blend.

Silica, one of the most abundant sources found on earth has been used in various engineering applications such as material science and medicine (Alhamali et al., 2016). Nanoscale silica has been commonly used to stabilize the elastomers as a rheological solution in the polymer industry. As a result, nano silica draw the attention of the pavement engineers regarding to polymer nanocomposite modification of asphalt cement due to its unique properties such as small particle size, high surface area to volume ratio, good dispersion ability and low cost (Alhamali et al., 2015). The addition of silica to SBS modified asphalt cement at 2, 4 and

6% by the wt. of asphalt was investigated by (Yusoff et al., 2019). Their findings demonstrated that, all modified asphalt yielded better rutting and fatigue resistance at high temperatures and/or low frequencies and at low temperatures and/or high frequencies respectively. Additionally, FT-IR analysis showed that polymer/nanosilica modified asphalt improved the aging resistance subsequently as the modifier content was increased. In another study, the effect of polymer nanocomposite modified asphalt cement with polypropylene polymer and nanosilica particles on the fatigue performance of asphalt mix concrete was investigated. The modifier content in the asphalt mix preparation was in the range of 0% - 4% by the weight of bitumen. The asphalt performance tests; flexural four point beam fatigue test, indirect tensile strength and indirect tensile stiffness modulus were performed. The results of their study showed that, up to 3% nano silica addition the fatigue resistance of the asphalt mixture was improved while, the optimum nano silica content that satisfied all the other performance properties was found to be 2% by the weight of polymer modified asphalt (Bala et al., 2018).

Alumina is another material that was used extensively in the literature either as sole modifier or as additive to polymer modified asphalt cement. For instance, (Al-Mansob et al., 2017) investigated the performance of epoxidised natural rubber modified asphalt using nano-alumina as additive. A distinction of their study from the others was that, a sonication method was used to disperse the nano aluminium particles inside the polymer-asphalt matrix. As a result, the agglomeration of nano particles was reduced significantly, improving the stability and compatibility of the additives. In addition, the addition of nanoalumina has been reported to improve the temperature sensitivity and rheological properties of the PMB.

A previous study conducted by (Sediq, 2018) used nano calcium and nano copper as secondary modifiers to ASA modified asphalt cement. Polymer modified binder (5% ASA by the weight of binder), ASA–nano calcium, and ASA–nano copper at concentrations of 3% and 5% by weight were characterized using a dynamic shear rheometer. Although the study was only limited to investigating the the behaviour of the material at high temperatures, it has demonstrated the ability of the polymer nanocomposites to improving the stability of the blends as well as improving the rheological characteristics at lower modifier concentrations. It was found that, 3% was the optimum addition of modifiers to maximise the stiffness of the material to resist rutting failure at high temperatures. Also, findings of

his study showed that the enhancement in rheological properties was more remarkable with the ASA-nano calcium modification while in the case of ASA-nano copper modification the enhancement was insignificant such that, almost a similar trend of increase in complex modulus was observed with sole modification of asphalt cement with ASA.

2.3 Modelling the Performance Characteristics of Asphalt Cement

2.3.1 Experimental modelling of AC

Asphalt has its use in various applications such as roofing, waterproofing and design of flexible pavement roads. For each application, it is essential to acquire knowledge about asphalt characteristic properties in order to evaluate its performance during the service life and also to assess its lifecycle cost analysis (Zhu et al., 2014). Since, the characteristic properties of asphalt vary depending on the source it is obtained from, (whether it is obtained from natural deposits or obtained from fractional distillation of crude oil) and also the distillation procedure, numerous grading systems for asphalt have been developed in order to classify and standardise the asphalt cement (Chattaraj, 2011). Penetration grading and viscosity grading were firstly adopted by agencies in the field of pavement design. These systems had their pros and cons which are as explained in Chapters 2.3.1.1 and 2.3.1.2. More recently, Superpave specification system which has been developed during the strategic highway research program is considered to be the latest advancements for asphalt cement characterisation and therefore, accepted by transportation authorisation agencies worldwide (Al-Omari et al., 2018). Superpave grading system is explained in Chapter 2.3.1.3 in more detail.

2.3.1.1 Penetration grading

The penetration grading has been adopted in the early 1900's in the European and ASTM standards as a measure of consistency of asphalt cement. Road designers directly used penetration value of asphalt to specify which penetration grade of asphalt should be selected depending on the temperature conditions (Apparao et al., 2013). Although the choice of asphalt binder characteristics for pavement design is more complex, the penetration grading provides basis to the selection of suitable asphalt binder whether it is to be used as a neat

binder or as a base to modified asphalt binder in the hot mix asphalt design (Chattaraj, 2011). Penetration grading requires the quantification for the penetration, softening point, flash point, ductility and asphalt solubility in trichloroethylene however penetration grading is designated within a range of penetration values solely. Penetration grading is designated with a “pen” abbreviation which is then followed with two numbers which the first number indicates the lower specified limit and the second number specifies the maximum penetration limit for an asphalt binder. The penetration grade ranges from 40-300. The selection of asphalt binder depends on the purpose of use and the place where it will be used (Al-Omari et al., 2018). For road construction, ASTM suggests the use of penetration grade asphalt such as 60/70, 80/100 and 40/50. If the temperature conditions are cold, a higher penetration grade is preferred to be used since, higher penetration indicates a softer material. For example, pen 80/100 penetration grade is typically used in colder regions such as Finland and Alaska. In cases, where the climate is expected to be warmer, a pen 60/70 grade is more suitable to be used. Pen 40/50 grade asphalt is the hardest grade and it is typically used in very hot climates such as Saudi Arabia and most of the African countries since, a stiffer asphalt is required in order to prevent the occurrence of rutting failure (Al-Omari et al., 2018).

The utilization of penetration grading continued from the early 1900’s to the beginning of 1960’s until it was replaced by the viscosity grading by many authorisation agencies. The shift from penetration grading to viscosity grading was due to the major drawbacks of the penetration grading such as penetration value being a measure at a single temperature, the empirical nature of measurement and penetration not being a fundamental engineering property of asphalt cement like the rotational viscosity (Chattaraj, 2011). It can be seen in Figure 2.13 that, due to viscoelastic nature of asphalt, although all asphalt samples A, B and C have the same penetration value at ambient temperature, the material behaviour is different at higher and lower temperatures. Considering that an asphalt concrete pavement may experience such erratic climate conditions during its service life, the penetration grade alone is said to be limited to provide reliable performance grade to determine the quality of asphalt pavements. (Apparao et al., 2013),

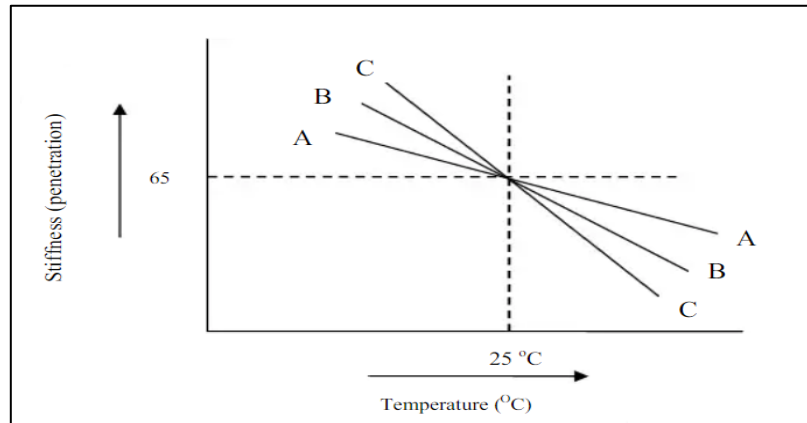


Figure 2.13: Penetration grading of three different pen 60/70 grade AC samples

2.3.1.2 Viscosity grading

Viscosity grading system was constructed based on the measurement of rotational viscosity of asphalt under unaged and short term aged conditions. Viscosity grade was developed in the early 1960's. The rotational viscosity test replaced the empirical penetration test as the primary asphalt binder characterization in the viscosity grading system (Chattaraj, 2011). Methods defined in the ASTM D5 and AASHTO T27 standards define the viscosity grade of asphalt.

The viscosity grading system has certain advantages compared to European system. Unlike penetration, rotational viscosity is a fundamental engineering parameter. The viscosity grading system also provides information on the consistency of asphalt at three different key temperatures; 25°C which is the approximate average ambient pavement temperature, 60°C which is the approximate maximal pavement surface temperature and 135°C which is the approximate asphalt mixing temperature. These three temperatures also provide an insight regarding to the temperature sensitivity of AC (Kim, 2008).

On the other hand, the viscosity grading system has certain downsides. Viscosity grading system is not able to assess the asphalt properties at low service temperatures. Also, when using the AR grading system, for the RTFO test residues, the viscosities may vary greatly within the same AR grade (Read et al., 2003). In addition to that, the viscosity test conducted at 135°C is representative for neat asphalt binder samples mixing temperature however, in the case of modified asphalt binders, the mixing temperatures may reach up to 200°C

therefore, the viscosity grading system may not be suitable to represent the grade of asphalt for modified asphalt cement (Chattaraj, 2011).

The viscosity grading system has been widely implemented from the 1960's to 1990's, but has been replaced since then in most countries. For instance, it has been replaced in the United States by the Superpave Performance Grading. It is still enforced in some countries such as India, Australia and in some regions in Africa and Latin America (Al-Omari et al., 2018).

2.3.1.3 Superpave performance grade (PG) specification

Penetration grading and viscosity grading specifications having major downsides as mentioned in Chapters 2.3.1.1 and 2.3.1.2, lead to the development of the Superpave performance grade specification due to growing concerns that are based on traffic loading, climate conditions and the effect of aging on asphalt pavements. The Superpave specifications became effective in use in 1993 after a five year project conducted in United States of America (USA) as part of the Strategic Highway Research Program (SHRP) (Jadidirendi, 2017). Unlike previous grading specifications, Superpave PG is a performance based specification rather than an empirical one. It accounts for how the asphalt binder is selected based on the climate where the pavement will be placed, the traffic it is expected to carry and the type of pavement distresses it may experience during its service life (Chin, 2009). An asphalt pavement is expected to perform under extreme climate conditions from the heat of summer to the frozen winter. It also has to carry varied traffic from small sports cars to heavily loaded trucks. The proper selection of asphalt binder to address these varying conditions is critical to good performance and therefore the Superpave PG specification was developed to address these issues (Read et al., 2003). The grading system is primarily based on the climate conditions as shown in Table 2.8.

Table 2.8: Superpave PG specification

	Temperature (°C)					
Temperature (°C)	52	58	64	70	76	82
-16	52-16	58-16	64-16	70-16	76-16	82-16

Table 2.8 Continued						
Temperature (°C)	52	58	64	70	76	82
-22	52-22	58-22	64-22	70-22	76-22	82-22
-28	52-28	58-28	64-28	70-28	76-28	82-28
-34	52-34	58-34	64-34	70-34	76-34	82-34
-40	52-40	58-40	64-40	70-40	76-40	82-40

With recent Superpave specification, asphalt binders are designated with a PG abbreviation which is then followed by the temperature ranges for which it will be used. As an example; For a PG 64-16 asphalt binder, the first number (64) is the expected high pavement surface temperature and the second number (-16) is the expected low pavement surface temperature that the binder will experience based on the climate where the pavement will be constructed. The expected high temperature is accepted to be the average of the seven days with the climax temperatures whereas, the low temperature grade is specified using the lowest temperature the pavement has experienced throughout the year (Al-Omari et al., 2018). It has to be noted that, these temperatures are not the atmospheric weather temperatures but the recorded asphalt pavement surface temperatures. There are numerous models available in the literature that has attempted to correlate the air temperatures with the pavement surface temperatures. (Arangi & Jain, 2015) have reviewed some of these modelling techniques. According to (Arangi & Jain, 2015), the pavement surface temperature can be modelled using meteorological data such as, daily ambient air temperatures, the amount of solar radiation, location latitude, humidity and wind speed in order to predict the pavement surface temperature that the asphalt will be exposed.

In Superpave specification, the binder grading is specified with 6°C increments of temperature. The selection of binder grade to be used in the field is performed by using the normal probability distribution for a seven day average of high temperature and at one day extreme low temperature (Jia et al., 2005). The grade selection by the relevant reliability levels are as demonstrated in Figure 2.14. It also has to be noted that, Superpave specification is developed in the US and although the highest possible pavement temperature in US was recorded as 70°C, two more high temperature grades are available as can be seen in Table 2.9. This is due to the Superpave standards specifying that the traffic loading should also be taken into consideration in the selection of binder grade. According to Superpave

specification if slow speed or heavier traffic is expected, the binder grade should be adjusted as much as increasing up to 2 grades where necessary so that a stiffer binder is used. Adjusting the binder grade to accommodate transient and stationary loads is referred to as “grade bumping” and it is as demonstrated in Table 2.9 (Bukowski, 2011).

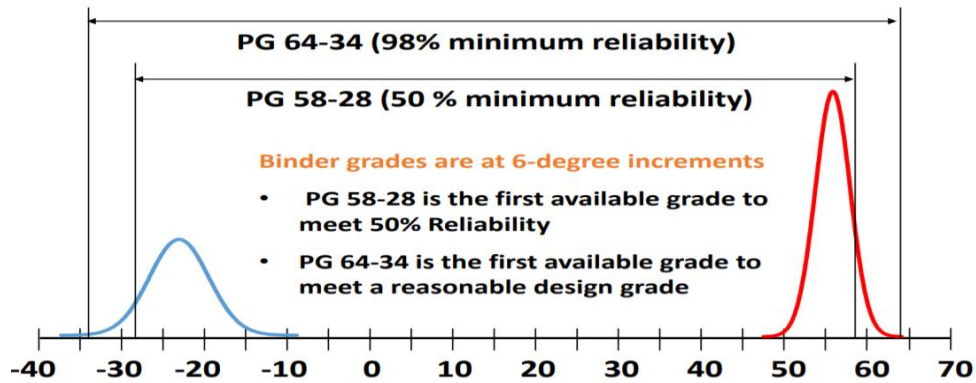


Figure 2.14: Superpave grade selection

Table 2.9: Superpave grade bumping

Original Grade	Grade for slow transient loads	Grade for stationary loads	20-year ESALs >30 million
PG 58-22	PG 64-22	PG 70-22	PG 64-22
PG 64-22	PG 70-22	PG 76-22	PG 70-22
PG 70-22	PG 76-22	PG 82-22	PG 76-22

Asphalt binder properties change with temperature. At high temperatures, it is a viscous fluid and at low temperatures, it acts as an elastic solid. Due to its viscoelastic nature, asphalt exhibits different behaviour at different temperatures. This variation in properties of asphalt is taken into consideration in the Superpave specification (Kim, 2008). As the asphalt binder ages in the pavement, its properties also change and this affects its performance. Due to aging, asphalt becomes stiffer and more brittle making it more prone to cracking. The Superpave specification addresses this by testing asphalt under varied temperatures and at various aging conditions such as short-term aging referred to as RTFO and long-term aging known as PAV condition in order to evaluate how the binder will perform as it ages (Read et al., 2003). Rutting of the pavement typically occurs early in asphalt pavement life and at

high temperatures. Cracking from traffic loading also known as fatigue cracking happens during its service life at moderate temperatures. Low temperature cracking also occurs later in the pavements service life caused by exposure to very low pavement surface temperatures (Ali et al., 2017). Figure 2.15 illustrates the typical tests required and the conditions at which the testing protocols are followed in the Superpave specification of performance grading (Jia et al., 2005).

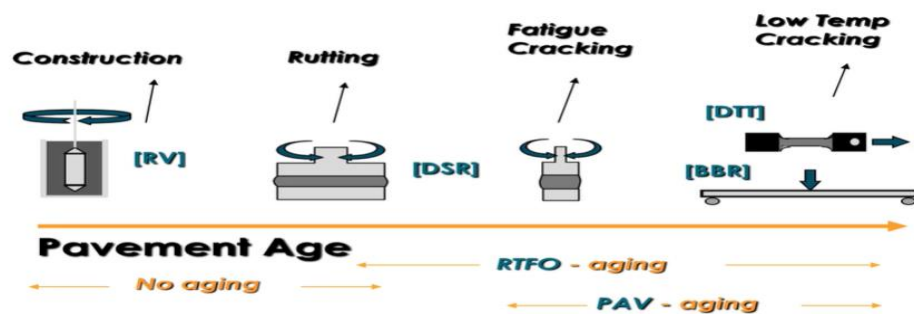


Figure 2.15: Superpave PG testing protocols

As seen in Figure 2.15, in order to evaluate the asphalt binder's early life conditions, testing is done at very high temperatures on unaged binders using a rotational viscometer (RV) to determine if it will be workable during construction. The asphalt binder is then tested at high pavement service temperatures using a dynamic shear rheometer (DSR) on the RTFOT short-term aged binder to determine the potential for rutting failure. To evaluate the binder's later life conditions, testing is done on PAV long-term aged binders at moderate temperatures to determine cracking that is associated with traffic loading and also the test is performed at very low temperatures to control low temperature thermal cracking properties. Direct tension tester (DTT) and bending beam rheometers (BBR) are also utilized in the assessment of long term aged performance of asphalt binders on low temperature cracking characteristics (Arshad & Qiu, 2012).

2.3.2 Soft computing modelling of performance parameters

The most recent advancements in the testing methods for the experimental evaluation of asphalt cement properties provided a more accurate assessment of asphalt cement

performance characteristics which enabled the design of better roads. However, the new testing technologies are not considered as time and resource friendly processes. Due to high number of tests needed to characterize asphalt cement and the high number of test repetitions required to increase consistency and reliability of the test results, a significant amount of materials are used and the testing procedures take considerable amount of time. Also, advanced laboratory facilities are essential to accommodate the test conditions which is of significance since, the availability and maintenance costs for the advanced laboratory equipment cannot be negligible (Fang et al., 2013). On this basis, many researchers were gravitated to minimising or eliminating some of the testing procedures by adopting mathematical and computational modelling approaches in order to predict significant parameters of asphalt cement that are related to its performance characteristics (Venudharan & Biligiri, 2017).

Computational modelling have been the most popular technique in numerous fields of engineering by researchers since the development of machine learning algorithms in the beginning of 1960's (Venudharan & Biligiri, 2017). Machine learning is considered to be a subset of artificial intelligence which adopts learning from sample data by training a set of input data points to predicting an outcome set of data points which is also referred to as computational predictive analytics. Artificial Neural Networks (ANN), Fuzzy Inference Systems (FIS), Adaptive Fuzzy Inference Systems (ANFIS), Support Vector Machines (SVM) and Genetic Algorithms (GA) are among the machine learning family that have been commonly utilized in many researches to model experimental outcomes of various engineering parameters (Abedali, 2015). As acknowledged in the literature, a considerable amount of research has been devoted to the modelling of fundamental engineering properties of asphalt concrete mixtures in the field of pavement engineering to predict the performance of asphalt pavement during its service life. However, limited attempts have been made to model the performance characteristics of asphalt cement that are fundamentally critical for determining the performance features of the hot mix asphalt design. (Kok et al., 2010).

Although artificial intelligence based modelling technique is applicable in many fields of engineering, an effective model is said to be the one which has the generalisation ability, meaning that, the model should also be able to predict new data points when untrained data sets are introduced in the model network (Yusoff et al., 2019). Numerous model developing

ideas have been suggested in the literature by a number of researchers. A study conducted by (Venudharan & Biligiri, 2017) found that mechanical test conditions such as the temperature and frequency at which the tests are carried out can predict the oscillatory DSR test performance. The significance of their study was to minimise the number of tests and repetitions that are required to plot a smooth master curve in the evaluation of rutting, fatigue and thermal cracking parameters. Another study conducted by (Kim et al., 2014) made a successful computational modelling effort to predict the short-term and long-term aged performance characteristics of asphalt cement from its unaged physical and rheological properties. Henceforth, the necessity for two aging simulation equipment were avoided and also a significant amount of resources were not wasted to repeat the tests under various aging conditions regarding to the evaluation of aged performance characteristics of asphalt cement. Furthermore, it was reported in a study conducted by (Tapkın et al., 2009) that, the strain accumulation in the actual as-laid pavement roads can be predicted from the repeated creep test results by using artificial neural network modelling. Their findings demonstrated that, it is possible to predict the accumulation of strain in the built pavement road before the construction which is also essential to eliminating the requirement for sample extraction and destructive testing procedures towards the performance evaluation of asphalt concrete pavement.

In this study, the mechanical test conditions and the concentration of modifiers in the blends were used as input parameters to predicting the output parameter which is the complex shear modulus of asphalt cement. Two different computational modelling techniques; ANN and ANFIS as explained in Chapters 2.3.2.1 and 2.3.2.2 were utilized. The motives of the author towards employing the computational modelling of experimental results was to explore the potential of the developed models to predict performance characteristics of asphalt cement under various conditions that the asphalt may experience during its service life since, superpave specification states that, the suitability of the type of asphalt cement to be used depends on these conditions which vary according to the volume and the type of traffic loading as well as the climate conditions of the region that the pavement will be placed.

2.3.2.1 Artificial neural network modelling

ANN is a soft computing method that belongs to the machine learning family which is inspired by the way a human brain functions biologically (DeRousseau et al., 2018). The principle of ANN is to construct a network structure that is similar to human nerve system while the difference between the two is that, ANN is composed of highly interconnected processing constituents called the artificial neurons, which operate in parallel logic and transmit information from one layer to others in serial operations (DeRousseau et al., 2018). ANN has previously been utilised to address the classification, prediction and optimisation problems because of its acknowledged efficiency in generating generalized models to solve nonlinear problems in various fields of engineering which are difficult to model using conventional statistical methods (Yusoff et al., 2019). In ANN modelling, firstly the input data is normalised by the eq. 2.11 in order to improve data integrity and reduce data redundancy since, the parameters of interest may have different dimensions (Alas & Ali, 2019).

$$X_{\text{normal}} = \frac{X - X_{\text{min}}}{X_{\text{max}} - X_{\text{min}}} \quad (2.11)$$

Where; X_{normal} is normalized observed data, x is observed actual data and x_{min} , and x_{max} are minimum and maximum values of found data respectively.

The network structure for ANN consists of 3 main layers and referred to as Multi-layer Perceptron (MLP). As illustrated in Figure 2.16, in an ANN network structure, information is processed at the neurons, and the signals are passed through the connection links, which are associated with weight vectors that determine the strength of the connections. The functions of these neurons are, first to sum up all the initially assigned weights from the lower layers and then to process the sum by a linear or non-linear activation function to determine the output signal from the given input signals (Alas et al., 2020). Although there are a number of activation functions available, non-linear functions have proven to better perform in cases of solving problems with high complexity and they are commonly used in many asphalt performance characteristics prediction models particularly for modified asphalt where the test outcomes involve high complexity due to nature of asphalt cement

viscoelastic behaviour under various conditions (Alas et al., 2020). According to (Venudharan & Biligiri, 2017), Pure-linear function is categorized as linear whereas, Hyperbolic tangent and Logarithmic-sigmoidal functions are classified as non-linear activation functions. As adopted in this study, Hyperbolic tangent activation function is given by eq. 2.12.

$$y_j = \frac{2}{1+e^{-2s_j}} \quad (2.12)$$

Where; s_j = input j^{th} neuron, y_j = output j^{th} neuron

A type of ANN network with abovementioned structure is known as a Feed Forward Multi-Layer Perceptron Neural Networks (FFMLPNN) model. Backpropagation method is commonly adopted with FFMLPNN in order to find the optimum weights as an iterative process to minimize the error between target and computed outputs with a selected accuracy. The iterative forward and backward passes are performed by using the backpropagation method as illustrated in Figure 2.16 and it is denoted as the model training phase (Baldo et al., 2018). Training algorithm is another parameter that has strong influence on the capacity of model to predict the desired outcomes. Levenberg-Marquardt (LVM), Gradient Descent (GD) and Scaled Conjugate Gradient (SCG) are among the most utilised functions due to their generalisation abilities. However, the selection of the training algorithm depends on the type of neural network to be modelled and the structure and complexity of the data to be fed into the network (Alas & Ali, 2019).

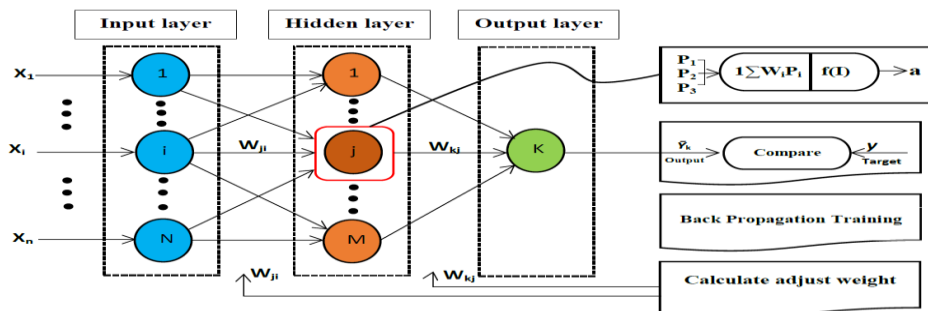


Figure 2.16: A three-layered feed-forward neural network with BP

An ANN model has three main aspects, which are the training, validation, and testing. The dataset is randomly divided among the aforementioned three aspects. The training data set is used for fitting the model. The validation data set is used to provide an unbiased evaluation of the model fit and to adjust the model hyperparameters. A common method adopted in the literature for minimizing the bias and variance is the cross-validation technique while the holds-out cross-validation and k-fold cross validation being the most widely adopted cross validation techniques (Reitermanova, 2010). (Esfandiarpour & Shalaby, 2017) stated that, the test dataset is used in the evaluation of model performance by using the untrained dataset. Data splitting has a significant influence on the performance of the final model regarding to introducing bias and variance into the developed model. Systematic Data Splitting Method, SBSS-N Data Splitting Method and DUBLEX Data Splitting Method are among the data splitting methods investigated by Wu et al., 2012 (Wu et al., 2012).

Machine learning algorithms are mainly divided into supervised and unsupervised learning. In supervised learning, the input and output variables are known and using activation functions the output parameters are attempted to be predicted, whereas, in unsupervised learning, the input data are known but there are no corresponding output data, and the algorithm is expected to underline the structure and distribution in the data points in order to predict the output data set (Baldo et al., 2018). As adopted in this study, in the FFMLPNN supervised learning with backpropagation method, the pursue is to perform forward and backward passes in order minimizing the error between predicted output and provided target data at predefined accuracy level (Venudharan & Biligiri, 2017). Evaluation of the model efficiency is performed in conjunction with statistical performance indicator metrics. The common measures adopted in various studies are Average Mean Error (MAE), Mean Squared Error (MSE), Root Mean Squared Error (RMSE), Average Percentage Error (APE), Correlation Coefficient (R) and Coefficient of Determination (R^2) (Abedali, 2015; Dutta et al., 2017; Kok et al., 2010). However, the statistical efficiency should not be considered alone, and the model validation with the abovementioned techniques should also be used to evaluate the generalization capacity of the network due to the overfitting concern (Kok et al., 2010).

Previously, significant amount of research have been dedicated to modeling the asphalt cement and asphalt concrete pavement performance characteristics by using ANN and other

soft computing techniques. (Liu et al., 2018) studied the ANN and Iowa models to predict dynamic modulus of base and recycled shingle asphalt mixtures with data from four different projects. The input parameters they have included in their models were the sieve test results on aggregates, air voids in HMA, the concentration of the binder, physical test results, applied frequency, and recycled asphalt shingle contents. The findings of their study showed that, ANN models were able to outperform Iowa models in terms of prediction accuracy. (El-Badawy et al., 2018) compared regression models and ANN models with Witczak and Hirsch predictive models for forecasting dynamic modulus of asphalt mixture. The database for their analytical models was obtained from the mechanical tests that were carried out in different countries using mixtures possessing different volumetric properties and aggregate gradations that yielded to a range of G^* and δ results. For three predictive models, the ANN models yielded better results than regression models over a large range of experimental datasets. In a study conducted by (Firouzinia & Shafabakhsh, 2018), it was stated that the asphalt mixtures are highly temperature susceptible and that, sole enhancement of binder rheological properties is not sufficient to overcome this problem. Thus additives should be used in asphalt mixtures. In their study, the influences of nano-silica at five different contents were investigated on the thermal susceptibility of asphalt mixture using experimental procedures and the ANN models. It was found that the modification of asphalt mixtures with nano-silica improved the temperature sensitivity of asphalt concrete and also, the ANN models which were developed using 5 input parameters of aged sample conditions, bitumen type, the percentage of the void, unaged bitumen conditions and temperature by using a training algorithm as Radial Basis Function (RBF) was able to sufficiently predict the experimental results. (Tapkın et al., 2009) presented a study to predict the strain accumulation in polypropylene (PP) modified marshal samples. The data observed from repeated creep tests were modelled in ANN and demonstrated positive similarities with the experimentally observed results. This study had its significance since, it allowed predicting strain accumulation on asphalt concrete using predefined asphalt mixture composition and test conditions without carrying out destructive mechanical testing. Modelling of asphalt was not limited to mixture conditions but also asphalt cement performance characteristics modelling related works are available in the literature. A comparative analysis was conducted between the performance of Multiple Linear Regression (MLR) models and ANN with base asphalt binder based on temperature, frequency, dynamic viscosity, shear stress

and strain as inputs and G^* as output (Abedali, 2015). (Ziari et al., 2018) performed a similar study with carbon nanotube (CNT) modified AC to predicting the permanent deformation using MLR and ANN. Both studies demonstrated that the ANN prediction performance outperformed the MLR models. (Kok et al., 2010) investigated the stiffness of base and modified bitumen by styrene-butadiene-styrene (SBS) with ANN using five different SBS concentrations, the temperature and applied frequencies as inputs and adopted various training algorithms. LVM algorithm was found to be the optimum algorithm for predicting G^* . (Venudharan & Biligiri, 2017) employed ANN to predict the rutting performance of asphalt binders with different Crumb Rubber (CR) gradations. The input parameters were considered as five different CR gradations, base binder viscosity, and test temperature and frequency. A various combination of architectures of neural networks were trained with different training and transfer function algorithms. The optimum network was found using the backpropagation method with SCG training algorithm.

2.3.2.2 Adaptive neuro fuzzy inference modelling

ANFIS is another artificial intelligence modelling technique that has been used in analytical modelling for numerous applications in engineering. ANFIS has been used widely in the prediction process due to its capability to deal with complex nonlinear problems (Parmar & Bhardwaj, 2015). The system of fuzzy modeling, developed by Takagi and Sugeno in 1985, has also found numerous practical applications in control and inference applications. (Pedrycz, 1993; Sugeno, 1985). ANFIS is a hybrid system that, combines the learning abilities of artificial neural networks (ANN) which is a data driven system and fuzzy inference systems (FIS) which is a knowledge based system to solve complex non-linear problems. The concept in ANFIS is that, the fuzzy part connects the imported and exported parameters and neural network determines the membership function's parameters. ANFIS is an adaptive and multilayer feed-forward network that contains nodes and links, the former performs a specific function on incoming information and the latter are used to connect the nodes (Gaya et al., 2014). The network structure of ANFIS is as illustrated in Figure 2.17 and it is composed of a 5 layer structure which is as represented in Figure 3.10.

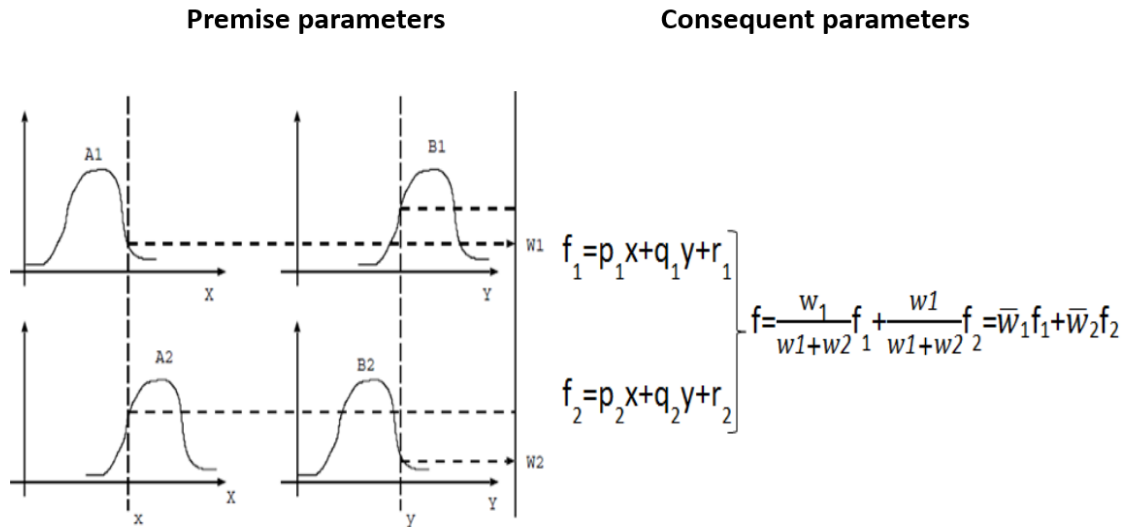


Figure 2.17: General structure of ANFIS

Unlike Boolean logic, fuzzy logic includes membership functions. A membership function is responsible for the fuzzification of the input variables which means assigning a quantified value to a numerical or linguistic variable within a specific range between zero and one. Common membership functions that are used in fuzzification involves the gaussian, gaussian-bell, triangular and trapezoidal functions. Fuzzification for crisp values are performed in the first layer. ANFIS is based on Sugeno fuzzy model which uses fuzzy reasoning mechanism, the Membership grades are associated with fuzzy if then rules. Layer 2 in the network structure is responsible for performing the fuzzy operations based on a number of “if then” rules as represented by eq. 2.13.

$$R_k: \text{IF } \mu_{A_i}(x) \text{ AND } \mu_{B_i}(y) \text{ THEN } f = p_k x + q_k y + r_k \quad (2.13)$$

Where; k is the number of rules A_i and B_i are the n fuzzy membership functions denoted by μ in the antecedent part of the rule R_k and p_k , q_k and r_k are the linear parameters of consequent part of the k^{th} rule.

Layer 3 is called to normalisation layer which calculates the normalised firing strength of a rule from the previous layer as a ratio of the i^{th} rule to all rules. Parameters in layers 4 and 5

are called the consequent parameters. The 4th layer calculates the effect of i^{th} rule in output of model and the 5th layer computes the overall output as the summation of all incoming signals.

The ANFIS is trained by a hybrid algorithm as presented by (Jang et al., 1997). The learning in ANFIS is in two phases which are the forward pass and the backward pass. The algorithm uses the least-squares approach in the forward pass to define the consequent parameters on layer 4. The errors are propagated backward in the backward pass and the premise components are modified by the gradient descent method (Solgi et al., 2017). Unlike the ANN technique, the inputs are not required to be normalised or standardised initially since the assigned membership functions are normalised in layer 3 automatically. After a series of forward and backward calculations, using the backpropagation method, the errors between the prediction and the actual data points are minimised and the output vectors are presented in the last layer (Cüneyt Aydin et al., 2006). Similar to ANN modelling and other computational modelling methods the model efficiency is evaluated by statistical indicator metrics such as MAE, MSE, RMSE, APE, R and R^2 (Cüneyt Aydin et al., 2006; Khademi et al., 2016; Yilmaz et al., 2011).

Many researchers have utilized fuzzy logic and ANFIS in the field of pavement engineering due to its adaptability and computational efficiency when dealing with the complex behaviour of pavement materials (Özgan et al., 2012; Yilmaz et al., 2011). (SERİN et al., 2013) modelled the marshal stability (MS) of light asphalt concrete manufactured by expansive clay with varied mixture properties and asphalt binder contents from 4.5% - 10.5% by using fuzzy logic. Their results showed that, the developed fuzzy logic model was able to predict the actual experimental results with RMSE value of 19.25 and a R^2 value of 0.775. The R^2 value they have achieved was slightly lower than the significance level which is specified as 0.80 in most of the high class investigations. (Specht & Khatchatourian, 2014) utilized MLR, ANN and fuzzy logic modelling techniques for predicting rotational viscosity of crumb rubber. Different crumb rubber contents, rubber particle size and various blending conditions such as the duration and the temperature were the input variables of the developed models. They have reported that, ANN and fuzzy logic models were able to better describe the experimental results than the MLR results. In addition to that, ANN model was the best performing model however, fuzzy logic model was found to perform better than the ANN in

cases where models were developed with limited data sets. ANFIS modelling has been used in a study conducted by (Özgan et al., 2012) to predicting the stiffness modulus of asphalt concrete. The tests were performed on asphalt samples that were subjected to different temperatures at various duration of exposure. Also, tests were performed on extracted asphalt samples from the concrete which were used in combination to form the input parameters. Their results have yielded a correlation coefficient of 0.94. Besides asphalt concrete modelling, ANFIS has also been previously utilised in a study conducted by (Yilmaz et al., 2011) to predict the complex modulus of ethylene-vinyl-acetate (EVA) modified asphalt cement. Statistical analysis of model performance analysis demonstrated that, ANFIS models were able to closely predict the experimental outcomes for different concentrations of EVA copolymer at a range of temperatures and frequencies. It was reported that, the optimum model was developed by reducing the number of membership functions and utilizing two different gauss input membership functions. A more recent study conducted by (Alas et al., 2020) performed a similar study on two different polymer-nano composite modified asphalt cements namely the ASA-Nanocopper and ASA-Nanocalcium. The concentration of modifiers in the asphalt cement and the mechanical test conditions; a range of temperatures and frequencies at which the experiments were conducted were used as input variable to predict an output parameter which was the complex modulus. ANN models were developed along with the ANFIS models and the model performance of two different technique were compared. The findings of their study demonstrated that, both the ANN and ANFIS models for predicting the outcomes of the DSR test results have shown to provide reliable models both with training and testing datasets. Using the results of the testing datasets, R^2 values of 0.996 and 0.920 were achieved for ANN and ANFIS models respectively.

2.4 Hot Mix Asphalt Design

The primary objective in the design of hot mix asphalt (HMA) is to produce an economical mixture of aggregates and asphalt that meets the requirements of the design. For a given specific project, there are standardised requirements to meet specified criteria. These criteria are based on the expected volume of traffic, the climatic conditions and the material selection (Kennedy et al., 1994). Since the traffic conditions and the impact of climate vary depending

on the location that the pavement is to be constructed, different agencies use different specifications that are required to be followed. It should also be noted that, when designing the asphalt mix concrete, the designer should not only consider the initial cost but also the life cycle cost since typically asphalt pavement roads have 10-15 years of service life (Tabatabaee & Bahia, 2012). On account for this, agencies demand certain design requirements for HMA in order to poses desirable characteristics which are explained in the following Chapter 2.4.1.

2.4.1 Requirements of HMA

Asphalt mix concrete pavement should be designed to withstand heavy traffic loads under adverse climatic conditions and to provide adequate structural and functional character to the pavement. The asphalt concrete should have adequate structural strength in order to resist failure by rutting at high temperatures and/or cracking at intermediate and low temperatures under repeated dynamic vehicular loading and it should also be able to provide a smooth driving experience for the driver as a functional character during its service life in order to avoid high maintenance cost or even in extreme cases the complete replacement (Nunn et al., 1997). Numerous mix design methods have been adopted by agencies however, in order to design the most suitable asphalt concrete, certain requirements are needed to be met regardless of the choice of design method. These requirements include asphalt concrete to have sufficient stability, durability, permeability, workability and skid resistance (Roberts et al., 2002).

Stability of HMA is the resistance that a pavement shows against flow in order to prevent the development of ruts and ripples due to repeated traffic loading. Since, stability is affected by the traffic conditions, a careful traffic condition survey should be conducted before implementing a design stability parameter for the pavement to be constructed and for this reason, agencies specify certain limits that needs to be met (Tarefder et al., 2003). Internal friction between the aggregate particles and the cohesion are the two factors influencing the stability of HMA therefore, it can be said that, the stability depends on the design aggregate structure (aggregate shape and texture) and the binder content. Using aggregates with angular shape and in rough texture form within the mixture was found to have positive effect

to prevent the mobility of aggregates and thus improving the stability (Adishesu & Naidu, 2011). Also, stability is affected by the binder content and its characteristics. Cohesion is the result of bonding of asphalt and aggregates in the mix. Cohesion increases with higher traffic loading rate and also under low pavement temperature conditions (high asphalt binder viscosity) (Read et al., 2003). Additionally, the amount of binder used in the mix is crucially important. There should be sufficient amount of binder to provide the binding action however, excessive asphalt content simply lubricates the mix rather than providing a binding effect and this only creates a thick layer of film on the aggregates resulting in loss of inter-particle friction thus, reducing the stability of the mixture (Sengoz & Topal, 2005).

Durability of asphalt concrete pavement is its ability to resist environmental factors and also to withstand various traffic conditions over the designed service life. Typically the service life of flexible asphalt pavement is designed to be 10-15 years (Yang et al., 2015). Aging of asphalt is the major durability concern. Aging in the long term is a result from oxidation of the asphalt binder which results in disintegration of aggregates due to stripping of asphalt coating around the aggregates (Lange & Stroup-Gardiner, 2007). Similar to stability concerns, durability of HMA is influenced by the design aggregate structure and also by the asphalt binder content. Common methods to improve the durability of HMA are; increasing the asphalt binder content, using dense gradation with strip resistant aggregates and reducing the permeability. Increasing the binder content in the mix is useful in enhancing the durability since, a thicker film of binder on the aggregates tends not to age as quickly as a thin film of asphalt and substantially, asphalt retains its characteristics for a longer period of time. Additionally increasing the binder content leads to lower air voids in the mix which improves the impermeability of mix against water and air. However, it should be noted that, air voids should be kept at certain levels (3% - 5% at construction stage) in order to allow for expansion of binder under warmer weather conditions and allow for flexibility under the effect of vehicular loading (secondary compaction). Using dense gradation when designing the mix also contributes to the pavement durability by providing abovementioned characteristics and also by providing a closer contact between the aggregate particles which improves the impermeability of HMA (Sreedhar & Coleri, 2018).

Permeability of asphalt significantly influences the durability of pavement. There have been different types of asphalt pavement roads constructed depending on the challenge to design

the most suitable and superior performing asphalt pavements. Porous or stone matrix asphalt (SMA) for example, have higher permeability to allow the passage of water to the lower layers which will then be transported to the drainage systems. However, for a dense graded asphalt, permeability should aimed to be minimised to prevent the passage of water and air since this would cause moisture damage (in case of presence of water) and early oxidation (in case of presence of oxygen) which would result in early deterioration of the asphalt pavement. Permeability and the percentage of air voids are therefore mentioned in conjunction when designing a HMA (Nejad et al., 2010). It is useful to note that, the character of the air voids such as; the size of the voids, the number of voids and the proximity of voids to the surface layer determine the degree of permeability for the asphalt mix concrete. All designed asphalt mixtures would show a level of permeability that is inevitable, but fine as long as the air voids remain within the restricted limits for each type of HMA (Mohammad et al., 2003).

Workability of HMA refers to the practicality of asphalt concrete to be laid and compacted on the construction site. Workability of a mixture can be adjusted by changing the aggregate type and/or gradation. Mixes that have too much coarse aggregates tend to segregate during the pavement construction which also increases the compaction effort. Also, mixes having excessive fine aggregates may lead HMA to become very tough and gummy making the concrete difficult to work with (Gudimettla et al., 2004). Although being a minor contributor, the asphalt binder also has role that determines the workability of HMA. Asphalt binder with low viscosity, particularly in the cases of modified binders results in low mixing and compaction temperatures. Asphalt is said to be less workable at low temperatures since this increases the effort to mix and compact the HMA properly (Ali et al., 2014). On the other hand asphalt that is highly workable leads to a tender HMA. Highly tender asphalt is unstable for proper placement and compaction. Shortage of fine aggregates in the mix, smooth rounded aggregate particles and the presence of moisture in the HMA are the major causes for tender mixes (Teh & Hamzah, 2019).

Skid resistance is one of the important surface characteristics of asphalt that needs to be addressed when designing the HMA. Sufficient skid resistance should be attained in order to prevent vehicles from skidding on the road surface particularly in the presence of water (Kogbara et al., 2016). Adequate contact should be maintained between the tyres of the

vehicle and the aggregates rather than hydroplaning on the road surface for safety of the road users. A rough surface with small stone chippings is desirable rather than a smooth driving surface in order to increase skid resistance (Sullivan, 2005). In addition to that, a bleeding surface (rich in asphalt content) results in reduction of skid resistance therefore, although up to a certain point, more asphalt content in the mix provides more durable pavement, excessive usage may lead to thick film of asphalt on the surface layers leading to lower skid resistance (White, 2018).

2.4.2 Superpave mix design method

Superpave mix design method was developed during the SHRP in 1993. The method was a replacement for the Hveem and Marshall Mix design methods (Hung, 2018). The objective of Superpave was to enhance the selection of materials and the design of mixtures by developing a method of design that accounts for traffic loading and environmental conditions. On this basis, new approaches have been developed to determine the performance of asphalt binders and mixtures. (Bahia et al., 2001). The Superpave system has two key components which are; 1. Performance based asphalt binder specification, 2. Volumetric mix design and analysis (Hung, 2018). Pavements undergo various traffic loading conditions and they are also required to serve in a wide range of climatic conditions. On this basis, the Superpave method incorporated a new binder specification and a suitable asphalt binder selection is based on this system which is explained in Chapter 2.4.2.3.1. Superpave mixes are also based on volumetric properties. The characteristics of the aggregates and the volumetric properties of the mix are also integral part of the Superpave mix design and are as explained in Chapter 2.4.2.3.2 (Little et al., 2018).

2.4.2.1.1 Asphalt binder selection

The selection of suitable asphalt binder is based on a new binder specification that is produced during the development of Superpave mix design method. Asphalt binders are classified into performance grades based on a range of climates and pavement temperatures. The specification sets certain physical properties that binders must meet. The specific climatic conditions at the paving site was decisive on the temperature at which certain

properties must be achieved. (Lucas, 1997). Superpave binders are classified by PG for performance graded ratings. The rating contains two numbers indicating high and low pavement temperatures. For example, a “PG 64-22” used in a Superpave mix is expected to be resistant to rutting and cracking at pavement temperatures as high as 64°C and as low as -22°C respectively. Firstly, to choose the suitable Superpave binder, the average maximum temperature of seven days and the minimum pavement design temperature for a specific job site must be identified. Recorded air temperatures from weather stations are converted to anticipated pavement temperatures by using standardised formula in the Superpave mix design protocols (Khan et al., 2013). For pavements at extreme climatic conditions, asphalt cement may be required to be modified and this is specified by the performance grading specifications for asphalt binders and it is as expressed in Table 2.8 (Jadidirendi, 2017). However, modified or not, the PG binder should possess the required properties to perform as expected during the service life of asphalt pavement. Testing asphalt binders for conformance with the Superpave specification requires several new laboratory equipment as shown in Figure 2.15 (Kennedy et al., 1994). However, PG rated binders require no changes to standard methods of handling, storing and transporting asphalt binders (Kennedy et al., 1994).

2.4.2.1.2 Design aggregate structure

Superpave mixes are also based on volumetric properties. The characteristics of the aggregate are determinant on certain volumetric properties such as the voids in the mineral aggregates, voids filled with asphalt and the percentage of air voids in the total compacted mix. These properties form the basis for selecting aggregate gradation and asphalt binder content in the mix (Shen et al., 2005). The Superpave system bases aggregate selection on consensus properties that apply equally on all locations. They include; angularity of the coarse and fine aggregates, flat and elongated particles and the clay content. In addition, highway agencies determine source properties in light of local or source conditions. Source properties include; toughness, soundness and deleterious materials. These tests for measuring aggregate properties are not new and they have also been used as parts of the conventional mix design procedures (Alshamsi, 2006). Furthermore, it should be noted that, aggregate selection in the mix design is generally limited to locally available sources. In

order to improve the properties of the asphalt mix and the performance of the pavement, the Superpave mix design provides a means for determining the optimum aggregate structure or gradation. Gradations are defined using the Federal Highway Administration 0.45 power chart which is illustrated in Figure 2.18 (Choudhary et al., 2018).

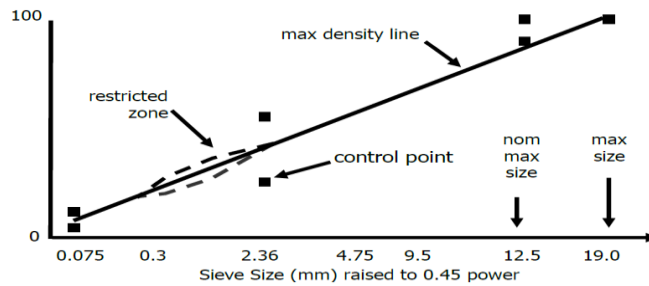


Figure 2.18: Federal Highway Administration 0.45 power chart

The chart is used to show the total particle size distribution for an aggregate blend. The chart is also useful in understanding how the aggregate particles fit together. The maximum density line is plotted from the origin through the maximum aggregate size (Kringos et al., 2013). The Superpave system adds two features to the 0.45 power chart namely the control points and the restricted zone. The control points serve as boundaries for the outer ranges of the sieves. Three sets of control points are plotted, one for the nominal maximum sieve, one for an intermediate sieve and one for the smallest sieve. Aggregate gradations must stay within the control points. The restricted zone is a warning zone providing a guideline for the mix designers. Gradations falling in the restricted zone may have excessive rounded natural sand. Mixes designed using such gradations often experience compaction problems during constructions and can be prone to rutting. For best design, mix designers should choose a gradation that falls between the control points and avoids the restricted zone (Read et al., 2003).

2.4.2.1.3 Sample preparation and compaction

Superpave mix design differs from Marshall Mix design not only by the addition of new testing methods but also in sample preparation and compaction type. A mechanical mixer is

used to mix the suitable PG grade asphalt binder and the designed aggregate structure. The mix is aged in an oven to simulate the aging that occurs during the construction process. The trial blends are evaluated by compacting the specimens and determining their volumetric properties (Peterson et al., 2004). The Superpave system uses a new method of laboratory compaction using a Superpave Gyrotory Compactor (SCG). SCG is reported to represent the actual field compaction better than the other compaction methods (Peterson et al., 2004). The asphalt mixture is loaded into a mould of 150mm in diameter. A ram loading system maintains a constant pressure of 600 kPa on the specimen. The mould is tilted at a slight angle of 1.25° and rotates while the load is being applied. The schematic showing the compaction method for SCG is illustrated in Figure 2.19 (Ismail et al., 2015). Three different gyration numbers are established in Superpave mix design. These are; the initial (N_{ini}), design (N_{des}) and maximum (N_{max}). N_{ini} is used as a measure of compactibility of the samples. Mixes that compact too quickly may result in tender mixes meaning that the proper construction is difficult and that, it will also be unstable under traffic loading during the service life. Commonly, mixes with excessive sand content fails this criteria (Dessouky et al., 2004). N_{des} is typically the design number of gyration and it is used to determine the OBC at 4% V_a in the mixture. N_{max} is used as a check to ensure that laboratory produced samples are not over densified since this would lower the air voids content in the total mix resulting in rutting failure (Mallick, 1999). The compaction levels depend on the expected traffic levels. Superpave specification states the required compaction levels and the allowable densities for dense graded asphalt concrete mix are demonstrated in Table 2.10 and Table 2.11 (Read et al., 2003).

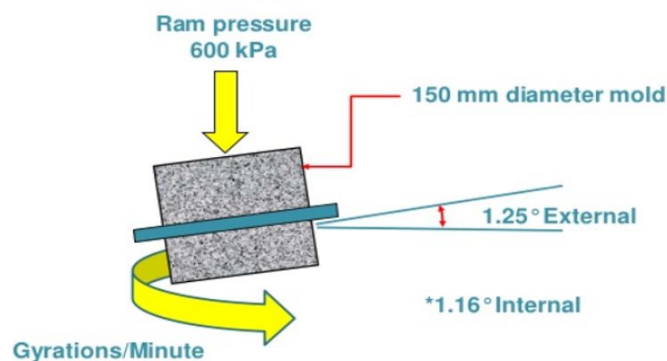


Figure 2.19: Superpave gyrotory compaction

Table 2.10: Superpave design compaction gyrations

20-yr Traffic Loading (in millions of ESALs)	Number of gyrations		
	Ninitial	Ndesign	Nmax
Less than 0.3	6	50	75
0.3-3	7	70	115
3-10	8	100	160
10-30	8	100	160
Greater than 30	9	125	205

Table 2.11: Superpave compaction density requirements

20-yr Traffic Loading (in millions of ESALs)	Required densities as percentage of TMD		
	Ninitial	Ndesign	Nmax
Less than 0.3	91.5	96	98
0.3-3	90.5	96	98
3-10	89	96	98
10-30	89	96	98
Greater than 30	89	96	98

Along with the asphalt binder selection and design aggregate structure volumetric properties of the mixture is integral part of the Superpave mix design procedure. With the aid of compacted samples by SCG and loose samples, specific gravities of the mixture are measured and therefore the volumetric properties are computed. Volumetric properties such as VMA, VFA and V_a are important parameters that define the optimum binder content for the mixture and they are also required to be within certain ranges depending on the aggregate structure and traffic loading conditions as specified in the Superpave mix design protocols (Read et al., 2003). These properties are explored in more detail in the following Chapter

2.4.3 HMA characteristics and behaviour

Hot mix asphalt is a composition of course aggregates, fine aggregates, asphalt binder and air voids. The density and volumetric analysis of these materials is an integral part of the mix design in order to decide the OBC to be used in the asphalt concrete mix with desirable properties. (Canestrari & Partl, 2015). As part of the Superpave mix design, voids analysis is performed to determine parameters such as VMA, VFA, V_a and Dust to asphalt ratio

(D/A). Figure 2.20 represents an asphalt concrete cross section and the volumetric phase diagram. Voids analysis is computed by measuring the specific gravities of aggregates, asphalt binder and the compacted mix samples in the laboratory environment (Bargegol et al., 2020).

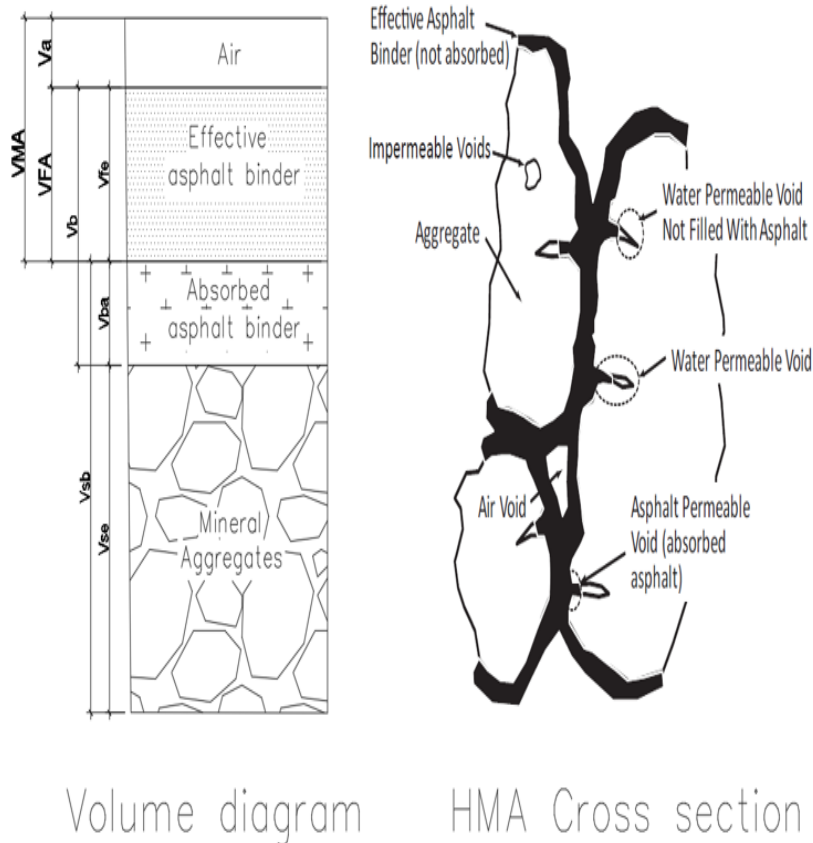



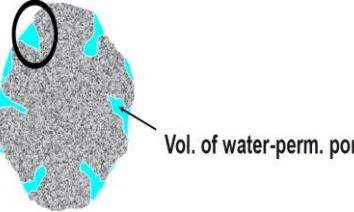
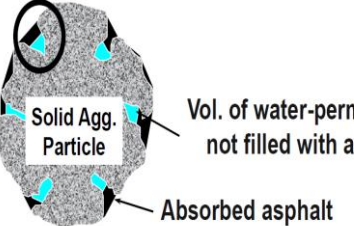
Figure 2.20: Compacted asphalt concrete cross section and volumetric phase diagram

2.4.3.1 Specific gravities

2.4.3.1.1 Specific gravity of aggregates

Specific gravity of an aggregate is defined as the ratio of the weight of aggregate to an equal volume of water at 23°C (Read et al., 2003). Three different specific gravities of aggregates are essential to understand the asphalt absorption level of aggregates in the asphalt concrete mix. These are the apparent specific gravity (G_{sa}), bulk specific gravity (G_{sb}) and effective specific gravity (G_{se}). The relationship between apparent, bulk and effective specific gravities of aggregates is demonstrated in Table 2.12 (Leckie & Beeson, 2018).

Table 2.12: Apparent, bulk and effective specific gravities of aggregates

Specific Gravity	Illustration	Formula
Apparent specific gravity		$G_{sa} = \frac{\text{Mass of oven dry agg.}}{\text{Vol. of agg.}}$
Bulk specific gravity	<p>Surface Voids</p>  <p>Vol. of water-perm. poi</p>	$G_{sb} = \frac{\text{Mass of oven dry agg.}}{\text{Vol. of agg. + Perm. pores}}$
Effective specific gravity	<p>Surface Voids</p>  <p>Solid Agg. Particle</p> <p>Vol. of water-perm not filled with a</p> <p>Absorbed asphalt</p>	$G_{se} = \frac{\text{Mass of oven dry agg.}}{\text{Vol. of agg. + Pores not absorb by asphalt}}$

Specific gravity of aggregates is used in Superpave mix design since, the aggregates asphalt absorption level is crucial to be known in order to estimate the effective asphalt binder content to be used in the mix design (Jadidirendi, 2017). Although mix design is a volumetric process, weights of the mix constituents are measured and then converted to volumes by using specific gravities. Accurate measurement of specific gravities is essential in the mix design since small changes may result in extreme alterations in the volumetric properties of asphalt mix concrete thus, leading to incorrect mix design proportions (Handbook, 2007). Aggregate absorption level is a major factor influencing the specific gravity of the total mixture. Aggregates which have high permeable surface voids, have higher mass due to water that is filled in the surface pores. Too high absorption level of aggregates leads to undurable asphalt pavements. Also, this indicates that, less binder is available to coat the aggregates thus, increases the total bitumen that is needed to be used in the total mixture (Read et al., 2003).

2.4.3.1.2 Bulk Specific Gravity

The bulk specific gravity (G_{mb}) of an asphalt mixture is used in the calculation of critical asphalt concrete mix parameters. G_{mb} has direct influence on parameters such as V_a and VMA and it is indirectly used in the calculation of the VFA (Garber & Hoel, 2014).

There have been numerous methods developed to measure G_{mb} of compacted asphalt mix samples. A common method to determine the G_{mb} of asphalt mixture is by calculating the compacted asphalt mix samples volume by subtracting the mass of specimen in water from the mass of a Saturated Surface Dry (SSD) conditioned specimen. SSD condition means that the samples internal air voids are filled with water while surface pores are dry. For this approach, a critical issue is that, if the air void content of the designed mix is high such as in the case in porous asphalt design, the water that fills the internal pores of the mixture drains out quickly as the sample is taken out from the water which may lead to inaccurate G_{mb} measurement (Li et al., 2011).

Other methods that have been used to measure G_{mb} of asphalt mixture includes, the water displacement method, Paraffin, Parafilm and Corelok techniques. The water displacement method is based on the Archimedes principle. The sample is weighted in a water bath and then out of the water bath and the difference in weights are used to find the amount of water displaced which is then converted to volume by using the specific gravity of water. The Paraffin method is a similar technique to water displacement method where melted paraffin wax is used instead of water since the wax is less likely to drain out after it is set. Another method to determine the G_{mb} is the Parafilm method. In this method, the sample is covered with a Parafilm and weighted in and out of the water. This allows better volume measurement since no water can penetrate inside the sample. Corelok is a more advanced version of Parafilm technique which the sample is sealed with a high quality plastic bag that is shrink-wrapped in a vacuum chamber. Although these techniques are used and theoretically produce reliable results, the application is difficult in practice and the test results are generally inconsistent. On this basis, the SSD conditioned G_{mb} measurements have been found to provide the most accurate and consistent results (Handbook, 2007).

The parameters that are measured with the SSD method are the G_{mb} and the percentage of water absorbed by volume. Typical values of G_{mb} for asphalt concrete mix are in the range

of 2.200-2.500 depending on the G_{mb} of aggregates, the compaction level and the bitumen content in the mix. Absorption level is typically below 2%. If test results reveal higher absorption levels then the paraffin technique is suggested to be performed rather than the SSD method (Nicholls et al., 2006).

2.4.3.1.3 Theoretical Maximum Specific Gravity

Theoretical Maximum Specific Gravity (G_{mm}) of a hot mix asphalt is the void less specific gravity of the mixture. G_{mm} can be multiplied by the density of water to obtain the density of the mixture, also referred to as the “Rice” density which was named after the founder of the test method (Mamlouk & Zaniewski, 2006). G_{mm} is a critical parameter in the hot mix asphalt design since it is used along with the bulk specific gravity to calculate the total air voids in the mixture. G_{mm} is also used in the assessment of compaction level for the HMA. In addition to that, using the G_{mm} , the amount of asphalt absorbed and therefore, the effective asphalt content can be calculated (Habib, 2013).

The basic principle of G_{mm} is to divide the mass of the loose sample, excluding air voids, by the volume of the sample. To determine its dry mass, a loose sample of HMA is weighed in dry condition, and then the Rice method procedure is used to determine the volume of the sample. The theoretical maximum specific gravity is then divided by its volume by the sample mass. Rice method procedure is applied to remove the air that is entrapped in the loose sample. The sample is placed inside a container and filled with water slightly above the sample level. Then a vacuuming process at 3.7 kPa is applied on the sample for 15 minutes together with an agitating movement of the container by virtue of the experimental set up to completely remove the air between the loose sample. After the Rice method procedure, the sample is either weighed in water or in air to calculate the volume of the sample and hence the G_{mm} .

Typical values for G_{mm} is between 2.400-2.700 depending on the specific gravities of aggregates and the bitumen content. It is observed in a number of studies that, extremely heavy or light aggregates in the mix may result in G_{mm} values outside the abovementioned range. Similar to G_{mb} , G_{mm} has no direct relation and influence on the performance properties of HMA however, the significance of determining the specific gravity of the mixes is that

they are essential to correctly proportion the volumetric properties which affect the overall performance of the asphalt mix concrete (Nicholls et al., 2006).

2.4.3.2 Air voids in mixture

Air void content (V_a) is one of the most important volumetric parameters that is considered in the mix design. It is expressed as a ratio of the total volume of air voids to the bulk volume of the compacted asphalt mix concrete. V_a in the asphalt mix is the pockets of air between the asphalt coated aggregate particles (Kushwaha & Swami, 2019). G_{mb} and G_{mm} of the asphalt mix are used in determining the air void content. The amount of air voids in the mix has a significant influence on the asphalt concrete pavement performance. The asphalt mix can be susceptible to water and air penetration if the air void content of the mix is high (above 8 percent), resulting in moisture damage and lower resistance to ageing. On the contrary, low asphalt content indicates to more asphalt binder usage in the mix which may result in bleeding and plastic deformation. Studies showed that, mixes that have air void content less than 2%-3% are likely to be prone to bleeding and rutting failure. The Superpave mix design method suggests that, providing that other volumetric parameter specifications are met, total air void content should be targeted to be close to 4% when designing the hot mix asphalt. The amount of V_a in the mix can be controlled by increasing or decreasing the fines proportion in the mix and/or increasing the binder content and by changing the gradation used for the mix (Karahancer et al., 2016).

2.4.3.3 Voids in mineral aggregates

The amount of void space between the aggregate particles and the effective asphalt binder which the aggregates do not absorb makes up the voids in the mineral aggregates (VMA) (McGennis et al., 1995). VMA is calculated as a percentage of the compacted asphalt mix's total volume. Since the total air void content is aimed to be close to 4%, VMA has significant role for determining the OBC for HMA. Higher values of VMA are preferable since, more space would be available to accommodate the effective binder content thus increasing the durability of the pavement. On this basis, Superpave mix design protocols restricts the lower

limits for VMA of a mixture based on the choice of nominal maximum aggregate size (See Table 2.13) (Read et al., 2003).

Table 2.13: Superpave hot mix asphalt VMA requirements

Nominal Maximum Aggregate Size (mm)	Minimum VMA requirement (%)
9.5	15.0
12.5	14.0
19.0	13.0
25.0	12.0
37.5	11.0

It should be noted that, mixes that have excessively high VMA is likely to have unacceptable low stability. On the other hand, if VMA is below the minimum requirements, there will be insufficient room in the mixture to accommodate enough bitumen to coat the aggregate particles. (Garber & Hoel, 2014). Mix designers often attempt to lower the VMA in order to lower the economic costs in mix production by lowering the amount of bitumen used in the mix design however, it has been found to be non-effective and more detrimental to pavement quality since mixes with a low VMA are more sensitive to small changes OBC (Rahman, 2004). The gradation selection for the mix design has significant role on the VMA of the asphalt mixture. Particularly, the use of fine aggregate fractions influences the VMA. Fine aggregates present in the mix tend to be absorbed by the asphalt and this causes increase in the bulk volume resulting in lower VMA(Read et al., 2003).

2.4.3.4 Voids filled with asphalt

The voids filled with asphalt (VFA) is the proportion of the VMA that contains the effective asphalt binder. It is expressed as a percentage of the VMA. Superpave specification limits the minimum VMA requirements due to durability concerns however, there are no specifications for the maximum VMA limits. The VFA requirement in the Superpave specification is due to limiting the maximum limits for the VMA since excessive VMA would cause stability concerns. On this basis, it can be said that, VFA, VMA, the binder content and the air void content in the mix are directly related. VFA is inversely related to

air voids (McGennis et al., 1995). According to the Superpave specifications the VFA requirement is based on the expected traffic loading and it is as demonstrated in Table 2.14 (Scarpas et al., 2012). The aim of VFA in light traffic situations is to avoid less durable HMA resulting from thin binder films on the aggregate particles. With a relatively low percentage of air voids, HMA intended for heavy traffic volumes may also not pass the VFA requirement even if the amount of air voids is within the appropriate range. The VFA requirement helps to avoid mixes that are vulnerable to rutting in heavy traffic situations because the low air void contents can be very important in terms of permanent deformation. (Mamlouk & Zaniewski, 2006).

Table 2.14: Superpave hot mix asphalt VFA requirements

Traffic 10⁶ ESAL's	Range of VFA (%)
<0.3	70-80
<1	65-78
<3	65-75
>3	65-75

2.4.3.5 Dust to asphalt ratio

Dust proportion in the mix which is also referred to as dust to asphalt ratio (D/A) is another parameter that was included in the Superpave mix design. D/A is defined as the ratio of the fine aggregates (aggregates that pass through the 0.75mm sieve) to the effective asphalt content (Al-Bayati & Tighe). According to the Superpave criteria, D/A is restricted to be in a range from 0.6-1.2. The effective asphalt content is used in the computation of D/A rather than the total asphalt content. The purpose for this is to limit the absorption level of bitumen by the aggregates since D/A results would be higher when computed using the effective asphalt content. FHWA's Asphalt Mixture Expert Task Group and the AASHTO Lead States also suggested that the criteria set for the D/A ratio in the Superpave specifications should be changed to 0.8-1.6 in the case of utilizing course aggregate gradation for the mix (Guide, 2001). The amount of fines or dust in the mix has significant influence on the VMA. An increase in the VMA is observed by lowering the dust proportion in the mix. This also indicates that, more asphalt binder is required due to increased VMA (Guide, 2001). Another parameter that has a relation to D/A ratio is a performance based characteristic which is the

rutting resistance. Based on findings of previously conducted study, the amount of rut depth that occurs in the HMA decreases significantly by increasing the D/A ratio in the mix (Cooley Jr et al., 2002). It should also be noted that, along with the amount of dust proportion in the asphalt mix, the aggregate type and the particle surface texture also has an influence on the rutting resistance as observed from the findings of (Cooley Jr et al., 2002) that, limestone and granite sources of aggregates yielded different results.

2.4.3.6 Optimum binder content

The amount of asphalt binder and air voids in the mixture are the most critical parameters when designing the hot mix asphalt and they form the basis of volumetric features. It is crucial to determine the binder content accurately in the laboratory environment and control it precisely during the manufacturing process in the production plant (Little et al., 2018). The optimum binder content is strongly dependent on the aggregate gradation. Mixes designed with fine aggregates require more binder due to increased aggregate surface area and inversely mixes designed with courser aggregates require less asphalt binder since, HMA with courser aggregates would have less total aggregate surface area (Read et al., 2003). Also the absorption level of the aggregates is a critical factor affecting the optimum binder content. Asphalt binder that is absorbed by the aggregates do not contribute to increasing the strength of the mix rather, it simply increases the cost of production since sufficient asphalt is still required to coat the aggregates that would provide the binding action (Mamlouk & Zaniewski, 2006). Asphalt binder content (P_b) and the effective asphalt binder content (P_{be}) are the terms used when determining the optimum binder content where, P_b is the term used for the total asphalt used in the mix design and P_{be} is the term used to express the available asphalt binder that coats the aggregates. Effective binder content is calculated based on the G_{sb} and the G_{se} of the aggregates. The higher the aggregate absorption, the greater would be the difference between G_{se} and G_{sb} (Read et al., 2003).

Determining the optimum binder content is an iterative laboratory testing procedure. Several trial mixes that are expected to have binder content that is close to the optimum binder content are prepared and tested for other volumetric properties. Mixes that satisfy the volumetric conditions and have air void content close to 4% are considered in the

determination of the optimum binder content (West et al., 2013). The air void content and the binder content used in the mix design are strongly related. Increasing the asphalt binder content leads to lower air void content and the opposite is versa. Increasing the asphalt binder enhances the durability of the mixture however, beyond certain point strength and stability of the mix gets reduced in excessive binder content usage which is illustrated in Figure 2.21 (Al-Mosawe & Thom, 2016).

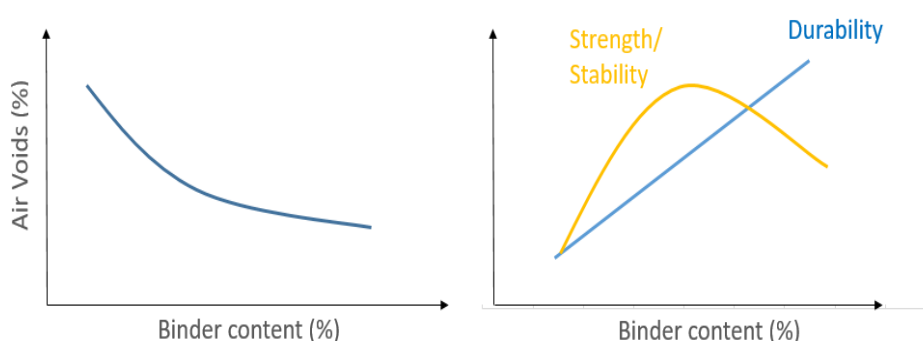


Figure 2.21: Relationship between air voids and asphalt content in the HMA

It is reported in numerous studies that, increasing the asphalt content more than the required optimum content not only leads to an uneconomical mix design but also makes asphalt concrete prone to bleeding and permanent deformation from the standpoint of appearance and performance. On the other hand, using a lower than required bitumen content will lead to a dry, stiff mixture that is difficult to place and compact and also be vulnerable to cracking and durability problems while having lower resistance to fatigue. (Dalhat et al., 2020). Since the air voids and the binder content in the mix are inversely related, the primary objective of the mix design is to find the fine balance between the two parameters to produce durable and stable mixes that possess desired performance characteristics.

2.4.4 HMA Moisture susceptibility

Moisture susceptibility is a major form of distress for a HMA which occurs because of the weakening of the adhesion bond between the mineral aggregates and the asphalt binder due

to the penetration of water and moisture into the HMA (Ali et al., 2018). It is crucially important to control the infiltration of water into the HMA to avoid moisture induced damage which results in failure of asphalt concrete against stripping and ravelling due to loss of adhesion between the asphalt binder and the mineral aggregates (Omar et al., 2020). Factors influencing the moisture susceptibility of HMA include; the mechanical and chemical properties of the aggregates and the asphalt binder, molecular orientation of the particles and the adhesion tension forces between the aggregates and the asphalt binder. However, moisture susceptibility is a complex phenomenon and therefore, by using physical testing procedures, it is difficult to determine which of the above mentioned mechanisms is the primary trigger to moisture damage (Caro et al., 2008). Common methods to reduce moisture susceptibility that have been proposed by numerous researches in the literature are; reducing the air void content of the HMA design to mitigate the penetration of water or using additives to modify the asphalt cement. Air void content of the HMA can be controlled by adjusting the aggregate gradation, bitumen content and the mixing and compaction conditions. Also, additives such as anti-stripping agents, hydrated lime, fly ash, crumb rubber, polymers and nanomaterials when used as modifiers to asphalt enhances the adhesion between the bitumen and aggregate and reduces the moisture induced damage for the HMA (Omar et al., 2020). To measure the moisture susceptibility of HMA, different test methods are available. Moisture damage of asphalt mixtures can be estimated by visual tests such as stripping tests, chemically by the image analysis techniques by using dedicated software or deterministic testing methods. Among these methods, a deterministic testing method that utilizes the modified lottman conditioning process which is then followed by the indirect tension test has been the most popular technique to assess the moisture susceptibility of HMA (Solaimanian et al., 2007). In the modified lottman test, the samples are subjected to partial vacuum saturation and optionally freeze and thaw cycles. After the modified lottman procedures, the conditioned and unconditioned samples are subjected to indirect tension test and the ratio between the tensile strength of the conditioned sample to the unconditioned sample is evaluated. According to Superpave specifications, a minimum ratio of 0.8 indicates that, the HMA demonstrates resistance to moisture damage (Hamedi et al., 2015).

CHAPTER 3

EXPERIMENTAL PROCEDURES AND DATA ANALYSIS

3.1 Materials and Sample Preparation

The virgin binder that was used as the base asphalt (also referred to as the control sample) was 80/100 penetration grade and it was obtained from Petronas Petroleum/ Malaysia. The type of polymer used in the modification process was an elastomeric polymer named Acrylate-Styrene-Acrylonitrile (ASA). ASA was used at 5% concentration by the weight of base binder since research conducted previously in the literature by (Ali et al., 2015) and (Mubaraki, 2019) reported this finding as the optimum polymer content to modify virgin asphalt. Current study introduced two different nanomaterials, nano silica (SiO_2) and nano iron dioxide (Fe_3O_4) which were added in the ASA modified asphalt to further form two different polymer-nanocomposite modified asphalt cements (PNCMAC). Physical properties of the abovementioned materials are provided in Table 3.1.

Hot melting technique was used to blend ASA- SiO_2 and ASA- Fe_3O_4 at 3%, 5% and 7% concentrations by the wt. of polymer modified AC. A high shear mixer was used to blend the PNCMAC's at 5000 rotations per minute (rpm) at $165^\circ\text{C} \pm 3^\circ\text{C}$ for 60 minutes. The shear rate, duration and the temperature at which the blending process was performed were selected by reviewing the previous research conducted with relevant materials and also by conducting the softening point analysis. Stabilisation of the softening point values was considered as an indication of fine dispersion of particles in the modified blends and hence selected as the optimum conditions for the blending process.

The design of hot mix asphalt (HMA) included finding the optimum binder content (OBC) by targeting 4% air voids and certain volumetric properties in 1100 gram of dense graded mixture samples prepared by using granite aggregates with AC-14 gradation. A laboratory asphalt mixer was used to mix the AC with mineral aggregates. Two different conditioning of samples were used in the testing and evaluation of HMA which were the loose samples and the compacted samples. Compaction process was performed with a SuperPave gyratory compactor by utilizing Superpave testing protocols. The design of HMA including the

aggregate properties, volumetric design and OBC is further explained in Chapter 3.4 in more detail.

Table 3.1: Physical properties of the base binder and the modifiers

Properties	Nano-Silica	Nano-Ironoxide
Formula	SiO ₂	Fe ₃ O ₄
Molecular Weight	6.3-6.49	N/A
Colour and Odour	White	Brown Powder/odourless
Form	Nano powder	Nano powder
Purity	0.9999	0.99
Average nanoparticle size (nm)	30- 50	60-80
Bulk Density (g/cm ³)	N/A	0.68
Melting Point (°C)	1600	1566
Solubility in Water	Insoluble	N/A

3.2 Testing Procedures

The laboratory testing standards for asphalt binders which were described in American Association of State Highway and Transportation Officials (AASHTO) and American Society for Testing and Materials (ASTM) standards were utilised in the investigation of physical and rheology related properties of PNCMAC's while, for the performance characteristics testing of HMA, SuperPave testing procedures were followed. The summary of the adopted procedures and a review of the latest advancements in the laboratory testing for asphalt binder and mixture procedures are provided in Chapter 2.3 and 2.4. The prepared samples were tested under fresh, short-term ageing and long-term ageing conditions. Rolling thin film oven (RTFO) and Pressure aging vessel (PAV) were used in the simulation of short-term and long-term ageing of samples. Conditioned samples were referred to as RTFO samples and PAV samples within the text. Each test was performed with at least 3 repetitions and average values were recorded in order to improve consistency of the results obtained. Experimental procedures and the number of tests conducted for asphalt binders and mixtures are demonstrated in Tables 3.2 and 3.3 respectively.

Table 3.2: Testing procedures for asphalt binders

Category	Test	Number of tests conducted									Total number of tests
		Base AC Condition			Base AC+ASA 5%+ SiO ₂ Condition			Base AC+ASA 5%+ Fe ₃ O ₄ Condition			
		Unaged	RTFO	PAV	Unaged	RTFO	PAV	Unaged	RTFO	PAV	
Physical tests	Penetration	3	-	-	9	-	-	9	-	-	312
	Softening point	3	3	-	9	9	-	9	9	-	
	Rotational viscosity	3	3	-	9	9	-	9	9	-	
	Ductility	3	-	-	9	9	-	9	9	-	
Temperature Sensitivity	Storage stability	3	-	-	9	-	-	9	-	-	
Chemical characterisation	XRD	3	-	-	9	-	-	9	-	-	
	FTIR	3	3	-	9	9	-	9	9	-	
Rheology	Frequency sweep	3	3	3	9	9	9	9	9	9	
	MSCR	-	3	-	-	9	-	-	9	-	

Table 3.3: Testing procedures for hot mix asphalt concrete

Category	Test	Number of tests conducted						Total number of tests
		Base AC		Base AC+ASA 5%+ SiO ₂ 5%		Base AC+ASA 5%+ Fe ₃ O ₄ 3%		
		Loose	Compacted	Loose	Compacted	Loose	Compacted	
Optimum binder content	Bulk specific gravity	12	12	12	12	12	12	198
	Maximum theoretical specific gravity	12	12	12	12	12	12	
Volumetric properties	Bulk specific gravity	3	3	3	3	3	3	
	Maximum theoretical specific gravity	3	3	3	3	3	3	
Moisture susceptibility	Indirect tension test	-	6	-	6	-	6	

3.2.1 Penetration test

The penetration test is an empirical testing procedure to determine consistency (hardness or softness) of bitumen samples. It measures the depth in tenths of a millimetre that a standard loaded needle (100g) penetrates into a sample prepared in a container at a depth at least 15 mm in excess of the expected penetration for 5 seconds. The apparatus assembly is as illustrated in Figure 3.1. Historically, penetration test was adopted in performance grading specifications. However, with the advancements in the assessment methods for rheology testing after SHRP, it has been started to be used as an independent traditional measure rather than performance grading of bitumen. Penetration grading being a single point measure at 25 °C and the empirical nature of testing method was found to be inefficient in deriving a meaningful engineering property (Kim, 2008). On this basis, penetration was used as a measure of solitary physical property in the bitumen characterization. Test method was followed as described in ASTM D-5.

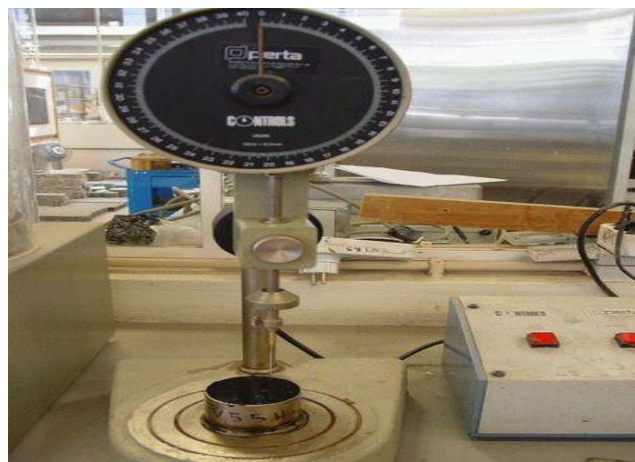


Figure 3.1: Penetration test apparatus assembly

3.2.2 Ring and ball softening point

Softening point was used as an index of consistency. The temperature at which the bitumen changes from semi-solid to liquid phase is defined as the softening point of the sample. ASTM D-36 was adopted in the softening point testing procedure. The recordings were measured as the temperature at which a steel ball passes through the bitumen sample in a

mould and falls through a height of 25mm when heated at a constant rate of 5°C per minute in water or glycerine (asphalt with softening point greater than 80 °C) heating medium. The test assembly is illustrated in Figure 3.2. Previously, softening point, a single point measure at 65°C has been attempted to be correlated with other conventional parameters (penetration and viscosity) in order to deriving rheological properties of bitumen however, these correlations mostly suffered from lack of generalization and low statistical significance (Kim, 2008). Therefore, herein, the test was used in the assessment of the stability of modified asphalt binders.

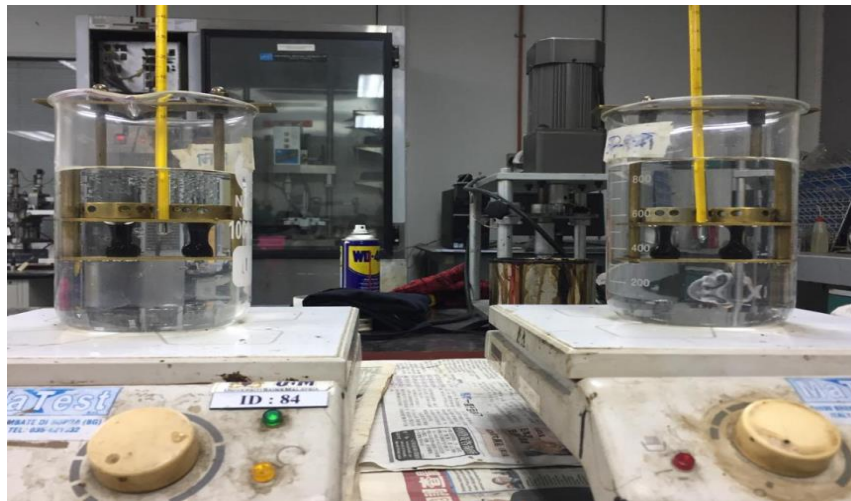


Figure 3.2: Ring and ball softening point test

3.2.3 Rotational viscosity

Viscosity refers to the fluidity of an asphalt which is denoted as the measure of materials resistance to flow. The viscosity test was utilized to assess the workability of AC during the pumping at the manufacturing process and practicality of handling of AC at the construction stage. A number of researchers in the past have attempted to relate viscosity along with other conventional physical properties to determine stiffness of AC however, their results were not satisfactory to describe such property (Read et al., 2003). Recent standards such as Superpave adopted viscosity as a measure for determining the mixing and compaction temperatures in the design of HMA. The RV test was performed according to the ASTM D4402 using a Brookfield viscometer with an inner concentric cylinder (as shown in Figure

3.3). Measurements for viscosity values were taken at every 15°C increments once the readings were stabilised within a range of temperatures between 120°C and 180°C in order to observe the variation in viscosity values at elevated temperatures and under constant rotation action at 20 rpm. The tests were performed on samples in fresh and short-term aged states to further assess aging behaviour because of loss of volatiles during the production and construction of AC in the field.



Figure 3.3: Rotational viscosity test

3.2.4 Ductility

Ductility is a characteristic of asphalt by virtue of which it can be elongated without breaking apart. The bituminous binder used in road construction should be ductile such that, it can take up the deflections that occur in them. Standards followed in the ductility measurement was ASTM D-113. The prepared samples were poured into briquette moulds of two ends of which one end was fixed and the other end was moving with a speed of 5 cm/min. Tests were conducted in water bath at uniform constant temperature at 25 °C. The testing procedure was as illustrated in Figure 3.4. The distance which the asphalt sample split upon pulling in the ductility apparatus was noted in cm. Ductility test results provided insight to creep behaviour and tensile properties for bituminous binders. However, like traditional methods of testing for physical properties of binders, this test has limited use since it is empirical and conducted at only one temperature (Read et al., 2003).



Figure 3.4: Ductility test

3.2.5 Storage stability test

The storage stability was used to assess the integrity and homogeneity of AC during storage at high temperatures in the production facility and while transporting the materials to the on-site. Since asphalt cement is a composite material, because of the different chemical composition, solubility and density of the polymer, nanomaterials and virgin asphalt and its constituents, the lighter components rise to the top portion. Eventually, instability of modified binders leads to phase separation and unreliable performance of asphalt pavements (Alhamali et al., 2015). The test procedure was followed by emptying prepared samples into the aluminium foil tubes which have a diameter of 3cm and a height of 16cm. Top of the aluminium tubes were closed and rested in an oven at ± 163 °C for 2 days in vertical position. After removing the tubes from the oven, the tubes were cooled down at room temperature and were split into 3 equal sections which the upper and lower third sections were taken for the softening point investigation. The test results were evaluated based on ASTM-D 5892.

3.2.6 Morphology analysis

3.2.6.1 XRD

XRD was a powerful method that was used to characterize the microstructure of asphalt binders. XRD provided insight about the crystalline and amorphous structure of the polymer nanocomposites which was essential to understand the level of reaction between the bitumen and the added modifiers (Ali et al., 2015). Nanomaterial and polymer interaction was further

assessed by measuring the difference in the interlayer spacing of the layered structure of nanomaterials. Evaluation of interlayer spacing enabled to explain the diffusivity of modifiers in the blends as well as to measure the morphological formation of intercalated and exfoliated polymer-nanocomposite structures (Zhu et al., 2014). The principle used by the XRD is demonstrated in Figure 3.5 and the calculation for the interlayer spacing between the particles using the Bragg's law is expressed in eq. 3.1 (Golestani et al., 2012).

$$2d_{001} \sin(\theta) = \gamma \quad (3.1)$$

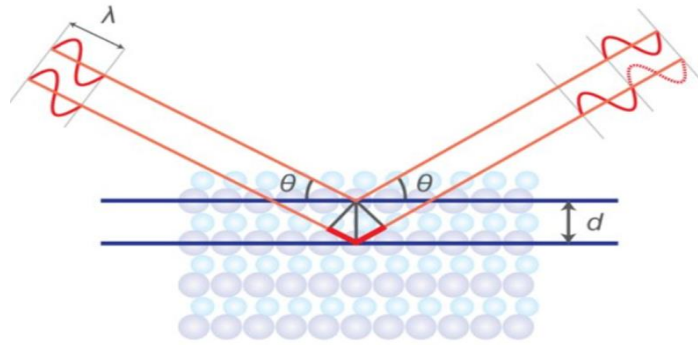


Figure 3.5: X-ray crystallography

Where, d_{001} is the spacing between the nanomaterial layers in the composite blends, θ is the diffraction angle and γ is the constant wavelength used by the diffractometer.

XRD test results were used in combination with the FT-IR analysis in order to characterize the microstructure of modified binders with the pursuit to understand the changes in rheological behaviour under various conditions. The XRD spectra were obtained with a diffractometer which imposed CuK α radiation ($k = 1.54 \text{ \AA}$) at room temperature. The scans were performed from 10° - 90° in the 2θ angle range. The scanning rate was $2^\circ/\text{minute}$.

3.2.6.2 Fourier-transform infrared spectroscopy (FTIR)

FTIR technique was used to observe the formation of new structural and functional groups due to interaction between base bitumen and the polymer nanocomposites. Through

identification of vibrational energy of molecules, FTIR detected the presence of base bitumen components and the molecules belonging to the modifier materials (Yusoff et al., 2019). The absorbed wavelength of the reflected beam represented specific functional groups and also aided in identifying the degree of chemical bonding. The technique was able to provide information regarding to chemical changes in the structural groups such as aromaticity and aliphaticity and also enabled to observe and quantitatively analyse the level of newly formed chemical structures; Carbonyl and sulfoxide in the assessment of aging resistance of modified binders. (H. Wang et al., 2020). The FTIR analysis was run on a Perkin Elmer spectrometer in the attenuated total reflectance (ATR) mode. The FTIR spectra was obtained in wavelengths from 600-4000 cm^{-1} at room temperature. The small samples of a drop size were prepared in blended phase and placed on top of the ATR crystal. FTIR machine attained the transmitted wavelengths of specific molecules by using the protocol described in Figure 3.6. The percentage transmittance were later converted to absorbance using eq. 3.2 in order to evaluate the volatilisation and oxygenation aging indexes by using a dedicated software; OriginPro version 9.0 which aided in the calculation of areas under the specific wavelength regions in the absorbance wavelength graph by using the integral area method (Hofko et al., 2018).

$$\% \text{ Absorbance} = 2 - \log(\% \text{ Transmittance}) \quad (3.2)$$

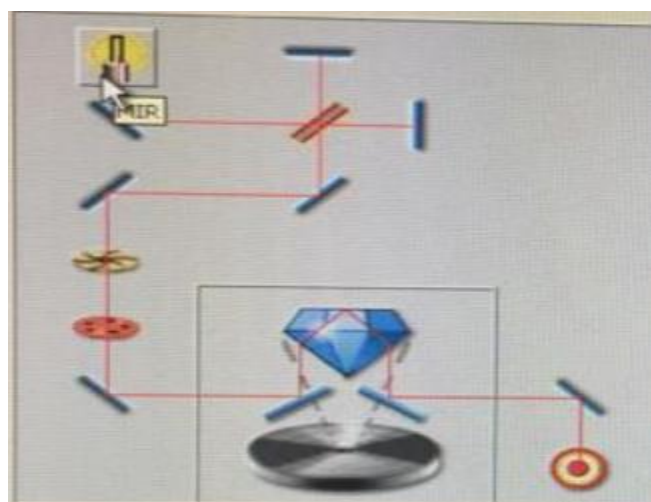


Figure 3.6: FTIR working principle

3.2.7 Sample conditioning

3.2.7.1 Short-term ageing

Short term ageing is referred to the condition when bituminous binders undergo irreversible property change due to the effect of heat and air during the mixing and paving operations (Lolly et al., 2017). A rolling thin film oven (RTFO) was used to simulate the short-term ageing behaviour to ensure that the “as-laid” properties of asphalt pavements meet the desired performance characteristics. The conditioning process was performed by following procedures in the ASTM D-2872. Pre-heated samples were filled into eight open mouth glasses by 35g in each bottle and placed into a carousel equipped oven as shown in Figure 3.7. The oven was set to rotate the glass bottles at 15 rpm for 85 minutes at 163°C under air blown pressure of 4 psi. The rotation action of the carousel enabled dispersion of asphalt particles while, a jet of air was blown at 4 psi at each rotation imitated the oxidation process. The test temperature was of a debate matter among numerous researchers. The test has been validated for virgin asphalt which undergoes mixing and laying temperatures commonly in the range of 160°C-170°C. In the case of modified binders where the viscosity values and hence, the mixing and compaction temperatures are increased significantly therefore, validity of the testing procedure has been questioned and several methods referred to as modified rolling thin film oven test (M-RTFO) was adopted in the literature (F. Wang et al., 2020). However, these efforts are not yet to replace the conventional RTFO test due to reliability issues such that RTFO testing is still the universally accepted technique that proved to represent the actual in-situ conditions and therefore, it was adopted within the scope of the experimental study herein (Southern, 2015).

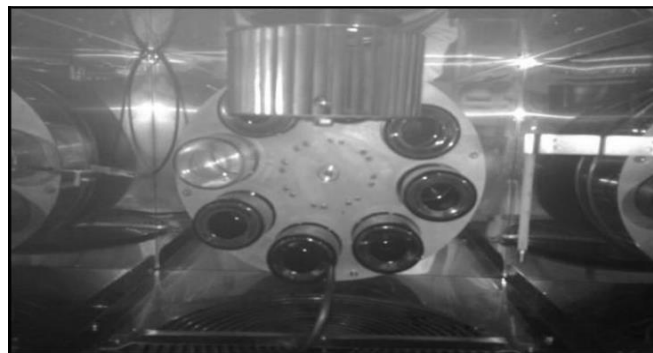


Figure 3.7: Rolling thin film oven test

3.2.7.2 Long-term ageing

Major forms of distresses that occur in pavements initiate and become intensive in the later times during the service life of pavements. Oxidation is a major factor that accounts for the long term aging of asphalt roads (Liu et al., 2019). Therefore a test method called the Pressure Aging Vessel (PAV) has been developed during the SHRP in order to imitate the long-term aging in pavements that occurs due to oxidation over a 7-10 year period. In the process of PAV aging, the short-term aged samples were used. Immediately after short-term conditioning, the samples which weight 50g were placed into special trays and placed in a heated, pressurised aging vessel for 20 hours at 300 psi. The test temperature selection varied depending on the climatic conditions. 90°C, 100°C or 110°C were chosen to represent cold, moderate and hot climate conditions respectively. ASTM D-6521 was the standard followed in PAV aging of samples. In the field application, the effect of long-term aging depends on several parameters eg; the thickness of asphalt layer and the volumetric characteristics of the HMA. In addition to that, PAV simulation in the laboratory does not account for the rate of aging due to ultraviolet radiation (Southern, 2015). Although, aforementioned disadvantages, PAV aging has been considered as the best method for simulating the long-term aging in asphalt binders considering the reasonable divergence between field observations and laboratory simulations for long-term aging of asphalt (Smith et al., 2019). Since fatigue and thermal cracking failures are of the primary concern in the long-term aged asphalt pavements, upon conditioning in the PAV, samples were taken to be tested in dynamic shear and bending beam rheometers in the evaluation of intermediate and low temperature performance characteristics of AC.

3.2.8 Dynamic shear rheometer

3.2.8.1 Frequency sweep test

A dynamic shear rheometer (DSR) shown in Figure 3.8, was used to conduct the frequency sweep tests. The tests were performed under strain controlled condition within linear viscoelastic region by applying stress in sinusoidal wave form which created a shearing action with oscillatory movements of fixed (bottom) and oscillating (top) plates of the DSR. The focus of the tests was to determine viscous and elastic components of asphalt binders

which constituted the rheological properties. Complex shear modulus (G^*) and phase angle (δ) were the two parameters revealed by the frequency sweep tests. G^* is the materials resistance to permanent deformation while δ is the lag between the applied shear stress and the resulted shear strain (Alas & Ali, 2019). Asphalt being a viscoelastic material refer that, its rheological behavior is dependent on frequency and temperature. Therefore the frequency sweep tests were performed at temperatures ranging from 10°C to 82°C with 6°C increments and a range of frequencies between 0.159 Hz and 15.92 Hz, where the former represented the anticipated field temperatures and the latter simulated the speed of traffic up to 90 km/hr (Ramadan & Abo-Qudais, 2017). The test was run in two phases. The high temperature characteristics for the asphalt binders were measured between 46°C - 82°C with a 25mm spindle diameter and 1mm sample thickness. In this range of temperatures, the tests were conducted on fresh and RTFO samples. To evaluating the viscoelastic properties of AC at low and intermediate temperatures between 4°C - 46°C, an 8mm diameter plate geometry and 2mm thickness of samples were tested under PAV aged conditions. Plate geometries are illustrated in Figure 3.8b. DSR was equipped with a temperature control unit and fluid bath system as shown in Figure 3.8c which was used in order to maintaining a stable temperature within $\pm 0.1^\circ\text{C}$ as suggested in the SuperPave specification. The frequency sweep test results were presented in isochronal curves where, G^* and δ variations at different temperatures were illustrated at specific frequencies. Another way to analyzing outcomes of the frequency sweep tests was the construction of master curves which enabled the representation of G^* and/or δ at a constant temperature which may be shifted horizontally across the temperature scale using time-temperature superposition theorem (Ali et al., 2015). Permanent deformation (rutting) and fatigue cracking failure parameters were further analyzed using the G^* and δ outcomes in the frequency sweep tests. More details regarding to master curve construction and rutting and fatigue parameters evaluation were given in Chapters 4.3.1.2 and 4.3.1.3 respectively.

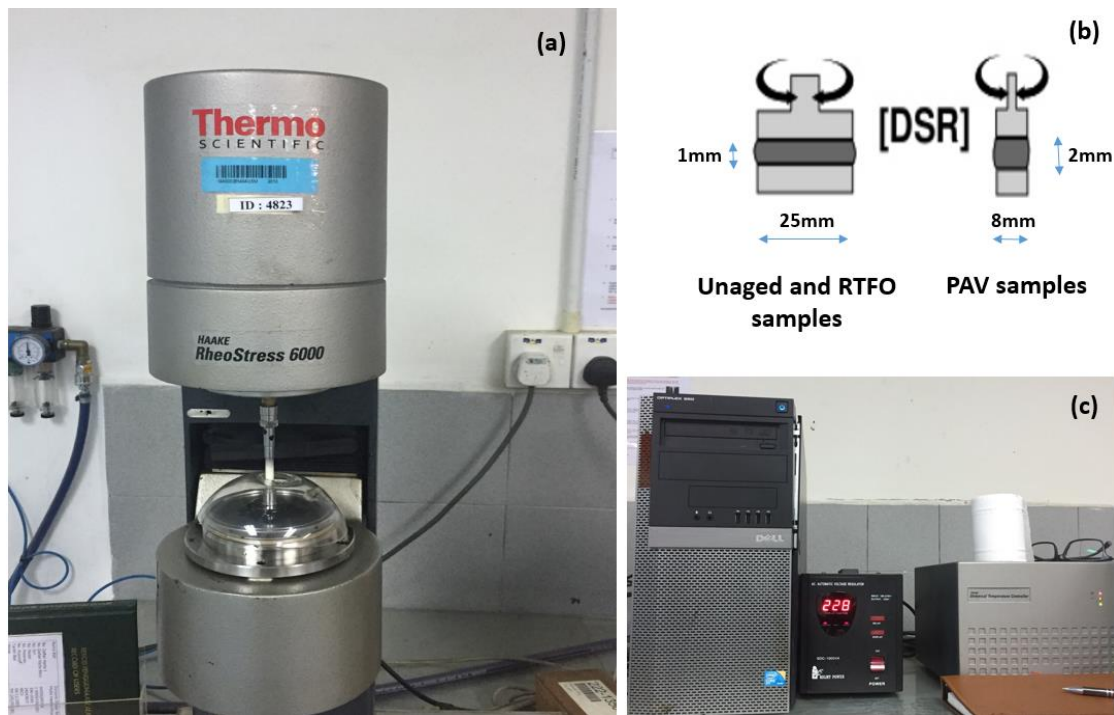


Figure 3.8: Dynamic shear rheometer (a) Main body (b) Spindle and plate geometry (c) Temperature control unit

3.2.8.2 Multiple Stress Creep Recovery (MSCR) test

MSCR test was conducted to simulate a continuous traffic loading in order to determine the amount of permanent deformation that occurs during the repeated dynamic loading. DSR was used with a 25mm plate geometry and 1mm sample thickness on RTFO aged samples. The standard protocols followed in the testing was as described in AASHTO TP70. MSCR test was performed at 64°C with 100 Pa and 3200 Pa stress levels which represented low and heavy traffic conditions respectively. Test procedure was started by applying a one second load in haversine form at 100 Pa which was followed by a resting period of nine seconds. The 10 second interval was considered as one cycle. After completing 10 consecutive cycles at 100 Pa, the test was further continued for another 10 cycles under 3200 Pa loading to complete a total of 20 cycles. At the end of each cycle and the beginning of the next cycle fluency and the recovered strain were recorded in order to compute the non-recoverable creep compliance and the percentage of elastic recovery by using eq. 3.3 and eq. 3.4 respectively.

$$J_{nr}(\sigma, N) = \frac{\varepsilon_{10}}{\sigma} \quad (3.3)$$

Where, J_{nr} is the non-recoverable creep compliance, $\varepsilon_{10} = \varepsilon_r - \varepsilon_0$ is the strain value at the end of recovery portion of each cycle, ε_r is the final strain in the recovery stage, ε_0 is the initial strain in the creep stage, σ is the applied stress level and N is the number of cycles.

$$\%R = \frac{\varepsilon_1 - \varepsilon_{10}}{\varepsilon_1} \times 100\% \quad (3.4)$$

Where, $\varepsilon_1 = \varepsilon_c - \varepsilon_0$ is the strain value at the end of creep portion of each cycle, ε_c is the final strain in the creep stage and $\%R$ is the percentage recovery.

The testing duration excluding the sample preparation was 15 minutes which was a major benefit over force ductility and elastic recovery tests that were considered as time and resource intensive testing methods (DuBois et al., 2014). Furthermore, based on strong correlation between the field and laboratory tested samples and dispute concerning the lack of efficiency in the frequency sweep testing due to linear viscoelastic region, the MSCR testing procedures have been considered as a superior technique to measure rutting potential of modified asphalt binders. (Anderson, 2014).

3.3 Heuristic Modelling for Viscoelastic Characteristics of Asphalt Cement

3.3.1 Multilayer perceptron neural networks

Artificial Neural Networks (ANN), a computer modelling tool that has been employed in optimization, regression and prediction modelling for numerous engineering applications, is a black box framework that is inspired by the way biological neurons work. An ANN model is composed of highly interconnected processing constituents called the artificial neurons, which operate in parallel logic and transmit information from one layer to others in serial operations (Liu et al., 2018). Among various type of ANN models, Feed Forward Multilayer Perceptron Neural Networks (FFMLPNN) were proven to be an efficient machine learning technique that has been utilized in the modelling of critical parameters of material properties

due to its generalization ability (Yusoff et al., 2019). With this type of network, information was processed at the neurons, and the signals were passed through connection links, which were associated with weight vectors that determine the strength of the connections. In the FFMLPNN model, the functions of these neurons were, first to sum up all the initially assigned weights from the lower layers and then to process the sum by a linear or non-linear activation function to determine the output signal from the given input signals (Ozgan, 2011). A commonly used nonlinear activation function, the hyperbolic tangent activation (given in eq. 3.5) function was adopted herein for the model development, since polymer and nanomaterial addition in the base bitumen was known to introduce a nonlinear feature to the failure behavior of PNCMAC's (Anderson, 2014; Venudharan & Biligiri, 2017).

$$f(a) = \frac{e^a - e^{-a}}{e^a + e^{-a}} = \frac{2}{1 + e^{-2a}} - 1 \quad (3.5)$$

The constructed FFMLPNN structure consisted of 3 layers which were the input, hidden and the output layers as illustrated in Figure 3.9. FFMLPNN utilized a supervised learning protocol meaning that, for a given set of input vectors, an output vector was supplied to the network and the system was expected to adjust its weights using forward and backward calculations to minimize the errors in prediction, which is also called the learning phase (Baldo et al., 2018). In the learning phase, various training algorithms such as Levenberg-Marquardt (LM), Gradient-Descent (GD) and Scaled Conjugate Gradient (SCG) which were the most commonly utilized training algorithms in ANN modelling for engineering applications were available. However, selection of the training algorithm depends on the type of neural network to be modelled and the structure and complexity of the dataset to be fed to the network (Kok et al., 2010).

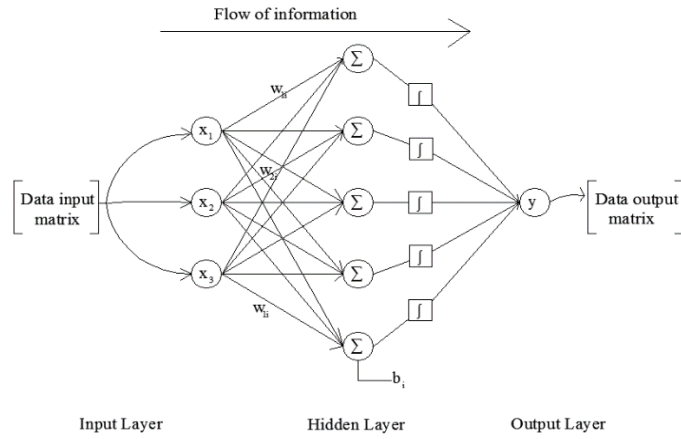


Figure 3.9: Schematic of FFNNM with backpropagation network

FFMLPNN model had three main aspects, which were the training, validation, and testing. The dataset was randomly divided among the aforementioned three aspects. The training data set was used for fitting the model. The validation data set was used to provide an unbiased evaluation of the model fit and to adjust the model hyperparameters and the test dataset was used to evaluate accuracy of the models constructed with untrained data points by adopting statistical performance indicator metrics such as the root mean square (RMSE) and the coefficient of determination (R^2) as given in eq. 3.6 and eq.3.7 respectively (Khademi et al., 2016; Yilmaz et al., 2011). Model validation was performed with k-fold cross-validation, even though others could also be used such as holdout or leave one out. An advantage of utilizing k-fold cross validation technique was that, each dataset (training, validation and testing datasets) were exchanged independently in every single round for 10 instances in order to avoid systematic biases in the data and to improve the accuracy of the predictive models. Apart from this, the efficiency of data usage was improved by running the models multiple times with various data splitting versions. (Abba et al., 2020).

$$\text{RMSE} = \sqrt{\frac{1}{n} \sum_{i=1}^n (\hat{Y}_i - Y_i)^2} \quad (3.6)$$

$$R^2 = 1 - \left[\frac{(Y - \hat{Y})^2}{(Y - Y_{\text{mean}})^2} \right] \quad (3.7)$$

Where, γ_i is the data observed in the experiments, $\hat{\gamma}_i$ is the ANN model predicted data and n is the number of target values.

Two different prediction models were developed for two different scenarios. In the first scenario, unaged G^* was the predicted target (output) using the PNC physical properties and the mechanical test conditions (frequency and temperature) as the input parameters while the second model (referred to as “RTFO G^* model” in the text) was aimed to predict the short term aged G^* using the same input parameters by excluding the physical properties and including the unaged G^* data points. Dataset used in the model development were obtained from the oscillatory DSR tests and included experimental results for both of the PNCMAC’s. The aim for including both PNCMAC in the datasets was first, to propagate the data points to improve efficiency of the model and second was to test the models generalisation ability.

A total number of 2210 data points for scenario 1 and 1768 data points for scenario 2 were used. Data splitting was proportioned in 70%, 15% and 15% ratio for training, validation and testing respectively. Prior to running the training, data was normalised using eq. 3.8 for reducing data redundancy and improving data integrity.

$$X_{\text{normal}} = \frac{X - X_{\text{min}}}{X_{\text{max}} - X_{\text{min}}} \quad (3.8)$$

Where; X_{normal} is the normalized data, x is the observed data and x_{min} , and x_{max} are the minimum and maximum of the experimentally observed data points respectively.

3.3.2 Adaptive neuro fuzzy inference system (ANFIS)

ANFIS is another artificial intelligence based technique that is able to solve complex non-linear problems that require human-thinking like expertise (Cüneyt Aydın et al., 2006). Similar to ANN, ANFIS is an adaptive multilayer feed-forward network that operates by learning the pattern within the dataset, by using the assistive numerical and linguistic variables to predict new outcomes from trained data sets (Gaya et al., 2014). ANFIS adopts a hybrid learning algorithm that combines the ANN’s data driven and fuzzy inference

system's (FIS) knowledge based abilities to maximising the accuracy of the prediction model. The learning phase in ANFIS was in two phases which were the forward and backward passes. The former was performed until layer 4 (illustrated in Figure 3.10) where the premise parameters were trained using the least squares method and the latter involved in adjusting the consequent parameters by using the Gradient Descent (GD) method (Orouskhani et al., 2013). An advantage of ANFIS was that, instead of using crispy data points that were used in Boolean logic, input and output parameters were first fuzzified by assigning membership functions such as trapezoidal, triangular and Gaussian in order to determine the membership grades for the input and output parameters and later, defuzzified to crispy outputs that can be interfered by engineers to perform numerical analysis (Solgi et al., 2017). ANFIS Model development was performed by using a Sugeno type fuzzy inference algorithm. A first order Sugeno type modelling involved a set of fuzzy if then rules as expressed in eq. 3.9 and 3.10.

$$\text{Rule (1): if } \mu(x) \text{ is } A_1 \text{ and } \mu(y) \text{ is } B_1; \text{ then } f_1 = p_1x + q_1y + r_1 \quad (3.9)$$

$$\text{Rule (2): if } \mu(x) \text{ is } A_2 \text{ and } \mu(y) \text{ is } B_2; \text{ then } f_2 = p_2x + q_2y + r_2 \quad (3.10)$$

For given inputs x and y , the membership function are indicated as A_1, B_1, A_2, B_2 , the outlet functions' parameters are $p_1, q_1, r_1, p_2, q_2, r_2$.

The structural formula and arrangement of the 5 layer ANFIS is illustrated in Figure 3.10 and explained by eq. 3.11-3.15 (Nourani et al., 2018).

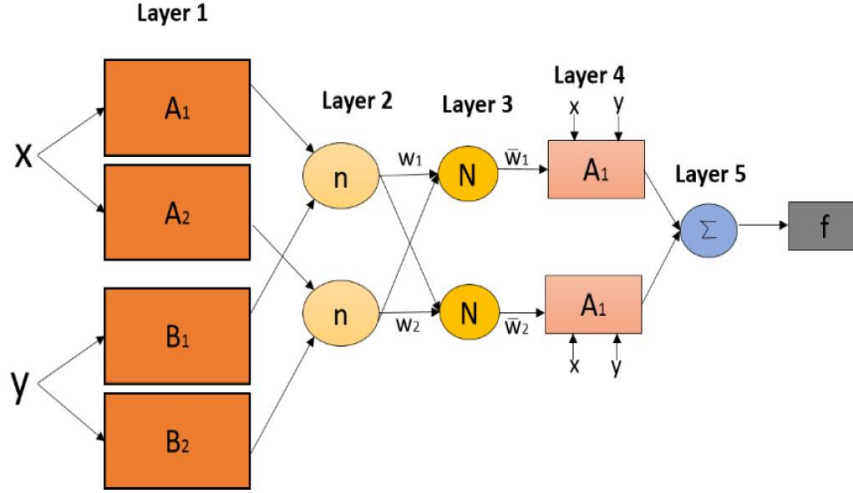


Figure 3.10: The general structure of ANFIS

Layer 1: The layer was responsible for fuzzification of the premise parameters,

$$Q_i^1 = \mu_{A_i}(x) \text{ for } i = 1,2 \text{ or } Q_i^1 = \mu_{B_i}(x) \text{ for } i = 3,4 \quad (3.11)$$

Q_i^1 stands for the membership grade for x and y inputs. The selected membership function was a Gaussian membership function since it reduces the error in the prediction process.

Layer 2: The layer calculated the firing strength of the i^{th} rule using T-norm fuzzy operations including the AND and OR operators.

$$Q_i^2 = w_i = \mu_{A_i}(x) \cdot \mu_{B_i}(y) \text{ for } i = 1,2 \quad (3.12)$$

Layer 3: The layer, also denoted as the normalisation layer calculated the ratio of i^{th} rule to all rules.

$$Q_i^3 = \bar{w}_i = \frac{w_i}{w_1 + w_2} \quad i=1, 2 \quad (3.13)$$

Layer 4: In this layer, each node i performed the subsequence rules as an adaptive node.

$$Q_i^4 = \bar{w}_i(p_i x + q_i y + r_i) = \bar{w}_i f_i \quad (3.14)$$

p_i, q_i, r_i , were the irregular parameters referred to as the consequent parameters.

Layer 5: The layer was responsible for defuzzification. Summation of all incoming signals from previous node and results were generated in a crisp value.

$$Q_i^5 = \bar{w}_i(p_i x + q_i y + r_i) = \sum_i \bar{w}_i f_i = \frac{\sum_i w_i f_i}{\sum_i w_i} \quad (3.15)$$

Dataset used, data splitting techniques and the scenarios created in the model development were entirely the same with the procedures that were followed in the FFMLPNN modelling which was described in Chapter 3.3.1. The objective in creating two different models using FFMLPNN and ANFIS was to assess the tangibility of both computational modelling techniques towards estimating the possible outcomes of experimental investigations conducted on similar type of modifiers with different compositions to the weight/volume of base binder over a wider range of test conditions without the necessity to repeating the experimental procedures.

3.4 Hot Mix Asphalt Design

The hot mix asphalt (HMA) design was performed in four stages. In the first stage, the modified asphalt binders and the aggregate type and gradation were selected. The asphalt binder selection was explained in Chapter 3.1 and it forms the foundations of the current study. The aggregate selection is commonly limited to the locally available sources. In the current study, granite aggregates with AC-14 gradation were used to prepare 1100 grams of asphalt concrete samples. The gradation limits used for AC-14 gradation is demonstrated in

Table 3.4. The second stage involved determination of the appropriate mixing and compaction temperatures for the asphalt mixtures using the RV of base and modified AC. In the third stage, the samples were prepared using a laboratory asphalt mixer. Following to the mixing process, loose samples (uncompacted samples) and the samples which were compacted by using a SGC were used to determine specific volumetric properties for the HMA samples. Volumetric properties included the Va, VMA, VFA and D/A ratio as specified in the Superpave mix design procedures and they were measured and computed to determine the OBC. Starting from 4.5% asphalt content and increasing with 0.5% increments at each trial, the OBC was determined for asphalt mix samples by targeting 4% air voids while meeting the other volumetric criteria. The final stage in the HMA design was to conduct moisture susceptibility tests on the asphalt mix samples with the OBC determined in stage 3.

Table 3.4: AC-14 Gradation

Sieve Size (mm)	Percentage Passing (%)
20	100
14	90-100
10	76-86
5	50-62
3.35	40-54
1.18	18-34
0.425	12-24
0.150	6-14
0.075	4-8

3.4.1 Mixing and compaction temperatures

The mixing and compaction temperatures for the hot mix asphalt (HMA) design was obtained from the log-viscosity-temperature graph based on RV of the AC. This method of estimation was specified in the ASTM D-2493 standards. RV test results at 135°C and 165°C for the asphalt binders were converted to log-style on the y-axis and plotted against the temperature parameter on the x-axis. Two lines were drawn horizontal to the y-axis to locate viscosity ranges corresponding to the mixing and compaction temperatures. Viscosity ranges at 0.17 ± 0.02 Pa-s correspond to the mixing temperature and 0.28 ± 0.03 Pa-s was the compaction temperature range. This procedure has been proven to be efficient for asphalt

mixes that are designed with virgin AC however, in the case of use of modified asphalt binders in the mix occasionally, the mixing and compaction temperatures may be too high due to increased viscosity of the modified asphalt binder which is not desirable in terms of energy consumption during the manufacturing process and also may result in deterioration of material properties due to exposure to extreme heat. Asphalt institute suggests that mixing temperatures should not exceed 200°C. In addition, the laboratory mixing and compaction temperatures are recommended by the Asphalt Institute to assess the design volumetric properties of the asphalt mixture and are not intended to reflect real field mixing and compaction temperatures at the project stage. (Yildirim et al., 2006).

3.4.2 Volumetric properties and the optimum binder content

Asphalt mix design is a volumetric process. Volumetric characteristics of an asphalt mixture is crucially important from the specification and the performance standpoint. Parameters such as the total air voids in the mix (V_a), voids in the mineral aggregates (VMA), voids filled with asphalt (VFA) and dust to asphalt (D/A) ratio are called the specification parameters and they are computed using the measured volumetric properties such as the specific gravity of the binder (G_b), bulk specific gravity of the mineral aggregates (G_{sb}), bulk specific gravity of the compacted mix (G_{mb}) and specific gravity of the void less volume of paving mix (G_{mm}). Other volumetric parameters that aids in computing the specification parameters include the effective specific gravity of the aggregates (G_{se}), the percent effective asphalt binder content (P_{be}) and the percent asphalt binder that is absorbed by the aggregates (P_{ba}).

From the measured parameters perspective, G_b is customarily provided by the manufacturer and it is not required to be tested if not for verification. Typical G_b values are between 1.02 and 1.05 and since it has very little difference and negligible influence on the overall results, the most commonly, suppliers data are credited.

The weight ratio of a known volume of aggregates, including permeable and impermeable voids, to the weight of an equivalent volume of water is referred to as G_{sb} . Asphalt mix design involves the use of coarse and fine aggregates in combination to form a suitable gradation formula for the hot mix asphalt design. Additionally, it is a common practice to

use aggregates from various sources to achieve the optimum gradation. Although, aggregates from different sources were not used in this study, the chosen gradation included coarse and fine aggregates, therefore the coarse aggregates specific gravity and the fine aggregates specific gravity were measured separately and computed to act as a single unit of G_{sb} by using eq. 3.16.

$$G_{sb} = \frac{100\%}{P_1/G_1 + P_2/G_2} \quad (3.16)$$

Where, G_{sb} is the bulk specific gravity of the aggregates, P_1 and P_2 are the percentage retained on the sieve for coarse and fine aggregates and G_1 and G_2 are the individual specific gravities for coarse and fine aggregates respectively.

The measurement techniques for the coarse and fine aggregate specific gravities are essentially similar. The oven dry mass, SSD mass and the mass of sample when submerged into water are required to compute both specific gravities. For the coarse aggregates that retain on the 4.755 mm sieve, the dry weight of the sample was measured, then the sample was submerged into water at room temperature for 15-19 hours and it was weighted again. Finally, the sample was taken out from the water bath, dried with a towel and the SSD weight was measured. For the fine aggregates passing through 4.75 mm sieve, the difference in mass measurement from the coarse aggregates was the SSD conditioning. For measuring the samples SSD weight, after removing the sample from the water, it was placed in a non-absorbent plate and dried by blowing warm air using a blow dryer. The sample was then, placed inside a cone shaped metal mould and tamped with 25 light drops by using a metal tamper. After that, the cone was lifted slightly. If the sample contained surface moisture, the cone shape retained its position. The test procedure was repeated by drying and cone testing until the sample is slumped. This condition was considered as the SSD condition and the sample was weighted to determine the SSD mass. The testing procedures for measuring the coarse and fine aggregate specific gravities can be found in AASHTO T-85 and AASHTO T-86 respectively. Using the three weights measured in oven dry, submerged into water and

SSD states, the samples apparent specific gravity, bulk specific gravity and water absorption were calculated by using eq. 3.17-3.19 respectively.

$$G_{sa} = \frac{A}{A-C} \quad (3.17)$$

$$G_{sb} = \frac{A}{B-C} \quad (3.18)$$

$$A\% = \frac{B-A}{A} \times 100\% \quad (3.19)$$

Where, G_{sa} is the apparent specific gravity, G_{sb} is the bulk specific gravity, $A\%$ is the absorption in percent, A is the mass of oven dry sample in air, B is mass of SSD sample in air and C is the mass of sample submerged into water.

The theoretical maximum specific gravity (G_{mm}) is the void less specific gravity of the asphalt mixture meaning that, the combined specific gravities of the asphalt binder and the aggregates is the theoretical maximum specific gravity of the mixture. Although there are no specific requirements and limits for the G_{mm} , it is an important HMA characteristic since it is used in computing the total air voids in the mixture. G_{mm} is also used to compute the effective specific gravity of the aggregates (G_{se}) which is substantially used to compute the percent effective asphalt binder content (P_{be}) and thereafter, D/A ratio by using eq. 3.20-3.22 respectively.

$$G_{se} = \frac{P_s}{\frac{100 - P_b}{G_{mm}} - \frac{P_b}{G_b}} \quad (3.20)$$

$$P_{be} = P_b - \left[P_s \times G_b \left\{ \frac{(G_{se} - G_{sb})}{(G_{se} \times G_{sb})} \right\} \right] \quad (3.21)$$

$$D/A = \frac{\% \text{pass \#200 (0.075mm)}}{P_{be}} \quad (3.22)$$

Where, G_{se} is the effective specific gravity of the aggregates, P_s is the percentage of aggregates in the mix, G_{mm} is the theoretical maximum specific gravity, P_b is the percentage of asphalt binder in the mix, G_b is the specific gravity of the asphalt binder, P_{be} is the percent effective asphalt binder, D/A is the dust to asphalt ratio and %Pass #200 is the percentage of fine aggregates or dust that passes through the sieve number 200 (0.075mm).

Theoretical maximum specific gravity is also called the rice gravity which was named after James Rice who developed the testing procedures for G_{mm} . The test procedure was conducted on loose HMA samples. After the mixing process, the loose sample was spread on a craft paper. During this step every single particle was separated from the others to prevent air voids stuck between the particles which would have resulted in skewing the test results. In the next step, the mass of the container was weighted empty and weighted again after filling the sample inside the container. After that, the container including the sample was filled with water at $25 \pm 0.5^\circ\text{C}$ until it has reached few centimetres above the sample and then it was placed onto a vacuum extractor. The vacuuming process was conducted at 3.7 ± 0.3 kPa for 15 minutes. The container was agitated by the mechanical agitator during this process. The container with the sample was then removed from the vacuum apparatus and placed inside a water bath at $25 \pm 0.5^\circ\text{C}$. After waiting for 10 minutes the samples weight was stabilised and the measured weight was recorded. The complete procedure for the rice method was as illustrated in Figure 3.11. Using the above weight measurements, G_{mm} was computed by eq. 3.23.

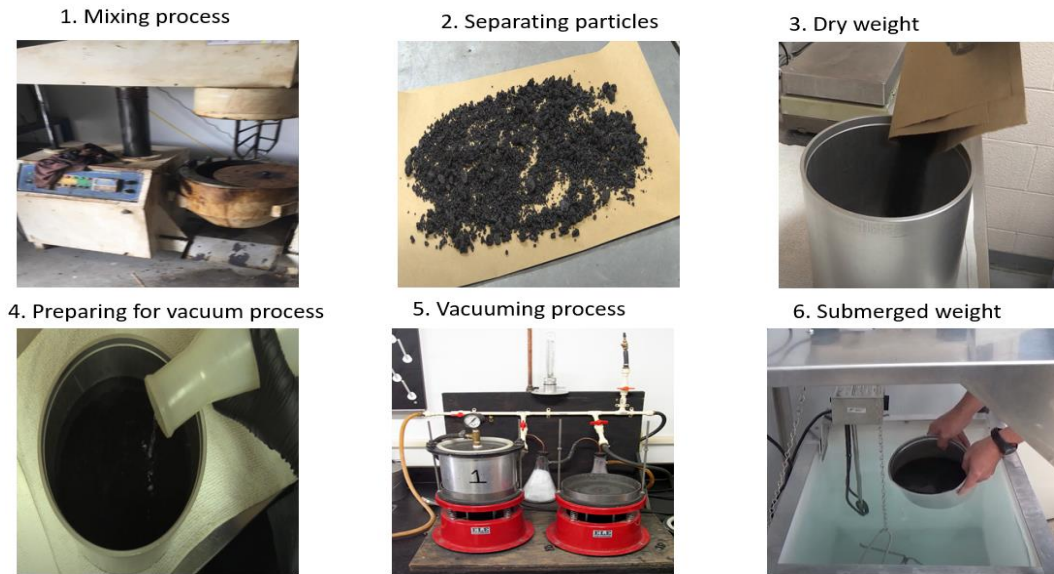


Figure 3.11: Rice method procedure

$$G_{mm} = \frac{A}{(A+D-E)} \quad (3.23)$$

Where, A is the dry mass of the sample, D is the mass of container filled with water and E is the mass of container and the sample filled with water after the rice method.

Bulk Specific gravity of the compacted mix (G_{mb}) is another important HMA characteristic as it is involved in most of the key mixture voids analysis. VMA and V_a are directly and VFA is indirectly influenced by the G_{mb} of the mixture which can also be deducted from eq. 3.25-3.27. A study conducted by (Gashi et al., 2017) reported that, it is crucially important to measure the loose and compacted samples specific gravities correctly since, small changes in G_{mm} and/or G_{mb} can result in significant discrepancy in V_a calculation thus, incorrectly calculated VMA and VFA leading to incorrect mix design proportions for the designer. It was reported in their study that, if G_{mb} is held constant, +0.01 change in G_{mm} causes +0.4% change in V_a . Additionally, if G_{mm} is held constant, +0.01 change in G_{mb} leads to -0.4 change for the V_a and also if G_{sb} and P_s are held constant +0.01 change in G_{mb} causes -0.4% change for the VMA. G_{mb} test was conducted on the compacted sample of asphalt mixture. The compaction was performed with a superpave gyratory compactor. The dry mass of the

compacted mix was measured and then the sample was submerged into water at $25\pm 0.5^{\circ}\text{C}$ and its weighted again to measure the submerged weight of the sample. Sample was then removed from the water bath, dried with a towel to remove the water from the surface pores and immediately weighted again to record the SSD mass. Three measured masses were then used to compute G_{mb} of the sample by using eq. 3.24. AASHTO T 166 was used for the testing procedure as it is illustrated in Figure 3.12.

$$G_{mb} = \frac{A}{(B-C)} \quad (3.24)$$

Where A is the dry mass of the sample in air, B is the mass of SSD sample in air and C is the mass of sample submerged in water.

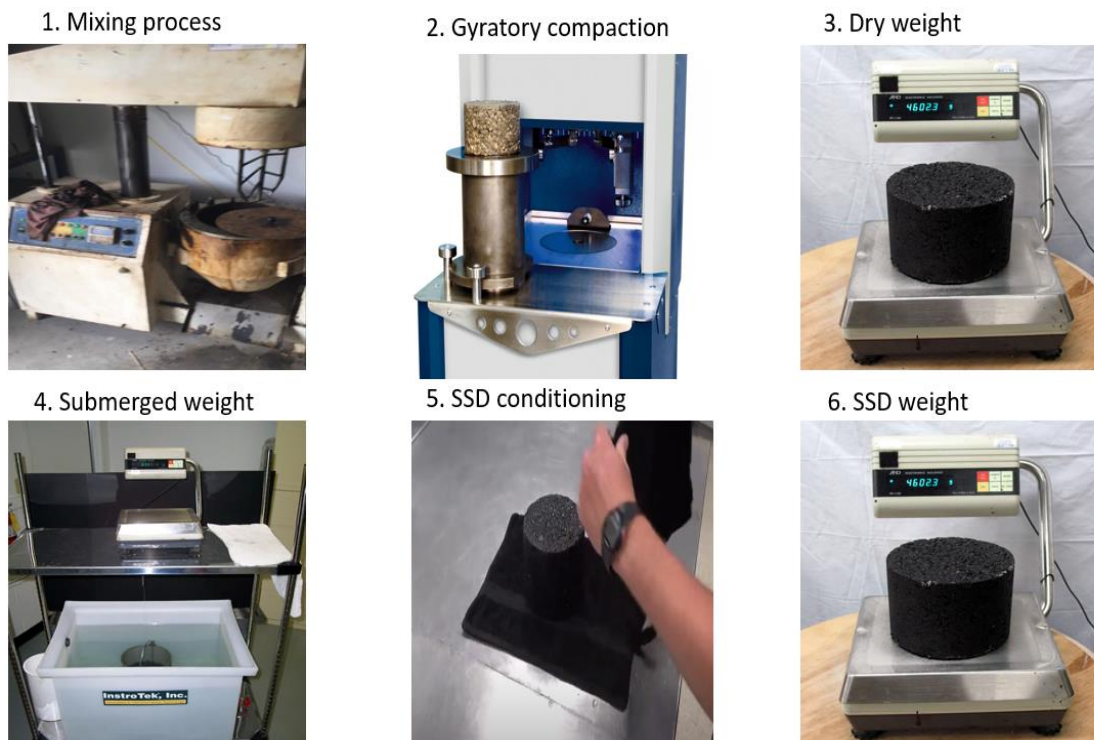


Figure 3.12: Determination of Bulk specific gravity of the mixture

Void analysis is an integral part of the Superpave mix design. Parameters such as V_a , VMA and VFA are called the specification parameters and they were computed using the specific gravities of the aggregates and the mixture by using eq. 3.25-3.27.

$$V_a = \left(1 - \frac{G_{mb}}{G_{mm}}\right) \times 100\% \quad (3.25)$$

$$VMA = 100 - \left[\frac{(G_{mb} \times P_s)}{G_{sb}}\right] \quad (3.26)$$

$$VFA = \frac{VMA - V_a}{VMA} \quad (3.27)$$

V_a refers to the small air pockets of air which remain in the final compacted mixture between the asphalt coated aggregate particles. In dense graded highway mixes, air voids are needed to allow for additional pavement compaction under the effect traffic loading to providing a small space for asphalt binder to flow during this subsequent compaction. The air void content for the laboratory mixes varies from 2% to 5% for most departments, while the mixes laid on the roadways are typically designed to 5% to 7.5% air voids. In a compacted state HMA, VMA denotes to the spaces of air between the mineral aggregates and the void spaces available for the effective asphalt binder. A higher VMA means that asphalt has more room available to accommodate effective binder to coat the aggregates, which improves the durability of the mixture. Thereby, in the Superpave requirements, a minimum VMA condition based on the nominal maximum aggregate size is set for HMA design. VFA is the proportion of air voids in the VMA that are filled with effective asphalt binder. Besides VFA is an indicator for a measure of durability, VFA is also correlated with the density of HMA. A low VFA indicates inadequate amount of effective asphalt binder in the mix to provide sufficient durability and the mixture is considered to be vulnerable to fatigue. If VFA is too high, then the available VMA is overfilled with asphalt and the mix would be likely to over densify and which leads to lower stability. On this basis, a range of VFA is specified considering the traffic loading that the pavement is expected to perform. According to the

Superpave specification the targeted V_a for the compacted mix should be around 4%. The VMA and VFA requirements as specified by the Superpave are presented in Tables 2.17 and 2.18 respectively.

3.4.3 Moisture susceptibility

Moisture susceptibility of an HMA is referred to as the weakening of the adhesion and cohesion bonds between the asphalt and the mineral aggregates because of infiltration of water in the mixture (Omar et al., 2020). Owing to complex mechanism of moisture susceptibility, it is difficult to identify a specific cause for moisture damage however, the level of moisture damage can be evaluated by using the indirect tension test after following a conditioning process (Solaimanian et al., 2007). Although a number of conditioning procedures are available in the literature, the modified lottman method was utilized in the present study. The capability of the modified lottman procedures regarding to the repeatability and reproducibility of test results was the primary justification for the means (Hamedi et al., 2015). A total of 6 test specimens were prepared for each sample at an average of $7\pm 0.5\%$ air void content. Half of the samples were conditioned while the other half was remained rested at room temperature. The conditioned samples were first subjected to a vacuum pressure of 13-67 kPa to achieve partial saturation between 70-80%. Later, the saturated samples were subjected to a 16 hour freeze cycle at -18°C which was then followed by the thaw cycle for 24 hours in a water bath that was maintained at 60°C . After completing these procedures, the samples were considered to be in conditioned state. Afterwards, the samples were tested for the indirect tensile strength by using the indirect tension test which applied a load at a constant rate of 50 mm/minute on the conditioned and unconditioned specimens. The tensile strength of the samples were computed by using eq. 3.28 and the mean of the test results for each group of specimens were determined as the average tensile strength of the samples. Finally, to evaluate the moisture susceptibility of the HMA, the tensile strength ratio (TSR) was computed by using eq. 3.29. The typical TSR values range between 70-90% while Superpave specification limits the TSR to a minimum of 80% (Solaimanian et al., 2007).

$$S_t = \frac{2P}{\pi tD} \quad (3.28)$$

$$\text{TSR} = \frac{S_2}{S_1} \quad (3.29)$$

Where; S_t is the tensile strength, S_2 and S_1 are the average tensile strength of conditioned and unconditioned samples respectively, P is the maximum load, t is the sample thickness and D is the sample diameter.

CHAPTER 4

RESULTS AND DISCUSSION

The physical, chemical and rheological properties for the ASA/Si and ASA/Fe modified AC at modifier concentrations 3, 5 and 7% by the weight were presented in this chapter. Along with the results from the conventional testing, the dynamic shear rheometer procedures by using frequency sweep tests and MSCR test results were analysed to characterize the performance characteristics of the samples at intermediate and high temperatures under fresh and short-term aging conditions. Additionally, long-term ageing condition was utilized to evaluating the performance characteristics for the low temperature properties. The morphological analysis was conducted by using XRD and FTIR techniques in order to identify the formation of new chemical and structural changes in the modified asphalt matrix which assisted in remarking the differences in the modified AC behaviour. Also, two different heuristic modelling techniques namely, the ANN and ANFIS were utilized to model the performance characteristics. Capability of the developed models to predict the experimental outcomes were analysed by using the statistical indicator metrics; R^2 and RMSE. Furthermore, after identifying the best performing composition for both modifiers, the performance investigations were conducted at the mixture level. Herein, volumetric properties for the HMA and the moisture susceptibility evaluation were presented.

4.1 Conventional Properties

Conventional properties of the PNC modified AC were evaluated based on the experimental outcomes from the physical testing procedures including the penetration, ductility, RV and the softening point tests. The test results were presented for unaged and short-term aged samples to further evaluate the aging index. The temperature susceptibility of AC was evaluated by using two different parameters, namely the PI and PVN indices. RV, Penetration, and the softening point parameters were measured to compute PI and PVN indices. Furthermore, the storage stability of the AC was analysed according to the results from the softening point test. Unconditioned and preconditioned sample softening point values were analysed to perform the storage stability analysis.

4.1.1 Penetration and softening point test results

Consistency of AC was determined based on its physical properties. Penetration value was one of the important physical properties of AC which has also been utilized in asphalt pavement industry as a classification method to grading of asphalt for various road use applications. For AC that is used in hot mix asphalt design, typical values of penetration values range between 25mm^{-1} and 200mm^{-1} where, the lower penetration indicates to a harder and higher penetration indicates to a softer asphalt binder. Penetration of AC depends on the crude oil origin and the processing method that it has undergone. For construction applications, the penetration of asphalt binder is generally provided by the manufacturer and maybe tested in the laboratory for verification. Penetration test results alone were not suitable to assess the performance of AC however, it was used as to identify the grade of asphalt binder. The penetration grade is abbreviated based on the lower and upper limits of the penetration test results. For example, as utilized in the present study, a penetration grade “pen 80/100” means that, the asphalt binder penetration value lies between the former and the later penetration values in mm^{-1} . Researchers have also conducted numerous studies to correlate the penetration of AC to its performance characteristics. For the same reason the penetration test was conducted in the current research to investigate the effect of change in penetration of AC due to the modification process and its influence on the physical properties of neat AC. The results of the penetration tests were illustrated in Figure 4.1.

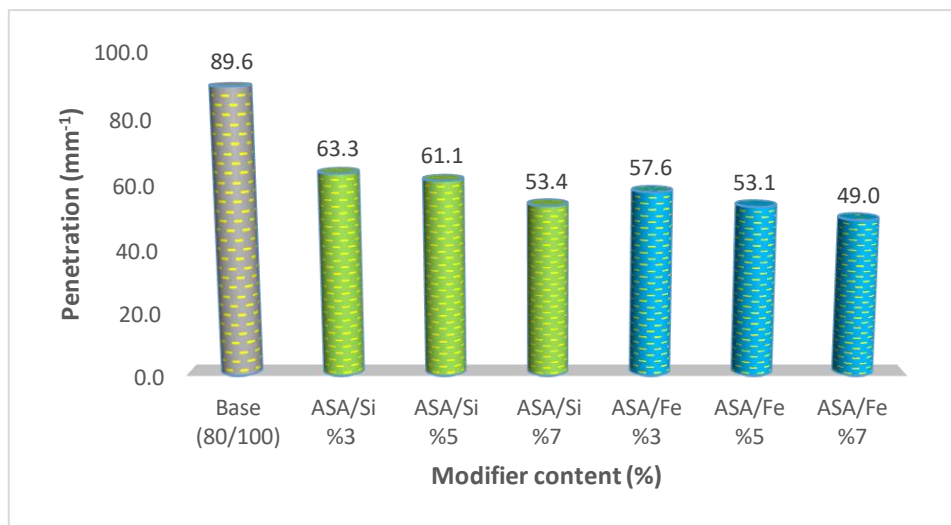


Figure 4.1: Penetration test results

It can be observed from Figure 4.1 that, for both types of polymer nanocomposites, the penetration of PNC modified AC decreased dramatically. Penetration value of 89.6 mm^{-1} for the base binder was a proof that the supplied asphalt was as specified by the manufacturer since it lies between the range of 80 mm^{-1} and 100 mm^{-1} . The decrease in the penetration values for the PNC modified AC was an indication for the stiffening of the materials due to the modification process. The increase in stiffness was a beneficial feature for the asphalt binders by means of enhancing the resistance to rutting failure at extreme temperatures. On the contrary, this have led to poor fatigue resistance for the asphalt binders at low temperatures due to reduced elastic properties. In a study conducted by (Junaid et al., 2018), two different penetration grade asphalt namely, pen 40/50 and pen 80/100 were compared by performance by utilizing the dynamic modulus test results. Findings of their study demonstrated that, the rutting resistance of pen 40/50 AC was significantly higher than the pen 80/100 AC while for the fatigue resistance parameter, pen 80/100 asphalt binder performed better than pen 40/50 asphalt binder. In another study conducted by (Pasandín & Pérez, 2014), it was stated that, by using a lower asphalt penetration grade AC, a better adhesive bonding between the AC and the mineral aggregates was achieved which resulted in more durable asphalt mixtures. Therefore, a reduction in the penetration value of the asphalt can lead to a more durable mixture. From the above discussions, it can be deduced that, the reduction of the penetration values were a result of the stiffening of the PNC modified AC which led to improved rutting resistance, higher durability and reduced fatigue resistance. It should be noted that, the choice of penetration grade of asphalt for paving applications depends on the climatic conditions and a fine balance of high temperature and low temperature properties should be achieved by selecting the appropriate penetration grade asphalt. On this basis the choice of asphalt penetration grade for the present study (pen 80/100) which was the average of the lowest and the highest available penetration grade asphalt was justified.

The softening point is another consistency parameter that was used to measure the temperature at which a sample reaches a certain softening under specified conditions. A higher softening point ensures that, asphalt binder resists against flow due to vehicular traffic loading. Also, higher softening point was an indication for lower temperature susceptibility. Expectedly, an asphalt binder with high softening point is favourable in the case for

pavement applications where the hot climate conditions are anticipated. Softening point and the penetration of AC were inversely proportional. A higher softening point corresponded to a lower penetration grade. Nevertheless, it was possible to increase or decrease the softening point separately from the penetration by using modifiers in AC. Sassobit is an interesting modifier in this regard. Studies conducted by (Wang et al., 2016) and (Zaumanis, 2011), showed that, modifying the base asphalt with Sassobit can lead to increase or decrease in both physical properties of the AC. Figure 4.2 illustrated the outcomes from the softening point tests.

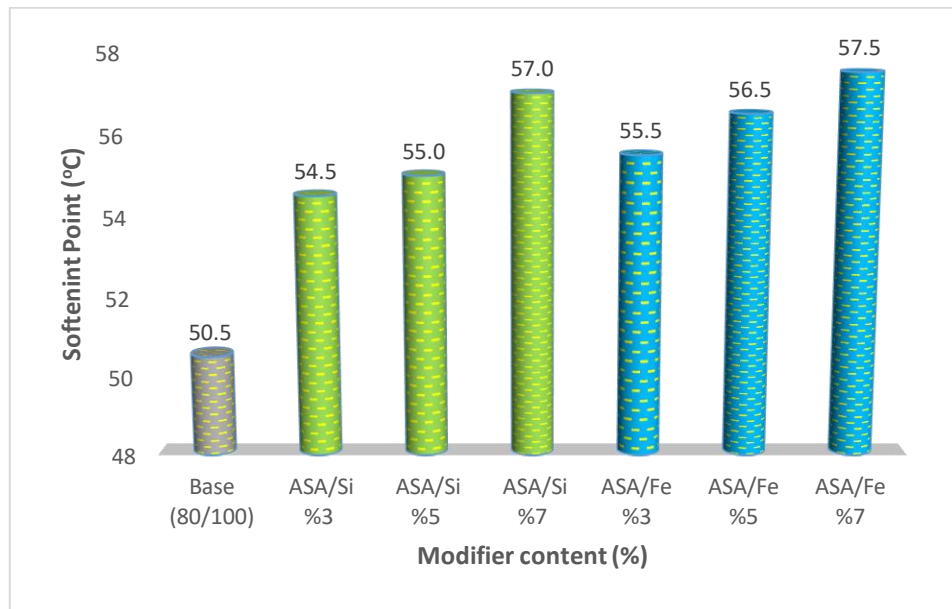


Figure 4.2: Softening points for the base and PNC modified AC

Results from Figure 4.2 showed that, for all binders the softening points were increased successively after adding the modifiers. Both PNC's demonstrated a similar trend of increase that are rather in the similar range. The higher softening point values were regarded to the corresponding reduction in the penetration which corroborated the stiffening of the binders. Based on the ring and ball softening point test results, PNC modified AC's were shown to possess better resistance to flow than the base AC. Higher softening point values with the addition of modifiers were also considered that, the temperature susceptibility for the modified asphalt binders were improved.

4.1.2 Rotational viscosity test results

The RV measurements at 135°C and 160°C were useful to evaluating the workability of AC during the production and construction stages. Although the rotational viscosity cannot describe fundamental rheological characteristics alone, it has been used together with the penetration and softening point parameters to assessing the temperature sensitivity of AC. The test results have also been adopted in grading for AC since the penetration grading alone suffers from the deficiency to properly designate the consistency of asphalt due to being a single point measurement. Foremost, the RV test results are critical for the asphalt mixture design, regarding to determination of the mixing and compaction temperatures. Higher viscosities yield to a less workable HMA due to increased stiffness which results in higher energy consumption in the production plant because of increased mixing temperatures and also it requires more effort to compacting the asphalt mix in the construction field. The rotational viscosity testing procedures were applied under fresh and short-term aging conditions for the base and PNC modified AC in a range of temperatures from 120°C to 180°C by 15°C increments in order to observe the variation of viscosity at elevated temperatures. Additionally, conducting the tests under fresh and short-term aging conditions enabled the computation of Viscosity Aging Index (VAI) which is explained later in Chapter 4.1.6. The RV measurements for the base AC, ASA/Si and ASA/Fe modified AC were presented in Figures 4.3a and 4.3b respectively.

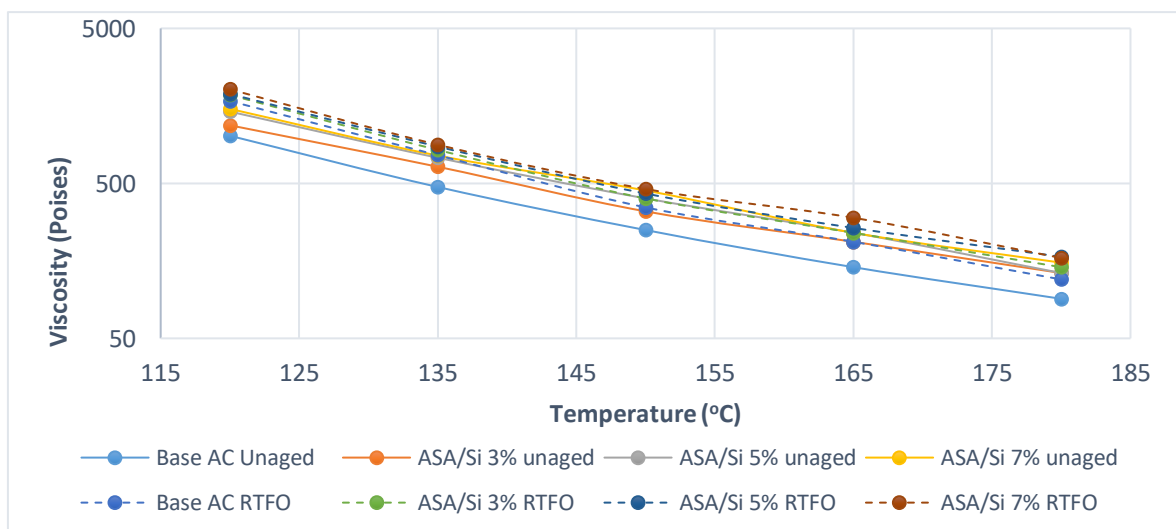


Figure 4.3a: Rotational viscosity test results for ASA/Si composites

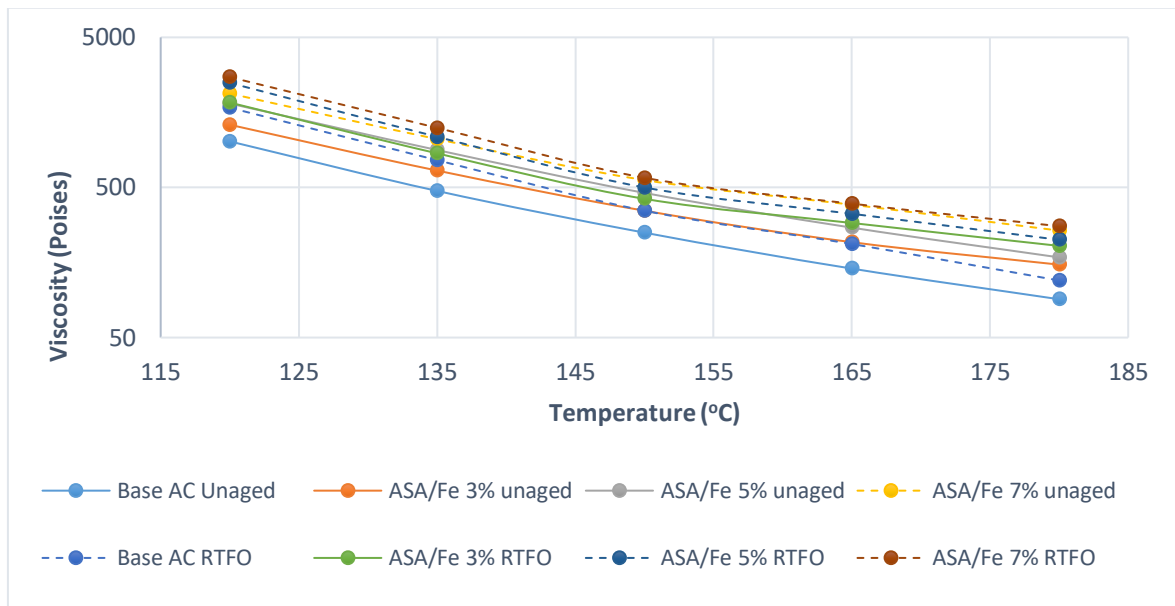


Figure 4.3b: Rotational viscosity test results for ASA/Fe composites

It can be observed from Figures 4.3a and 4.3b that, the viscosity values for all samples were reduced as the test temperature increased regardless of the modifier content. This was due to the viscoelastic nature of asphalt. Furthermore, the increase in the modifier content resulted in higher viscosities because of stiffening of the asphalt due to the modification process. In addition to that, short-term aged samples demonstrated higher viscosities compared to the unaged samples. This was an expected outcome from the tests since, AC whether it is modified or neat is known to undergo age hardening due to exposing to high temperatures and air pressure during the short term aging. The samples which contained the highest percentage of modifier concentrations possessed the highest viscosities at 120°C which were 2020 Poises for the ASA/Si and 2718 Poises for the ASA/Fe composites at 7% modifier contents by the weight of asphalt. The viscosities for both of the polymer nanocomposites were reduced significantly compared to the findings of a research conducted by (Ali et al., 2015) which utilized ASA as sole modifier to base AC of 60/70 grade. However, it is difficult to distinguish whether the difference in viscosities was a result of the influence of the additives or the effect of the penetration grade of AC since, different penetration grades were utilized in the two studies. Nevertheless, it can be concluded that, with the application of polymer nanocomposites in the current study, the workability of the AC was improved and the mixing and compaction temperatures were reduced owing to achieving lower viscosities.

4.1.3 Ductility test results

A property of a bitumen by virtue of which it can be elongated without breaking apart is referred to as the ductility of AC. The asphalt binder used in road construction should be ductile such that, it can take up the deflections that occur in them. The ductility test results were also an indication for; the cohesiveness of the binders and the mineral aggregates, the cracking resistance and the temperature susceptibility of AC. In the present day, the ductility test is rarely used as a method of rheological characterisation since more advanced techniques to assess the viscoelastic behaviour of AC such as the DSR testing procedures have been adopted after the SHRP. However, the test is still performed for research purposes as a performance indicator for asphalt modification. The results from the ductility tests were illustrated in Figure 4.4. As suggested by the Superpave specifications, the minimum ductility requirement which is 100cm for the neat AC was met since the ductility of base AC was 164cm. A sharp decrease in ductility for both PNC modified AC were observed after the modification process as a result from the stiffening of the AC. A different ductile behaviour was observed when the AC were modified with 5% modifier concentrations. The reason for such behaviour change was related to the instability of the modified samples due to phase separation and agglomeration which is difficult to explain by the ductility test results but analysed by more advanced techniques which are explained in detail in Chapters 4.2 and 4.3.

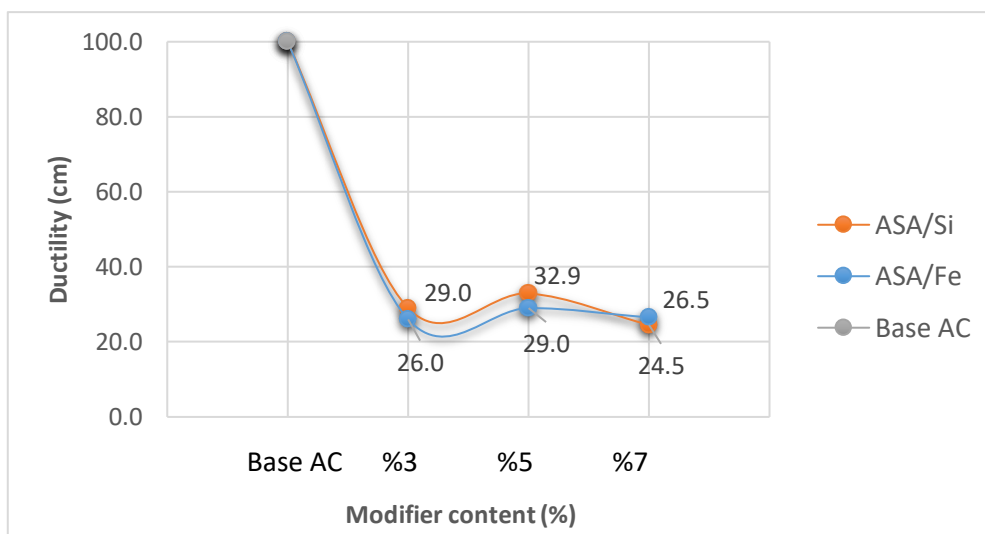


Figure 4.4: Ductility test results

4.1.4 Temperature sensitivity analysis

Asphalt is a thermoplastic material, meaning that its physical properties are time and temperature dependent. As the physical properties of asphalt change at elevated temperatures, its consistency and temperature susceptibility are affected. Computed by the penetration value of AC at 25°C and the softening point values, the Penetration Index (PI) is one of the parameters that was used to evaluate the temperature susceptibility of PNC modified AC. Another parameter used for this purpose was the Penetration Viscosity Number (PVN) which was computed by eq. 2.3 based on the penetration and rotational viscosity test results at reference temperatures of 25°C and 135°C respectively, while PI was computed by using eq. 2.1. (Al-Mansob et al., 2017). The computed PI and PVN indices were associated with the temperature susceptibility of AC and the analytical outcomes were demonstrated in Table 4.1.

Table 4.1: PI index and PVN

	Penetration	Softening point	Viscosity at 135 C	PI	PVN
Base (80/100)	89.6	50.5	474.0	0.4340	1.8194
ASA/Si %3	63.3	54.5	648.0	0.4584	1.8525
ASA/Si %5	61.1	55.0	888.0	0.4787	1.9507
ASA/Si %7	53.4	57.0	1050.0	0.5713	1.9726
ASA/Fe %3	57.6	55.5	640.0	0.4368	1.8252
ASA/Fe %5	53.1	56.5	732.0	0.4493	1.8506
ASA/Fe %7	49.0	57.5	756.0	0.4630	1.8483

A PI value for asphalt binders range from -3 to +7, where lower values indicate a more temperature susceptible AC. As can be deduced from Table 4.1, the reduced penetration values and higher softening points after the modification process indicated that, the base AC became stiffer with the addition of polymer nanocomposites at higher concentrations. Furthermore, the increased PI and PVN numbers show that the modification process have led to an improved temperature susceptibility for the modified samples. The PVN index for ASA/Fe 7% was slightly smaller than that of the ASA/Fe 5%. It can also be observed that, as compared with the base AC, for the ASA/Fe samples, the change in PI and PVN indices were less significant compared to change in PI and PVN indices for the ASA/Si composites.

4.1.5 Storage stability analysis

Storage stability at high temperatures, is an important property for a modified AC that is used in the evaluation of integrity and homogeneity of asphalt mixtures during storage and handling of AC in the field. Although polymer-modified AC offers significant improvement in the properties of AC, many researchers' findings have indicated that the phase separation problem due to dissimilarity between the polymer and asphalt chemical structure such as the solubility and density are the causes of instability and incompatibility in polymer modified AC which limits their application (Yin & Moraes, 2018). The phase separation is associated with the accumulation of polymer particles in the top section of the AC at high temperatures, which forms a steady position. Although, other test methods for evaluating the storage stability of the AC such as the RV and DSR techniques were available, the softening point test results, as utilized in numerous high class investigations were utilized in the present study due to its simplicity. The disparity between the softening point of the upper and lower sections of the asphalt samples extracted from the aluminium foil tubes was measured to analyse the storage stability. According to the literature, although a difference of up to 4°C-4.5°C, between the top to bottom parts of the conditioned samples was considered within acceptable limits, the common perception among the researchers is that in order to classify AC as storage stable, the difference in softening points should not exceed 2.5°C (Bala, Napiah, et al., 2017). The results of the addition of ASA/Si and ASA/Fe at 3, 5 and 7% by the weight of ASA modified AC are illustrated in Figure 4.5.

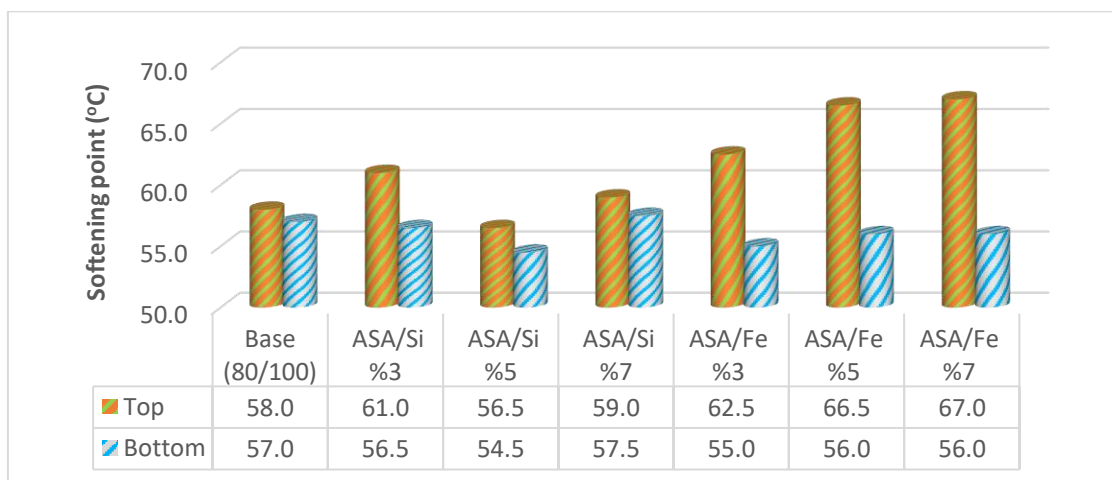


Figure 4.5: Storage stability results

From Figure 4.5 it was observed that, the storage stabilities for the ASA/Si samples were improved as the modifier to asphalt concentration was increased. It was observed that, the softening point of the sample extracted from the top part of the conditioned sample was not higher than 2.5°C for 5% and 7% ASA/Si modified AC, while at 3% ASA/Si concentration, the difference in softening points was 4.5°C. On the contrary, ASA/Fe modified AC samples demonstrated poor storage stability. The top section of the samples were significantly higher than the bottom sections. The differences were 7.5°C, 10.5°C and 11°C for ASA/Fe 3, 5 and 7% compositions respectively. A previous study conducted on ASA modified AC by (Ali et al., 2015) stated in their findings that, a disparity for the softening points between the top of the samples and bottom of the samples were observed to reach up to 12°C, displaying signs of a phase separated structure of asphalt and polymer matrix. Based on the experimental outcomes from the present study and the findings of (Ali et al., 2015), it can be concluded that, ASA/Si composites were able to improve the storage stability of AC while, ASA/Fe composites were ineffective in this context since, the addition of Fe in the ASA modified AC yielded to an insignificant improvement for the storage stability as compared to the findings of the previous research conducted on AC that was modified with ASA alone.

4.1.6 Aging index for AC

The aging of AC during the production stage and over the service course is a major durability concern because it causes hardening of the AC that alters its physical properties and rheological behaviour. As a result of the age hardening, the asphalt becomes stiffer and more brittle due to increased viscosities which makes it vulnerable to cracking. The aging occurs due to oxygenation, volatilization and polymerisation or it may occur due to the thixotropic nature of the asphalt material. Current available experimental methods are not sufficient to measure the degree of aging that occurs in the asphalt binder directly rather, a characteristic property comparison between the unaged samples and the samples which are subjected to aging procedures enable the quantification of the aging impact by using a parameter called the aging index. In this study, two different physical tests namely the softening point and the RV tests were conducted under fresh and short-term aging conditions to computing the aging indices for the PNC modified AC by using eq. 4.1.

$$\text{Aging index} = \frac{S_{\text{RTFO}} - S_{\text{unaged}}}{S_{\text{RTFO}}} \quad (4.1)$$

Where, S_{RTFO} is for the conditioned samples in a rolling thin film oven, and S_{unaged} is the unconditioned samples.

Figure 4.6 illustrated the aging index based on RV test results at elevated temperatures. The softening point aging index was also computed for each PNC modified AC and the results were tabulated in Table 4.2.

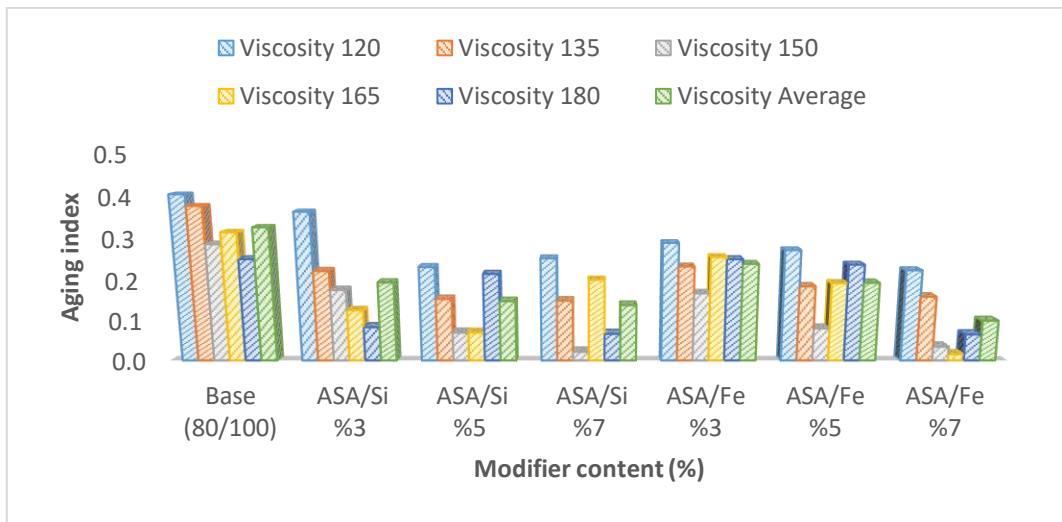


Figure 4.6: Viscosity aging index at elevated temperatures

The results displayed in Figure 4.6 demonstrated that, the viscosity aging index (VAI) for both polymer nanocomposites were reduced (on average) with the increase in modifier content, indicating an improvement in the aging resistance. The aging index for the ASA/Fe composites were successively reduced at all test temperatures while for the ASA/Si composites, deviations in the aging resistance trend particularly for 5% and 7% modifier concentrations were observed at elevated temperatures. This outcome was interpreted as the ASA/Si composite modified AC was less stable and more susceptible to changes in temperature as compared to the ASA/Fe composite samples in regard of the resistance to aging.

Table 4.2: Softening point aging index

Aging index	Base (80/100)	ASA/Si %3	ASA/Si %5	ASA/Si %7	ASA/Fe %3	ASA/Fe %5	ASA/Fe %7
Softening point (Unaged)	50.5	54.5	55	57	55.5	56.5	57.5
Softening point (RTFO)	57.5	59	59	59.5	61	61.5	63
Softening point Aging index	0.1217	0.0763	0.0678	0.0420	0.0902	0.0813	0.0873

As deduced from Table 4.2, for the ASA/Si composites, the gap between the unaged and short-term aged softening points were reduced significantly by increasing the modifier content. The difference in softening points between the unconditioned and conditioned samples were 4.5°C, 4°C and 2.5°C for ASA/Si 3, 5 and 7% concentrations respectively. The softening point for the ASA/Fe composites were slightly higher than the ASA/Si composites after the rolling thin film oven aging process. However, the gap between unconditioned and conditioned samples were higher and relatively in the same range rather than lowering which was the case for the ASA/Si composites. The softening point test results which were obtained from the unaged and short-term aged samples also enabled the computation of aging index and the quantitative analysis of the aging resistance of the PNC modified AC. A lower aging index indicated improved aging resistance while higher aging index represented the opposite. Compared to the base binder, the aging resistance of the ASA/Si composites were improved by 37.30%, 44.29% and 65.48% for ASA/Si 3%, 5% and 7% compositions. For the ASA/Fe composites the enhancement was 25.88%, 33.20% and 28.27% for ASA/Fe 3%, 5% and 7% respectively.

4.2 Chemical Structure and Morphology Analysis

The influence of the polymer nanocomposites on the performance characteristics of AC was evaluated according to the empirical and simulative testing procedures. It was observed that, the behaviour of PNC modified AC varied with different compositions. In order to understand the changes in the behaviour, XRD and FTIR techniques were utilized. The former was used to analyse the internal structure of asphalt and the later was used to identify the formation of new chemical and structural bondings due to the modification process.

4.2.1 X-ray diffraction

The analysis of changes in the internal structure (asphalt-polymer-nanomaterial matrix) of the PNC modified AC was performed by the X-Ray diffraction (XRD) method. A Bruker type D8 X-ray diffractometer was used in the investigation. The amorphous and crystalline structures were identified with the assistance of XRD plots. In Figures 4.7a and 4.7b, the XRD spectra for the base AC, additives alone and the blended polymer nanocomposites were illustrated. In a XRD plot, straight plateau with one or more smooth curves which are also called the mountain valley indicates the amorphous structures while, sharp and high/low peaks indicate that a material has a crystalline or semi-crystalline structures. The difference between the two different structures was the reactivity of the additives in the asphalt matrix. Formation of crystalline structures was a sign that, additives have interacted with the asphalt chemical composition to form new chemical structures whereas, an amorphous structure indicated low reactivity. It can be observed from Figures 4.7a and 4.7b that, base AC nanosilica and ASA/Si composites had an amorphous structure with a mountain valley around 20-25 degrees in the 2-theta angle range. ASA polymer, nano iron oxide and ASA/Fe composites were observed to have a semi crystalline structure. Sharp peaks around 32, 37, 46 and 65 degrees for the ASA and peaks around 30, 35, 43, 56 and 63 degrees for the nano iron oxide were associated to the presence of high reactivity in the asphalt matrix. ASA/Fe composites were observed to possess both an amorphous structure and semi-crystalline structures together due to the interaction between the additives and the base AC.

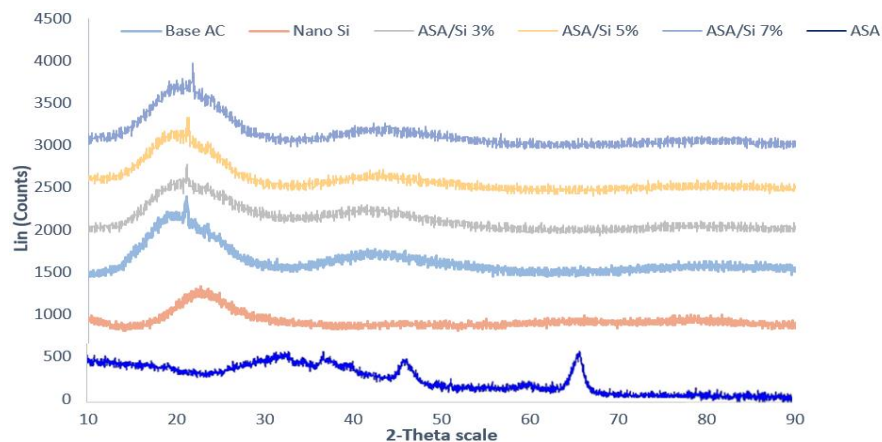


Figure 4.7a: XRD plot for ASA/Si composites

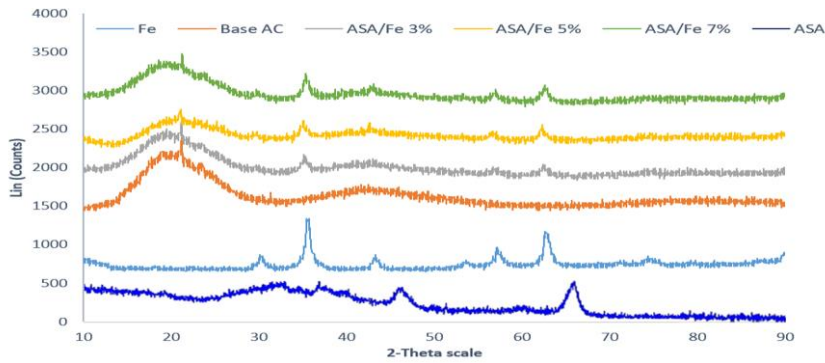


Figure 4.7b: XRD plot for ASA/Fe composites

Another outcome from the XRD plots was the interlayer spacing between the layered silicates of the nanomaterials. The interlayer spacing (d-spacing in XRD analysis) was computed with a dedicated software by using the Bragg's law expressed in eq. 3.1. D-spacing was a sign of formation of phase separated, intercalated and/or exfoliated structures of PNC modified AC. A higher d-spacing indicated insertion of polymers in-between the layered structure to form intercalated or exfoliated structures, while lower d-spacing indicated the opposite which resulted in phase separated structures.

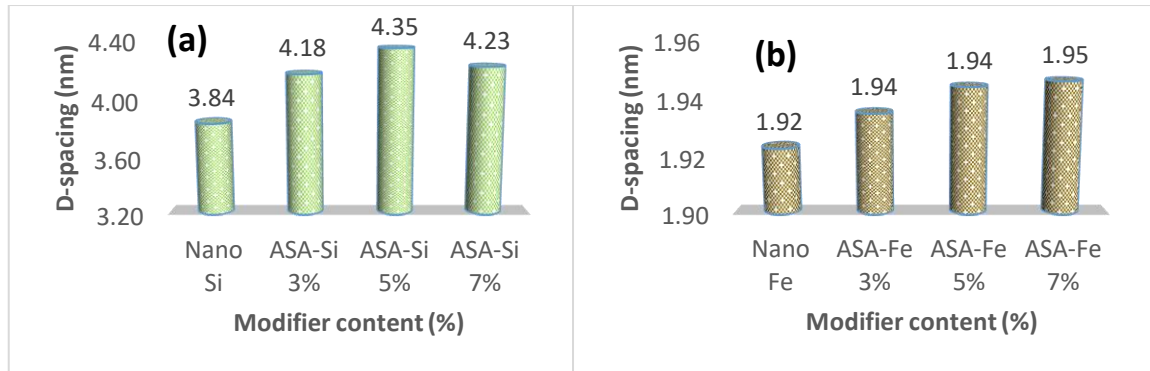


Figure 4.8: D-spacing for PNC modified AC (a) ASA-Si (b) ASA-Fe compositions

Based on findings from a previous study conducted by (Golestani et al., 2012), it was reported that, little or no change in the interlayer spacing is an indication of phase separation, d-spacing around 4nm was considered as proof of formation of intercalated structures while d-spacing differences around 8nm, the material was said to possess an exfoliated structure. From Figure 4.8, d-spacing for ASA/Si composites were shown to increase up to 5% ASA/Si

addition while for the ASA/Fe composites, the change in d-spacing was barely significant. Intercalated and exfoliated structures was a sign of better dispersion of additives in the asphalt matrix while phase separation was an undesired phenomenon which resulted in lower stability and lower aging resistance for the PNC. The results from the XRD analysis were a justification for the better storage stability and aging resistance as presented in the findings of Chapters 4.1.5 and 4.1.6.

4.2.2 Fourier infrared spectroscopy

The FTIR analysis was employed to observe the chemical interactions between the additives and the base asphalt during the modification process. Additionally, with the FTIR analysis, the effect of aging on the chemical composition of the PNC modified AC was investigated. The FTIR investigation was performed in a spectra of wavenumbers from 4000 cm^{-1} - 600 cm^{-1} . The most significant changes occurred below the 2000 cm^{-1} which is also called the fingerprint region. Identified chemical structures and formation of new functional groups in this particular region enabled the analysis of aging resistance and performance behavior of modified asphalt cement. The evidence of the formed groups were illustrated in Figures 4.9a and 4.9b and the associated IR bands were demonstrated in Table 2.5. As observed from the FTIR spectra, for both PNC's, there was no formation of new chemical structures due to the modification process since, the characteristic peaks at specific wavelengths were not shifted in the horizontal direction. Also, FTIR technique was particularly useful in describing the changes in chemical composition of asphalt-polymer nanocomposite matrix after being exposed to aging conditions. During the aging process, chemical composition of the bitumen may change due to bonding with oxygen. Structural groups such as the carbonyl and sulfoxide compounds were the most significant parameters that were used to evaluate the effect of chemical transformation on the aging resistance. Appearance of these compounds in higher peak concentration was an indication of a lesser aging resistance for the PNC modified AC. Additionally, functional groups such as the aromatic and aliphatic compounds were related to the aging of asphalt cement and therefore they were monitored during the aging process. A quantitative analysis was performed to identify the level of formations of new and differential structural and functional groups by computing the areas under the characteristic peaks at different wavelengths. A tangential integration method was utilized

to measure the area for each characteristic peak from valley to valley with the aid of a dedicated software (Origin Pro 9.1), then eq. 2.11 was utilized to compute the group index. The results of the quantitative analysis were illustrated in Figures 4.10a to 4.10d.

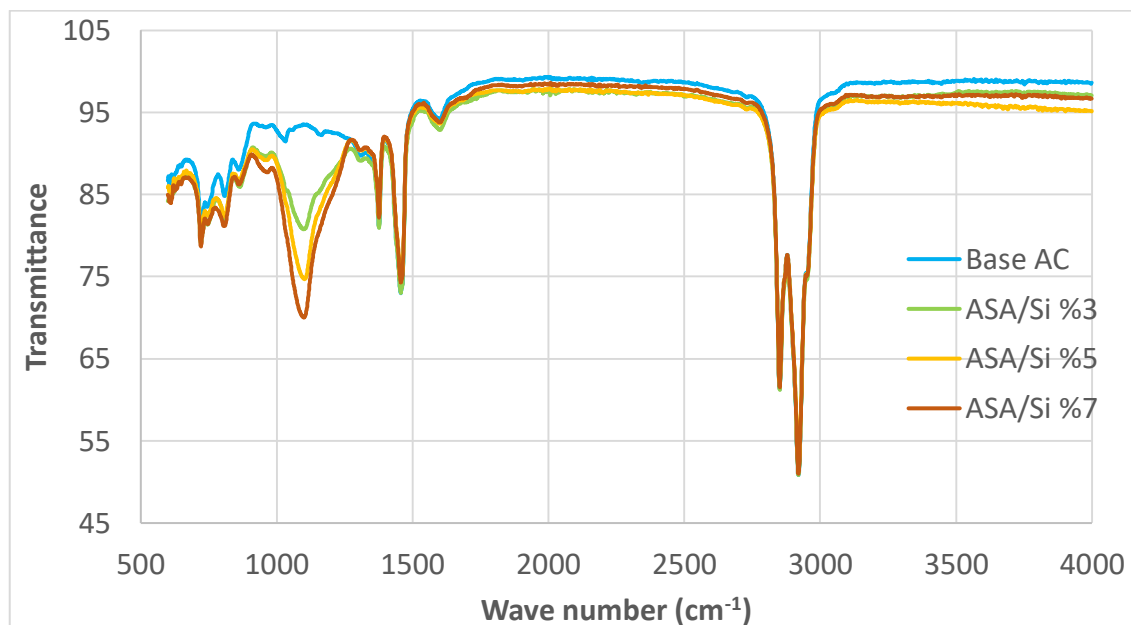


Figure 4.9a: Spectrum pattern for the ASA/Si composite binders

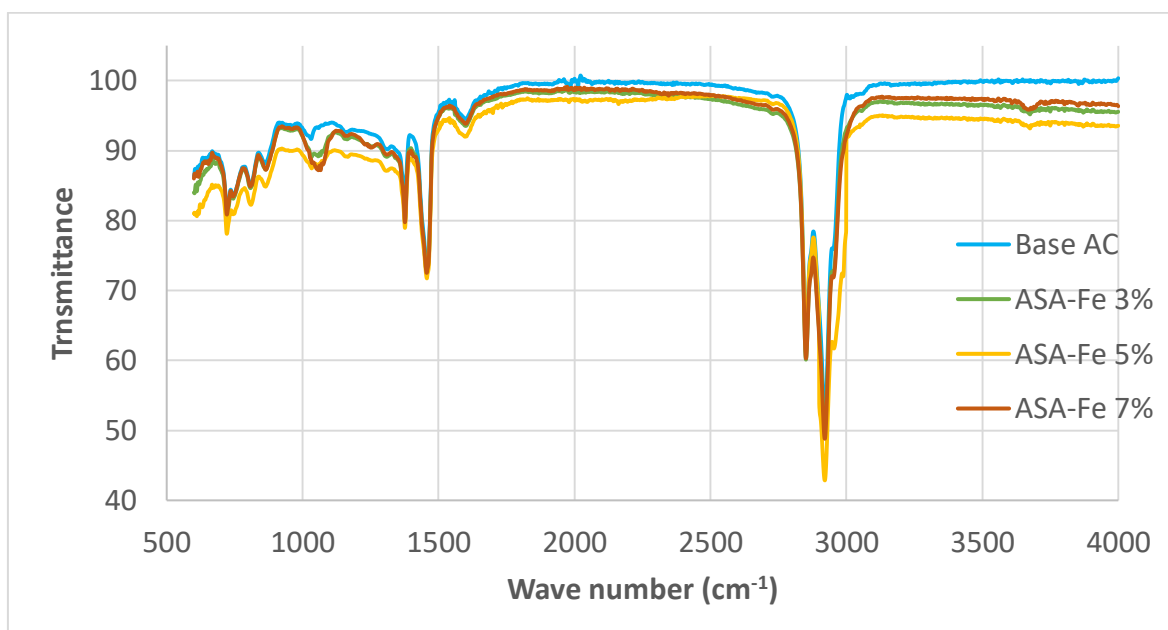


Figure 4.9b: Spectrum pattern for the ASA/Fe composite binders

The existence of aliphatic structures was apparent in the FTIR spectra in a wavelength ranges of 1376 cm^{-1} and 1460 cm^{-1} . The presence of aliphatic structures was evident by the symmetric and asymmetric carbon and hydrogen bending vibrations. Aliphatic structures were the light components in the asphalt matrix which may be volatilized because of the presence of high temperature during the processing of asphalt and/or transformed to form aromatic rings when interacting with the additives. From Figure 4.10a, it was observed that, aliphaticity of all binders were reduced consistently after short-term age conditioning the samples where, the samples were exposed to high temperature for 2 hours. Additionally a reduction of aliphaticity was noted by increasing the modifier content which was attributed to the interaction between the chemical composition of additives and the base asphalt. The aromatic structures were existed in the FTIR spectra at 1600 cm^{-1} wavelength. An increase in the aromatics index was observed for the neat binder, ASA/Si at 3% and ASA/Fe at 3% and 5% concentrations after being exposed to aging procedures. This was related to the equivalent descention in the aliphatic index. However, for ASA/Si 5% and 7% and ASA/Fe 7%, a reduction in the aromatics was observed after short-term aging. This was associated to continued interaction between the additives with bitumen to absorb aromatic structures. Sulfoxides and carbonyls were the main oxidation products of the bitumen aging due to sulphur double binding with oxygen ($\text{S}=\text{O}$) and carbon double bonding with oxygen ($\text{C}=\text{O}$). They appear in the wavelengths of 1034 cm^{-1} and 1700 cm^{-1} in the FTIR spectra respectively. Although the sulfoxide band was visible for the base binder, it was not apparent for the ASA/Si modified binders due to the overlapping phenomena of the bonds in the spectra since the silica and oxygen bonds of silicon dioxide (SiO_2) was present within the same band wavenumbers. For the ASA/Fe composite modified binders, this peak was visible and sulfoxide index was computed and the results were illustrated in Figure 4.10c. A reduction in the sulfoxide group after applying the aging conditions was an indication for improved aging resistance. Up to 5% addition of ASA/Fe composite, the gap between the unaged and RTFO aged samples were reduced while, for the ASA/Fe 7% the gap has increased. A possible mechanism for this behaviour could be the excessive phase separation phenomenon between the additives and the base binder. Another group that was associated with the aging index was the carbonyl group. The peaks for carbonyl group were missing in the FTIR spectra for the ASA/Fe composites. This was associated with the formation of sulfoxide compounds which were more reactive compared to the carbonyl compounds. This outcome

showed that, the ASA/Fe modified AC samples were not affected further due to the aging process. On the other hand, although the sulfoxide groups were missing, the carbonyl group was present for the ASA/Si composites. It can be observed from Figure 10d that, the carbonyl index increased after aging however, with the addition of ASA/Si, the gap between the unaged and aged binders was significantly decreased which indicated that, by increasing the amount of modifiers in the blend, the aging resistance of the asphalt was increased.

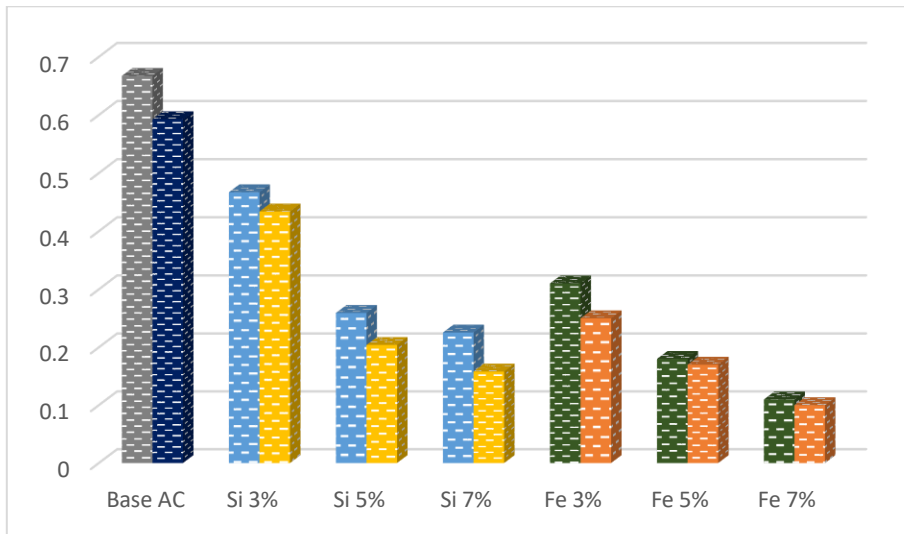


Figure 4.10a: Aliphatic index

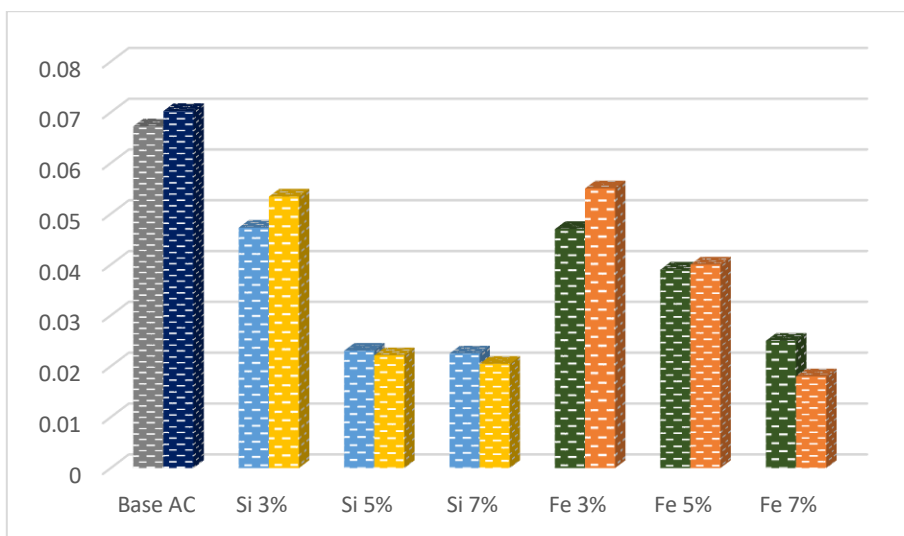


Figure 4.10b: Aromatics index

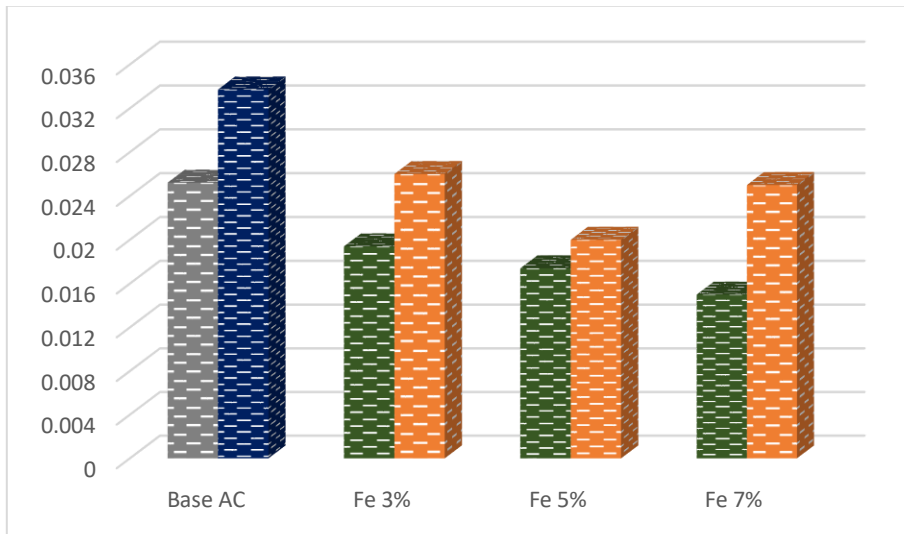


Figure 4.10c: Sulfoxide index

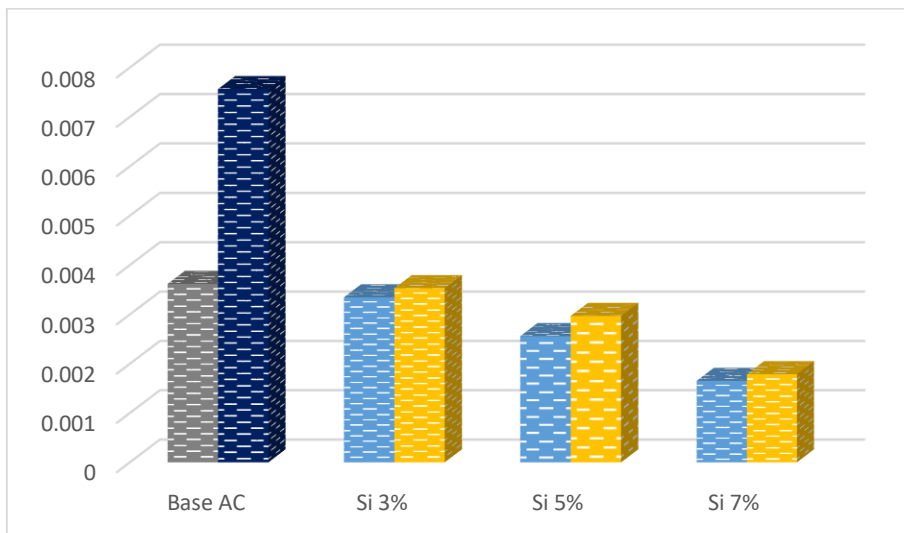


Figure 4.10d: Carbonyl index

4.3 Performance Characteristics

Asphalt exhibits viscoelastic and thermoplastic behaviour meaning that, at different frequencies and temperatures its rheological properties are dependent on its viscous and elastic components. On this basis, it is more reliable to evaluate the performance of asphalt by using the aforementioned components along with the physical and chemical property testing procedures. A DSR was utilized to provide two different kinds of rheological

assessment for the base and PNC modified AC. Namely, these tests were the frequency sweep test and the MSCRT. The former testing procedures represented the stiffness (G^*) and the elastic modulus (δ) for the AC while, for the later experimental technique, the outcomes were presented in non-recoverable creep compliance (J_{nr}) and the elastic recovery (%R). More detailed information regarding to the test parameters utilized and the test outcomes are explained in the following Chapters 4.3.1 and 4.3.2.

4.3.1 Frequency sweep test

The frequency sweep test was performed by using a DSR machine. The test was conducted under strain controlled condition which enabled the tests to be conducted within the viscoelastic zone. The maximum shear strain was set to 12.5% and the frequency sweep testing procedures were applied on this shear strain level. After defining the maximum shear strain level, the frequency sweep tests were conducted under various temperatures (10, 16⁺⁶ up to 82°C) using two different spindles; 8mm and 25mm and two different thicknesses of samples; 1mm and 2mm for the low and high temperatures respectively. A range of frequencies starting from 0.159 Hz up to 15.92 Hz were used as the frequency test parameter. The most significant outcomes from the frequency sweep test were the G^* and δ . These output parameters enabled the graphical representation of the performance characteristics of base and the PNC modified AC in isochronal plots and rheological master curves. Further, the outcomes were used in the computation of the rutting and fatigue resistance parameters.

4.3.1.1 Isochronal plots

Isochronal plots allowed the viscoelastic features of base and modified AC such as the G^* versus temperature at certain frequencies to be displayed. The effects of the modification process on the stiffness and temperature susceptibility of AC were visualised in isochronal plots. The results from the isochronal plots which represented the stiffness and elasticity of binders from 10°C to 82°C at two different frequencies; 0.159 Hz and 15.92 Hz were illustrated in Figures 4.11 and 4.12 for ASA/Si and ASA/Fe composite modified AC respectively. The results illustrated in Figure 4.11a and 4.11b showed that, at high temperatures (above 46°C), the base AC demonstrated the lowest G^* and 5% ASA/Si has

the highest G^* . G^* for the ASA/Si at 7% concentration was insignificantly less than that of the G^* for ASA/Si 5% at high temperatures however, it was observed that ASA/Si 5% performed better than the ASA/Si 7% at low temperatures due to lesser G^* (below 46°C to 10°C). At low temperatures, the G^* was the minimum for the ASA/Si 3% which was followed with an increasing trends for base AC, ASA/Si 5%, and ASA/Si 7% successively whereas, the G^* for the base AC and ASA/Si 5% were almost identical. This outcomes were interpreted as, ASA/Si composites were able to continuously improve the viscoelastic properties of base AC up to 5% addition of the modifiers both at high temperatures and at low temperatures. At 7% ASA/Si composition, the G^* was higher compared to base AC at high temperatures but it was lower compared to ASA/Si 5% and G^* for base AC was less than the G^* for ASA/Si 7% which means that, at low temperatures the elastic properties of base AC was better than the ASA/Si 7%. A possible outcome for different behaviour of ASA/Si 7% can be attributed to instability of the blend due to agglomeration of the nanoparticles at higher modifier content in the PNC modified AC matrix. The isochronal plots illustrated in Figures 4.11a (G^* at 0.159 Hz) and 4.11b (G^* at 15.92 Hz) followed a similar trend. Additionally, the results showed that the influence of additives were more prominent at high frequencies and temperatures. The isochronal for the ASA/Fe modified AC were presented in Figure 4.12. The results showed that, the base AC has the lowest stiffness and the highest elasticity while, ASA/Fe 3% has the highest stiffness and the lowest elasticity both at high and low temperatures. The G^* for the ASA/Fe 5% and 7% lied between the base AC and the ASA/Fe 3% while ASA/Fe 5% was observed to perform slightly better than the ASA/Fe 7%. In general, it can be concluded that, since all modified binders demonstrated higher stiffness both at high and low temperatures, ASA/Fe composites were able to improve the high temperature performance characteristics of base AC but they were inefficient in improving the low temperature performance characteristics.

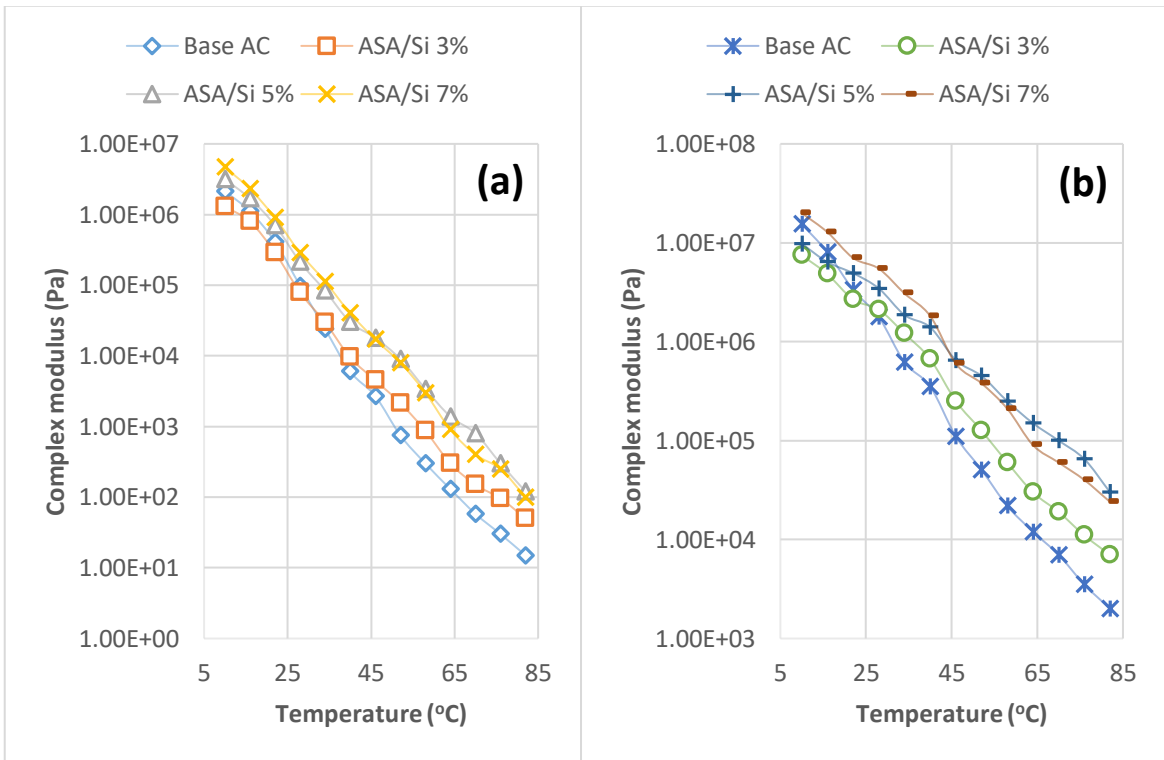


Figure 4.11: Isochronal plots for ASA/Si composites at (a) 0.159Hz (b) 15.92Hz

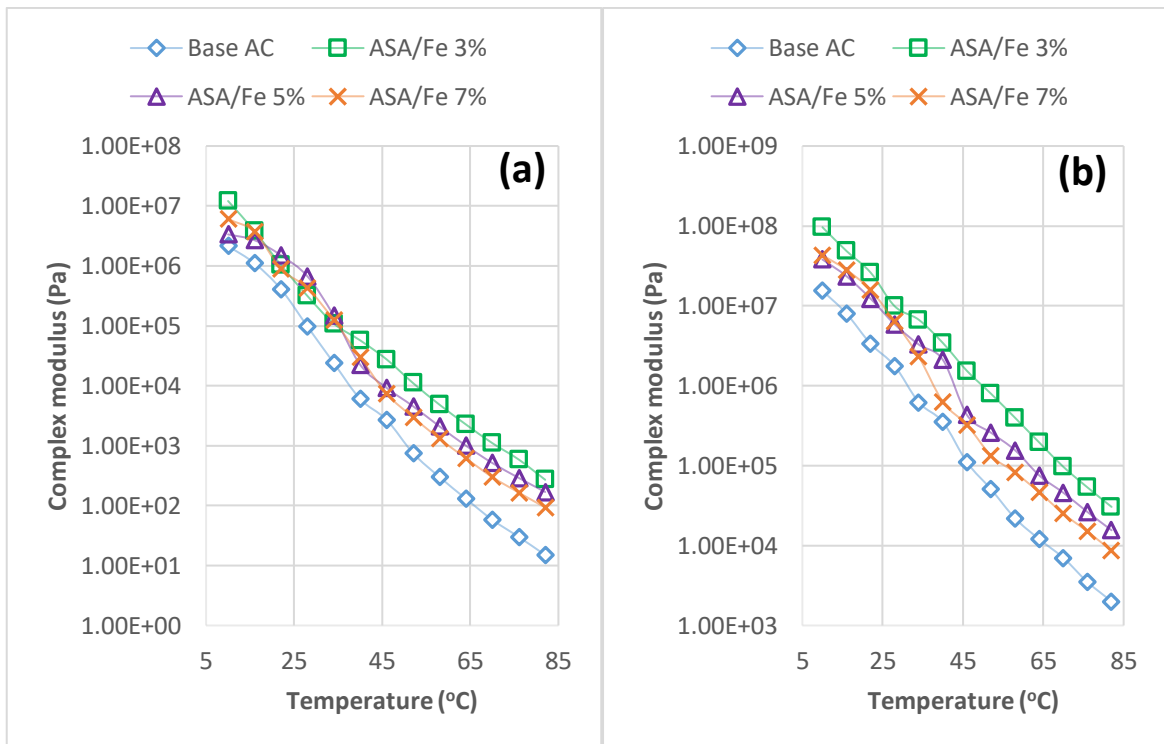


Figure 4.12: Isochronal plots for ASA/Fe composites at (a) 0.159Hz (b) 15.92Hz

4.3.1.2 *Master curves*

One of the most fundamental and effective representation methods to analyse the viscoelastic properties of asphalt that has been adopted without exception in the high class investigations has been the master curves therefore, to better characterise and understand the rheological performance of base and PNC modified AC, master curves were constructed. A master curve is a representation of stiffness (G^*) in a range of temperatures and frequencies which is displayed in a single graph. To construct a master curve, time-temperature superposition theorem was utilized which was, the shifting of the G^* data points at different temperatures observed from the experiments in the horizontal axis (range of frequencies) to plotting a single smooth curve. Herein, a reference temperature of 64°C was selected and the data points at the other temperatures were shifted horizontally to and fro by using the convenient shift factors. Figures 4.13 and 4.14 illustrated the complex modulus master curves in fresh and short term aged states for ASA/Si and ASA/Fe composites respectively. Greater complex modulus at high temperatures and higher elasticity at low temperatures were the favourable viscoelastic properties of AC. Low temperature elastic properties were illustrated in the previous chapter (Chapter 4.3.1.1) with the aid of isochronal plots while the master curve outcomes for the high temperature permanent deformation characteristics are evaluated herein. From Figures 4.13a and 4.14a, it was observed that, the stiffness of all PNC modified AC's were higher than the base asphalt under unaged conditions, indicating that the modification process has led to enhanced complex modulus. The increase in G^* was more remarkable for the ASA/Fe composites than the ASA/Si composites. This showed that, the ASA/Fe composites were more suitable for paving applications in regions where the high temperature conditions are anticipated. It was also noted that, the influence of the additives when used in different concentrations affected the rheological behaviour of the PNC modified AC. The maximum enhancement in G^* were obtained at 5% ASA/Si and 3%ASA/Fe compositions and therefore they were considered to be the optimum compositions for improving the high temperature performance characteristics of AC, as further addition of PNC resulted in lower enhancement in the rheological properties of AC. The reduction in G^* was attributed to the occurrence of agglomeration of the nanoparticles in the case of ASA/Si composites while formation of the phase separated structures was one of the possible causes for this reduction in enhancement in performance characteristics for

the ASA/Fe composites. From the literature review, it was acknowledged that the nano particles tend to agglomerate and form clusters within the composite asphalt matrix which may have led to reduction in the performance enhancement at usage in higher concentrations. On the other hand, the phase separation phenomenon for the ASA/Fe composite modified AC was a possible cause for reduced G^* which was also evidential from the storage stability test results and the chemical characterisation tests. Furthermore, as observed from the Figures 4.13b and 4.14b, the master curves constructed after the short-term aging procedures followed a similar trend for the modified and base asphalt; therefore, the increase in the G^* was attributed to the short-term aging of the asphalt phase rather than the rearrangement of the polymer/nanocomposite particles. On this basis, the increase in G^* after undergoing short-term aging was referred to as hardening of the materials due to volatilization and oxygenation and no new chemical structures were formed after applying the short-term aging procedures which was also validated by the FTIR analysis in the chemical characterisation analysis (see Chapter 4.2.2). However, it is noteworthy to mention that, a relatively small increase in G^* for the PNC modified AC's compared to the base AC can be related to improved aging resistance and improved temperature susceptibility.

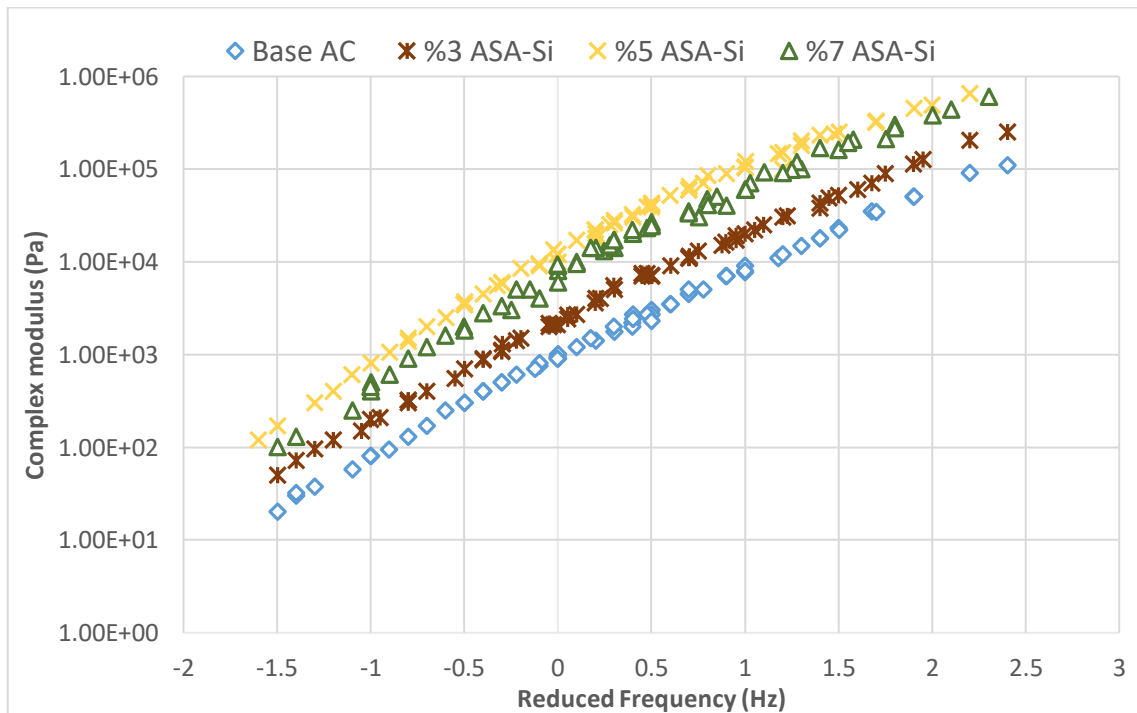


Figure 4.13a: G^* for unaged base and ASA/Si modified AC

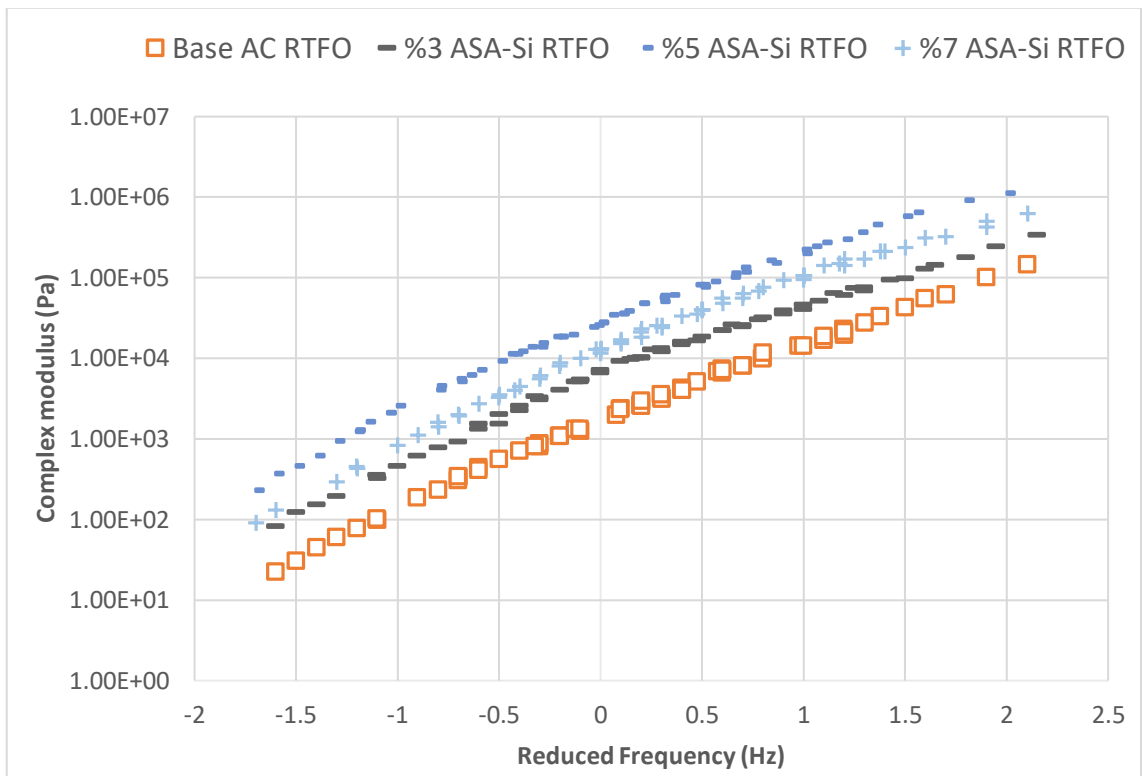


Figure 4.13b: G^* for RTFO aged base and ASA/Si modified AC

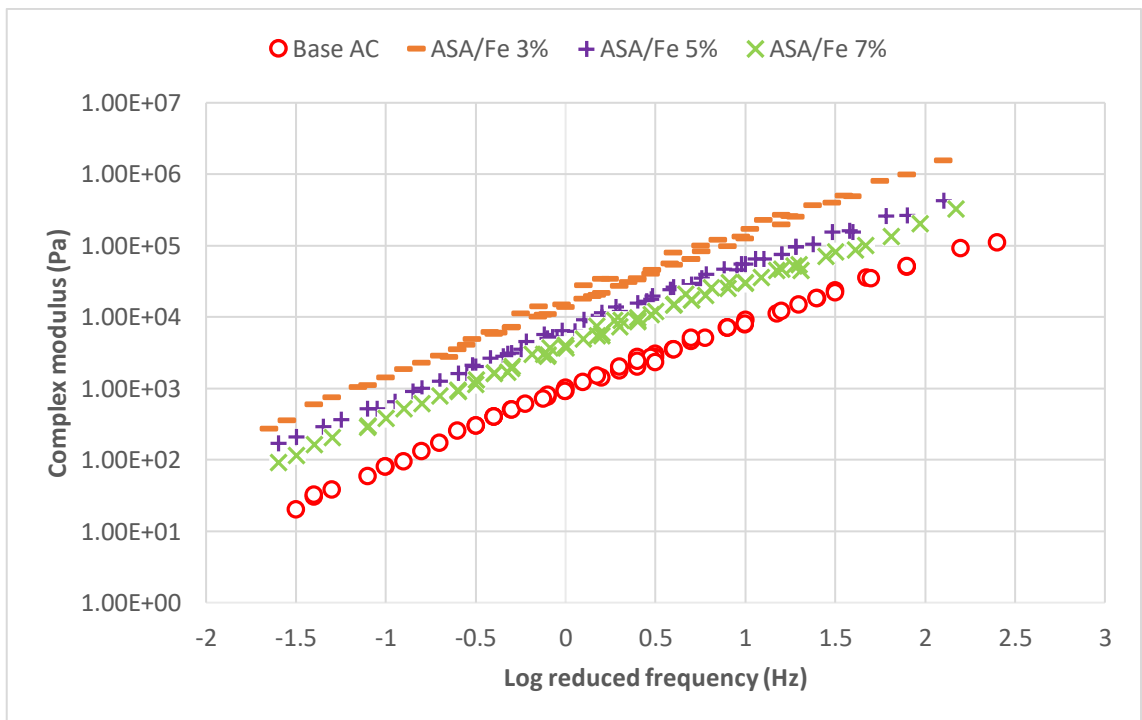


Figure 4.14a: G^* for unaged base and ASA/Fe modified AC

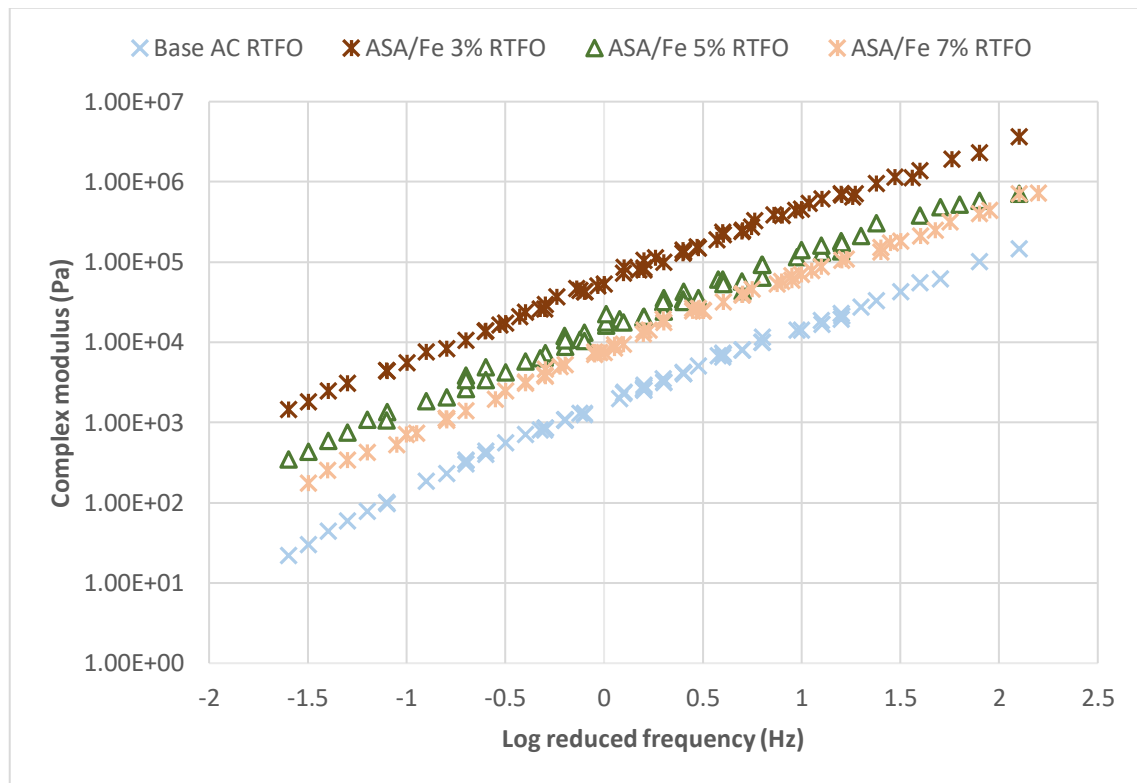


Figure 4.14b: G^* for RTFO aged base and ASA/Fe modified AC

4.3.1.3 Rutting and fatigue resistance parameters

The rutting resistance is the ability of asphalt binder to resist permanent deformation at high temperatures. Rutting resistance is defined as the ratio of the viscous and the elastic portions of an asphalt binder and it is denoted with the formula $G^*/\sin \delta$. According to Superpave standards, at a loading rate of 1.592 Hz, a minimum of 1 kPa is the allowable requirement for an unaged sample of binder. The rutting parameter was evaluated in a range of temperatures from 46°C- 82°C at a loading rate of 1.592 Hz by using the G^* and δ outcomes from the frequency sweep test results. As illustrated in Figure 4.15a, $G^*/\sin \delta$ was the lowest for base AC. Binders containing ASA/Si composites up to 5% by the weight of bitumen demonstrated the highest $G^*/\sin \delta$ value, while the addition of ASA/Si composites above 5% concentration led to reduced $G^*/\sin \delta$. The compatibility problem between the polymer nanocomposite and the binder was considered to be the factor leading to the reduction in rutting resistance parameter at 7% ASA/Si concentration. From Figure 4.15b, it was observed that, among all of the compositions for the PNC modified AC including the ASA/Si

composites, the ASA/Fe composite modified AC at 3% modifier content resulted in the highest $G^*/\sin\delta$. For the ASA/Fe composites at 5% and 7% modifier content, although the $G^*/\sin\delta$ was higher compared to the base AC, they were considerably lower as compared to the ASA/Fe 7% and also ASA/Si composites at 5 and 7% modifier contents. The different behaviour was associated to the phase separation between the polymer and the nanoparticles. In general, it can be concluded that, the rutting performance of all the PNC modified AC were enhanced significantly compared to the base binder and satisfied the minimum requirement of 1 kPa at 1.592 Hz and at 64°C.

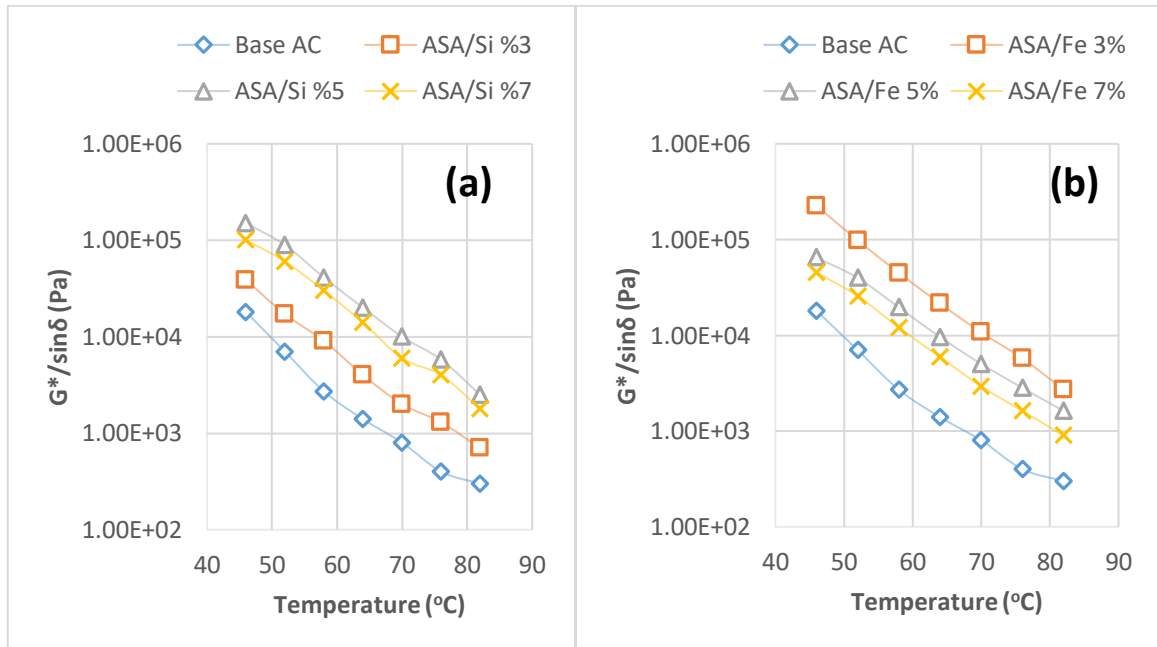


Figure 4.15: Rutting resistance parameter (a) ASA/Si (b) ASA/Fe composites

The effect of additives on the low temperature fatigue cracking behaviour of AC was analysed by the fatigue resistance parameter which was denoted by the formula $G^*.\sin\delta$. The minimised $G^*.\sin\delta$ parameter was an indication of better fatigue cracking resistance for the AC. The Superpave method considers 5000 kPa as the maximum limit of fatigue cracking at low and intermediate temperatures. From Figures 16a and 16b it can be observed that, the Superpave maximum criteria was met for ASA/Si composites at a temperature of 18°C while, the ASA/Fe composite modified AC samples were shown to be resistant to fatigue

cracking at temperatures around 26°C. Additionally, as illustrated in Figure 15.b, the ASA/Fe composites were shown to demonstrate weaker fatigue resistance than the base AC which was due to the higher stiffness of the polymer/nanocomposites due to the modification process. On the other hand, ASA/Si composite modified AC at 3% and 5% compositions were found to have lower $G^* \cdot \sin\delta$ compared to the base AC and at 7% composition the results were slightly similar to the $G^* \cdot \sin\delta$ at temperatures up to 15°C. Beyond this trend, $G^* \cdot \sin\delta$ for PNC modified AC were increase continuously. This outcome demonstrated that the ASA/Si composite modified binders were able to improve both the high and low temperature performance characteristics of AC while ASA/Fe composites were only efficient in enhancing the high temperature performance characteristics of AC.

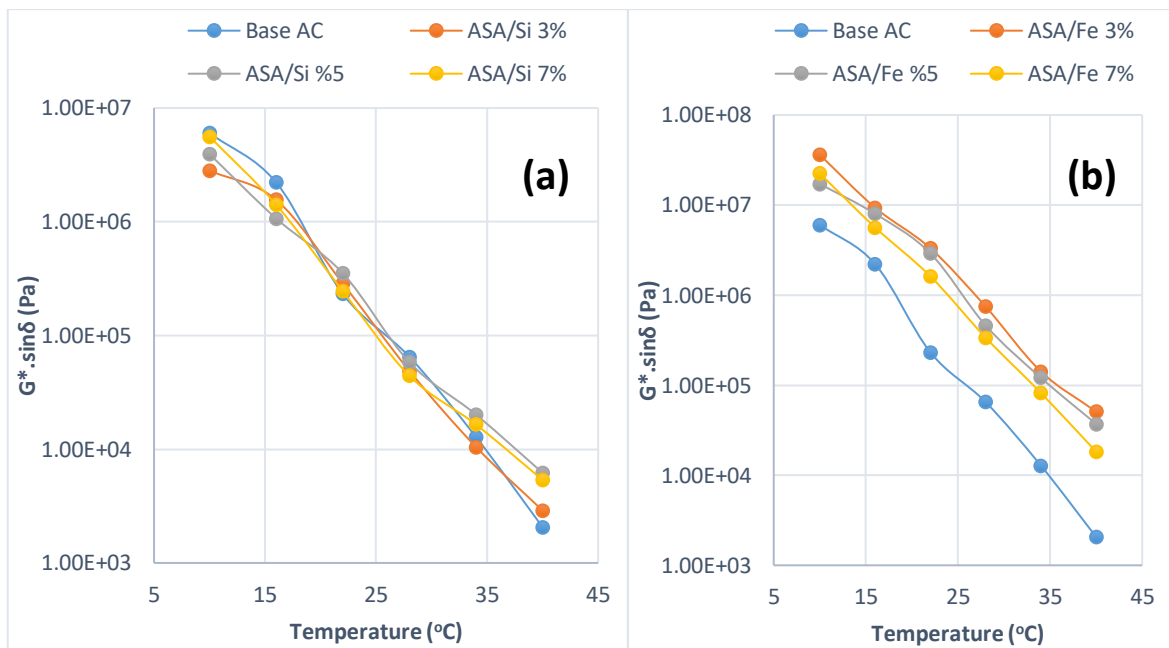


Figure 4.16: Fatigue resistance parameter (a) ASA/Si (b) ASA/Fe composites

4.3.2 MSCR test

The MSCR test was utilized to simulate the movement of traffic flow on the highway surface and to evaluate the resistance and recovery of asphalt binder against rutting. The test procedure involved two phases. The first phase was the creep phase which the samples were subjected to a constant load for nine seconds and the second phase was the recovery phase

which the asphalt samples were rested at recovery for one second. The two phases were completed in a 10 seconds interval which is considered as one cycle. The test was conducted at two different loading levels which were the 100 Pa and 3200 Pa to represent the low stress and high stress traffic scenarios respectively. The test temperature was 64°C which was determined by the binder grade according to the Superpave performance grading criteria. The test was run continuously without a halt at low and high stress levels where ten consecutive cycles were applied at the former stress level which was then followed by another 10 consecutive cycles at the latter stress level. The cumulative strain, non-recovered creep compliance and the percent recovery were the outcomes from the MSCR test. Figure 4.17 and 4.18 displayed the creep and creep recovery schemas for the base AC, ASA/Si and ASA/Fe composite modified AC's, while parts a and b for each figure was presented separately for distinguishing the effect of loading rate at the low stress and high stress levels. It was observed that, the accumulation of strain was higher for the ASA/Si composites than the ASA/Fe composite modified binders. This was due to ASA/Fe composite modified binders yielded better resistance to permanent deformation (rutting) at high temperatures which was also evidential from the frequency sweep test results. Further, it was observed from the differences in parts a and b from Figures 4.17 and 4.18 that, at 3200 Pa stress level the accumulated strains were significantly higher than at the lower stress level at 100 Pa. Additionally, it is noteworthy to mention that, the gap of strain accumulation between the base and PNC modified AC for both modifiers reduced at higher stress levels which indicated that the influence of additives were more prominent at low stress levels.

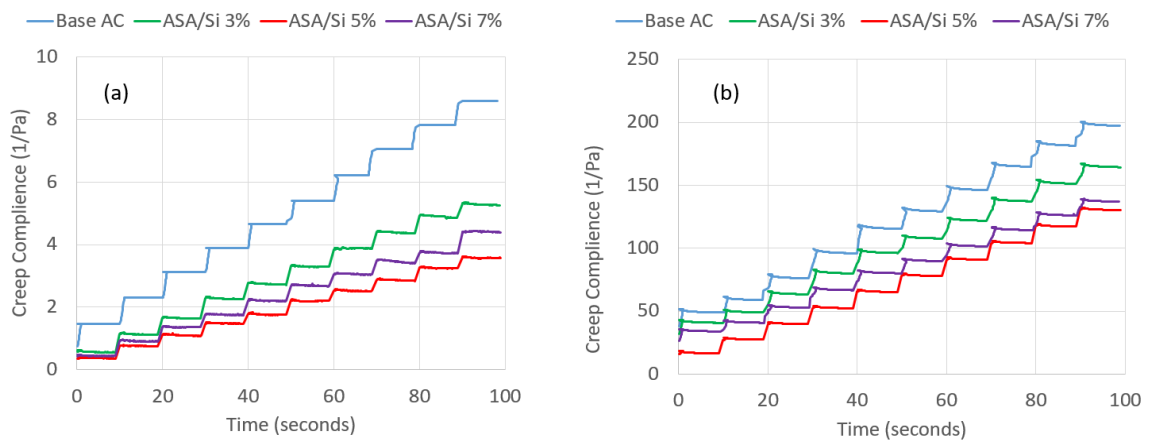


Figure 4.17: Creep compliance for ASA/Si composites (a) 100 Pa (b) 3200 Pa

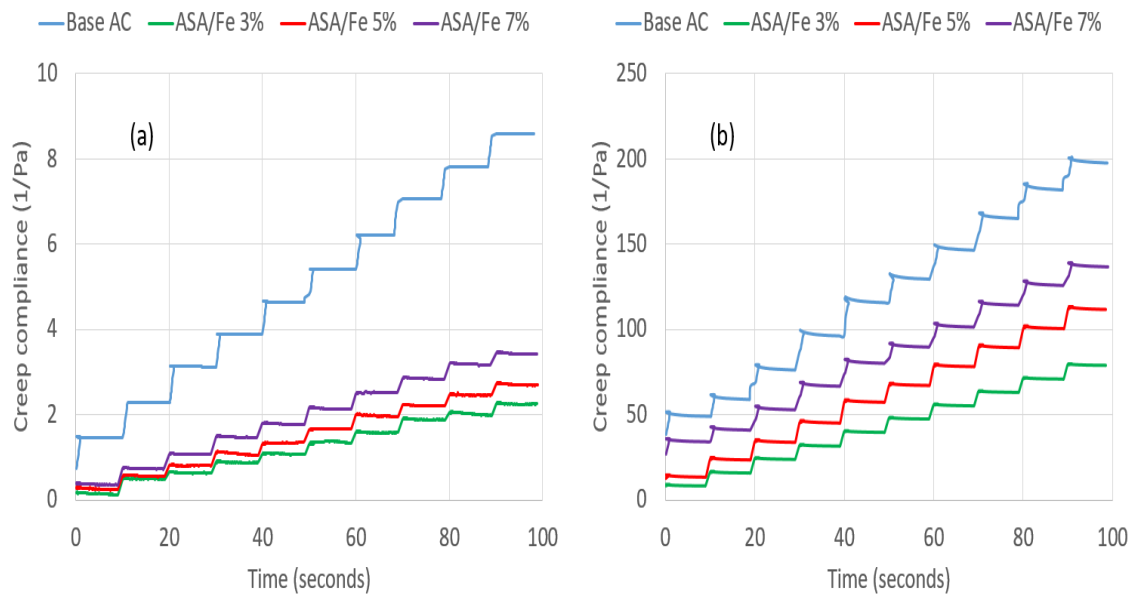


Figure 4.18: Creep compliance for ASA/Fe composites (a) 100 Pa (b) 3200 Pa

The influence of additives on the performance characteristics was further investigated by analysing the non-recovered strain after the loading phase and the recovery rate during the resting period. Non recoverable strain was denoted as the J_{nr} and the recovery rate was referred to as the %R. A higher R% and a lesser J_{nr} were the favourable properties of AC in order to improving the viscoelastic behaviour of AC. From Figure 4.19, enhancement in the elastic recovery (%R) for the ASA/Si composite modified AC up to 5% composition was observed, while this increase was less for the 7% ASA/Si modifier content. At 100 Pa stress level, the percentage increase for the ASA/Si at 3, 5 and 7% contents compared to the base asphalt were 39.5%, 92.8% and 52.0% respectively, while at the 3200 Pa stress level the percentage increase were 93.4%, 199.0% and 95.0%. The percentage increase in terms of %R was 81.1%, 65.0% and 32.6% at 100 Pa and it was 173.1%, 154.9% and 100.61% at 3200 Pa for the ASA/Fe composite modified binders. Apart from the %R, the computed J_{nr} results illustrated in Figure 4.20 demonstrated that, the non-recoverable creep was reduced after the modification process. The reduction of the J_{nr} for the ASA/Si composites compared to the base AC were 22.0%, 43.5% and 17.7% at the 100 Pa stress level and it was 31.9%, 41.30% and 12.9% for ASA/Si 3, 5 and 7% respectively. For the ASA/Fe composites 3, 5 and 7% addition of additives resulted in reduction of J_{nr} by 48.8%, 37.8% and 20.27% at 100 Pa stress level and by 51.3%, 41.3% and 26.1% at 3200 Pa stress level respectively.

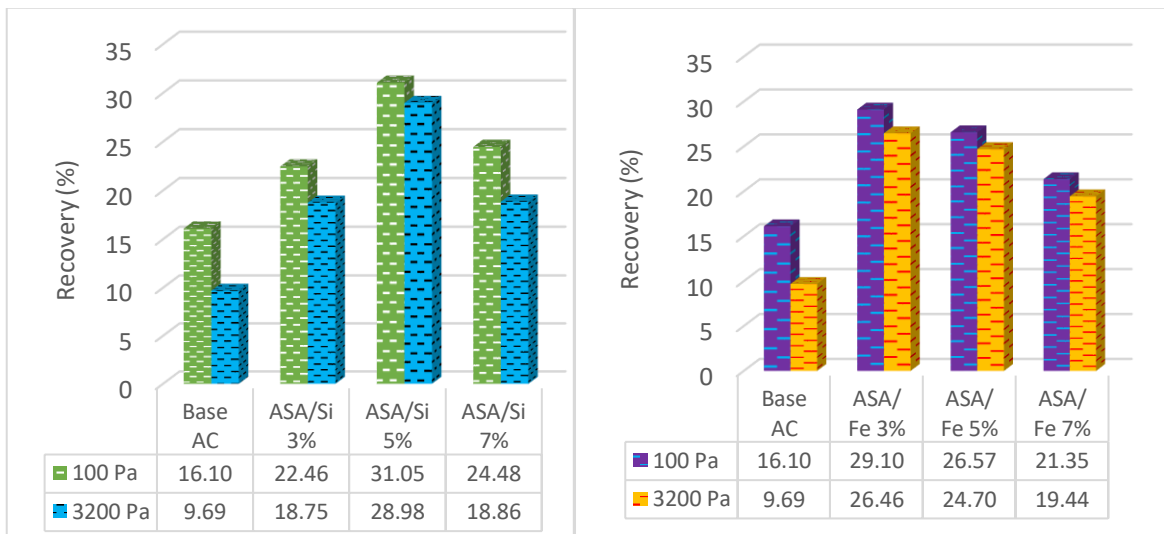


Figure 4.19: Elastic recovery for base, ASA/Si and ASA/Fe composites

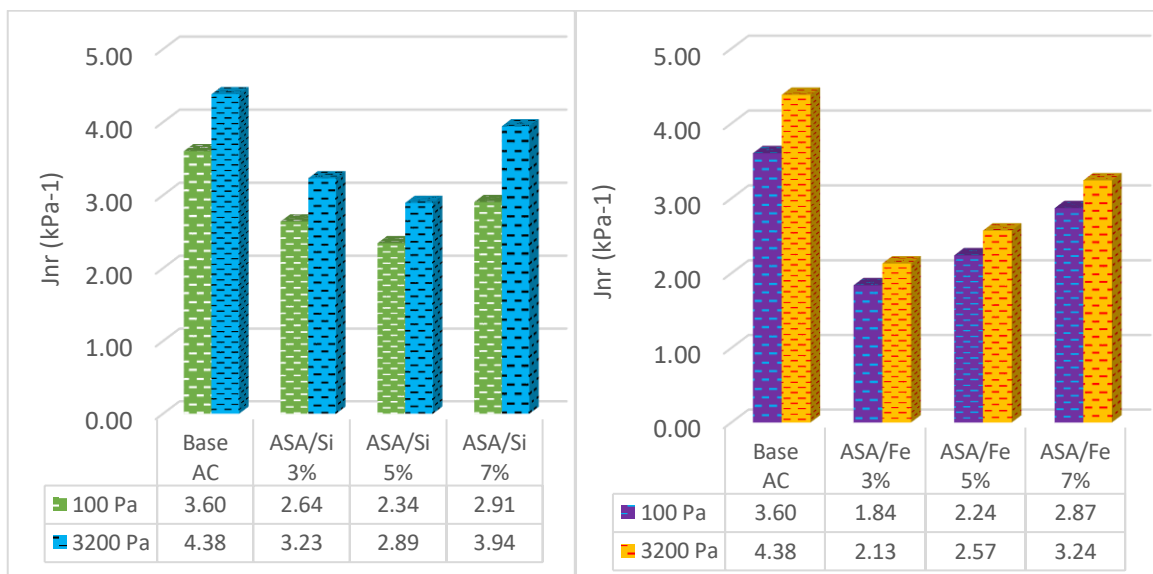


Figure 4.20: Non-recoverable creep compliance for base, ASA/Si and ASA/Fe composites

4.4 Heuristic Modelling Of Performance Characteristics

The performance characterisation of AC by experimental investigations involves time and resource intensive testing procedures that challenge to acquire advanced laboratory equipment and well maintained testing facilities. On this basis, an abundant research have been available in the literature which focus on developing statistical and computer aided

models to estimate AC's output characteristics along with the experimental investigations (Venudharan & Biligiri, 2017). For the same purpose, two different computer modelling techniques namely; the ANN and ANFIS were utilized in the current study to develop two different models by each artificial intelligence machine learning algorithms. The models were labelled as scenario 1 and scenario 2 where, the former was targeted to predict the G^* for polymer nanocomposite modified AC from the physical test results and the experimental set-up and the latter scenario was develop to predict the G^* outcome for the RTFO aged samples from the samples G^* in fresh state and the mechanical testing conditions. The descriptive statistics for the inputs and output parameters which were observed from the experimental investigations were presented in Table 4.3. Penetration, softening point, test temperature and frequency were the inputs and the unaged G^* was the output parameter for scenario 1. Test temperature and frequency and the G^* in unaged state were the input and G^* in RTFO state was the output parameters in scenario 2.

Table 4.3: Model Scenarios and descriptive statistics for the input and output parameters

	Penetration (mm⁻¹)	Soft. Point (°C)	Temp (°C)	Freq. (Hz)	Unaged G* (Pa)	RTFO G* (Pa)
Mean	59.7310	55.1429	64.0000	4.2634	27032.8367	47233.2908
Standard Error	0.6115	0.1048	0.5721	0.2414	3563.9254	5383.4413
Kurtosis	1.3505	0.1451	-1.2506	0.4654	27.7874	30.3371
Skewness	1.6502	-1.0717	-0.0091	1.3322	4.8314	4.8393
Range	40.6000	7.0000	36.0000	15.7610	649989.140	1099976.95
Minimum	49.0000	50.5000	46.0000	0.1590	4178.0000	9515.0000
Maximum	89.6000	57.5000	82.0000	15.9200	657000.000	1130000.00

4.4.1 Artificial neural network

ANN is an artificial intelligence based modelling technique which works by mimicking the functioning of a human brain. This way, ANN is considered to be a black box model that consists of artificial neurons rather than biological neurons. Matlab 2013a's neural network tool was utilised for developing the models for both scenarios. Among the various types of ANN available in the literature, a Feed Forward Multi-Layer Perceptron (FFMLP) model was the most suitable model for the current study. A supervised learning approach was utilized in which the input and output parameters were supplied in the network and the

system was expected to learn the pattern in the datasets by training to be able to predict new set of data points which were untrained by the network. The principle of the learning phase in ANN was based on iterative process. The system performed series of forward and backward calculations to adjust its weights in order to minimize the error between the actual and the experimentally observed data points. By adjusting the initially assigned weights after each forward and backward calculations, the input parameters were associated to new connection weights which were computed by eq. 4.2. One cycle of forward and backward pass calculation is called an epoch. The number of epoch was significant in determining the efficiency of an ANN network. The errors between the predicted and the actual data points should be in decreasing trend after each epoch otherwise, the model suffered from the overfitting phenomenon. An over fitted models lacks the efficiency to perform accurate predictions for untrained data sets therefore, it should be avoided. The epoch performance of the models developed for scenario 1 and 2 were illustrated in Figures 4.21a and b.

$$y = \sum_{i=1}^a w_i x_i + w_o \quad (4.2)$$

Where, x is the input parameter, y is the output parameter, w_i is the associated weight that corresponded to the input parameter and w_o is the bias.

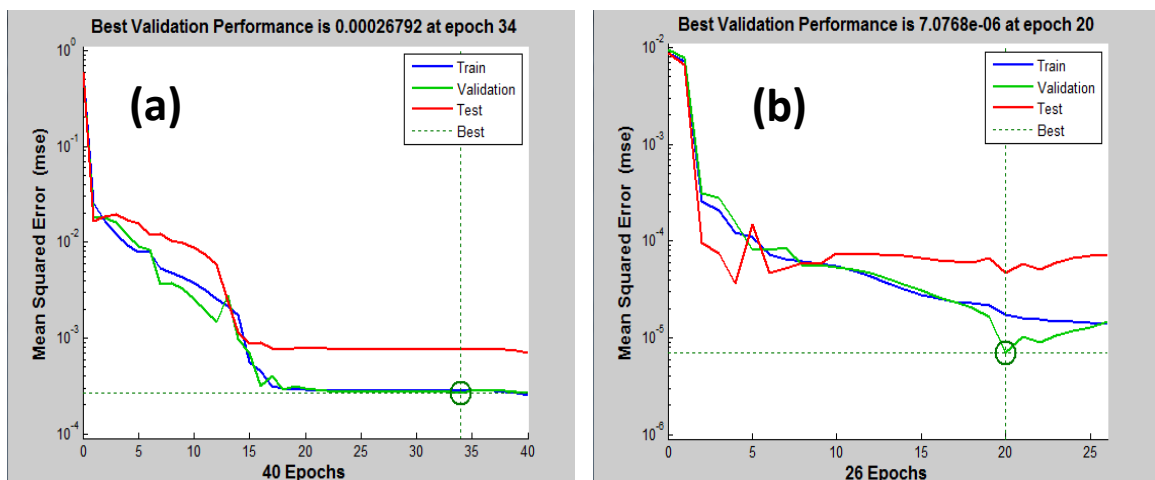


Figure 4.21: Total number of epochs for (a) Scenario 1 and (b) Scenario 2

In the forward pass calculations, an activation function was utilised to introduce non-linearity since, the asphalt cement is a complex material which behaves non-linearly under various loading and temperature conditions. The hyperbolic tangent function as expressed in eq. 3.5 was found to be the most suitable activation function for this purpose by trial and error. Additionally, although other algorithms such as GD and SCG were available, the LM learning algorithm was found to be the best working algorithm for models developed in both scenarios. The constructed network structure consisted of 3 layers which were the input, hidden and output layers. In scenario 1, there were 4 inputs and 1 output parameter and in scenario 2, there were 3 inputs and 1 output parameters. The middle layer was referred to as the hidden layer which linked the input and output layers by enabling the transformation of the forward and backward pass calculations. The neuron number in the hidden layer varies depending on the complexity of a model. In the current study an extra neuron from the number of neurons in the input layer was used which was also suggested in a number of researches available in the literature. Alternating the number of neurons in the hidden layer was also attempted however, based on the prediction performance of the developed models, an extra neuron in the hidden layer provided the best performing models in both scenarios compared to the others. In order to evaluate the efficiency of the models, a data splitting technique was applied. 70% of the data warehouse was used for the training of the neural network while the remaining 30% was shared equally between the validation and testing datasets to evaluating the performance of the prediction models with the untrained data points. Two different statistical indicator metrics which were the Root Mean Squared Error (RMSE) and the coefficient of determination (R^2) were used to assess the performance of models using the training and testing datasets. Additionally, the goodness of fit measures from the software output were obtained and plotted in Figures 4.22a and 4.22b. The computed statistical indicator metrics showed that, for scenario 1, R^2 value of 0.980 and RMSE of 1.49E-06 for the training dataset and R^2 value of 0.969 and RMSE of 2.25E-06 were observed for the testing dataset. In the case of scenario 2. The R^2 values were 0.909 and 0.856 and RMSE values were 3.64E-05 and 5.37E-04 for the training and testing datasets respectively. From these findings it can be concluded that the model developed for scenario 1 outperformed the model in the scenario 2 which was derived from the higher R^2 and lower RMSE values.

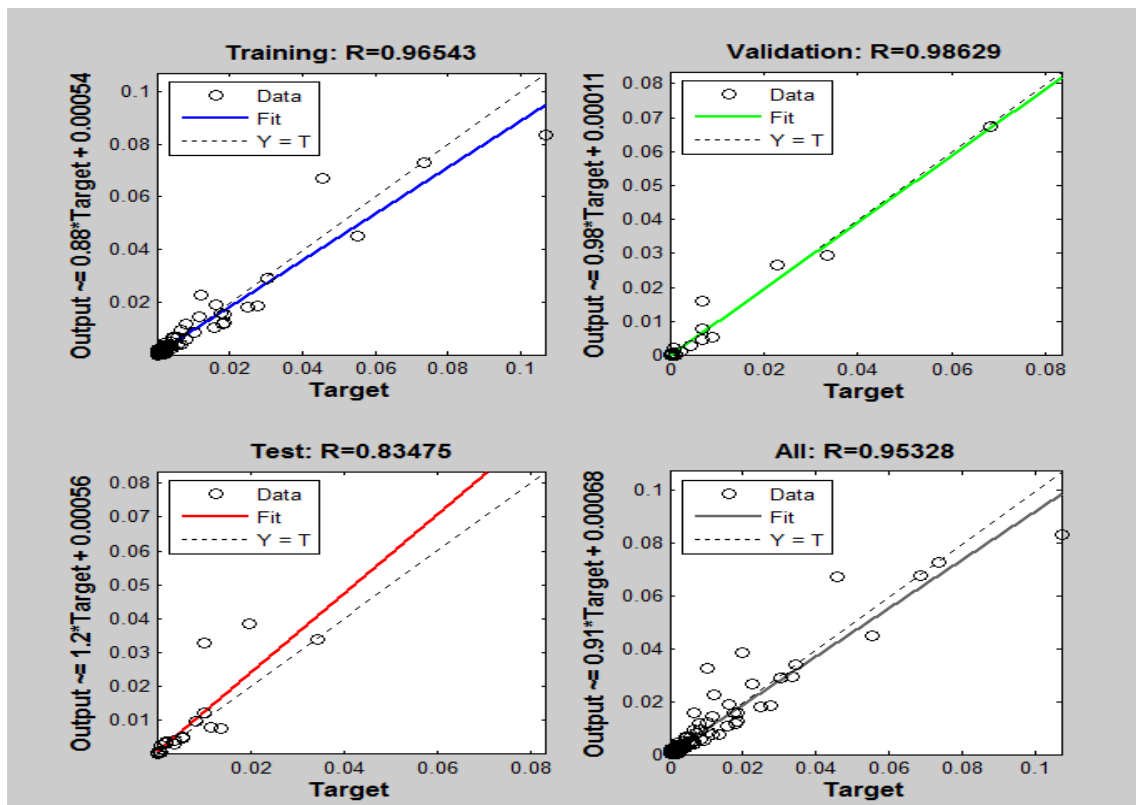
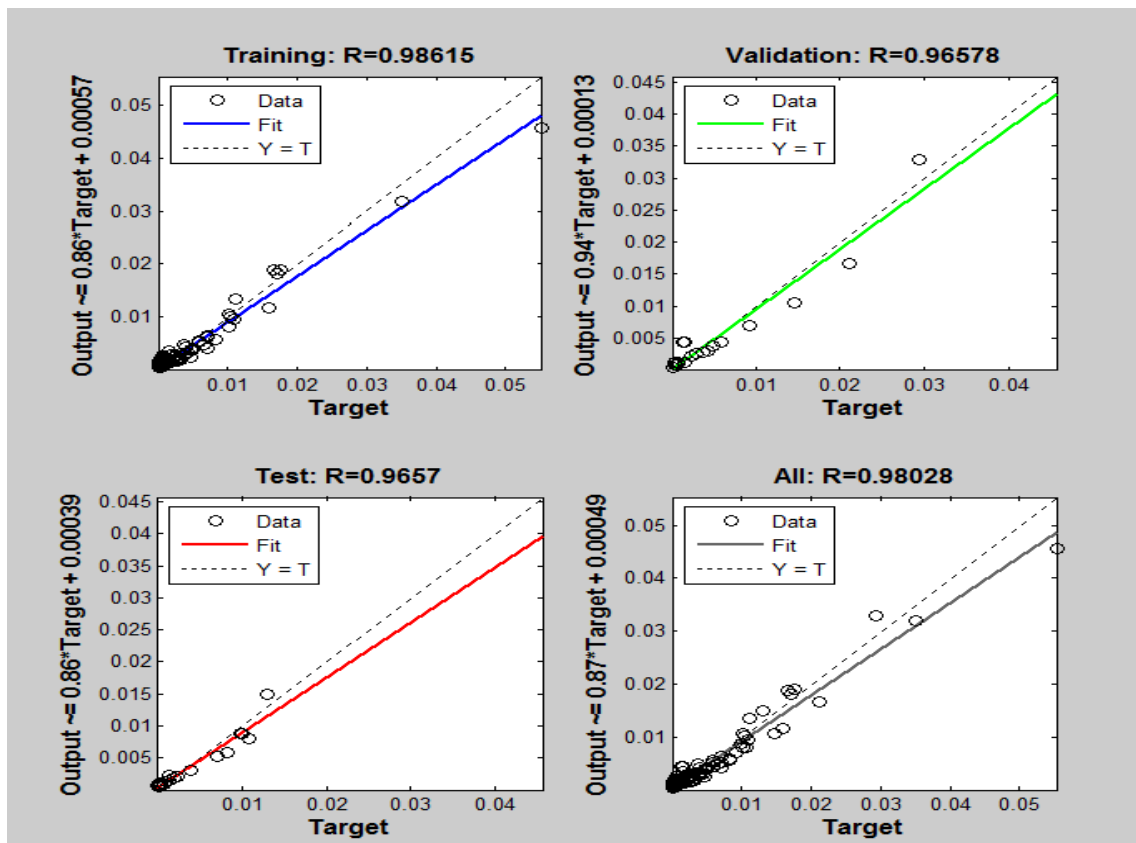


Figure 4.22: Measure of goodness of fit for (a) Scenario 1 and (b) Scenario 2

4.4.2 Adaptive neuro fuzzy inference system

Another modelling technique adopted in the present study was the ANFIS computational modelling tool which used a hybrid learning system. A hybrid system is an artificial intelligent system that is framed by combining at least two intelligent technologies. In ANFIS, a hybrid system was formed by combining the special features of ANN and Fuzzy Inferences Systems (FIS). ANN is a data driven system while the ANFIS is a knowledge based system. The hybrid learning system which combined the learning abilities of the ANN and FIS was an effective tool to solve complex engineering problems that include highly nonlinear relationship between the input and output data sets. ANFIS which belongs to a branch of adaptable FFMLP consisted of a number of inputs and an output variable which were connected by a Sugeno type if then rules based fuzzy reasoning mechanism as demonstrated in eq. 3.9 and eq. 3.10. ANFIS models were developed by using the same input and output variables that were expressed in ANN modelling. Similar to ANN, ANFIS learning phase was performed in two phases which was the forward pass and backward pass calculations. The network structure for ANFIS was made up of 5 layers which was illustrated in Figure 3.10. In the forward pass calculations, the consequent parameters were identified by the least squares method which performed computations until layer four and a backpropagation method was applied in the backward pass calculations by using the gradient descent algorithm to estimating the most accurate premise parameters. An additional advantage of the ANFIS was the fuzzification of the input and output parameters. Fuzzification enabled the classification of the variables in a grey scale rather than adopting a Boolean logic which was consisted of sharp limits. In the first layer of ANFIS, the variables of concern were fuzzified by assigning membership functions to the consequent and premise parameters. This could have been achieved by adopting various membership functions such as triangular, trapezoidal, bell shaped, sigmoidal and Gaussian, that are available in the Matlab ANFIS tool however, by trial and error, the Gaussian membership function was found to be the most optimum type for developing the models in both scenarios. To measure the efficiency of the developed models, the total data set was shared between the training, validation and the testing datasets in a ratio of 70%, 15% and 15% respectively. Herein and for the ANN models, K-Fold data splitting technique was employed. In K-Fold technique, the data sets were randomly divided into four equal subsets and shared between the data set

variants. This procedure was repeated 4 times for training, validating and testing the data sets which was also called the 4-Fold cross validation method. A benefit of this method was to optimize and to improve the efficiency of the models by separating the datasets for training, validation and testing to individual datasets at each round of running the models. Similar to the performance assessment methods used for the ANN models, the performance evaluation for the ANFIS models were conducted by the RMSE and R^2 . The statistical indicator metrics from the ANFIS and also from the ANN prediction models were tabulated in Table 4.4 to enable comparison between the performance of the models for two different scenarios and to identify the most efficient models. Additionally, the statistical goodness-of-fit measure for the regression performance and the ANFIS network checking performance were illustrated in Figure 4.23a and 4.23b respectively. Finally, a point to point comparison between the experimentally observed and ANFIS model predictions were plotted in Figure 4.24a and 4.24b for scenario 1 and scenario 2 respectively.

Table 4.4: Statistical indicator metrics

		Scenario 1		Scenario 2	
		Train	Test	Train	Test
ANN	R2	0.980	0.969	0.909	0.856
	RMSE	1.49E-06	2.25E-06	3.64E-05	5.37E-04
ANFIS	R2	0.934	0.901	0.854	0.668
	RMSE	1.48E-05	9.74E-05	2.35E-04	1.04E-03

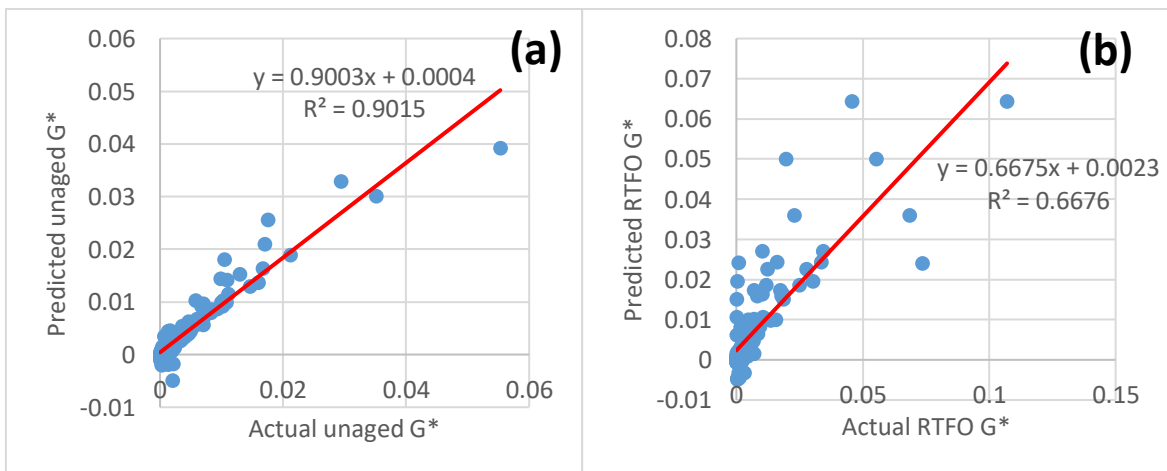


Figure 4.23: ANFIS model regression performance (a) Scenario 1 (b) Scenario 2

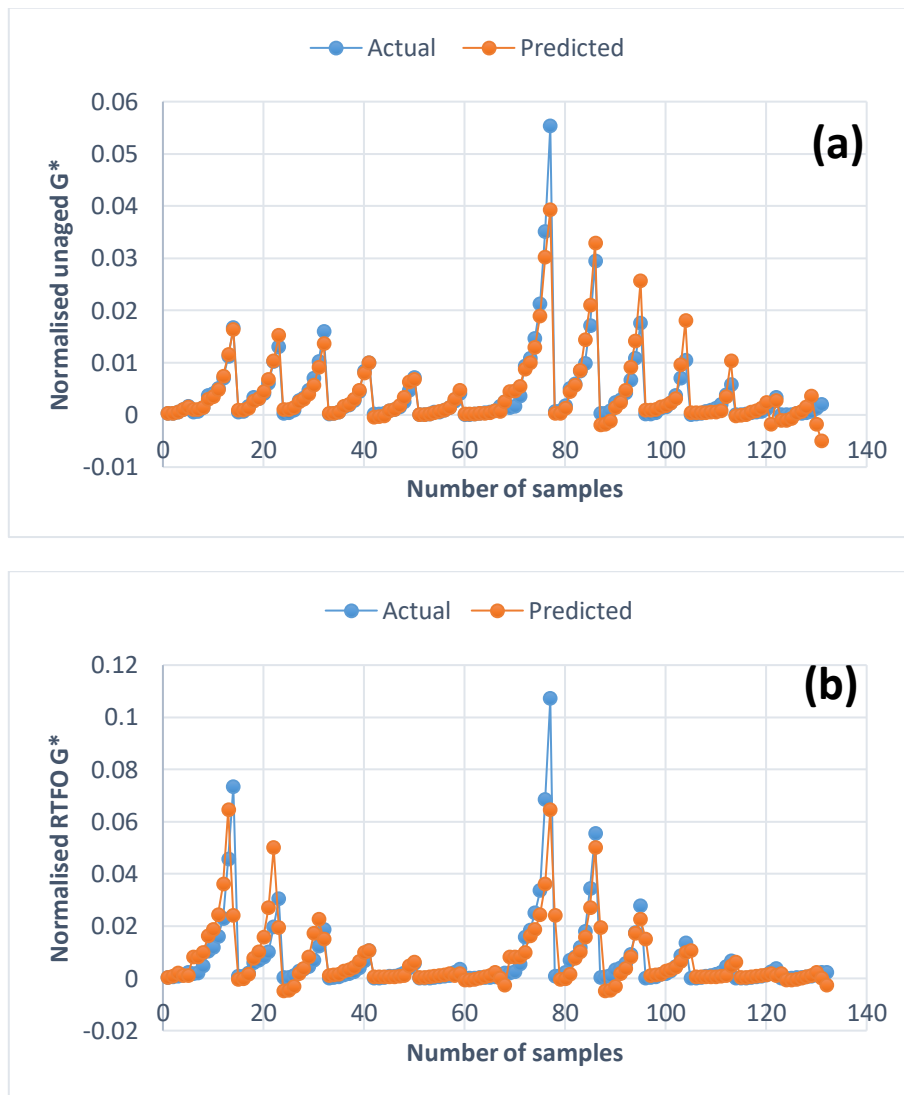


Figure 4.24: Discrepancy between actual and predicted data (a) Scenario 1 (b) Scenario 2

Based on the statistical indicator metrics, in the first scenario the G^* in unaged state was able to be predicted in both techniques at high accuracy with R^2 values above 0.90 for the testing datasets. In the second scenario, the capacity of ANN model to predict the G^* in RTFO condition from the test parameters and the G^* in unaged state was efficient with R^2 value of 0.856 and RMSE of $5.37E-04$ while the ANFIS model was not able to produce reliable models. Significantly low R^2 value obtained from the testing dataset was the cause for poor prediction performance. Additionally, the unreasonable gap between the R^2 value for the training and testing datasets indicated that the model suffered from the overfitting phenomenon.

4.5 Hot Mix Asphalt Design

The hot mix asphalt (HMA) design was conducted for the base and PNC modified AC considering the optimum performing compositions for the ASA/Si and ASA/Fe composites. ASA/Si 5% and ASA/Fe 3% compositions were found to be the superior performing modified AC among the other compositions according to the results from the physical, morphological and rheological evaluation performed in the asphalt binder level. Superpave design procedures were applied in the HMA design for the current study. The design was based on suitable binder and aggregate selection (aggregate type and gradation), volumetric analysis to finding the optimum binder content (OBC) and performance testing to evaluating the influence of the additives on the moisture susceptibility and performance characteristics in the mixture level. Granite aggregates were used in the HMA design since, they were the commonly utilised and locally available source in the region. Although other aggregate gradations could have been selected, AC-14 aggregate gradation was utilised to minimise the sample size and hence to minimise the amount of materials used to design the HMA concrete samples. The prepared samples were weighted 1100 grams. The mixed (loose) and compacted samples were prepared for base and each PNC modified AC to verify the volumetric properties, determining the optimum binder content (OBC) and to evaluating the influence of volumetric characteristics regarding to the performance characteristics of hot mix asphalt concrete. Trial and error method was followed for determining volumetric properties and the OBC for the mix design. Firstly, the samples were prepared at 4 different binder contents; 4.5%, 5%, 5.5% and 6% by the wt. of asphalt mixture. The volumetric properties were measured at each binder content and the Superpave mix design parameters were assessed to determining the volumetric properties and the OBC which are explained in Chapter 4.5.1.

4.5.1 Mix design parameters and volumetric properties

The Superpave mix design parameters were adopted in the preparation of HMA samples. The asphalt concrete test samples were prepared by using a mechanical laboratory asphalt mixer. The compaction process was performed by a Superpave Gyrotory Compactor (SGC). For compacting the samples, N_{design} was selected as 125 times compaction from the

AASHTO N_{design} table to represent heavy traffic loading that is greater than 30 million ESALs. The mixture preparation temperatures and the compaction temperatures were set based on RV of the asphalt cement. The RV test results for asphalt binders at 135°C and 165°C were converted to log-style on the vertical axis and plotted against the temperature on the horizontal axis as illustrated in Figure 4.25. Two lines were drawn horizontal to the y-axis at 0.17 Pa.s and 0.28 Pa.s to locate the viscosity ranges which corresponded to the mix and compacted sample temperatures respectively. The interval for the mixing and compaction temperatures for base AC, ASA/Fe 3% and ASA/Si 5% which were observed from Figure 4.25 were tabulated in Table 4.5.

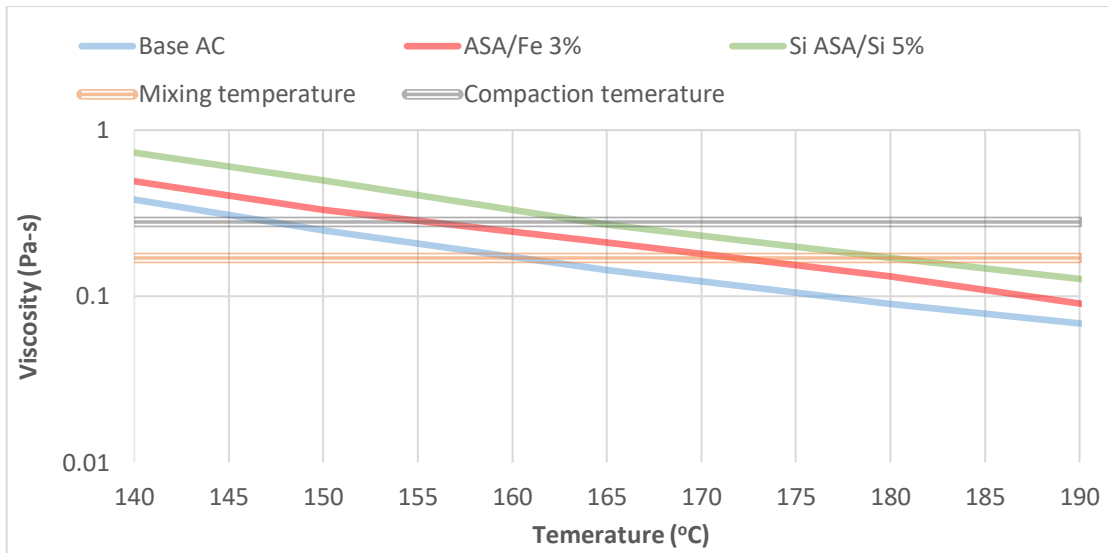


Figure 4.25: Mixing and compaction temperatures

Table 4.5: Mixing and compaction temperatures

	Mixing temp. (°C)		Compaction temp. (°C)	
	Min	Max	Min	Max
Base AC	159	163	146	149
ASA/Fe 3%	169	173	153	156
ASA/Si 5%	177	182	161	166

In the next step of HMA design, mix and compacted samples were prepared. Three samples for base AC and for each PNC modified AC at four different aforementioned binder contents

were left in loose state to determining the G_{mm} and the same amount of samples were compacted by using a SGC to determining the G_{mb} of sample mixes. Asphalt mix design was a volumetric process. The volumetric characteristics of an asphalt mixture were crucially important from the specification and performance standpoint. Parameters such as the V_a , VMA, VFA and D/A are the main characteristics of an HMA that were specified and standardised in Superpave specifications. However, it is difficult to analyse the volumetric properties of HMA directly rather, specific gravities such as the G_{sb} , G_{mm} and G_{mb} were measured experimentally and then converted to volumes by using the weight-volume relationship. V_a , VMA, VFA and D/A were computed by using eq. 3.25, 3.26, 3.27 and 3.22 respectively. The primary target was to achieve 4% V_a , regardless of the traffic level. This was because if the V_a content was higher, the mixture would be susceptible to more air and water entering in the asphalt pavement which causes age hardening and moisture damage. On the contrary, if the V_a content was low, the mixes would have been prone to bleeding and plastic deformation. VMA is the total of the void spaces plus the effective binder content in the mixture. Since V_a was constant due to design requirements, VMA was influenced by the effective binder content. A higher VMA results in a requirement for more asphalt to coat the aggregates which increases the durability of the mix however, it should be noted that, excessively high VMA leads to an uneconomic mix design and lower stability. On this basis Superpave standards set a minimum requirement for the VMA based on the nominal maximum aggregate size. For a mix design that contained the maximum nominal aggregate size of 19mm, the Superpave minimum VMA requirement is 13%. VMA ratios lower than the specification indicated that, there would not be sufficient voids to accommodate adequate space for the effective asphalt. VFA is another parameter that is associated to the VMA of a mix design. The proportion of the VMA which contains the effective binder is referred to as the VFA. The VFA requirement in the Superpave specification was due to limiting the maximum percentage for the VMA since excessive VMA would cause stability concerns. VFA requirement was based on the anticipated traffic conditions which was greater than 30 million ESAL'S. The standard requirement for the VFA was between 65%-75%. A final parameter evaluated for the volumetric analysis was the D/A ratio which is the ratio of the fine aggregates to the effective asphalt content. According to the Superpave criteria, D/A is restricted to be in a range from 0.6-1.2. D/A ratio and VMA are inversely proportional. A lower D/A ratio causes increase in the VMA thus, leading to more effective asphalt content

in the mix. Additionally, the amount of rut depth that occurs in the HMA is known to decrease significantly by increasing the D/A ratio in the mix. The above mentioned parameters were computed in order to determining the OBC for the control sample and PNC modified HMA samples. The OBC of an HMA is inversely proportional to the V_a . Increase in the OBC leads to improved durability for the mixture however, beyond certain point, strength and stability of the mix gets reduced in excessive binder content usage. By using the results of the voids analysis, the volumetric properties of the base and PNC modified HMA are demonstrated in Table 4.6.

Table 4.6: Volumetric characteristics of HMA

Mix Properties	Base AC	ASA/Fe 3%	ASA/Si 5%	Criteria
V_a (%)	4	4	4	4
VMA (%)	16.11	16.48	17.17	<13
VFA (%)	74.5	75	74.3	65-75
D/A ratio	0.87	0.93	0.95	0.6-1.2
OBC (%)	5.39	5.75	5.92	-

4.5.2 Moisture susceptibility

The moisture susceptibility is referred to as the loss of ability of asphalt to bond with the mineral aggregates due to the infiltration of water and moisture in the asphalt concrete mixture. This phenomenon leads to moisture induced damage which results in major pavement distresses such as ravelling and stripping. Because these modes of failure have a complex mechanism that cannot be measured directly, the moisture susceptibility testing of HMA was the appropriate method to evaluate the moisture induced damage on the HMA samples. The modified lottman method was utilized for the moisture susceptibility tests since this method was proven to correlate well with the actual field performance (Hamedi et al., 2015). Six samples for each type of mixtures were prepared and compacted at air void contents around 7%. Three of these samples were left unconditioned while, the remaining samples were conditioned by first, applying a vacuum pressure of 13-67 kPa to partially saturate the samples between 70-80% and then applying a freezing and thawing cycles at -18°C for 16 hours and at 60°C for 24 hours respectively. After this procedure, the unconditioned and conditioned samples were tested by using the indirect tensile strength

(ITS). The results from the ITS test were computed by using eq. 3.28 to find tensile strength of the samples. Figure 4.26 illustrates the tensile strength of the conditioned and unconditioned samples. It can be observed that, the tensile strength of the modified samples were improved compared to the base binder which was the influence of the additives in the PNC modified AC. Additionally, the tensile strength of the conditioned samples were lower than the unconditioned samples. This was an expected outcome which demonstrated the occurrence of deterioration on the asphalt mix concrete samples when subjected to moisture conditions. Furthermore, by using the tensile strength of the conditioned and unconditioned samples, the tensile strength ratio (TSR) was computed. TSR was an indication of moisture susceptibility of HMA. The Superpave standards limits the TSR to a limit of 80%. Figure 4.26 illustrated that, the tensile strength for the unconditioned, dry samples were increased compared to the control HMA. The increase in tensile strength indicated that the modified mixes possessed better fracture energy. The increase in tensile strength for ASA/Si 5% was significantly higher than the ASA/Fe 3%. On the other hand, the differences in ITS results between the conditioned and unconditioned samples demonstrated that, ASA/Fe 3% was less susceptible to moisture damage than the ASA/Si 5%. The TSR values observed from Figure 4.27 showed that, the moisture susceptibility of ASA/Fe 3% was improved compared to the unmodified control sample while the moisture susceptibility was degraded for ASA/Si 5%. This outcome for the ASA/Si 5% was contradictory to the findings of (Taherkhani & Tajdini, 2019; Yusoff et al., 2014) and verified by the findings of (Hasaninia & Haddadi, 2017; Razavi & Kavussi, 2020).

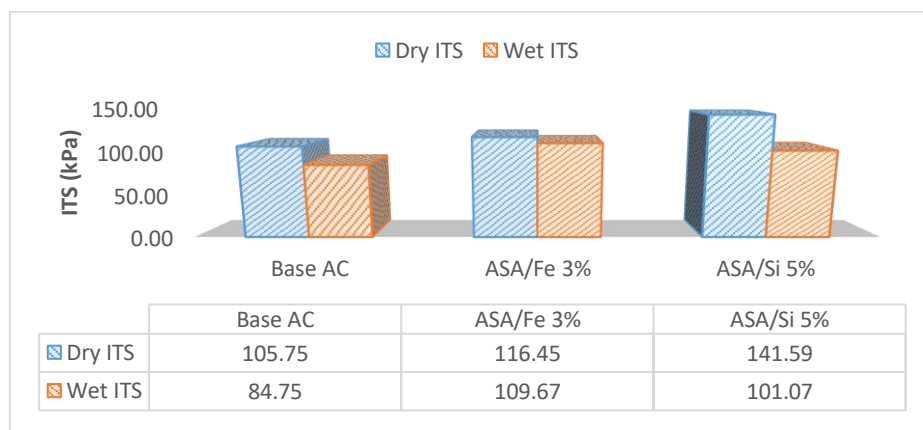


Figure 4.26: Tensile strength of control and modified HMA

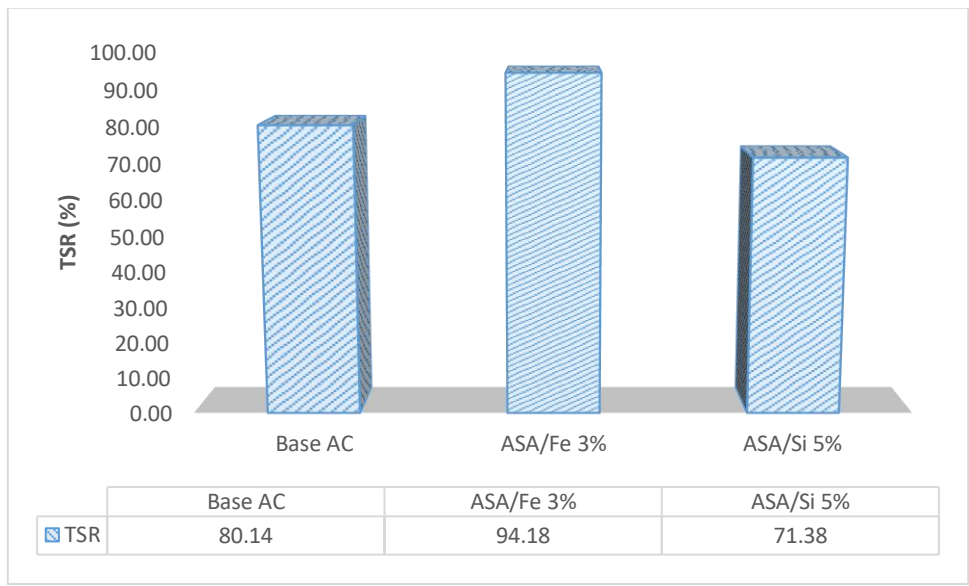


Figure 4.27: Tensile strength ratio

CHAPTER 5

CONCLUSION

5.1 Summary of the findings

The influence of ASA/Si and ASA/Fe composite modifiers were evaluated under unaged, RTFO and PAV conditions with respect to physical, chemical and rheological properties at the binder level. Additionally, heuristic modelling techniques; ANN and ANFIS were implemented to develop AI models that can estimate the performance characteristics of AC from the experimental outcomes. Furthermore, the superior performing compositions for each types of PNC modified AC were selected, and HMA parameters were designed and tested for moisture susceptibility at the mixture level. During the modification process ASA was used in 5% concentration whereas, the addition of nano silica and nano ironoxide was 3, 5 and 7% by the weight of AC. The significant findings based on the aforementioned investigations are summarised as followed;

- From the DSR test results, it was observed that, 3% addition of nano ironoxide in the blend resulted in the highest complex modulus at high temperatures which indicated enhanced rutting resistance. However, the increase in the rutting resistance was at the cost of reduced fatigue resistance due to increased brittleness. ASA/Fe composite modified AC demonstrated phase separated structures. This was evident from the storage stability test results and it was confirmed by the XRD analysis. The formation of phase separation inhibited the further enhancement in rutting resistance at the higher concentration compositions for ASA/Fe composites.
- For the ASA/Si composite modified AC, the improvement in viscoelastic characteristics was consistent up to 5% addition of nano silica in the blend. Beyond this composition, a reduced enhancement in performance characteristics was observed. Although the enhancement in rutting resistance for the ASA/Si composites was lower than the ASA/Fe composites, ASA/Si composites were also able to improve the low temperature performance characteristics of AC. The stability of ASA/Si composites were improved after the modification process however, at 7% content, ASA/Si composites demonstrated lower enhancement in viscoelastic

properties. A possible cause for this outcome was due to the agglomeration of nanosilica particles in the asphalt/polymer nanocomposite matrix. From the durability standpoint, ASA/Si modified AC demonstrated better aging resistance at all compositions compared to base AC and ASA/Fe modified AC. Also, this finding was verified by the FTIR analysis.

- The performance characteristics of the base and PNC modified AC were modelled by employing ANN and ANFIS. Two different model scenarios were developed. These scenarios were labelled as scenario 1 and scenario 2. R^2 and RMSE results showed that, ANN was able to predict the G^* in both scenarios with high accuracy. Also, ANFIS model developed for scenario 1 was able to predict G^* with high accuracy however, ANFIS model for scenario 2 was inefficient due to low R^2 and also due to the significant difference in R^2 values between the training and testing datasets.
- The design of asphaltic mixtures was performed for the optimum compositions of modified binders. The optimum performing PNC was 5% for the ASA/Si and it was 3% for the ASA/Fe compositions. Mix design was a volumetric process. From the volumetric characteristics the OBC of the HMA were found to be 5.39%, 5.75% and 5.92% for base AC, ASA/Fe 3% and ASA/Si 5% respectively. In terms of moisture susceptibility, it was observed that ASA/Fe 3% composition was the least moisture susceptible AC while ASA/Si 5% was found to be the most susceptible mix to moisture induced damage.

5.2 Future research recommendations:

The current research can be upgraded further with the following future research recommendations;

- The findings of the current study can be used as foundations to investigate the influence of additives more comprehensively by using simulative testing methods at the mixture level. This would enable designers and engineers to reach to a better conclusion prior to any field application.

- The performance of the modified binders can be investigated by using different penetration grades of asphalt as base to modifiers at the binder level. Also, the influence of aggregate gradations and the effect of different types of aggregates can be investigated for the asphaltic mixture design. Additionally, economical aspects of the design shall be analysed regarding to feasibility of the designed mix and aggregates/binders that are obtained from RAP or RAS sources may be utilized to improve the design economically.

REFERENCES

- Abba, S., Pham, Q. B., Usman, A., Linh, N. T. T., Aliyu, D., Nguyen, Q., & Bach, Q.-V. (2020). Emerging evolutionary algorithm integrated with kernel principal component analysis for modeling the performance of a water treatment plant. *Journal of Water Process Engineering*, 33, 101081.
- Abed, A., & Oudah, A. (2018). Rheological properties of modified asphalt binder with nanosilica and SBS. *In the 2nd International Conference on Engineering Sciences the IOP Conf. Ser. Mater. Sci. Eng* (pp. 433).
- Abedali, A. H. (2015). Predicting complex shear modulus using artificial neural networks. *Journal of Civil Engineering and Construction Technology*, 6(3), 15-26.
- Abhilash, V., Rajender, N., & Suresh, K. (2016). X-ray diffraction spectroscopy of polymer nanocomposites, S. Thomas D. Rouxel, D. Ponnamma (Eds.), *Spectroscopy of Polymer Nanocomposites* (pp. 410-451). India: Elsevier.
- Adishesu, G. N. P., & Naidu, G. (2011). Influence of coarse aggregate shape factors on bituminous mixtures. *International journal of engineering research and applications*, 1(4), 2013-2014.
- Airey, G., Grenfell, J., Apeageyi, A., Subhy, A., & Presti, D. L. (2016). Time dependent viscoelastic rheological response of pure, modified and synthetic bituminous binders. *Mechanics of time-dependent materials*, 20(3), 455-480.
- Airey, G. D. (2002). Use of black diagrams to identify inconsistencies in rheological data. *Road Materials and Pavement Design*, 3(4), 403-424.
- Airey, G. D. (2003). Rheological properties of styrene butadiene styrene polymer modified road bitumens. *Fuel*, 82(14), 1709-1719.
- Al-Bayati, H. K., & Tighe, S. (2018). Evaluating the effects of mineral filler on the volumetric properties of HMA mixtures based on Superpave mix design specifications. *In Bâtir la Société de Demain* (pp. MA77-1-10). Canada: Fredicton.

- Al-Khateeb, G. G., & Al-Akhras, N. M. (2011). Properties of Portland cement-modified asphalt binder using Superpave tests. *Construction and Building Materials*, 25(2), 926-932.
- Al-Khateeb, G. G., & Ramadan, K. Z. (2015). Investigation of the effect of rubber on rheological properties of asphalt binders using superpave DSR. *KSCE Journal of Civil Engineering*, 19(1), 127-135.
- Al-Mansob, R. A., Ismail, A., Rahmat, R. A. O., Borhan, M. N., Alsharif, J. M., Albrka, S. I., & Karim, M. R. (2017). The performance of epoxidised natural rubber modified asphalt using nano-alumina as additive. *Construction and Building Materials*, 155, 680-687.
- Al-Mansob, R. A., Ismail, A., Yusoff, N. I. M., Albrka, S. I., Azhari, C. H., & Karim, M. R. (2016). Rheological characteristics of unaged and aged epoxidised natural rubber modified asphalt. *Construction and Building Materials*, 102, 190-199.
- Al-Mosawe, H. (2016). *Prediction of permanent deformation in asphalt mixtures* (Doctoral dissertation), University of Nottingham, United Kingdom.
- Al-Omari, A. A., Khedaywi, T. S., & Khasawneh, M. A. (2018). Laboratory characterization of asphalt binders modified with waste vegetable oil using SuperPave specifications. *International Journal of Pavement Research and Technology*, 11(1), 68-76.
- Alas, M., & Ali, S. I. A. (2019). Prediction of the High-Temperature Performance of a Geopolymer Modified Asphalt Binder using Artificial Neural Networks. *Int. J. Technol*, 10, 417-427.
- Alas, M., Ali, S. I. A., Abdulhadi, Y., & Abba, S. (2020). Experimental Evaluation and Modeling of Polymer Nanocomposite Modified Asphalt Binder Using ANN and ANFIS. *Journal of Materials in Civil Engineering*, 32(10), 04020305.
- Alhamali, D. I., Wu, J., Liu, Q., Hassan, N. A., Yusoff, N. I. M., & Ali, S. I. A. (2016). Physical and rheological characteristics of polymer modified bitumen with nanosilica particles. *Arabian Journal for Science and Engineering*, 41(4), 1521-1530.
- Alhamali, D. I., Yusoff, N., Wu, J., Liu, Q., & Albrka, S. I. (2015). The effects of nano silica particles on the physical properties and storage stability of polymer-modified bitumen. *Journal of Civil Engineering Research*, 5(4A), 11-16.

- Ali, A., Abbas, A., Nazzal, M., Alhasan, A., Roy, A., & Powers, D. (2014). Workability evaluation of foamed warm-mix asphalt. *Journal of Materials in Civil Engineering*, 26(6), 04014011.
- Ali, S. I. A., Abdulwahid, R., Eidan, M. L., & Md Yusoff, N. I. (2018). Evaluation of moisture and ageing effects on calcium carbonite nanoparticles modified asphalt mixtures. *International Journal of Engineering Research in Africa*, 34, 40-47.
- Ali, S. I. A., Ismail, A., Karim, M. R., Yusoff, N. I. M., Al-Mansob, R. A., & Aburkaba, E. (2017). Performance evaluation of Al₂O₃ nanoparticle-modified asphalt binder. *Road Materials and Pavement Design*, 18(6), 1251-1268.
- Ali, S. I. A., Ismail, A., Yusoff, N. I. M., Karim, M. R., Al-Mansob, R. A., & Alhamali, D. I. (2015). Physical and rheological properties of acrylate–styrene–acrylonitrile modified asphalt cement. *Construction and Building Materials*, 93, 326-334.
- Alshamsi, K. S. (2006). *Development of a mix design methodology for asphalt mixtures with analytically formulated aggregate structures* (Doctoral dissertation), Louisiana State University, USA.
- Ameri, M., Mansourian, A., & Sheikhmotevali, A. H. (2012). Investigating effects of ethylene vinyl acetate and gilsonite modifiers upon performance of base bitumen using Superpave tests methodology. *Construction and Building Materials*, 36, 1001-1007.
- Anderson, M. (2014). Introduction to the multiple-stress creep-recovery (MSCR) test and its use in the PG binder specification. *In the 54th Annual Idaho Asphalt Conference* (pp. 507-520). Moscow: Asphalt Institute.
- Apparao, G., Rajesh, G., & Raju, S. G. (2013). Grading System in Paving Bitumen—An Indian Scenario. *International Journal of Civil Engineering and Technology (IJCIET)*, 4(2), 208-214.
- Arabani, M., & Faramarzi, M. (2015). Characterization of CNTs-modified HMA's mechanical properties. *Construction and Building Materials*, 83, 207-215.
- Arangi, S. R., & Jain, R. (2015). Review paper on pavement temperature prediction model for Indian climatic condition. *Int. J. of Innovative Research in Adv. Engineering*, 2(8), 1-9.

- Arshad, A. K., Samsudin, M. S., Masri, K. A., Karim, M. R., & Halim, A. A. (2017). Multiple stress creep and recovery of nanosilica modified asphalt binder. *In the International Symposium on Civil and Environmental Engineering* (pp. 103- 111). MATEC Web of Conferences.
- Arshad, H., & Qiu, Y. J. (2012). Evaluation of Local Asphalt Binders under Superpave Specification. *Applied Mechanics and Materials, 178–181*, 1509–1512.
- Bahia, H. U., Hanson, D., Zeng, M., Zhai, H., Khatri, M., & Anderson, R. (2001). Characterization of modified asphalt binders in superpave mix design.
- Bala, N., Kamaruddin, I., Napiah, M., & Danlami, N. (2017). Rheological and rutting evaluation of composite nanosilica/polyethylene modified bitumen. *In the Proceedings of the 7th International Conference on Key Engineering Materials (ICKEM 2017)* (pp. 201-207). Penang, Malaysia: IOP Conference Series.
- Bala, N., Kamaruddin, I., Napiah, M., & Sutanto, M. H. (2019). Polymer nanocomposite-modified asphalt: characterisation and optimisation using response surface methodology. *Arabian Journal for Science and Engineering, 44(5)*, 4233-4243.
- Bala, N., Napiah, M., & Kamaruddin, I. (2018). Effect of nanosilica particles on polypropylene polymer modified asphalt mixture performance. *Case studies in construction materials, 8*, 447-454.
- Bala, N., Napiah, M., Kamaruddin, I., & Danlami, N. (2017). Rheological properties investigation of bitumen modified with nanosilica and polyethylene polymer. *International journal of advanced and applied sciences, 4(10)*, 165-174.
- Baldo, N., Manthos, E., & Pasetto, M. (2018). Analysis of the Mechanical Behaviour of Asphalt Concretes Using Artificial Neural Networks. *Advances in Civil Engineering, 2018*, 1650945.
- Bargegol, I., Sakanlou, F., Sohrabi, M., & Hamed, G. H. (2020). Investigating the Effect of Metal Nanomaterials on the Moisture Sensitivity Process of Asphalt Mixes. *Periodica Polytechnica Civil Engineering, 65(1)*, 15-25.

- Bastos, J. B., Babadopulos, L. F., & Soares, J. B. (2017). Relationship between multiple stress creep recovery (MSCR) binder test results and asphalt concrete rutting resistance in Brazilian roadways. *Construction and Building Materials*, 145, 20-27.
- Becker, Y., Mendez, M. P., & Rodriguez, Y. (2001). Polymer modified asphalt. *Vision tecnologica*. 9(1), 39-50.
- Behnood, A., & Gharehveran, M. M. (2019). Morphology, rheology, and physical properties of polymer-modified asphalt binders. *European Polymer Journal*, 112, 766-791.
- Bhargava, S., Raghuwanshi, A. K., & Gupta, P. (2016). Nanomaterial Compatibility and Effect on Properties of Base Bitumen Binder and Polymer Modified Bitumen. *IJISSET-International Journal of Innovative Science, Engineering & Technology*, 3(6), 276-282.
- Bitumen, S. (1995). *The shell bitumen industrial handbook*. London, UK: Thomas Telford.
- Branthaver, J. (1993). Binder Characterization and Evaluation, vol. 2: Chemistry. Washington, DC: Strategic Highway Research Program, National Research Council: Technical Report, SHRP-A-368.
- Brasileiro, L., Moreno-Navarro, F., Tauste-Martínez, R., Matos, J., & Rubio-Gámez, M. d. C. (2019). Reclaimed polymers as asphalt binder modifiers for more sustainable roads: A Review. *Sustainability*, 11(3), 646.
- Brovelli, C., Hilliou, L., Hemar, Y., Pais, J., Pereira, P., & Crispino, M. (2013). Rheological characteristics of EVA modified bitumen and their correlations with bitumen concrete properties. *Construction and Building Materials*, 48, 1202-1208.
- Bukowski, J. (2011). The multiple stress creep recovery procedure: Washington DC: Federal Highway Administration of United States Department of
- Cai, L., Shi, X., & Xue, J. (2018). Laboratory evaluation of composed modified asphalt binder and mixture containing nano-silica/rock asphalt/SBS. *Construction and Building Materials*, 172, 204-211.
- Caro, S., Masad, E., Bhasin, A., & Little, D. N. (2008). Moisture susceptibility of asphalt mixtures, Part 1: mechanisms. *International Journal of Pavement Engineering*, 9(2), 81-98.

- Chattaraj, R. (2011). Bitumen Grading system—from penetration grading to viscosity grading—A step towards better quality control. *Indian Highways*, 39(2), 39-45.
- Cháves-Pabón, S., Rondón-Quintana, H., & Bastidas-Martínez, J. (2019). Aging of asphalt binders and asphalt mixtures. Summary part i: effect on physical-chemical properties. *Technology*, 10(12), 259-273.
- Chin, C. (2009). Performance graded bitumen specifications. *In the Road Engineering Association of Asia and Australasia (REAAA) Conference* (pp. 10p). Incheon, Korea: Songdo Convensisa.
- Choudhary, R., Kumar, A., & Murkute, K. (2018). Properties of waste polyethylene terephthalate (PET) modified asphalt mixes: dependence on PET size, PET content, and mixing process. *Periodica Polytechnica Civil Engineering*, 62(3), 685-693.
- Commission, E. (2011). Commission Recommendation of 18 October 2011 on the definition of nanomaterial (2011/696/EU). *Official Journal of the European Communities: Legis*, 275, 38.
- Cooley Jr, L., James, R. S., & Buchanan, M. S. (2002). Development of Mix design criteria for 4.75 mm superpave mixes, *Transportation Research Record*, 1819(1), LVR8-1039
- Corbett, L., & Merz, R. (1975). Asphalt binder hardening in the Michigan Test Road after 18 years of service. *Transportation research record*, 544, 27-34.
- Crucho, J., Picado-Santos, L., Neves, J., & Capitão, S. (2019). A Review of Nanomaterials' Effect on Mechanical Performance and Aging of Asphalt Mixtures. *Applied Sciences*, 9(18), 3657.
- Crucho, J. M. L., das Neves, J. M. C., Capitão, S. D., & de Picado-Santos, L. G. (2018). Mechanical performance of asphalt concrete modified with nanoparticles: Nanosilica, zero-valent iron and nanoclay. *Construction and Building Materials*, 181, 309-318.
- Cüneyt Aydın, A., Tortum, A., & Yavuz, M. (2006). Prediction of concrete elastic modulus using adaptive neuro-fuzzy inference system. *Civil Engineering and Environmental Systems*, 23(4), 295-309.

- Dahunsi, B. I., Olufemi, S., Akinpelu, M., & Olafusi, O. S. (2013). Investigation of the properties of “pure water” sachet modified bitumen. *Civil and Environmental Research*, 3(2), 47-61.
- Dalhat, M., Osman, S., Alhuraish, A.-A. A., Almarshad, F. K., Qarwan, S. A., & Adesina, A. Y. (2020). Chicken Feather fiber modified hot mix asphalt concrete: Rutting performance, durability, mechanical and volumetric properties. *Construction and Building Materials*, 239, 117849.
- DeRousseau, M., Kasprzyk, J., & Srubar III, W. (2018). Computational design optimization of concrete mixtures: A review. *Cement and Concrete Research*, 109, 42-53.
- Dessouky, S., Masad, E., & Bayomy, F. (2004). Prediction of hot mix asphalt stability using the superpave gyratory compactor. *Journal of Materials in Civil Engineering*, 16(6), 578-587.
- Dony, A., Zyian, L., Drouadaine, I., Pouget, S., Faucon-Dumont, S., Simard, D., . . . Nicolai, A. (2016). MURE National Project: FTIR spectroscopy study to assess ageing of asphalt mixtures. Paper presented at the Proceedings of the E&E congress.
- DuBois, E., Mehta, Y., & Nolan, A. (2014). Correlation between multiple stress creep recovery (MSCR) results and polymer modification of binder. *Construction and Building Materials*, 65, 184-190.
- Dutta, S., Murthy, A. R., Kim, D., & Samui, P. (2017). Prediction of compressive strength of self-compacting concrete using intelligent computational modeling. *Comput. Mater. Contin*, 53, 167-185.
- Ehinola, O. A., Falode, O. A., & Jonathan, G. (2012). Softening point and Penetration Index of bitumen from parts of Southwestern Nigeria. *Nafta*, 63(9-10), 319-323.
- El-Badawy, S., Abd El-Hakim, R., & Awed, A. (2018). Comparing Artificial Neural Networks with Regression Models for Hot-Mix Asphalt Dynamic Modulus Prediction. *Journal of Materials in Civil Engineering*, 30(7), 04018128.
- Esfandiarpour, S., & Shalaby, A. (2017). Local calibration of creep compliance models of asphalt concrete. *Construction and Building Materials*, 132, 313-322.

- Ezzat, H., El-Badawy, S., Gabr, A., Zaki, E.-S. I., & Breakah, T. (2016). Evaluation of asphalt binders modified with nanoclay and nanosilica. *Procedia Engineering*, *143*, 1260-1267.
- Fang, C., Yu, R., Liu, S., & Li, Y. (2013). Nanomaterials applied in asphalt modification: a review. *Journal of Materials Science & Technology*, *29*(7), 589-594.
- Fernandes, M. R. S., Forte, M. M. C., & Leite, L. F. M. (2008). Rheological evaluation of polymer-modified asphalt binders. *Materials research*, *11*(3), 381-386.
- Fernández-Gómez, W. D., Rondón Quintana, H., & Reyes Lizcano, F. (2013). A review of asphalt and asphalt mixture aging: Una revisión. *Ingeniería e investigación*, *33*(1), 5-12.
- Firouzinia, M., & Shafabakhsh, G. (2018). Investigation of the effect of nano-silica on thermal sensitivity of HMA using artificial neural network. *Construction and Building Materials*, *170*, 527-536.
- Gallego, J., Rodríguez-Alloza, A. M., & Giuliani, F. (2016). Black curves and creep behaviour of crumb rubber modified binders containing warm mix asphalt additives. *Mechanics of time-dependent materials*, *20*(3), 389-403.
- Galooyak, S. S., Dabir, B., Nazarbeygi, A. E., & Moeini, A. (2010). Rheological properties and storage stability of bitumen/SBS/montmorillonite composites. *Construction and Building Materials*, *24*(3), 300-307.
- Gama, D. A., Júnior, J. M. R., de Melo, T. J. A., & Rodrigues, J. K. G. (2016). Rheological studies of asphalt modified with elastomeric polymer. *Construction and Building Materials*, *106*, 290-295.
- Garber, N. J., & Hoel, L. A. (2014). *Traffic and highway engineering*: Cengage Learning.
- García-Morales, M., Partal, P., Navarro, F., & Gallegos, C. (2006). Effect of waste polymer addition on the rheology of modified bitumen. *Fuel*, *85*(7-8), 936-943.
- García-Morales, M., Partal, P., Navarro, F., Martínez-Boza, F., Gallegos, C., González, N., Muñoz, M. (2004). Viscous properties and microstructure of recycled eva modified bitumen. *Fuel*, *83*(1), 31-38.

- García-Morales, M., Partal, P., Navarro, F., Martínez-Boza, F., & Gallegos, C. (2007). Processing, rheology, and storage stability of recycled EVA/LDPE modified bitumen. *Polymer Engineering & Science*, 47(2), 181-191.
- Gashi, E., Sadiku, H., & Misini, M. (2017). A review of aggregate and asphalt mixture specific gravity measurements and their impacts on asphalt mix design properties and mix acceptance. *International Journal of Advanced Engineering Research and Science*, 4(5), 237182.
- Gaya, M. S., Wahab, N. A., Sam, Y., & Samsudin, S. I. (2014). ANFIS modelling of carbon and nitrogen removal in domestic wastewater treatment plant. *Jurnal Teknologi*, 67(5), 29-34
- Ghaffari, A., Sharifi, K., & Ivakpour, J. (2017). An experimental study on the effects of temperature and asphaltene content on the rheological behavior of vacuum residues. *Petroleum Science and Technology*, 35(8), 768-774.
- Ghasemi, M., Marandi, S. M., Tahmooresi, M., Kamali, J., & Taherzade, R. (2012). Modification of stone matrix asphalt with nano-SiO₂. *Journal of Basic and Applied Scientific Research*, 2(2), 1338-1344.
- Goh, S. W., Akin, M., You, Z., & Shi, X. (2011). Effect of deicing solutions on the tensile strength of micro-or nano-modified asphalt mixture. *Construction and Building Materials*, 25(1), 195-200.
- Golestani, B., Nejad, F. M., & Galooyak, S. S. (2012). Performance evaluation of linear and nonlinear nanocomposite modified asphalts. *Construction and Building Materials*, 35, 197-203.
- Gudimettla, J. M., Cooley Jr, L. A., & Brown, E. R. (2004). Workability of hot-mix asphalt. *Transportation research record*, 1891(1), 229-237.
- Guide, S. M. D. (2001). Westrack Forensic Team Consensus Report. Washington, DC.
- Gulzar, S., & Underwood, S. (2019). Use of Polymer Nanocomposites in Asphalt Binder Modification. S. ul-Islam and B.S. Butola (Eds.), *Advanced Functional Textiles and Polymers: Fabrication, Processing and Applications*, (pp. 405-432). Raleigh, USA: Wiley.

- Habib, N. Z. (2013). *Morphology and rheology of PP and LLDPE modified bitumens and their effect on asphalt mix properties* (Doctoral dissertation), Universiti Teknologi Petronas, Malaysia.
- Hamed, G. H., Moghadas Nejad, F., & Oveisi, K. (2015). Investigating the effects of using nanomaterials on moisture damage of HMA. *Road Materials and Pavement Design*, 16(3), 536-552.
- Hamed, G. H., & Tahami, S. (2018). The effect of using anti-stripping additives on moisture damage of hot mix asphalt. *International Journal of Adhesion and Adhesives*, 81, 90-97.
- Hamid, A., Baaj, H., & El-Hakim, M. (2019). Enhancing Asphalt Cement Properties Using Geopolymer-Based On Fly Ash and Glass Powder. *In the 7th CSCE International Specialty Conference on Engineering Mechanics and Materials* (pp. MAT55-1-10). Laval, Canada: CSCE.
- Handbook, A. (2007). *Asphalt handbook*. Lexington: Asphalt Institute.
- Hardin, J. C. (1995). *Physical properties of asphalt cement binders*. Philadelphia, PA: ASTM International.
- Hasaninia, M., & Haddadi, F. (2017). The characteristics of hot mixed asphalt modified by nanosilica. *Petroleum Science and Technology*, 35(4), 351-359.
- Hasaninia, M., & Haddadi, F. (2018). Studying engineering characteristics of asphalt binder and mixture modified by nanosilica and estimating their correlations. *Advances in materials science and engineering*, 2018, 1-9.
- Hofko, B., Alavi, M. Z., Grothe, H., Jones, D., & Harvey, J. (2017). Repeatability and sensitivity of FTIR ATR spectral analysis methods for bituminous binders. *Materials and Structures*, 50(3), 187.
- Hofko, B., Porot, L., Cannone, A. F., Poulidakos, L., Huber, L., Lu, X., Grothe, H. (2018). FTIR spectral analysis of bituminous binders: reproducibility and impact of ageing temperature. *Materials and Structures*, 51(2), 45.
- Honarmand, M., Tanzadeh, J., & Beiranvand, M. (2019). Bitumen and its modifier for use in pavement engineering. S. Hemeda (Eds.), *Sustainable Construction and Building Materials* (pp. 250-270). London, UK: IntechOpen.

- Hung, S. S. (2018). *Performance Assessment of Asphalt Mixes Containing Reclaimed Asphalt Pavement and Tire Rubber* (Doctoral dissertation), University of California, USA.
- Iskender, E. (2016). Evaluation of mechanical properties of nano-clay modified asphalt mixtures. *Measurement*, 93, 359-371.
- Ismail, W. A., Endut, I. R., & Ishak, S. Z. (2015). Polyacrylate Modified Binder for Sustainable Asphalt Pavement Performances Using Superpave Mix Design, *Applied Mechanics and Materials*, 747, 238-241.
- Jadidirendi, K. (2017). *Evaluation of the Properties of Rubberized Asphalt Binders and Mixtures* (Doctoral dissertation), University of Nevada, USA.
- Jahromi, S. G., & Khodaii, A. (2009). Effects of nanoclay on rheological properties of bitumen binder. *Construction and Building Materials*, 23(8), 2894-2904.
- Jain, S., Joshi, Y., & Goliya, S. (2013). Design of rigid and flexible pavements by various methods & their cost analysis of each method. *International Journal of Engineering Research and Applications*, 3(5), 119-123.
- Jia, Y., Cao, R.-j., & Translation, B.-j. L. (2005). *Superpave fundamentals reference manual*. China: China Communications Publishing & Media Management Co., Ltd.
- Joshi, C., Patted, A., Archana, M., & Amarnath, M. (2013). Determining the rheological properties of asphalt binder using dynamic shear rheometer (DSR) for selected pavement stretches. *International Journal of Research in Engineering and Technology*, 11, 192-196.
- Junaid, M., Irfan, M., Ahmed, S., & Ali, Y. (2018). Effect of binder grade on performance parameters of asphaltic concrete paving mixtures. *International Journal of Pavement Research and Technology*, 11(5), 435-444.
- Karahancer, S. S., Eriskin, E., Sarioglu, O., Capali, B., Saltan, M., & Terzi, S. (2016). Utilization of Arundo donax in Hot Mix Asphalt as a fiber. *Construction and Building Materials*, 125, 981-986.
- Kennedy, T. W., Huber, G. A., Harrigan, E. T., Cominsky, R. J., Hughes, C. S., Von Quintus, H., & Moulthrop, J. S. (1994). Superior performing asphalt pavements (Superpave): The product of the SHRP asphalt research program.

- Khademi, F., Jamal, S. M., Deshpande, N., & Londhe, S. (2016). Predicting strength of recycled aggregate concrete using artificial neural network, adaptive neuro-fuzzy inference system and multiple linear regression. *International Journal of Sustainable Built Environment*, 5(2), 355-369.
- Khan, K. M., Sultan, T., Farooq, Q. U., Khan, K., & Ali, F. (2013). Development of Superpave Performance Grading Map for Pakistan. *Life Science Journal*, 10(7s), 355-362.
- Khordehbinan, M., & Kaymanesh, M. R. (2020). Chemical analysis and middle-low temperature functional of waste polybutadiene rubber polymer modified bitumen. *Petroleum Science and Technology*, 38(1), 8-17.
- Kim, Y.-J., Kotwal, A., Kim, H., & Lee, S.-J. (2014). Stiffness Prediction of Recycled Aged CRM Binders Using an Artificial Neural Network. *International Journal of Pavement Research and Technology*, 7(1), 9.
- Kim, Y. R. (2008). *Modeling of asphalt concrete*. North Carolina, NC: ASCE Press.
- Kogbara, R. B., Masad, E. A., Kassem, E., Scarpas, A. T., & Anupam, K. (2016). A state-of-the-art review of parameters influencing measurement and modeling of skid resistance of asphalt pavements. *Construction and Building Materials*, 114, 602-617.
- Kok, B. V., Yilmaz, M., Sengoz, B., Sengur, A., & Avci, E. (2010). Investigation of complex modulus of base and SBS modified bitumen with artificial neural networks. *Expert Systems with Applications*, 37(12), 7775-7780.
- Kordi, Z., & Shafabakhsh, G. (2017). Evaluating mechanical properties of stone mastic asphalt modified with Nano Fe₂O₃. *Construction and Building Materials*, 134, 530-539.
- Kringos, N., Birgisson, B., Frost, D., & Wang, L. (2013). *Multi-Scale modeling and characterization of infrastructure materials*. Stockholm: Springer.
- Kushwaha, P., & Swami, B. (2019). A Study on Moisture Susceptibility of Foamed Bitumen Mix Containing Reclaimed Asphalt Pavement. *Transportation Infrastructure Geotechnology*, 6(2), 89-104.
- Lange, C. R., & Stroup-Gardiner, M. (2007). Temperature-dependent chemical-specific emission rates of aromatics and polyaromatic hydrocarbons (PAHs) in bitumen fume. *Journal of Occupational and Environmental Hygiene*, 4(S1), 72-76.

- Leckie, J., & Beeson, M. (2018). HMA Spec Revisions and Testing 2018.
- Lee, H. J., Lee, J. H., & Park, H. M. (2007). Performance evaluation of high modulus asphalt mixtures for long life asphalt pavements. *Construction and Building Materials*, 21(5), 1079-1087.
- Lee, S.-Y., Mun, S.-H., Jin, J.-H., & Hong, Y.-K. (2011). Modification of Asphalt by in-situ Polymerization. *Elastomers and Composites*, 46(3), 257-261.
- Little, D. N., Allen, D. H., & Bhasin, A. (2018). *Modeling and design of flexible pavements and materials*. Texas, TX: Springer.
- Liu, F., Zhou, Z., Zhang, X., & Wang, Y. (2019). On the linking of the rheological properties of asphalt binders exposed to oven aging and PAV aging. *International Journal of Pavement Engineering*, 1-10.
- Liu, J., Yan, K., Liu, J., & Zhao, X. (2018). Using artificial neural networks to predict the dynamic modulus of asphalt mixtures containing recycled asphalt shingles. *Journal of Materials in Civil Engineering*, 30(4), 04018051.
- Lolly, R., Zeiada, W., Souliman, M., & Kaloush, K. (2017). Effects of short-term aging on asphalt binders and hot mix asphalt at elevated temperatures and extended aging time. *In the the MATEC Web of Conferences (pp. 120-137)*. USA: ASCMCES.
- Lu, X., Isacson, U., & Ekblad, J. (1999). Phase separation of SBS polymer modified bitumens. *Journal of Materials in Civil Engineering*, 11(1), 51-57.
- Lucas, D. (1997). *Superpave System: Designing and Building More Durable Asphalt Pavement*. Washington, DC: TR News.
- Mahali, I., & Sahoo, U. C. (2019). Rheological characterization of Nanocomposite modified asphalt binder. *International Journal of Pavement Research and Technology*, 12(6), 589-594.
- Mallick, R. B. (1999). Use of Superpave gyratory compactor to characterize hot-mix asphalt. *Transportation research record*, 1681(1), 86-96.
- Mamlouk, M. S., & Zaniewski, J. P. (2006). *Materials for civil and construction engineers*. New Jersey, NJ: Pearson.

- Mantilla-Forero, J. E., & Castañeda-Pinzón, E. A. (2019). Assessment of simultaneous incorporation of crumb rubber and asphaltite in asphalt binders. *Dyna*, 86(208), 257-263.
- McGennis, R., Anderson, R., Kennedy, T., & Solaimanian, M. (1995). Background of Superpave Asphalt Mixture Design and Analysis, US Department of Transportation Federal Highway Administration, Publication No: FHWA-SA-95-003, 172p.
- Moghaddam, T. B., Karim, M. R., & Abdelaziz, M. (2011). A review on fatigue and rutting performance of asphalt mixes. *Scientific Research and Essays*, 6(4), 670-682.
- Mohammad, L. N., Herath, A., & Huang, B. (2003). Evaluation of Permeability of Superpav® Asphalt Mixtures. *Transportation research record*, 1832(1), 50-58.
- Mubaraki, M. (2019). The Effect of Modified Asphalt Binders by Fourier Transform Infrared Spectroscopy, X-Ray Diffraction, and Scanning Electron Microscopy. *Journal of Materials and Engineering Structures «JMES»*, 6(1), 5-14.
- Murali, M., Suganthi, P., Athif, P., Bukhari, A. S., Mohamed, H. S., Basu, H., & Singhal, R. (2017). Histological alterations in the hepatic tissues of Al₂O₃ nanoparticles exposed freshwater fish *Oreochromis mossambicus*. *Journal of Trace Elements in Medicine and Biology*, 44, 125-131.
- Nejad, F. M., Aflaki, E., & Mohammadi, M. (2010). Fatigue behavior of SMA and HMA mixtures. *Construction and Building Materials*, 24(7), 1158-1165.
- Nicholls, C., Roberts, C., & Samuel, P. (2006). *Implications of implementing the European asphalt test methods*. Wokingham, UK: Transport and Road Research Laboratory.
- Nunn, M., Brown, A., Weston, D., & Nicholls, J. (1997). *Design of long-life flexible pavements for heavy traffic*. Wokingham, UK: TRL Limited.
- Omar, H. A., Yusoff, N. I. M., Mubaraki, M., & Ceylan, H. (2020). Effects of moisture damage on asphalt mixtures. *Journal of Traffic and Transportation Engineering (English Edition)*, 7(5), 600-628.
- Orouskhani, M., Mansouri, M., Orouskhani, Y., & Teshnehlab, M. (2013). A hybrid method of modified cat swarm optimization and gradient descent algorithm for training ANFIS. *International Journal of Computational Intelligence and Applications*, 12(02), 1350007.

- Ozgan, E. (2011). Artificial neural network based modelling of the Marshall Stability of asphalt concrete. *Expert Systems with Applications*, 38(5), 6025-6030.
- Özgan, E., Korkmaz, I., & Emiroğlu, M. (2012). Adaptive neuro-fuzzy inference approach for prediction the stiffness modulus on asphalt concrete. *Advances in Engineering Software*, 45(1), 100-104.
- Parmar, K. S., & Bhardwaj, R. (2015). River water prediction modeling using neural networks, fuzzy and wavelet coupled model. *Water resources management*, 29(1), 17-33.
- Pasandín, A., & Pérez, I. (2014). Effects of the asphalt penetration grade and the mineralogical composition on the asphalt-aggregate bond. *Petroleum Science and Technology*, 32(22), 2730-2737.
- Pedrycz, W. (1993). *Fuzzy control and fuzzy systems*. Somerset, UK: Research Studies Press Ltd.
- Petersen, J. C. (2000). Chemical composition of asphalt as related to asphalt durability. T.F. Yen and G.V. Chilinganan (Eds.), *Developments in petroleum science* (Vol. 40, pp. 363-399). New York, NY: Elsevier.
- Petersen, J. C. (2009). A review of the fundamentals of asphalt oxidation: chemical, physicochemical, physical property, and durability relationships. Transportation Research Circular (E-C140).
- Peterson, R. L., Mahboub, K. C., Anderson, R. M., Masad, E., & Tashman, L. (2004). Comparing Superpave gyratory compactor data to field cores. *Journal of Materials in Civil Engineering*, 16(1), 78-83.
- Pirmohammad, S., Majd-Shokorlou, Y., & Amani, B. (2019). Experimental investigation of fracture properties of asphalt mixtures modified with Nano Fe₂O₃ and carbon nanotubes. *Road Materials and Pavement Design*, 1-23.
- Ponniah, J., & Kennepohl, G. (1996). Polymer-modified asphalt pavements in Ontario: Performance and cost-effectiveness. *Transportation research record*, 1545(1), 151-160.
- Porto, M., Caputo, P., Loise, V., Eskandarsefat, S., Teltayev, B., & Oliviero Rossi, C. (2019). Bitumen and bitumen modification: A review on latest advances. *Applied Sciences*, 9(4), 742.

- Pyshyev, S., Gunka, V., Grytsenko, Y., & Bratychak, M. (2016). Polymer modified bitumen. *Chemistry & Chemical Technology*, 10(4s), 631-636.
- Rahman, M. (2004). *Characterisation of dry process crumb rubber modified asphalt mixtures* (Doctoral dissertation), University of Nottingham, United Kingdom.
- Ramadan, K. Z., & Abo-Qudais, S. A. (2017). Effect of Superpave short-term aging on binder and asphalt mixture rheology. *Periodica Polytechnica Transportation Engineering*, 45(4), 196-205.
- Read, J., Whiteoak, D., & Hunter, R. N. (2003). *The shell bitumen handbook*. London, UK: Thomas Telford.
- Redelius, P., & Soenen, H. (2015). Relation between bitumen chemistry and performance. *Fuel*, 140, 34-43.
- Reitermanova, Z. (2010). Data splitting. *In the WDS'10 Proceedings of Contributed Papers, Part I* (pp. 31–36). Prague, Czech Republic: MATFYZPRESS.
- Rezaei, S., Ziari, H., & Nowbakht, S. (2016). Low temperature functional analysis of bitumen modified with composite of nano-SiO₂ and styrene butadiene styrene polymer. *Petroleum Science and Technology*, 34(5), 415-421.
- Roberts, F. L., Mohammad, L. N., & Wang, L. (2002). History of hot mix asphalt mixture design in the United States. *Journal of Materials in Civil Engineering*, 14(4), 279-293.
- Rossi, C. O., Spadafora, A., Teltayev, B., Izmailova, G., Amerbayev, Y., & Bortolotti, V. (2015). Polymer modified bitumen: Rheological properties and structural characterization. *Colloids and Surfaces A: Physicochemical and Engineering Aspects*, 480, 390-397.
- Samiey, B., Cheng, C.-H., & Wu, J. (2014). Organic-inorganic hybrid polymers as adsorbents for removal of heavy metal ions from solutions: a review. *Materials*, 7(2), 673-726.
- Scholz, T. V. (1995). *Durability of bituminous paving mixtures* (Doctoral dissertation), University of Nottingham, United Kingdom.
- Sediq, P. A. (2018). *Characterization of Asphalt Binder Modified with Nanocomposite* (Master dissertation), Near East University. TRNC.

- Shen, D.-H., Kuo, M.-F., & Du, J.-C. (2005). Properties of gap-aggregate gradation asphalt mixture and permanent deformation. *Construction and Building Materials*, 19(2), 147-153.
- Sirin, O., Paul, D. K., & Kassem, E. (2018). State of the art study on aging of asphalt mixtures and use of antioxidant additives. *Advances in Civil Engineering*, 2018.
- Smith, B. T., Bazuhair, R. W., Daranga, C., Baumgardner, G. L., & Howard, I. L. (2019). Comparing Laboratory Pressure Aging Vessel Conditioning to Field Aging of Asphalt Binder within Compacted Mixtures. *Journal of Materials in Civil Engineering*, 31(11), 04019271.
- Solaimanian, M., Bonaquist, R. F., & Tandon, V. (2007). Improved conditioning and testing procedures for HMA moisture susceptibility (Vol. 589): Transportation Research Board.
- Solgi, A., Zarei, H., Nourani, V., & Bahmani, R. (2017). A new approach to flow simulation using hybrid models. *Applied Water Science*, 7(7), 3691-3706.
- Sotiriadis, G. (2016). *Asphalt transport pavements: causes of deterioration, methods of maintenance and suggestions/guidelines for new smart methods* (Doctoral dissertation), Cyprus University of Technology, Cyprus.
- Southern, M. (2015). A perspective of bituminous binder specifications. S. Huang and H. D. Benedetto (Eds.), *Advances in Asphalt Materials* (pp. 1-27). Brussels, Belgium: Wood Head Publishing.
- Specht, L., & Khatchatourian, O. (2014). Application of artificial intelligence to modelling asphalt–rubber viscosity. *International Journal of Pavement Engineering*, 15(9), 799-809.
- Sreedhar, S., & Coleri, E. (2018). Effects of binder content, density, gradation, and polymer modification on cracking and rutting resistance of asphalt mixtures used in Oregon. *Journal of Materials in Civil Engineering*, 30(11), 04018298.
- Sugeno, M. (1985). *Industrial applications of fuzzy control*. New York, NY: Elsevier Science Inc.
- Sullivan, B. (2005). Development of a fundamental skid resistance asphalt mix design procedure. *In the Proceedings, International Conference on Surface Friction* (pp. 15-30). Christchurch, New Zealand: TRANSIT NEW ZEALAND.

- Sun, D., & Lu, W. (2006). Phase morphology of polymer modified road asphalt. *Petroleum Science and Technology*, 24(7), 839-849.
- Tabaković, A., & Schlangen, E. (2015). Self-healing technology for asphalt pavements. Hager M., van der Zwaag S., Schubert U. (Eds.), *Advances in Polymer Science* (pp. 285-306). Switzerland: Springer.
- Tabatabaee, H. A., & Bahia, H. U. (2012). Life cycle energy and cost assessment method for modified asphalt pavements. *Procedia-Social and Behavioral Sciences*, 54, 1220-1231.
- Tapkın, S., Çevik, A., & Uşar, Ü. (2009). Accumulated strain prediction of polypropylene modified marshall specimens in repeated creep test using artificial neural networks. *Expert Systems with Applications*, 36(8), 11186-11197.
- Tarefder, R., Zaman, M., & Hobson, K. (2003). A laboratory and statistical evaluation of factors affecting rutting. *International Journal of Pavement Engineering*, 4(1), 59-68.
- Tauste, R., Moreno-Navarro, F., Sol-Sánchez, M., & Rubio-Gámez, M. (2018). Understanding the bitumen ageing phenomenon: A review. *Construction and Building Materials*, 192, 593-609.
- Teh, S. Y., & Hamzah, M. O. (2019). Asphalt mixture workability and effects of long-term conditioning methods on moisture damage susceptibility and performance of warm mix asphalt. *Construction and Building Materials*, 207, 316-328.
- Venudharan, V., & Biligiri, K. P. (2017). Heuristic principles to predict the effect of crumb rubber gradation on asphalt binder rutting performance. *Journal of Materials in Civil Engineering*, 29(8), 04017050.
- Viswanath, D. S., Ghosh, T. K., Prasad, D. H., Dutt, N. V., & Rani, K. Y. (2007). *Viscosity of liquids: theory, estimation, experiment, and data*. Netherlands: Springer Science & Business Media.
- Wang, H., Liu, X., Apostolidis, P., van de Ven, M., Erkens, S., & Skarpas, A. (2020). Effect of laboratory aging on chemistry and rheology of crumb rubber modified bitumen. *Materials and Structures*, 53(2), 1-15.

- Wang, T., Yang, R., Li, A., Chen, L., & Zhou, B. (2016). Effects of sasobit and its adding process on the performance of rubber asphalt. *Chemical Engineering Transactions*, 51, 181-186.
- West, R. C., Willis, J. R., & Marasteanu, M. O. (2013). Improved mix design, evaluation, and materials management practices for hot mix asphalt with high reclaimed asphalt pavement content (Vol. 752): Transportation Research Board.
- White, G. (2018). State of the art: Asphalt for airport pavement surfacing. *International Journal of Pavement Research and Technology*, 11(1), 77-98.
- Wu, J. (2009). *The influence of mineral aggregates and binder volumetrics on bitumen ageing* (Doctoral dissertation), University of Nottingham, United Kingdom.
- Yang, J., & Tighe, S. (2013). A review of advances of nanotechnology in asphalt mixtures. *Procedia-Social and Behavioral Sciences*, 96, 1269-1276.
- Yang, R., Kang, S., Ozer, H., & Al-Qadi, I. L. (2015). Environmental and economic analyses of recycled asphalt concrete mixtures based on material production and potential performance. *Resources, Conservation and Recycling*, 104, 141-151.
- Yao, H., You, Z., Li, L., Lee, C. H., Wingard, D., Yap, Y. K., Goh, S. W. (2013). Rheological properties and chemical bonding of asphalt modified with nanosilica. *Journal of Materials in Civil Engineering*, 25(11), 1619-1630.
- Yildirim, Y., Ideker, J., & Hazlett, D. (2006). Evaluation of viscosity values for mixing and compaction temperatures. *Journal of Materials in Civil Engineering*, 18(4), 545-553.
- Yilmaz, M., Avcı, E., Şengür, A., Şengöz, B., & Kök, B. V. (2010). Investigation of complex modulus of base and SBS modified bitumen with artificial neural networks. *Expert Systems with Applications* 37(12), 7775-7780
- Yilmaz, M., Kok, B. V., Sengoz, B., Sengur, A., & Avcı, E. (2011). Investigation of complex modulus of base and EVA modified bitumen with Adaptive-Network-Based Fuzzy Inference System. *Expert Systems with Applications*, 38(1), 969-974.
- Yin, F., & Moraes, P. R. (2018). Storage Stability Testing of Asphalt Binders Containing Recycled Polyethylene Materials: Phase II-A Study Report, Prepared for the Plastics Industry Association.

- You, Z., Mills-Beale, J., Foley, J. M., Roy, S., Odegard, G. M., Dai, Q., & Goh, S. W. (2011). Nanoclay-modified asphalt materials: Preparation and characterization. *Construction and Building Materials*, 25(2), 1072-1078.
- Yuanita, E., Hendrasetyawan, B., Firdaus, D., & Chalid, M. (2017). Improvement of polypropylene (PP)-modified bitumen through lignin addition. *In the IOP Conference Series: Materials Science and Engineering* (pp. 223-232). Medan, Indonesia: IOP Publishing.
- Yusoff, N. I. M., Alhamali, D. I., Ibrahim, A. N. H., Rosyidi, S. A. P., & Hassan, N. A. (2019). Engineering characteristics of nanosilica/polymer-modified bitumen and predicting their rheological properties using multilayer perceptron neural network model. *Construction and Building Materials*, 204, 781-799.
- Zare-Shahabadi, A., Shokuhfar, A., & Ebrahimi-Nejad, S. (2010). Preparation and rheological characterization of asphalt binders reinforced with layered silicate nanoparticles. *Construction and Building Materials*, 24(7), 1239-1244.
- Zaumanis, M. (2011). *Warm mix asphalt investigation* (Master dissertation), Riga Technical University, Denmark.
- Zhang, C., Xu, T., Shi, H., & Wang, L. (2015). Physicochemical and pyrolysis properties of SARA fractions separated from asphalt binder. *Journal of Thermal Analysis and Calorimetry*, 122(1), 241-249.
- Zhang, P., Guo, Q., Tao, J., Ma, D., & Wang, Y. (2019). Aging mechanism of a diatomite-modified asphalt binder using Fourier-Transform Infrared (FTIR) Spectroscopy analysis. *Materials*, 12(6), 988.
- Zhu, J., Birgisson, B., & Kringos, N. (2014). Polymer modification of bitumen: Advances and challenges. *European Polymer Journal*, 54, 18-38.
- Ziari, H., Amini, A., Goli, A., & Mirzaiyan, D. (2018). Predicting rutting performance of carbon nano tube (CNT) asphalt binders using regression models and neural networks. *Construction and Building Materials*, 160, 415-426.
- Zorn, S., Mehta, Y., Dahm, K., Batten, E., Nolan, A., & Dusseau, R. (2011). Rheological properties of the polymer modified bitumen with emphasis on SBS polymer and its

microstructure Road Materials and New Innovations in Pavement Engineering. *In the GeoHunan International Conference* (pp. 41-48). Hunan, China: ASCE.

Appendices

Appendix 1: XRD analysis results for ASA/Si and ASA/Fe composites

20-angle	Base AC	Fe	ASA/Fe 3%	ASA/Fe 5%	ASA/Fe 5%	Si	ASA/Si 3%	ASA/Si 3%	ASA/Si 3%
10.000	480	266	494	377	419	410	485	567	626
10.020	454	316	463	372	433	442	511	628	595
10.039	474	279	476	383	452	408	543	597	509
10.059	477	262	481	342	439	446	512	601	609
10.079	446	306	478	387	419	448	546	636	590
10.099	477	286	468	365	452	467	534	639	561
.
.
.
.
.
.
89.927	536	387	451	455	411	364	549	452	521
89.947	506	354	468	412	435	373	480	481	506
89.967	555	361	483	412	448	387	515	519	556
89.987	515	385	465	450	451	375	507	511	489
90.006	518	377	420	426	437	372	540	490	505

*Some or all data, models, or code that support the findings of this study are available from the corresponding author upon reasonable request. Please contact mustafa.alas@neu.edu.tr for full data.

Appendix 2: FTIR analysis results for ASA/Si composites

Wave number cm-1	Unaged FT-IR				Short-term aged FT-IR			
	Base AC %T	ASA/Si 3% %T	ASA/Si 5% %T	ASA/Si 7% %T	Base AC %T	ASA/Si 3% %T	ASA/Si 5% %T	ASA/Si 7% %T
4000	100.34	97.08	98.73	97.82	98.61	97.03	95.14	96.68
3999	100.29	97.08	98.79	97.86	98.58	97.05	95.16	96.68
3998	100.23	97.09	98.86	97.90	98.54	97.06	95.18	96.69
3997	100.19	97.08	98.89	97.94	98.51	97.04	95.18	96.68
3996	100.14	97.09	98.85	97.96	98.49	97.02	95.17	96.69
3995	100.07	97.10	98.77	97.94	98.50	97.01	95.17	96.70
.
.
.
.
.
605	87.34	84.85	87.58	85.51	86.00	85.99	85.35	84.17
604	87.38	84.86	87.65	85.76	86.40	85.93	85.38	84.38
603	87.15	84.63	87.56	85.63	86.92	86.00	85.65	84.58
602	86.78	84.40	87.30	85.13	87.26	86.17	85.97	84.73
601	86.50	84.26	86.94	84.64	87.15	86.26	86.04	84.86
600	86.38	84.18	86.50	84.39	86.67	86.23	85.86	84.96

*Some or all data, models, or code that support the findings of this study are available from the corresponding author upon reasonable request. Please contact mustafa.alas@neu.edu.tr for full data.

Appendix 3: FTIR analysis results for ASA/Fe composites

Wave number cm-1	Unaged FT-IR				Short-term aged FT-IR			
	Base AC %T	ASA/Fe 3% %T	ASA/Fe 5% %T	ASA/Fe 7% %T	Base AC %T	ASA/Fe 3% %T	ASA/Fe 5% %T	ASA/Fe 7% %T
4000	100.34	104.29	104.45	98.05	98.61	96.34	95.55	93.55
3999	100.29	104.28	104.45	98.07	98.58	96.38	95.53	93.53
3998	100.23	104.24	104.44	98.07	98.54	96.43	95.51	93.51
3997	100.19	104.20	104.50	98.07	98.51	96.48	95.50	93.50
3996	100.14	104.18	104.49	98.06	98.49	96.52	95.51	93.51
3995	100.07	104.28	104.48	98.07	98.50	96.54	95.51	93.51
.
.
.
.
.
605	87.34	86.48	84.70	84.54	86.00	86.48	84.70	84.54
604	87.38	86.58	84.28	84.22	86.40	86.58	84.28	84.22
603	87.15	86.69	84.00	83.73	86.92	86.69	84.00	83.73
602	86.78	86.70	83.89	83.36	87.26	86.70	83.89	83.36
601	86.50	86.44	83.93	83.28	87.15	86.44	83.93	83.28
600	86.38	86.00	84.00	83.42	86.67	86.00	84.00	83.42

*Some or all data, models, or code that support the findings of this study are available from the corresponding author upon reasonable request. Please contact mustafa.alas@neu.edu.tr for full data.

Appendix 4: Complex modulus for ASA/Si and ASA/Fe composites

Temp (°C)	Freq. (Hz)	Base AC	ASA/Si 3%	ASA/Si 5%	ASA/Si 7%	ASA/Fe 3%	ASA/Fe 5%	ASA/Fe 7%
		G* (Pa)	G* (Pa)	G* (Pa)	G* (Pa)	G* (Pa)	G* (Pa)	G* (Pa)
46	0.159	2700	4178	18215	17000	27495	9209	7370
46	0.2	3000	7113	28954	20000	33943	11420	8982
46	0.5	7000	16240	60384	47000	78143	26070	20772
46	1.592	18000	38087	150000	100000	223860	64730	45030
46	2	23000	52000	200000	168800	262470	75470	51961
.
.
.
.
.
82	2	400	900	3700	2800	4022	2035	1135
82	3	600	1400	5500	5000	5992	3043	1696
82	5	900	2100	9500	9300	9877	5058	2807
82	10	2000	5500	22000	17000	19370	9868	5481
82	15.92	2300	7000	30000	24000	30472	15540	8626

*Some or all data, models, or code that support the findings of this study are available from the corresponding author upon reasonable request. Please contact mustafa.alas@neu.edu.tr for full data.

Appendix 5: MSCR test results for ASA/Si composites at 100 and 3200 Pa

Stress level (Pa)	Base AC		ASA/Si 3%		ASA/Si 5%		ASA/Si 7%	
	time (s)	creep (1/Pa)	time (s)	creep (1/Pa)	time (s)	creep (1/Pa)	time (s)	creep (1/Pa)
100	0.193	0.741	0.198	0.573	0.153	0.356	0.155	0.432
100	0.288	0.827	0.290	0.579	0.280	0.363	0.270	0.449
100	0.368	0.899	0.368	0.588	0.363	0.356	0.365	0.440
100	0.445	0.969	0.483	0.594	0.440	0.353	0.445	0.454
100	0.575	1.086	0.643	0.594	0.558	0.388	0.520	0.458
100
100
100
100
100
100	97.916	8.592	98.439	5.258	3.578	98.529	4.374	98.591
100	98.034	8.592	98.551	5.262	3.579	98.661	4.380	98.669
100	98.126	8.592	98.649	5.257	3.571	98.739	4.376	98.804
100	98.206	8.592	98.724	5.263	3.583	98.819	4.383	98.886
100	98.286	8.592	98.839	5.262	3.578	98.934	4.375	98.964
3200	0.231	38.405	0.198	32.004	0.155	15.720	0.160	26.670
3200	0.326	40.032	0.293	33.360	0.275	16.190	0.293	27.800
3200	0.416	41.198	0.370	34.332	0.368	16.540	0.368	28.610
3200	0.556	42.509	0.445	35.424	0.448	16.790	0.445	29.520
3200	0.652	44.424	0.568	37.020	0.528	17.020	0.523	30.850
3200
3200
3200
3200
3200
3200	98.479	197.323	98.714	164.436	98.719	130.341	98.349	137.030
3200	98.594	197.309	98.794	164.424	98.794	130.343	98.429	137.020
3200	98.681	197.294	98.874	164.412	98.869	130.345	98.509	137.010
3200	98.756	197.280	98.951	164.400	98.981	130.337	98.639	137.000
3200	98.831	197.280	99.079	164.400	99.074	130.327	98.716	137.000

*Some or all data, models, or code that support the findings of this study are available from the corresponding author upon reasonable request. Please contact mustafa.alas@neu.edu.tr for full data.

Appendix 6: MSCR test results for ASA/Fe composites at 100 and 3200 Pa

Stress level (Pa)	Base AC		ASA/Fe 3%		ASA/Fe 5%		ASA/Fe 7%	
	time (s)	creep (1/Pa)	time (s)	creep (1/Pa)	time (s)	creep (1/Pa)	time (s)	creep (1/Pa)
100	0.193	0.741	0.158	0.170	0.160	0.271	0.198	0.372
100	0.288	0.827	0.275	0.169	0.298	0.278	0.290	0.376
100	0.368	0.899	0.370	0.164	0.375	0.276	0.368	0.382
100	0.445	0.969	0.445	0.156	0.455	0.276	0.483	0.386
100	0.575	1.086	0.525	0.175	0.568	0.287	0.643	0.386
100
100
100
100
100
100	97.91	8.592	97.80	2.257	98.75	2.691	97.89	3.425
100	98.03	8.592	98.01	2.252	98.83	2.696	97.99	3.423
100	98.12	8.592	98.08	2.258	98.91	2.700	98.07	3.419
100	98.20	8.592	98.16	2.254	99.04	2.699	98.15	3.419
100	98.28	8.592	98.24	2.246	98.00	3.578	98.27	3.418
3200	0.231	38.405	0.153	8.559	0.170	12.670	0.198	25.651
3200	0.326	40.032	0.283	8.709	0.305	13.050	0.293	26.880
3200	0.416	41.198	0.363	8.812	0.383	13.230	0.370	27.712
3200	0.556	42.509	0.443	8.875	0.465	13.440	0.445	28.642
3200	0.652	44.424	0.558	8.989	0.598	13.750	0.568	29.410
3200
3200
3200
3200
3200
3200	98.47	197.323	98.20	78.933	98.07	111.595	98.71	135.130
3200	98.59	197.309	98.28	78.927	98.14	111.596	98.7	135.133
3200	98.68	197.294	98.40	78.917	98.22	111.583	98.87	135.129
3200	98.75	197.280	98.48	78.906	98.35	111.581	98.95	135.128
3200	98.83	197.280	98.56	78.918	98.43	111.582	99.07	135.128

*Some or all data, models, or code that support the findings of this study are available from the corresponding author upon reasonable request. Please contact mustafa.alas@neu.edu.tr for full data.

Appendix 7: ANN model results

Data point	Scenario 1					Scenario 2					
	Training		Testing			Training		Testing			
	Actual	Predicted	Data point	Actual	Predicted	Data point	Actual	Predicted	Data point	Actual	Predicted
1	4.76E-04	1.32E-02	1	1.83E-04	6.00E-04	1	1.36E-02	3.19E-02	1	1.65E-03	3.30E-03
2	1.09E-02	1.40E-02	2	2.83E-04	7.00E-04	2	2.09E-02	3.25E-02	2	2.02E-03	3.60E-03
3	2.50E-02	2.11E-02	3	4.81E-04	7.00E-04	3	5.00E-02	3.76E-02	3	4.70E-03	6.40E-03
4	5.84E-02	5.82E-02	4	9.75E-04	8.00E-04	4	1.27E-01	5.73E-02	4	1.02E-02	1.21E-02
5	8.00E-02	7.43E-02	5	1.57E-03	2.00E-03	5	1.55E-01	6.61E-02	5	1.18E-02	1.42E-02
.
.
.
.
.
306	2.49E-03	2.10E-03	306	2.48E-04	2.00E-04	306	3.71E-03	2.66E-02	306	3.98E-04	1.00E-04
307	0.00E+00	1.00E-04	307	3.80E-04	3.00E-04	307	1.96E-06	2.70E-03	307	6.70E-04	1.00E-04
308	4.12E-06	1.00E-04	308	6.38E-04	6.00E-04	308	7.77E-06	2.80E-03	308	1.33E-03	3.00E-04
309	3.41E-05	1.00E-04	309	1.26E-03	1.20E-03	309	5.06E-05	2.90E-03	309	2.11E-03	1.90E-03
310	1.42E-04	4.00E-04	310	2.01E-03	2.80E-03	310	2.04E-04	4.30E-03	310	2.11E-03	3.20E-03

*Some or all data, models, or code that support the findings of this study are available from the corresponding author upon reasonable request. Please contact mustafa.alas@neu.edu.tr for full data.

Appendix 8: ANFIS model results

	Scenario 1			Scenario 1			Scenario 2			Scenario 2		
	Training			Testing			Training			Testing		
Data point	Actual	Predicted	Data point	Actual	Predicted	Data point	Actual	Predicted	Data point	Actual	Predicted	
1	4.14E-03	1.36E-02	1.00E+00	1.83E-04	2.00E-04	1.00E+00	1.36E-02	1.19E-02	1.00E+00	2.60E-04	3.00E-04	
2	4.60E-03	1.41E-02	2.00E+00	2.83E-04	3.00E-04	2.00E+00	2.09E-02	1.30E-02	2.00E+00	3.98E-04	8.00E-04	
3	1.08E-02	1.75E-02	3.00E+00	4.81E-04	5.00E-04	3.00E+00	5.00E-02	2.23E-02	3.00E+00	6.70E-04	1.90E-03	
4	2.77E-02	2.99E-02	4.00E+00	9.75E-04	1.00E-03	4.00E+00	1.27E-01	5.28E-02	4.00E+00	1.33E-03	1.00E-03	
5	3.54E-02	3.45E-02	5.00E+00	1.57E-03	1.50E-03	5.00E+00	1.55E-01	6.51E-02	5.00E+00	2.11E-03	1.00E-03	
.	
.	
.	
.	
306	2.49E-03	7.36E-02	3.06E+02	2.48E-04	6.00E-04	3.06E+02	3.71E-03	1.24E-02	3.06E+02	3.98E-04	4.00E-04	
307	0.00E+00	1.26E-02	3.07E+02	3.80E-04	1.50E-03	3.07E+02	1.96E-06	1.50E-03	3.07E+02	6.70E-04	1.00E-03	
308	4.12E-06	1.24E-02	3.08E+02	6.38E-04	3.50E-03	3.08E+02	7.77E-06	1.40E-03	3.08E+02	1.33E-03	2.20E-03	
309	3.41E-05	1.08E-02	3.09E+02	1.26E-03	1.90E-03	3.09E+02	5.06E-05	9.00E-04	3.09E+02	2.11E-03	1.00E-04	
310	1.42E-04	5.20E-03	3.10E+02	2.01E-03	5.00E-03	3.10E+02	2.04E-04	1.00E-03	3.10E+02	2.11E-03	2.80E-03	

*Some or all data, models, or code that support the findings of this study are available from the corresponding author upon reasonable request. Please contact mustafa.alas@neu.edu.tr for full data.

CURRICULUM VITAE

1. **Name –Last Name:** MUSTAFA ALAS

2. **Date of Birth:** 03.05.1990

3. **Title:** LECTURER

4. **Education:**

Degree	Department	University	Year
BSc.	Civil & Environmental Engineering	University of Southampton	2011
MSc.	Civil & Environmental Engineering	Near East University	2016
PhD.	Civil & Environmental Engineering	Near East University	2021 (Expected)

5. **Academic Title:** Msc.

Date for Assist. Professor title:

Date for Associate Professor title:

Date for Professor title:

6. **Master and PhD Thesis Supervised:**

6.1. **Master's thesis**

6.2. **PhD thesis**

7. **Publications**

7.1. **Articles published in international peer-reviewed journals (SCI & SSCI & Arts and Humanities)**

1. Experimental Evaluation and Modelling of Polymer Nanocomposite Modified Asphalt Binders Using ANN and ANFIS. *Journal of Materials in Civil Engineering*. (2020).
2. The High Temperature Performance Evaluation of Polymer/Nanocomposite Modified Asphalt Cement. *Teknik Dergi*. (Prescript) (2022).

7.2. **Articles published in other international peer-reviewed journals**

1. Prediction of the High-Temperature Performance of a Geopolymer Modified Asphalt Binder Using Artificial Neural Networks. *International journal of technology*. (2019).

7.3. **Bulletins presented in international scientific meetings and published in proceedings**

7.4. **International books or sections of books published**

7.5. **Articles published in national journals**

7.3. **Bulletins presented in national scientific meetings and published in proceedings**

7.7. **Other publications**

7.8. **International Citations**

Number of citations: 7

8. **National & International Project**

9. **Scientific and Professional Memberships**















K.T.M.M.O.B CHAMBER OF CIVIL ENGINEERS

10. Awards

11. Undergraduate or Graduate courses taught in the last two years:

Academic Year	Semester	Course Name	Hours per Week		Number of Students
			Theory	Application	
2018/2019	Spring	Technical Drawing	2	2	24
		Cad and 3D Printing	2	2	17
2019/2020	Fall	Technical Drawing	2	2	58
		Cad and 3D Printing	2	2	16
		Statics and Mechanics	4	-	110
		Structural analysis	4	-	158
	Spring	Technical Drawing	2	2	33
		Cad and 3D Printing	2	2	24
2020/2021	Fall	Technical Drawing	2	2	59
		Cad and 3D Printing	2	2	27

SIMILARTIY CHECK

<input type="checkbox"/>	AUTHOR	TITLE	SIMILARITY	GRADE	RESPONSE	FILE	PAPER ID	DATE
<input type="checkbox"/>	Mustafa Alias	Abstract	0% 	--	--		1524865184	05-Mar-2021
<input type="checkbox"/>	Mustafa Alias	Conclusion	0% 	--	--		1524372219	04-Mar-2021
<input type="checkbox"/>	Mustafa Alias	Introduction	2% 	--	--		1524365494	04-Mar-2021
<input type="checkbox"/>	Mustafa Alias	Results and discussion	6% 	--	--		1524371522	04-Mar-2021
<input type="checkbox"/>	Mustafa Alias	Literature Review	12% 	--	--		1524368932	04-Mar-2021
<input type="checkbox"/>	Mustafa Alias	Methodology	14% 	--	--		1524370243	04-Mar-2021
<input type="checkbox"/>	Mustafa Alias	Thesis all chapters	14% 	--	--		1524870761	05-Mar-2021



Assoc. Prof. Dr. Shaban Ismael Albrka

ETHICS LETTER

REF: 60/2020

TO THE INSTITUTE OF GRADUATE STUDIES

REFERENCE: MUSTAFA ALAS (20166246)

I would like to inform you that the above candidate is one of our postgraduate students in Civil Engineering department. He is taking thesis under my supervision on the thesis entailed: *The Performance Characteristics of Polymer Nanocomposite Modified Binders and Asphalt Mixtures*. The data used in his study was our own data obtained from experimental work conducted by the student in Malaysia.

Please do not hesitate to contact me if you have any further queries or questions.

Thank you very much indeed.

Best Regards,



Dr. Shaban Isamel Albrka

Civil Engineering Department,

Faculty of Civil and Environmental Engineering,

Near East Boulevard, ZIP: 99138

Nicosia / TRNC, North Cyprus,

Mersin 10 – Turkey.

Email: shabanismeal.albrka@neu.edu.tr